Aspects in Limb Development in Fossil and Recent Eureptiles: Morphological and Histological Approaches

---

Dissertation

zur

Erlangung der naturwissenschaftlichen Doktorwürde
(Dr. sc. nat.)

vorgelegt der

Mathematisch-naturwissenschaftlichen Fakultät

der

Universität Zürich

von

Jasmina Hugi

aus

Winterthur ZH

Promotionskomitee

Prof. Dr. Marcelo R. Sánchez-Villagra
(Leiter und Vorsitz der Dissertation)
Prof. Dr. Johannes Müller
Dr. Mark N. Hutchinson
Dr. Torsten M. Scheyer
Prof. Dr. Michel C. Milinkovitch
Dr. Heinz Furrer

Zürich, 2011

Aspects in Limb Development in Fossil and Recent Eureptiles: Morphological and Histological Approaches

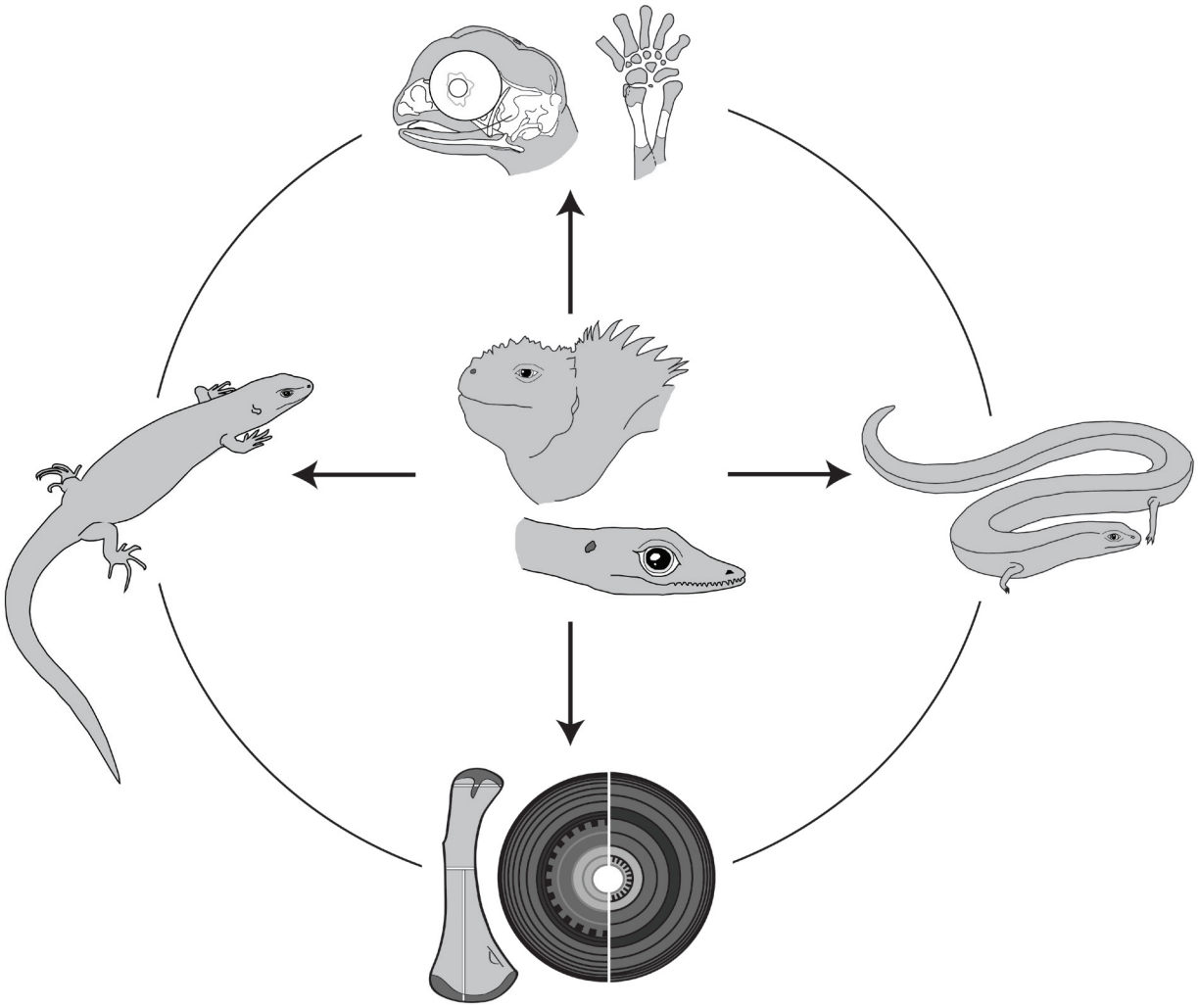

Drawing: J. Hugi

Content **Page Number**

Acknowledgment

Firstly, I'd like to say a massive thank you to Marcelo Sánchez and Torsten Scheyer for supervising my work. This work wouldn't have been possible without them and I'm honoured to be working with such enthusiastic scientists and dear friends. I'd also like to thank Heinz Furrer (Zürich), Raphael Winkler (Basel), Mark-Oliver Rödel (Berlin), Wolfgang Böhme (Bonn), Günther Köhler (Frankfurt), Alan Levotin (California), Mike Thompson and Jacquie Herbert (Sydney), Mark Hutchinson, Sonja Dewdney and the Australian Reptile Breeding Facility (Echunga, South Australia), Ian Williams, Aaron Fenner for assisting in the field and for the provision of bone samples and embryos. I'd like to thank especially Mark Hutchinson with whom I share the enthusiasm for herps. Ursina Koller for letting me use her stunning photographies of the marine and land iguanas from Galapagos. Nadav Pezaro from the University of Sydney and once again Ian Williams for beautiful pics of lizards that I was allowed to use in my thesis. Katja Polachowski, Claude Monnet, Naoki Morimoto, James Neenan, Laura Wilson, Christian Mitgutsch, Christian Kolb, Nicole Klein (Bonn), Martin Sander (Bonn), Johannes Müller (Berlin), Beat Häusler, Markus Hebeisen, Rosemarie Roth, Leonie Pauli, Julia Huber, Beat Scheffold, Jérôme Gapany for sharing their great knowledge with me. Many thanks to everyone of the Paleontological Institute, the Paleontological and Zoological Museum of the University of Zürich. I'd also like to thank my office mates, Kenneth de Baets and Carlo Romano for our excellent working atmosphere! Kenneth is especially thanked for his great catching skills in the Australian fields and for his wonderful company during our trip. Last but not least, I'd like to thank my friends and family for their love and patience, and everyone else who has helped guide me through the ups and downs of the last years.

This work is for Philipp and my mum and dad for the best support they could have given Kump'l and me.

Abstract

Evolutionary changes in lifestyle (e.g., terrestrial vs. aquatic modes of life) within tetrapod vertebrate clades are known to influence limb morphology. Modified limb morphotypes can reveal changes in the osteogenetic sequences (order in bone formation) and bone histology (microstructure of bone) in comparison to the plesiomorphic ancestral condition. Osteogenetic sequences are conserved in Recent terrestrial surface dwelling lacertilian squamates with non-reduced limbs, but are largely variable in the rest of the tetrapods. However, similar evolutionary trends in the order of osteogenesis and in bone microstructure are often displayed in tetrapods with equal habit preferences. Hence, these features can be used as evolutionary markers for specific modes of life.

This hypothesis is tested in growth series of fossil (e.g., pachypleurosaurids) and Recent eureptiles (e.g., marine iguana and other iguanine and scincid lizards) by using a combination of morphological and histological approaches. This thesis focuses on heterochronic events (evolutionary changes in developmental timing) during osteogenesis and on changes in the bone histology during ontogeny of living and fossil clades with different modes of life as a case study. The innovative aspects of the thesis reside in (A) the sampling of taxa and growth stages to study the evolution of eureptilian development in a broad phylogenetic and ecomorphological spectrum, (B) the integration of neontological data of different limb morphotypes, osteogenetic sequences and bone histology, and (C) the correlation of osteogenetic sequences and bone histology of unique fossil ontogenetic material from the UNESCO World Heritage Site Monte San Giorgio (Switzerland, Italy).

In one part of the thesis I examine the osteogenetic sequences in terrestrial surface dwelling lizards with non-reduced limbs and no body elongation. Results reveal conserved osteogenetic sequences for this specific limb morphotype which is hypothesised to be the plesiomorphic ancestral condition for terrestrial surface dwelling eureptiles. Recent subsurface dwelling lizard species, in contrary, show heterochronic shifts in the ossification sequences in comparison to surface dwelling relatives. The number of heterochronic shifts increases with an increasing fossorial lifestyle, therefore changes in the osteogenetic sequences correlate to the lifestyle in different lizard ecomorphs. The change from limbed locomotion to lateral undulation in fossorial lizard morphotypes is also observed in fossil and Recent eureptiles that secondarily adapted to aquatic environments, including the four pachypleurosaurids from Monte San Giorgio, but also the marine iguana (*Amblyrhynchus cristatus*) from the Galapagos Archipelago. The high abundance and unique preservation of pachypleurosaurids reveals detailed information on the osteogenesis in all four pachypleurosaurid species that all share features with both Recent terrestrial surface dwelling (e.g., scincid and iguanid lizards) and secondarily aquatic reptiles (e.g., turtles, crocodiles) by showing an increasing trend towards the “aquatic” condition with decreasing stratigraphical age.

In another part of the thesis, I examine the bone microstructure of the pachypleurosaurids from Monte San Giorgio in comparison with the data of the Recent amphibious marine iguana and with completely terrestrial iguanid relatives. Results reveal an intraspecific distribution of “terrestrial” and “aquatic” characters for the four pachypleurosaurids in relation to the data of Recent reptiles with terrestrial and aquatic modes of life. These histological inferences are based on variation in the bone deposition rate and remodelling processes that both lead to a variety of different bone matrices and vascularisation patterns that can be put into an evolutionary and developmental context reflecting two trends in habit preferences.

Key words: Limb Development, Eureptilia, Bone Histology, Osteogenesis, Modes of Life

Zusammenfassung

Die Morphologie (äussere Erscheinung) der Arme und Beine von Tetrapoden (vierbeinige Wirbeltiere) widerspiegelt die jeweilige Lebensart (z. B., terrestrisch, aquatisch). Die Lebensart beeinflusst aber nicht nur das äussere Aussehen der Extremitäten, sondern auch deren inneren knöchernen Aufbau (Knochenhistologie), sowie die Reihenfolge des Zeitpunktes wann ein Skelettelement verknöchert wird (Verknöcherungssequenz). Studien zeigen, dass Verknöcherungssequenzen von terrestrischen Eidechsen (Lepidosauria, Squamata) eher träge gegenüber Veränderungen sind, während andere vierbeinige Landtiere eine Vielzahl von Varianten zeigen. Auffällig ist, dass Reptilien mit einer ähnlichen Lebensweise oft ähnliche Tendenzen in den Verknöcherungssequenzen und der Knochenhistologie zeigen; dies meist unabhängig von ihrem Verwandtschaftsgrad. Eine logische Schlussfolgerung könnte daher sein, dass ähnliche Veränderungen in den Extremitäten der Reptilien bezüglich der Morphologie, der Verknöcherungssequenz, wie auch in der Knochenhistologie evolutionäre Marker für einen ähnlichen Lebensstil sind.

Da die Lebensweise in heutigen Reptilien meistens sehr gut bekannt ist, können wir Daten der Morphologie, Knochenhistologie und Verknöcherungssequenzen in den Kontext der Ökologie zu setzen. Diese Erkenntnisse erlauben in einem zweiten Schritt, Rückschlüsse auf die mögliche Lebensweise fossiler Verwandten zu ziehen, was Gegenstand meiner These ist. Ich kombiniere (A) erstmalig neugewonnene Daten aus der Morphologie, Knochenhistologie und den Verknöcherungssequenzen aus einem (B) grossen Datensatz von rezenten Reptilien mit unterschiedlichen Lebensarten. Anschliessend werden die Resultate mit (C) einzigartigem fossilen Material aus der Schweiz (Pachypleurosauria vom Monte San Giorgio) korreliert.

Im ersten Teil der These studiere ich die Verknöcherungssequenzen in heutigen, an Land lebenden, Eidechsen, welche fünfgliedrige Arme und Beine und keine Verlängerung der Wirbelsäule zeigen. Dieser ursprüngliche Eidechsentyp, der an der Erdoberfläche lebt, zeigt sehr wenig bis keine Variation in der Verknöcherungssequenz, die als ursprüngliches (plesiomorphes) Ossifikationsmodell der frühen terrestrischen Eureptilien, die unter anderem die Sauropterygier und Eidechsen umfassen, genommen wird. Die Resultate sind die Grundlage für eine weitere Verknöcherungssequenz-Studie über verwandte Eidechsen mit einer grabenden, d.h. vorwiegend im Bodengrund aufhaltenden Lebensweise. Der Vergleich der Daten zeigt, dass die grabende Lebensweise der Eidechsen direkt mit Änderungen in der Verknöcherungssequenz korreliert, die wiederum mit morphologischen Veränderungen, z. B., dem Verlust der Fingerglieder und der Verlängerung der Wirbelsäule einhergeht. Eidechsen mit einer grabenden Lebensweise bewegen sich ähnlich durch das Substrat, wie Reptilien, die sich sekundär an ein Leben im Wasser angepasst haben (z. B., der rezente Meeresleguan, *Amblyrhynchus cristatus*, von Galapagos und die fossilen Pachypleurosaurier von Monte San Giorgio). Die hervorragende Erhaltung der Pachypleurosaurier, die vor 241 Millionen Jahren in der Schweiz gelebt haben, erlaubt ausserdem eine umfassende und einzigartige Studie über die Verknöcherungssequenzen aller vier Arten. Die Resultate zeigen, dass die vier Pachypleurosaurier ähnliche Muster in den Verknöcherungssequenzen rezenter Reptilien mit einer aquatischen, bzw. grabenden Lebensweise haben.

Der zweite Teil der These behandelt Veränderungen in der Knochenhistologe von Eureptilien mit unterschiedlichen Lebensweisen. Die Meeresleguane von Galapagos sowie ihre terrestrischen Verwandten (andere Leguanartige) dienen als rezentes Vergleichsmaterial zu den fossilen Pachypleurosauriern. Meeresleguane zeigen eine sehr dichte und dicke Knochenmanschette in ihren Armen und Beine, welche mit grosser Wahrscheinlichkeit dem Auftrieb der Lunge während ihren Tauchgängen ausgleichend entgegen wirken soll. Terrestrisch lebende Verwandte hingegen zeigen den typischen Knochenaufbau anderer terrestrischer Reptilien mit einer eher dünnen, aber stabilen Knochenmanschette. Die Knochenhistologie der Meeresleguane ähnelt in groben Zügen

derjenigen der Pachypleurosaurier, welche denselben Knochentyp zeigen. Leichte Unterschiede in der Vaskularisierung und in der Organisation der Kollagenfasern desselben Knochentyps der vier Pachypleurosaurier korrelieren zu früheren morphologischen Studien und erhärten den Hinweis auf zwei unterschiedliche Lebensweisen innerhalb dieser vier Arten.

Schlüsselwörter: Entwicklung der Arme und Beine, Eureptilien, Knochenhistologie, Verknöcherung, Lebensweise

Chapter 1:

Introduction

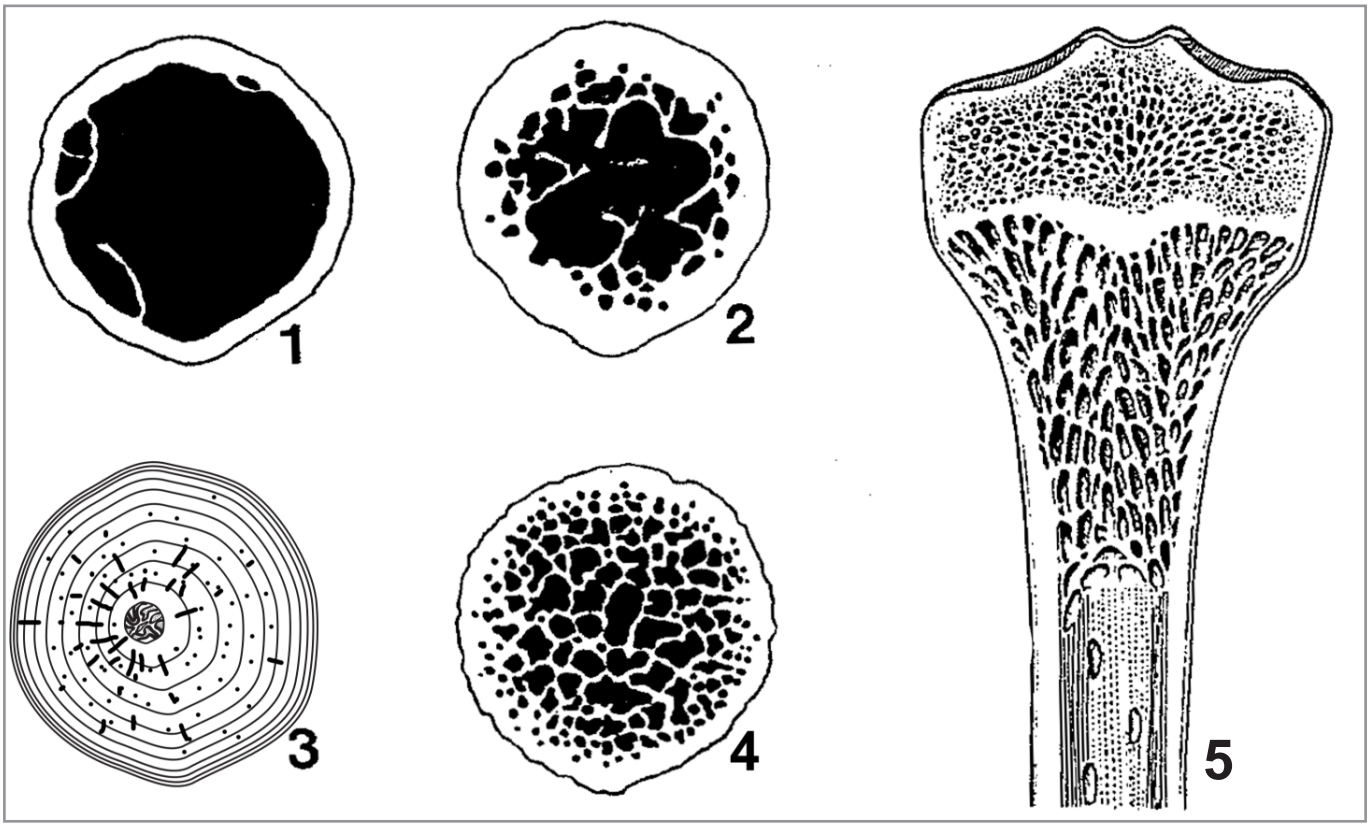

1: Flying vertebrate
2: land dwelling vertebrate
3: secondary aquatic vertebrate, bottom dweller
4: secondary aquatic vertebrate, fast swimmer, open sea
5: Longitudinal section of a long bone

After Francillon-Vieillot 1990, modified

Why using limbs as study system?

The modular nature and high diversity of tetrapod limbs, influenced by evolution and development, makes them an excellent study object for the morphological, histological and genetic basis (e.g., Shubin et al., 1997; Arthur et al., 1999; Bell et al., 2003; Carroll et al., 2005; Tanaka and Tickle, 2007; Richardson et al., 2009). Major topics in limb evolution address questions such as (modified from Hall 2007 in "On the nature of limbs by Owen, 1849"): 1) how secondarily aquatic tetrapods modify their limbs? And 2) What are the mechanisms which underlie digit or limb loss, notably in reptiles? Answers to these questions have been achieved through the examination of transformation series of different morphotypes in adult ontogenetic stages (Greer et al., 1998; Wiens and Slinghoff, 2001; Wiens et al., 2006), by documenting molecular cascades during the early skeletogenesis (Shapiro, 2002; Bell et al., 2003; Tanaka and Tickle, 2007), and by assessing the order in the chondrification and osteogenetic sequences in cleared and double-stained embryological series (e.g., Dingerkus and Uhler, 1977; Rieppel, 1993 a, b; Nye et al., 2003; Shapiro et al., 2003; Werneburg et al., 2009). This last method visualises one of the important early stages in the development of limbs that comprise processes of mesenchymal condensation and chondrification. Condensation and chondrification follows a conservative and general pattern in tetrapods involving branching and segmentation events (e.g., Shubin and Alberch, 1986; Oster et al., 1988).

Early development of limbs

Skeletal development generally comprises a cascade of events that involve different cellular processes (i.e., migration, adhesion, proliferation, growth, apoptosis) which are subject to different genetic controls (Hall, 2005). During condensation, dispersed cell populations gather together to differentiate into one single type of tissue such as for example a cartilaginous matrix as the basis for the development of endoskeletal bone, or to differentiate into bone directly for the development of dermal bone. Endoskeletal bone development includes chondrification and subsequent ossification which includes resorption and replacement of previously hypertrophied chondrocytes by osteoblasts. Collagenous fibrils are assembled into fibres or fibre bundles, whereas osteoblasts start to mineralise the matrix by precipitating osteoid, which is later mineralised into hydroxyl apatite, according to the spatial organisation of the fibrils or matrix. Dermal bones in contrast form in the dermis via intramembraneous or metaplastic ossification, without differentiation of transitory cartilages (modified from Francillon-Vieillot et al., 1990; Hall, 2005).

Two pathways of limb development in tetrapods

Condensation and chondrification processes follow two conserved pathways during the development of the limbs in tetrapods that distinguish urodeles from amniotes and anurans (Fig. 1 from Fröbisch, 2008). Three basic processes of condensation and subsequent chondrification are responsible for the patterning of the tetrapod limb. The first step is the formation of the stylopodium as a de novo condensation (e.g., Shubin and Alberch, 1986; Blanco and Alberch, 1992; Fabrezi et al., 2007). In amniotes and anurans, the zeugopodial elements follow by bifurcation with the postaxial ulna/fibula leading before the preaxial radius/tibia. Both zeugopodial condensations give rise

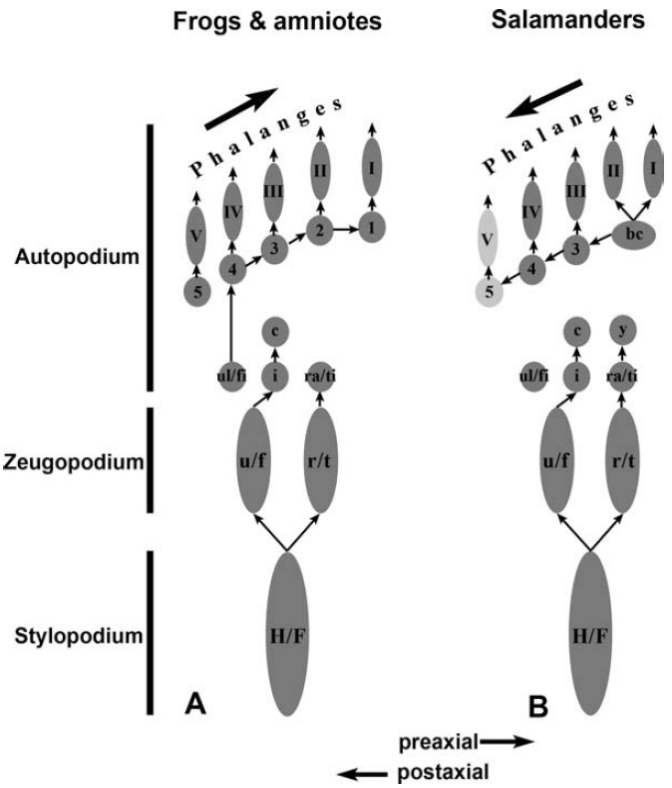

Fig. 1. Sketch of the two pathways of condensation and chondrification patterns during early skeletal development of the tetrapods (from Fröbisch, 2008). **A**. Postaxial dominance in the autopodial region of anurans and amniotes, **B**. Preaxial dominance in the autopodial region of urodeles. Abbreviations: bc, basale commune; c, centrale; H/F, humerus/femur; i, intermedium; r/t radius/tibia; ra/ti, radiale/fibulare; u/f, ulna/fibula; ul/fi, ulnare/fibulare; y, element y.

to mesopodial elements by another bifurcation event, which again establish more mesopodials through segmentation or bifurcation. The postaxial mesopodial elements, i. e., the ulnare and fibulare, initiate the formation of the digital arch starting with the segmentation of distal carpal/tarsal-4. Bifurcations of distal carpal/tarsal-4 produce distal carpal/tarsal-3 and metacarpal/tarsal-4. The mesopodial elements form the phalangeal elements in a distinct postaxial order (digit IV > V, III > II > I) through segmentation (e.g., Shubin and Alberch, 1986; Oster et al., 1988).

Contrary to amniotes and anurans, urodeles show a strict preaxial dominance in the bifurcation process of the zeugopodial region with the preaxial radius/tibia leading before the postaxial ulna/fibula. The preaxial dominance is also reflected in the mesopodial formation, as well as in the establishment of the phalanges. Hence, the digital arch displays a preaxial order forming in the sequence of II > I > III > IV > (V) (e.g., Schmalhausen, 1910; Shubin and Wake, 2003; Fröbisch, 2008). In contrast to the pattern in amniotes and anurans, four variations are found within the general salamander condensation patterns, each in a different salamander family (e.g., Shubin and Alberch, 1986; Vorobyeva and Hinchliffe, 1996; Franssen et al., 2005).

The subsequent ossification processes are less conserved in amniotes, anurans and urodeles, hence revealing more interspecific and in some cases intraspecific variability (e.g., Blanco and Alberch, 1992; Cohn et al., 2002; Shubin and Wake, 2003; Fröbisch, 2008). The relative position in the osteogenetic order, thus the relative timing of a skeletal element to begin and end ossification, has a functional role. Skeletal elements which ossify late during the ontogeny tend to be more likely reduced or lost in the evolution of limbs (e.g., Greer, 1987; Hall, 2007; Shapiro et al., 2007). The vast differences in the order of ossification reveal phylogenetic relationships but also convergent features as a result of similar changes in the life modes and functional requirements (e.g., Rieppel, 1993a, b, 1994; Caldwell 2002; Storrs, 2003; Shapiro et al., 2003; Sheil and Greenbaum, 2005; Werneburg et al., 2009). Those changes not only influence the order of the timing when elements start ossification, but also the morphology, as well as the microstructure of the bone (e.g., Buffrénil and Mazin, 1989; Castanet et al., 1993; Ricqlès and Buffrénil, 2001). The changes in the

microstructure of the limb bones are as manifold as the variety of different limb morphotypes. Data inferred from the microstructure of bones shed light on the modes of life, i.e. the bone growth, physiology, habitat (for example whether terrestrial or aquatic) and demography based on skeletochronology (e.g., Francillon-Vieillot et al., 1990; Sander, 1990; Castanet and Baez, 1991; Buffrénil and Castanet, 2000; Chinsamy-Turan, 2005; Klein et al., 2009).

The bone microstructure in tetrapods

Bones are flexible structures that are shaped in a multitude of interwoven processes during the entire ontogeny influenced by internal and external factors (Castanet et al., 1993; Castanet, 2006). The modifications in the microstructure of tetrapods which returned to an aquatic life reveal both phylogenetic affiliation, as well as convergent trends in ecology, functional requirements and/or physiology (e.g., Ricqlès and Buffrénil, 2001). The long bones of terrestrial tetrapods often show a medullary cavity surrounded by a rather thin cortex which leads to light, but robust bones. During the ontogeny of the “terrestrial type” endoskeletal bones, the perichondrium and endochondrium stop producing cartilage and osteoblast activity starts, released by the periosteum and endosteum, for subsequent periosteal and endosteal ossification. The periosteum is located at the outer surface of the bone and is characterised by a centrifugal mode of bone deposition, whereas the endosteum is placed on the inner surface of the medullary cavity of the bone showing centripetal bone deposition (Hall, 2005). Hence, the majority of cartilage does not persist during the ontogeny of terrestrial tetrapods and the bone is under constant remodelling by outer, centrifugal bone accretion and internal resorption along the inner bone surface (Francillon-Vieillot et al., 1990). As a result, a medullary cavity is built in the diaphyseal and metaphyseal region of the long bones. Secondarily aquatic tetrapods, in contrast, reveal two trends. Some lineages of aquatic tetrapods markedly reduced the overall mass of their skeleton in comparison to close terrestrial relatives (e.g., Buffrénil et al., 1986; Robineau and Buffrénil, 1993; Ricqlès and Buffrenil, 2001; Fig. 2), whereas others increase

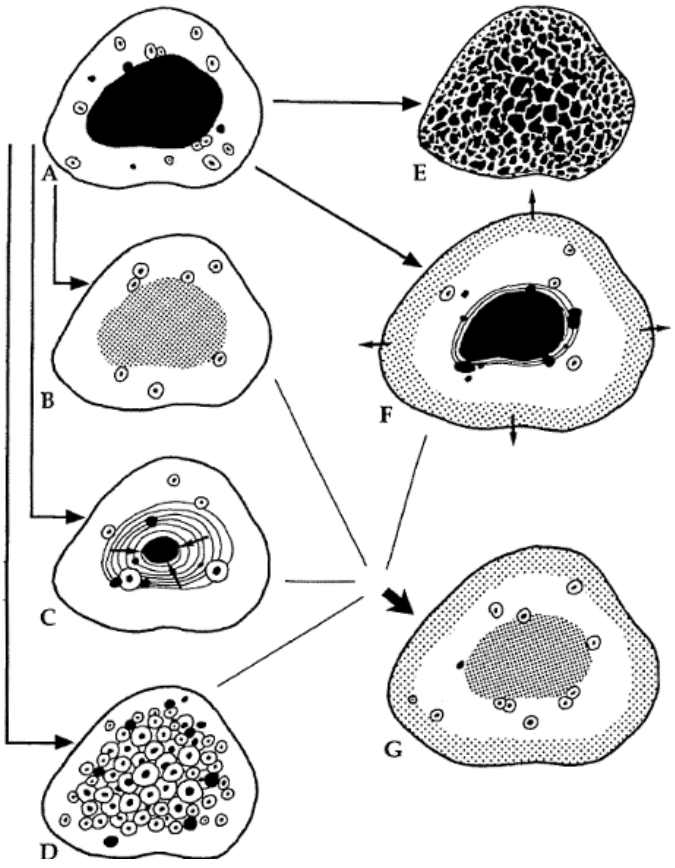

Fig. 2. Sketch of the different trends in the specialisations of the bone structure in aquatic tetrapods (from Ricqlès and Buffrénil, 2001). A, Plesiomorphic tubular organisation of long bones in terrestrial tetrapods. **B,** Osteosclerotic state by inhibition of chondroclastic and, pro parte, osteoclastic activities. **C**, Osteosclerotic state by endosteal filling of bone cavities, including the marrow cavity. **D**, Osteosclerotic state related to Haversian remodelling. **E**, Osteoporotic-like state in quick swimming forms in often open sea environments. **F**, Pachyostosis by hyperplasy of the periosteal cortex. **G,** Pachyosteosclerosis combining pachyostosis with one of the various types of osteosclerosis.

the skeletal mass in different ways (e.g., Buffrénil et al., 1990; Domning and Buffrénil, 1991; Ricqlès and Buffrenil, 2001; Fig. 2). The decrease in the skeletal mass is a common trend in quick swimming forms, hence among anurans, marine turtles, marine mesosuchian crocodilians, ichthyosaurs, adult plesiosaurs and pliosaurs, adult mosasaurs, and modern cetaceans (e.g., Leclair et al., 1993; Rhodin et al., 1981; Buffetaut, 1979; Buffrénil and Mazin, 1990; Wiffen et al., 1995; Sheldon, 1997; Felts and Spurrell, 1965). All of these aquatic tetrapods show a lessening of the thickness of compact cortical bone by remodelling which results in cancellous bone and/or an expansion of the medullary cavity. In contrast, slow, demersal swimmers often show an increase of bone compactness (e.g., Buffrénil and Schoevaert 1988; Buffrénil and Mazin 1989). The increase in skeletal mass is achieved either by 1) absence or a poor development of the marrow cavity, or 2) hyperplasy of the cortex, 3) incomplete resorption of calcified cartilage in the medullary region which are densely invaded by globuli ossei in some cases, 4) a complete resorption of the endochrondral cartilaginous matrix with a later exceptionally dense deposition of endosteal bone in the marrow cavity. Number 1 to 2 are defined as pachyostosis, whereas number 3 to 4 are defined as osteosclerosis (after Ricqlès and Buffrénil, 2001). A combination of both conditions is called pachyosteosclerosis and has been described among aquatic fossil reptiles such as Permian mesosaurs and Triassic pachypleurosaurids (e.g., Nopcsa and Heidsieck, 1934; Zangerl, 1935; Ricqlès, 1975), which mainly involves number 1 to 3 and partly number 4.

Eureptiles as study objects and what about osteogenesis in this group?

Reptilia comprises parareptiles and eureptiles (after Laurin and Reisz, 1995). Eureptilia includes Diapsida and its fossil relatives (Captorhinidae, Araeoscelidia and *Paleothyris*), whereas parareptiles include Testudines, Procolophonidae, Pareiasauria and Millerettidae (after Laurin and Reisz, 1995). I follow the traditional ideas for reptile interrelationships by excluding Testudines from the Diapsida being aware of the fact that their phylogeny is still debated (e.g., Tsuji and Müller, 2009; Lyson et al., 2010). I use the term reptile for data that refers to the entire group of Reptilia (Parareptilia and Eureptilia). The use of the term eureptile refers to data based on own results of sauropterygians and lizards and their hypothesised ancestor (see below; Chapter 4).

The 18,000 living eureptilian species (inclusive birds; sensu Modesto and Anderson, 2004) are only a tiny fraction of their total diversity that first originated at least 305 million years before present (Reisz and Müller, 2004; Pough et al., 2008). Aquatic eureptiles were especially species-rich during the Middle Triassic to the Late Cretaceous which is also reflected by their manifold number of bone formation pathways. Although the worldwide distribution is reflected in a large variety of different lifestyles, the terrestrial surface dwelling mode of life is regarded as the plesiomophic condition, thus being thought to be responsible for their successful radiation during the Mesozoic and Cenozoic era (Romer, 1956).

The plesiomorphic ancestral eureptile shares the same limb morphology (Romer, 1956), except for the number of mesopodial or sesamoid bones with Recent terrestrial

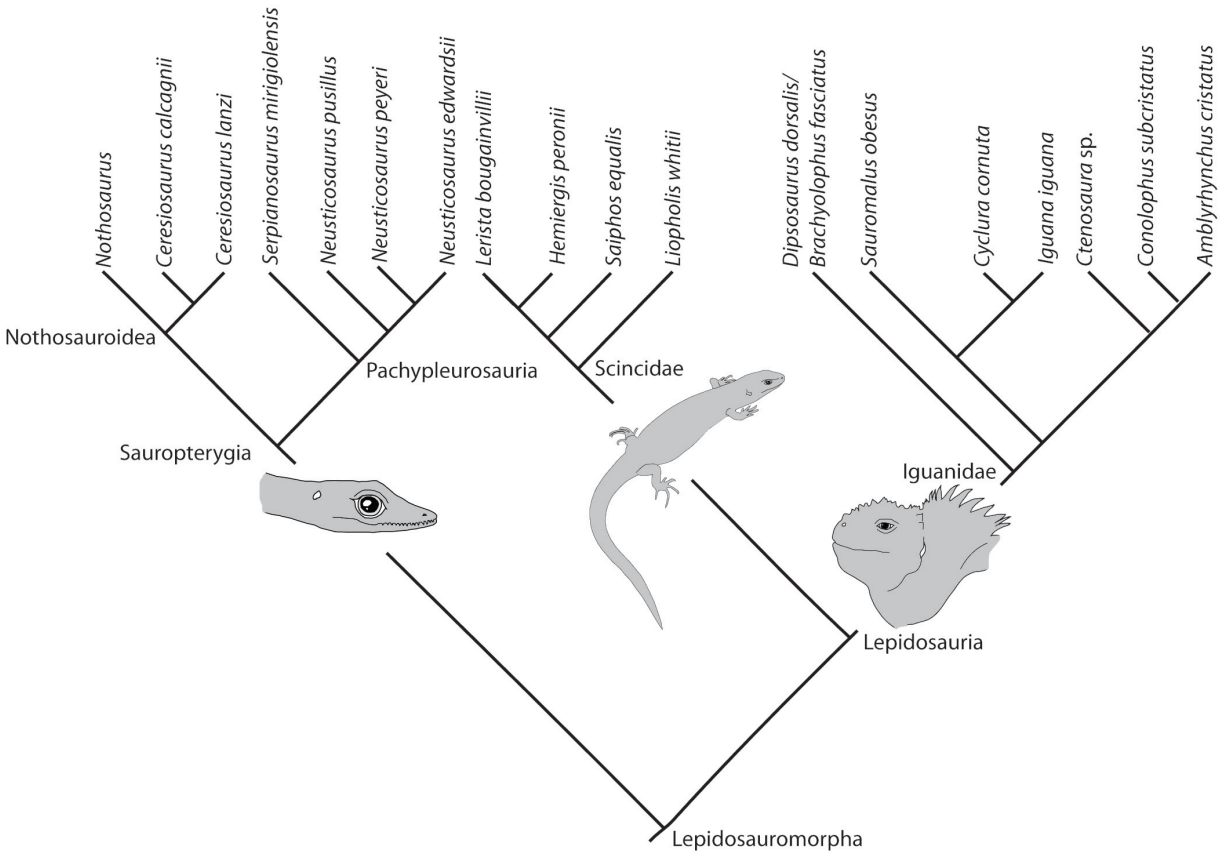

Fig. 3. The phylogeny of the studied eureptilian Lepidosauromorpha (Reeder, 2002; Wiens and Hollingsworth, 2002; Sander, 1989; Rieppel, 2000).

surface dwelling lepidosaurs with non-reduced limbs (e.g., Agamidae: Mathur and Goel, 1976; Lacertidae: Rieppel, 1992, Gekkonidae: 1994; Scincidae: Mohammed et al., 1995; Iguanidae: Lobo et al., 1995) and is hypothesised to 1) have had the same terrestrial mode of life (e.g., Canoville and Laurin, 2010), as well as the same conserved osteogenetic sequences in its limbs (Rieppel, 1992; Caldwell, 1994; Fröbisch, 2008; Hugi et al., 2010: basic study for this thesis). The fact that Recent terrestrial surface dwelling lepidosaurs with non-reduced limbs recapitulate the order of the condensation and chondrogenesis pathway in their osteogenetic sequences (exception: mesopodial region and fifth digit) might be further evidence for a plesiomorphic ancestral condition for at least the eureptiles.

Reptiles with an aquatic lifestyle often show modifications in their limb morphotype, in their osteogenetic sequences and in their bone histology compared to related terrestrial forms. In many cases, their limbs are reduced in total length and/or in the phalangeal formula (e.g., Sander, 1989; Carroll and Gaskill, 1985; Greer et al., 1998; Wiens and Slinghoff, 2001; Wiens et al., 2006). Changes in the mode of life accompany modifications in the microstructure of the bones (e.g., Buffrénil and Schoevaert, 1988; de Ricqlès, 1974a, b; Caldwell, 1997; O'Connor, 2004). Reptiles with aquatic or semi-aquatic modes of life either show an increased bone deposition rate that results in the predominant presence of highly

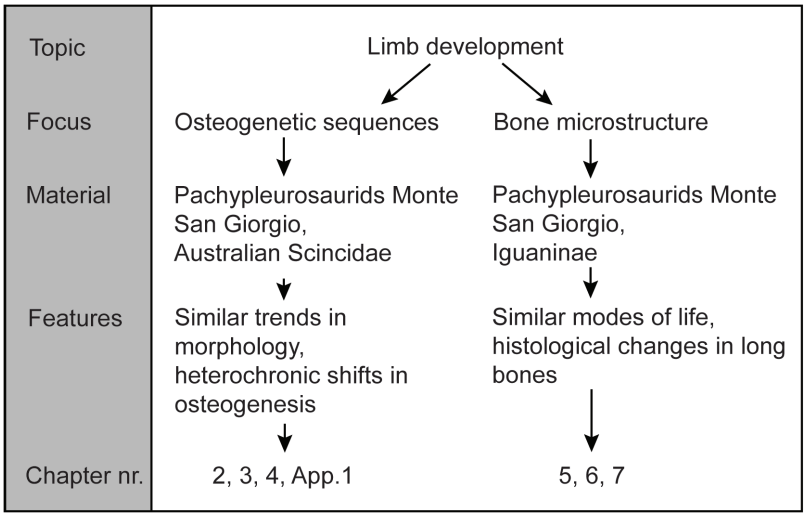

Fig. 4. Scheme showing the limb development as the main topic of the PhD project with two main focuses. The two focuses lie on the bone microstructure and the osteogenetic sequences during the development of the limbs in two different eureptilian groups, the sauropterygians and squamates.

vascularised fibrolamellar bone (e.g., Wiffen et al., 1995; Sheldon, 1997; Kolb et al., 2011) or display slowly deposited avascular lamellar-zonal bone (Chapter 4 to 7; Buffrénil and Rage, 1993; Buffrénil et al., 2008; Woodward and Horner, 2010). Sauropterygians are one group of fossil eureptiles that show both histological types as adaptation to a marine mode of life. They have been preserved in large quantity and high quality (Zangerl, 1935; Sander, 1990; Wiffen et al., 1995; Caldwell, 1997; Rieppel, 2000). The Sauropterygia are regarded as the extinct sister group of the Lepidosauria, which comprises the Rhynchocephalia and the Squamata (e.g., Benton, 1993; Lee et al., 2008). The Sauropterygia combine the Placodontia and the Eosauropterygia including the Pachypleurosauria, Nothosauroidea, and Pistosauroidea (after Rieppel, 2000). The close phylogenetic relationship of the Lepidosauromorpha that include the fossil Sauropterygia and the Recent Lepidosauria (Fig. 3) is supported by several morphological peculiarities such as shared cranial structures (Müller, 2004; Hill 2005), the occurrence of similar transformation events based on changes in the number of the presacral vertebrae (Müller, 2003) and in the phalangeal count (Fig. 4; Carroll and Gaskill, 1985; Greer, 1987, 1990; Sander, 1989; Wiens, 2009). Some fossil findings preserve data on the ossification in fossil lepidosauromorphs and reveal a similar order as in Recent terrestrial lepidosaurian relatives (Caldwell, 1994, 1997).

Pachypleurosaurids from Monte San Giorgio

The pachypleurosaurids are small marine sauropterygians that lived during the Middle Triassic in Europe, North America and China (Rieppel, 2000) with excellent fossil sites at the Monte San Giorgio UNESCO World Heritage Site along the Swiss and Italian border (Carroll and Gaskill, 1985; Sander, 1989; Furrer, 1995; Röhl et al., 2001). The pachypleurosaurids are morphologically similar to Recent terrestrial surface dwelling lizards, but also reveal similar bone histological data, i.e., the exclusive presence of lamellar-zonal bone in the cortex (e.g., Fig. 4; Ricqlès, 1976; Patnaik et al., 1981; Zug and Rand, 1987; Sander, 1990; Buffrénil and Francillon-Vieillot, 2001; Klein, 2010).

Aims and overview

The main goal of this thesis is to explore if osteogenesis, including the order in the ossification sequences and the bone microstructure, reflects not only phylogeny but also convergences as a result of similar modes of life in both fossil and Recent eureptilian taxa. Data comprise extant aquatic and terrestrial surface dwelling and subsurface dwelling lacertilian squamates and extinct aquatic sauropterygians with similar morphological trends (Figs. 3 and 4; Chapter 2 to 7). The aspects of this project reside in the (A) unique material which is based on fossil and Recent material to study the evolution of eureptilian development, the (B) correlation of osteogenetic sequences and bone microstructure, the (C) integration of neontological and paleontological data of different limb morphotypes, osteogenetic sequences and bone histology.

Chapter 2 is the basic study for all other chapters of this thesis. I document the first comprehensive survey of the ossification sequences in Recent surface dwelling lacertilian squamates with well developed limbs. The conserved ossification sequences in lacertilian squamates with terrestrial surface dwelling modes of life are hypothesised to be the plesiomorphic ancestral model for terrestrial surface dwelling eureptilians. In a second step, I correlate these findings to closely related subsurface dwelling lizard species with an increasing degree of limb reduction (Chapter 3). The detected heterochronic shifts in the ossification sequences of subsurface dwelling lizard species compared to surface dwelling species with non-reduced limbs are similar to the osteogenetic data of the fossil pachypleurosaurids which are the study focus in Chapter 4. Chapter 5 to 7 considers the microstructural changes in the long bones during the ontogeny of eureptiles with terrestrial and aquatic modes of life in comparison to reptiles in general. I present the first comprehensive sampling of Recent iguanine lizards including the land iguana, *Conolophus subcristatus*, and the marine iguana, *Amblyrhynchus cristatus*, from the Galapagos Archipelago, as well as give detailed information on the bone histology of them in comparison to all four pachypleurosaurids and two *Ceresiosaurus* spp. (Nothosauroidea) from Monte San Giorgio.

Appendix 1 represents one co-authored publication on the ossification sequences of pleurodire and cryptodire turtles with different lifestyles, that is used as complementary study for further data comparison within the Reptilia (following the nomenclature of Laurin and Reisz, 1995).

Literature Cited

Arthur, W., Jowett, T., Panchen, A. 1999. Segments, limbs, homology, and co-option. *Evolution and Development* 1(2): 74-76.

Benton, M. J. 1993. Reptilia. In: The Fossil Record 2, M. J. Benton (Ed.), Chapman & Hall, London, pp. 681-715.

Bell, S. M., Schreiner, C. M., Waclaw, R. R., Campbell, K., Potter, S. S., Scott, W. J. 2003. Sp8 is crucial for limb outgrowth and neuropore closure. *PNAS* 100(21): 12195-12200.

Blanco, M. J., Alberch, P. 1992. Caenogenesis, developmental variability, and evolution in the carpus and tarsus of the marbled newt *Triturus marmoratus*. *Evolution* 46: 677-687.

Buffetaut, E. 1979. A propos d'un crâne

de *Metriorhynchus* (Crocodylia, Mesosuchia) de Bavent (Calvados) l'allègement des os crâniens chez les Metriorhynchidae et a sa signification. *Bulletin de la Société Géologique de Normandie* 66: 77-83.

Buffrénil, V. de, Syre, J.-Y., Schoevaert, D. 1986. Comparaison de la structure et du volume squelettiques entre un delphinidé (*Delphinus delphis* L.) et un mammifére terrestre (*Panthera leo* L.). *Canadian Journal of Zoology* 64: 1750-1756.

Buffrenil, V. de, Schoevaert, D. 1988. On how the periosteal bone of the delphinid humerus becomes cancellous: ontogeny of a histological specialization. *Journal of Morphology* 198: 149-164.

Buffrénil, V. de, Mazin, J.-M. 1989. Bone histology of *Claudiosaurus germaini* (Reptilia, Claudiosauridae) and the problem of pachyostosis in aquatic tetrapods. *Historical Biology* 2: 311-322.

Buffrenil, V. de, Mazin, J.-M. 1990. Bone histology of the ichthyosaurs: comparative data and functional interpretation. *Paleobiology* 16(4): 435-447.

Buffrénil, V. de, Rage, J.-C. 1993. La pachyostose vertébrale de *Simoliophis* (Reptilia, Squamata) donne comparative set considérations fonctionnelle. *Annales de Paléontologie* (Vert.-Invert.) Paris 79(4): 315-335.

Buffrénil, V. de, Castanet, J. 2000. Age estimation by skeletochronology in the Nile monitor (*Varanus niloticus*), a highly exploited species. *Journal of Herpetology* 34(3): 414-424.

Buffrénil, V. de, Francillon-Vieillot, H. 2001. Ontogenetic changes in bone compactness in male and female nile monitors (*Varanus niloticus*). *Journal of Zoology* 254: 539-546.

Buffrénil, V. de, Bardet, N., Pereda-Suberbiola, X., Bouya, B. 2008. Specialization of bone structure in *Pachyvaranus crassispondylus* Arambourg, 1952, an aquatic squamate from the Late Cretaceous of the southern Tethyan margin. *Lethaia* 41: 59-69.

Canoville, A., Laurin, M. 2010. Evolution of humeral microanatomy and lifestyle in amniotes, and some comments on palaeobiological inferences. *Biological Journal of the Linnean Society* 100: 384-406.

Caldwell, M. W. 1994. Developmental constraints and limb evolution in Permian and extant lepidosauromorph diapsids. *Journal of Vertebrate Paleontology* 14: 459-471.

Caldwell, M. W. 1997. Limb osteology and ossification patterns in *Cryptoclidus* (Reptilia: Plesiosauria) with a review of sauropterygian limbs. *Journal of Vertebrate Paleontology* 17: 295-307.

Caldwell, M. W. 2002. From limbs to fins: Limb evolution on fossil marine reptiles. *American Journal of Medical Genetics* 112: 236-249.

Carroll, R., Gaskill, P. 1985. The nothosaur *Pachypleurosaurus* and the origin of plesiosaurs. *Philosophical Transactions of the Royal Society of London, Biological Science* 309(1139): 343-393.

Carroll, S. B., Grenier, J. K., Weatherbee, S. D. 2005. From DNA to Diversity – Molecular Genetics and the Evolution of Animal Design, Second Edition. Blackwell Publishing, Malden, MA.

Castanet, J. 2006. Time recording in bone microstructures of endothermic animals;

functional relationships. *Comptes Rendus Palevol* 5: 629-636.

Castanet, J., Francillon-Vieillot, H., Meunier, F. J., Ricqlès, A. de. 1993. In: Bone and Individual Aging, B. K. Hall (Ed.), Bone, Vol. 7. Bone Growth-B. CRC Press, Boca Raton, Florida, pp. 245-283.

Castanet, J., Baez, M. 1991. Adaptation and evolution in *Gallotia* lizards from the Canary Islands: age, growth, maturity and longevity. *Amphibia-Reptilia* 12: 81-102.

Chinsamy-Turan, A. 2005. The Microstucture of Dinosaur bone, deciphering Biology with Fine-Scale Techniques. The Johns Hopkins University Press, Baltimore and London, 188 p.

Cohn, M. J., Lovejoy, C. O., Wolpert, L., Coates, M. I. 2002. Branching, segmentation and the metapterygial axis: pattern versus process in the vertebrate limb. *BioEssays* 24: 460-465.

Dingerkus, G., Uhler, L. D. 1977. Enzyme clearing of Alcian Blue stained whole small vertebrates for demonstration of cartilage. *Stain Technology* 52: 229-232.

Domning, D., Buffrénil, V. de. 1991. Hydrostasis in the Sirenia: quantitative data and functional interpretations. *Marine Mammal Science* 7: 331-368.

Fabrezi, M., Abdala, V., Oliver, M. I. M. 2007. Developmental basis of limb homology in lizards. *The Anatomical Record* 290: 900-912.

Felts, W. J. L., Spurrell, F. A. 1965. Structural orientation and density in cetacean humeri. *American Journal of Anatomy* 116: 171-203.

Francillon-Vieillot, H., Buffrénil, V. de, Castanet, J., Géraudie, J., Meunier, F. J., Sire, J. Y., Zylberberg, L., Ricqlès, A. de. Microstructure and mineralization of vertebrate skeletal tissues. 1990. Chapter 20. In: Skeletal Biomineralization: Patterns, Processes and Evolutionary Trends, J.G. Carter (Ed.), Volume I., Van Nostrand Reinhold, New York, pp. 471-530.

Franssen, R. A., Marks, S., Wake, D., Shubin, N. 2005. Limb chondrogenesis of the seepage salamander, *Desmognathus aeneus* (Amphibia: Plethodontidae). *Journal of Morphology* 265: 87-101.

Fröbisch, N. B. 2008. Ossification patterns in the tetrapod limb – conservation and divergence from morphogenetic events. *Biological Reviews* 83: 571-600.

Furrer, H. 1995. The Kalkschieferzone (Upper Meride Limestone) near Meride (Canton Ticino, Southern Switzerland) and the evolution of a Middle Triassic intraplatform basin. *Eclogae Geologicae Helvetiae* 88(3): 827-852.

Greer, A. 1987. Limb reduction in the lizard genus *Lerista*. 1. Variation in the number of phalanges and presacral vertebrae. *Journal of Herpetology* 21: 267-276.

Greer, A., Caputo, V., Lanza, B., Palmieri, R. 1998. Observations on limb reduction in the scincid lizard genus *Chalcides*. *Journal of Herpetology* 32: 244-252.

Greer, A. 1990. Limb reduction in the scincid lizard genus *Lerista*. 2. Variation in the bone complements of the front and rear limbs and the number of postsacral vertebrae. *Journal of Herpetology* 24: 142-150.

Hall, B. K. 2005. Bones and Cartilage: Developmental and Evolutionary

Skeletal Biology. Elsevier Academic Press Amsterdam, 760 p.

Hall, B. K. 2007. Owen: on the nature of limbs, a discourse. R. Amundson (Ed.), Introductory essays by R. Amundson, K. Padian, M. P. Winsor, J. Coggon. The University of Chicago Press, Chicago and London, 126pp.

Hill, R. V. 2005. Integration of morphological data sets for phylogenetic analysis of Amniota: the importance of integumentary characters and increased taxonomic sampling. *Systematic Biology* 54(4): 530-547.

Klein, N. 2010. Long bone histology of Sauropterygia from the Lower Muschelkalk of the Germanic Basin provides unexpected implications for phylogeny. *PLoS ONE* 5(7): e11613. doi:10.1371/journal.pone.0011613

Klein, N., Scheyer, T., Tütken, T. 2009. Skeletochronology and isotopic analysis of a captive individual of *Alligator mississippiensis* Daudin, 1802. *Fossil Record* 12(2): 121-131.

Kolb, C., Sánchez-Villagra, M. R., Scheyer, T. M. 2011. The palaeohistology of the basal ichthyosaur *Mixosaurus* Baur, 1887 (Ichthyopterygia, Mixosauridae) from the Middle Triassic: palaeobiological implications. *Comptes Rendues Palevol* [doi:10.1016/j.crpv.2010.10.008].

Laurin, M., Reisz, R. R. 1995. A reevaluation of early amniote phylogeny. *Zoological Journal of the Linnean Society* 113: 165-223.

Leclair, R. C., Lamontagne, C., Aubin, A. 1993. Allométrie de la masse du squelette chez les amphibiens anoures. *Canadian Journal of Zoology* 71: 352-357.

Lee, M. S. Y., Reeder, T. W., Slowinski, J. B., Lawson, R. 2008. Resolving reptile relationships: molecular and morphological markers. In: Assembling the Tree of Life, J. Cracraft and M. J. Donoghue (Eds.), Oxford University Press, New York, pp. 451-467.

Lobo, F., Abdala, F., Scrocci, F. 1995. Desarollo del esqueleto de *Liolaemus scapularis* (Iguanidae: Tropuridae). *Bollettino del Museo Regionale di Scienze Naturali*, *Torino* 13 (1): 77-104.

Lyson, T. R., Bever, G. S., Bhullar, B.-A. S., Joyce, W. G., Gauthier, J. A. 2010. Transitional fossils and the origin of turtles. *Biology Letters* 6: 830-833.

Mathur, J. K., Goel, S. C. 1976. Patterns of chondrogenesis and calcification in the developing limb of the lizards *Calotes versicolor*. *Journal of Morphology* 149: 401-420.

Modesto, S. P., Anderson, J. S. 2004. The phylogenetic definition of Reptilia. *Systematic Biology* 53: 815- 821.

Mohammed, M. B. H., Khalife, S. A., El-Sayad, F. I., Ibrahim, S. A. 1995. Comparative analysis of ossification in the appendicular skeleton in some scincid lizards (Scincidae: Reptilia). *Journal of Egyptian German Society of Zoology* 17 (B): 93-119.

Müller, J. 2003. Early loss and multiple return of the lower temporal arcade in diapsid reptiles. *Naturwissenschaften* 90: 473-476.

Müller, J. 2004. The relationships among diapsid reptiles and the influence of taxon selection. In: Recent Advances in the Origin and Early Radiation of Vertebrates, G. Arratia, M. V. H. Wilson

and R. Cloutier (Eds.), pp. 379-408, Verlag Dr. Friedrich Pfeil, München.

Nopcsa, F., Heidsieck, E. 1934. Über eine pachyostotische Rippe aus der Kreide Rügens. *Acta Zoologica* 15: 431-455.

Nye, H. L. D., Cameron, J. A., Chernoff, E. A. G., Stocum, D. L. 2003. Extending the table of stages of normal development in the axolotl: Limb development. *Developmental Dynamics* 226: 555-560.

O'Connor, P. M. 2004. Pulmonary pneumaticity in the postcranial skeleton of extant aves: a case study examining Anseriformes. *Journal of Morphology* 261: 141-161.

Oster, G. F., Shubin, N. H., Murray, J. D., Alberch, P. 1988. Evolution and morphogenetic rules: the shape of the vertebrate limb in ontogeny and phylogeny. *Evolution* 42: 862-884.

Patnaik, B. K., Behera, H. N. 1981. Age determination in the tropical agamid garden lizard, *Calotes versicolor* Daudin, based on bone histology. *Experimental Gerontology* 16: 295-307.

Pough, F., Janis, C. M., Heiser, J. B. 2008. Vertebrate Life. Harvey Pugh, 8th edition, Upper Saddle River, N.J. Prentice Hall.

Reeder, T. W. 2002. A phylogeny of the Australian Sphenomorphus group (Scincidae: Squamata) and the phylogenetic placement of the crocodile skinks (*Tribolonotus*): Bayesian approaches to assessing congruence and obtaining confidence in maximum likelihood inferred relationships. *Molecular Phylogenetics and Evolution* 27: 384-397.

Reisz, R. R., Müller, J. 2004. The comparative method for evaluating fossil calibration dates: a reply to Hedges and Kumar. *Trends in Genetics* 20 (12): 596-597.

Rhodin, A. G. J., Ogden, J. A., Conlogue, G. J. 1981. Chondro-osseous morphology of *Dermochelys coriacea*, a marine reptile with mammalian skeletal features. *Nature* 290: 244-246.

Richardson, M. K., Gobes, S. M., van Leeuwen, A. C., Polman, J. A., Pieau, C., Sánchez-Villagra, M. R. 2009. Heterochrony in limb evolution: developmental mechanisms and natural selection. *Journal of Experimental Zoology B Molecular Development Evolution* 312B: 639-664.

Ricqlès, A. de. 1974a. Recherches paléohistologiques sur les os long des tétrapodes. V. Cotylosaures et mésosaures *Annales de Paléontologie* 60: 1-39.

Ricqlès, A. de. 1974b. Recherches paléohistologiques sur les os long des tétrapodes.IV. Eothériodontes et pélycosaures. *Annales de Paléontologie* 60: 171-216.

Ricqlès, A. de. 1975. Recherches paléohistologiques sur les os longs des tétrapodes. VII. Sur la classification, la signification fonctionnelle et l'histoire des tissus osseux des tétrapodes. *Annales de Paléontologie* (Vertébrés) 61: 51-129.

Ricqlès, A. de. 1976. On bone histology of fossil and living reptiles, with comments on its functional and evolutionary significance, In: Morphology and Biology of Reptiles, A. de Bellairs and C. B. Cox (Eds.), Linnean Society Symposium, Series 3, Academic press, London, pp. 123-150.

Ricqlès, A. de, Buffrénil, V. de. 2001. Bone histology, heterochronies and the return of tetrapods to life in water: were are we? In: Secondary Adaptation of Tetrapods to Life in Water, J.-M. Mazin and V. de

Buffrénil (Eds.), pp. 289-310, Dr. Friedrich Pfeil, München, Germany.

Rieppel, O. 1992. Studies on skeleton formations in reptiles. III. Patterns of ossification in the skeleton of *Lacerta vivipara* Jacquin (Reptilia: Squamata) *Fieldiana*, *Zoology, N.S.* 68: 1-25.

Rieppel, O. 1993a. Studies on skeleton formation in reptiles - patterns of ossification in the skeleton of *Chelydra serpentina* (Reptilia, Testudines). *Journal of Zoology*, *London* 231: 487-509.

Rieppel, O. 1993b. Studies on skeleton formation in reptiles. V. Patterns of ossification in the skeleton of *Alligator mississipiensis* Daudin (Reptilia, Crocodylia). *Zoological Journal of the Linnean Society* 109: 301-325.

Rieppel, O. 1994. Studies on skeleton formation in reptiles. Patterns of ossification in the limb skeleton of *Gehyra oceanica* (Lesson) and *Lepidodactylus lugubris* (Duméril and Bibron). *Annales des Sciences Naturelles, Zoologie*, *Paris* 15: 83-91.

Rieppel, O. 2000. Sauropterygia I: Placodontia, Pachypleurosauria, Nothosauroidea, Pistosauroidea. In: Encyclopedia of Paleoherpetology, P. Wellnhofer (Ed.), Verlag Dr. Friedrich Pfeil, München, p. 334.

Robineau, D., Buffrénil, V. de. 1993. Nouvelles données sur la masse due squelette chez les grands cétacés (Mammalia, Cetacea). *Canadian Journal of Zoology* 71: 828-834.

Röhl, H.-J., Schmid-Röhl, A., Furrer, H., Frimmel, A., Oschmann, W., Schwark, L. 2001. Microfacies, geochemistry and palaeoecology of the Middle Triassic Grenzbitumenzone from Monte San Giorgio (Canton Ticino, Switzerland). *Geologia Insubrica* 6(1): 1-13.

Romer, S. 1956. Osteology of the Reptiles. The University of Chicago Press, Chicago & London, pp. 3-772.

Sander, P. M. 1989. The pachypleurosaurids (Reptilia: Nothosauria) from the Middle Triassic of Monte San Giorgio (Switzerland) with the description of a new species. *Philosophical Transactions of the Royal Society of London, Biological Science* 325 (1230): 561-666.

Sander, P. M. 1990. Skeletochronology in the small Triassic reptile *Neusticosaurus*. *Annales des Sciences Naturelles, Zoologie*, *Paris* 13ème Série 11: 213-217.

Shapiro, M. D. 2002. Developmental morphology of limb reduction in *Hemiergis* (Squamata: Scincidae): chondrogenesis, osteogenesis, and heterochrony. *Journal of Morphology* 254: 211-231.

Shapiro, M. D., Hanken, J., Rosenthal, N. 2003. Developmental basis of evolutionary digit loss in the Australian lizard *Hemiergis*. – *Journal of Experimental Zoology (Molecular and Developmental Evolution)* 297 B: 48-56.

Shapiro, M. D., Shubin, N. H., Downs, J. P. 2007. Limb diversity and digit reduction in reptilian evolution. In: Hall BK, editor. Fins into limbs. The University of Chicago Press. pp. 225–244.

Sheil, C. A., Greenbaum, E. 2005. Reconsideration of skeletal development of *Chelydra serpentina* (Reptilia: Testudinata: Chelydridae): evidence for intraspecific variation. *Journal of Zoology, London* 265: 235-267.

Sheldon, M. A. 1997. Ecological implications of mosasaur bone microstructure. In: Ancient Reptiles, J. M. Callaway and E. L. Nicholls (Eds.), Academic Press: pp. 333-354.

Schmalhausen, J. J. 1910. Die Entwicklung des Extremitätenskelettes von *Salamandrella kayserlingii*. *Anatomischer Anzeiger* 37: 431-446.

Shubin, N. H., Alberch, P. 1986. A morphogenetic approach to the origin and basic organisation of the tetrapod limb. *Evolutionary Biology* 20: 319-387.

Shubin, N. H., Tabin, C., and Carroll, S. B. 1997. Fossils, genes and the evolution of animal limbs. *Nature* 388: 639-648.

Shubin, N. H., Wake, D. B. 2003. Morphological variation, development, and evolution of the limb skeleton of salamanders. In: Amphibian Biology, vol. 5, H. Heatwole and M. Davies (Eds.), Surrey Beatty & Sons PTY limited, Chipping Norton, pp.1782-1808.

Storrs, G. W. 1993. Function and phylogeny in sauropterygian (Diapsida) evolution. American *Journal of Science* 293A: 63-90.

Tanaka, E. M., Tickle, C. 2007. The development of fins and limbs. In Fins into Limbs, B. K. Hall (Ed.), The University of Chicago Press, Chicago, pp. 65-78.

Tsuji, L. A., Müller, J. 2009. Assembling the history of the Parareptilia: phylogeny, diversification, and a new definiton of the clade. *Fossil Record* 12: 71-81.

Vorobyeva, E. I., Hinchliffe, R. J. 1996. Developmental pattern and morphology of *Salamandrella keyserlingii* limbs (Amphibia, Hynobiidae) including some evolutionary aspects. *Russian Journal of Herpetology* 3: 68-81.

Werneburg, I., Hugi, J., Müller, J., Sánchez-Villagra, M. R. 2009. Embryogenesis and ossification of *Emydura subglobosa* (Testudines, Pleurodira, Chelidae) and patterns of turtle development. *Developmental Dynamics* 238: 2770-2786.

Wiens, J., Slingluff, J. L. 2001. How lizards turn into snakes: a phylogenetic analysis of body-form evolution in anguid lizards. *Evolution* 55: 2303-2318.

Wiens, J., Brandles, M. C., Reeder, T. W. 2006. Why does a trait evolve multiple times within a clade? Repeated evolution of snakelike body form in squamate reptiles. *Evolution* 60: 123-141.

Wiens, J. J. 2009. Estimating rates and patterns of morphological evolution from phylogenies: lessons in limb lability from Australian *Lerista* lizards. *Journal of Biology* 8: 19.

Wiens, J. J., Hollingsworth, B. D. 2002. War of the iguanas: conflicting molecular and morphological phylogenies and long-branch attraction in iguanid lizards. *Systematic Biology* 49(1): 143-159.

Wiffen, J., Buffrénil, V. de, Ricqlès, A. de, Mazin, J. M. 1995. Ontogenetic evolution of bone structure in Late Cretaceous Plesiosauria from New Zealand. *Geobios* 28(5): 625-640.

Woodward, H., Horner, J. 2010. Osteohistological analysis of *Alligator mississippiensis* indicates absence of fibrolamellar bone in crocodylians and confirms determinate growth with first report of external fundamental systems: implications for tetrapod osteohistology. *Journal of Vertebrate Paleontology* 28(3): 190A.

Zangerl, R. 1935. *Pachypleurosaurus edwardsi* Cornalia. Osteologie, Variationsbreite, Biologie. In: Triasfauna der Tessiner Kalkalpen IX *Pachypleurosaurus* Schweizer, B. Peyer (Ed.), *Abhandlungen der Schweizerischen Palaeontologischen Gesellschaft* 66, 80 p.

Zug, G. R., Rand, A. S. 1987. Estimation of age in nesting female *iguana iguana*: testing skeletochronology in a tropical lizard. *Amphibia-Reptilia* 8: 237-250.

Chapter 2:

Chondrogenic and ossification patterns and sequences in white's skink *Liopholis whitii* (Scincidae, Reptilia)

Jasmina Hugi, Christian Mitgutsch and Marcelo R. Sánchez-Villagra

Published in *Zoosystematics and Evolution* 86 (1), 21–32, 2010 / DOI 10.1002/zoos.200900011

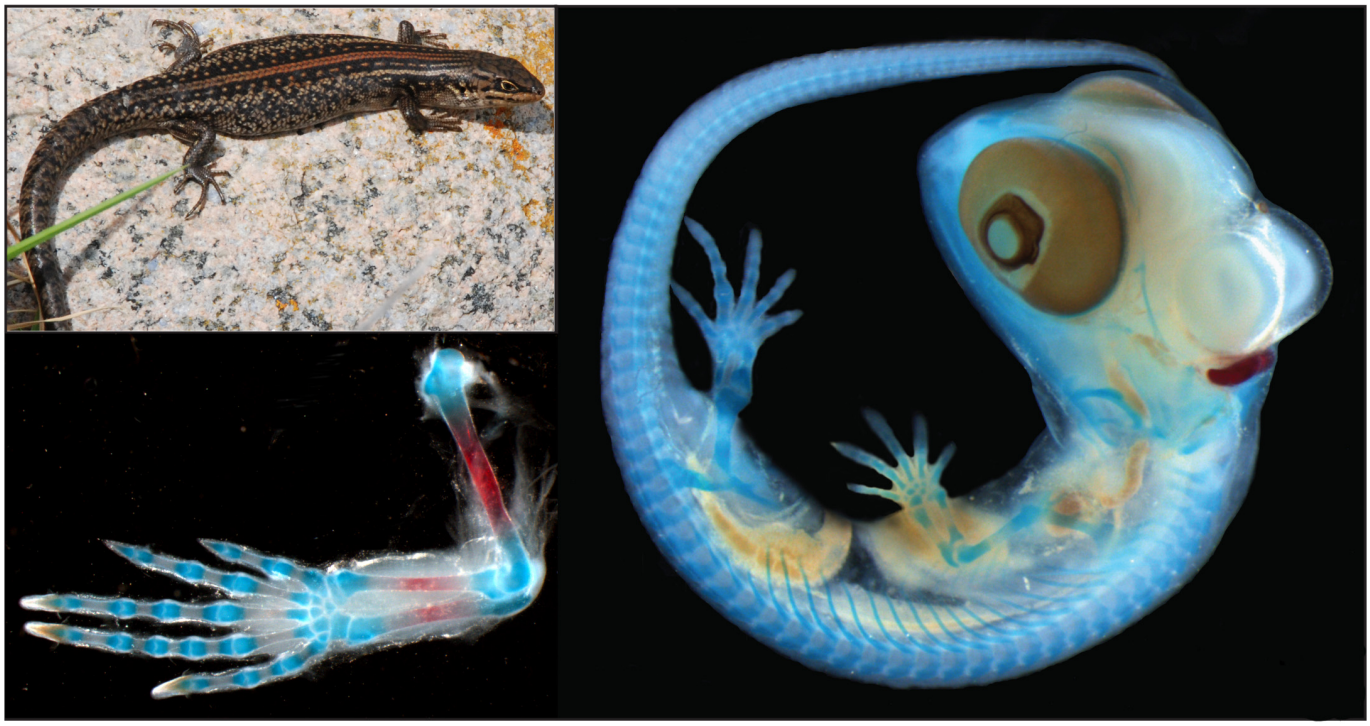

Photographs of embryos: J. Hugi
Picture upper left: Ian Williams

WILEY-VCH museum für naturkunde

Chondrogenic and ossification patterns and sequences in White's skink *Liopholis whitii* (Scincidae, Reptilia)

Jasmina Hugi*, Christian Mitgutsch and Marcelo R. Sánchez-Villagra

Paleontological Institute and Museum, University of Zürich, Karl Schmid-Strasse 4, Zürich 8006, Switzerland

Received 15 June 2009
Accepted 27 August 2009
Published 17 March 2010

Key Words

lizard
heterochrony
chondrification
skeletogenesis
cranium
postcranium

Abstract

The prenatal patterns and sequences of chondrogenesis and ossification are described for the skink *Liopholis whitii*; eight embryos and one adult specimen were examined. Cranial ossification begins in elements of the braincase and the palate, followed by areas of the lower jaw and the cranial roof. Ossification proceeds anteroposteriorly along the axial skeleton and from proximal to distal in the forelimbs and hind limbs. In the zeugopods, the ossification progresses from posterior to anterior, while there is also a strict postaxial order in the autopods with the predominance of digit III in the forelimb and digit IV in the hind limb. Ossification of the femur and tibia starts before the corresponding elements of the forelimb, but simultaneously with the onset in clavicles. Elements of the hind limb display advanced ossification with respect to their forelimb counterparts, with earlier uptake of Alizarin Red in the tarsals, metatarsals and phalanges. The preaxial area of the fused astragalocalcaneum-complex is first to begin ossification among the tarsals. The sequence of ossification is mostly conserved in the skeleton of squamates, as shown in a comparative analysis of heterochrony, but some shifts were found in cranial, vertebral and autopodial regions.

Introduction

The genus *Liopholis* includes common lizards widely distributed in the Australian continent. The ecology, life-history and behaviour of this taxon have been studied in several populations (Gardner et al. 2002; Chapple 2003). The viviparous White's skink, *Liopholis whitii* (= *Egernia whitii*; Gardner et al. 2008) is a member of this group; in this species stable social aggregations are developed and high levels of long-term social and genetic monogamy have been observed (e.g., Chapple & Keogh 2004, 2005). Besides its well known ecology, life-history and behaviour, morphological studies focusing on the limbs have been neglected. Limbs are of highly modular nature (e.g. Greer 1991; Greer et al. 1998). Skeletal modifications are among the first physical elements to adapt to a different habitat or mode of life (e.g., Liem et al. 2001). Patterns and sequences of chondrogenic and skeletal formation are useful tools for addressing questions of homology, convergence as well as for elucidating phylogenetic relationships on different taxonomic levels (e.g., Fabrezi et al. 2007; Fröbisch 2008). Publications focusing on chondrogenic and skeletal events of squamates are no rarity as patterns and sequences have been studied for several decades (e.g., Bellairs & Kamal 1981; Shubin & Alberch 1986; Mohammed et al. 1995; Maisano 2001; Fröbisch 2008). Early studies focused on chondrogenic events (e.g., Bellairs & Kamal 1981; Shubin & Alberch 1986), while later studies documented ossification events (e.g., Rieppel 1994; Mohammed et al. 1995; Rieppel & Zaher 2001; Maisano 2002a, b; Jerez & Tarazona 2008). Furthermore, studies of squamate ontogeny generally dealt either with prenatal or postnatal development (Bellairs & Kamal 1981; Mohammed et al. 1995; Maisano 2001) rather documenting events in selected regions (i.e. only cranium) than in the whole skeleton (e.g., Skinner 1973; Mathur & Goel 1976; Mohammed 1991; Good 1995; Shapiro 2002; Shapiro et al. 2003, 2008; Fröbisch 2008). Here the chondrogenic and ossification patterns and sequences of the entire skeleton of *Liopholis whitii* are described. Included in this study is also a description of the adult skeletal constitution of the manus and pes as well as an overview and compar-

* Corresponding author, e-mail: jasmina.hugi@pim.uzh.ch

ison with literature of squamates' chondrogenesis and skeletogenesis patterns and sequences.

Material and methods

The study is based on one adult individual (SVL 68 mm) and eight embryos of *Liopholis whitii* (numbered from 102 to 109, SVL 13.4–31.4 mm) from the South Australian Museum in Adelaide (Australia). The series is housed in the Natural History Museum in Berlin (Germany) as part of the embryological collection. Embryos were dissected out of ethanol fixed female specimens and subsequently fixed in 4 % neutral buffered formaldehyde.

Morphological description is based on observations with a Leica MZ-16 dissection microscope; pictures were taken with a DFC 420C digital camera and IM 50 software; drawings were produced using a camera lucida and subsequently refined using Photoshop CS3©. The embryos are ordered based on their body lengths (using digital callipers to the nearest 0.1 mm). Body length is defined as the distance between the tip of the snout and the end of the cloaca, a standard measurement in squamate research (Maisano 2001, 2002a, b). The specimens were already cleared and double-stained when measured and thus each size must be regarded as minimum. The heads of embryos 105 and 109 were not available for skeletogenic studies, because they will be used in another study. As a consequence the SVL of embryo 105 and 109 is an approach by summing up the length of the head with the length of the body. The clearing and double-staining procedure follows the protocol of Dingerkus & Uhler (1977), with modifications by Hiroshi Nagashima, Kobe (pers. comm. 2007).

The results are compared to data for squamates from several clades (Tab. 1). Event-pairing (Velhagen 1997) is applied to compare data from 5 out of 25 species.

Table 2 summarizes information for the five species included.

Twenty species for which some information is available are excluded from the study due to incomplete information or lack of resolution. However, relevant developmental aspects regarding all 25 species are partly included in the discussion. For each of the five species included in the event-pairing, a character matrix is constructed in which the very first visible onset of ossification among the 39 elements listed in Table 2 is related to every other event. This results in 741 event pairs for each species. Three character states reflect the timing of one event relative to another: before 0), simultaneously (1), or after (2). Simultaneous events, which are ties, probably result from a lack in resolution, since it is unlikely that ossification of two or several bones occurs at exactly the same time. In Table 2, some elements are treated as parts of skeletal groups as defined in terms of function and/or topographical region and/or members of a metameric series. The first structure that ossifies within each group is taken to represent the onset of ossification of the group as a whole (e.g., jugal in the dermatocranium). Besides grouping of elements, in Table 2 some skeletal elements are neither included in groups nor listed singly (e.g., pisiforme, radiale, phalanges) due to invariable timing of onset of ossification (postnatal ossification/never ossifies) or a lack in resolution in all examined squamates (e.g., phalanges). As Table 2 gives a rough overview about the events of onsets of ossification in

Table 1. Summary of squamate skeletogenesis studies and species relevant for this work (* refer to Tabs 2 and 4). ext. morph. – external morphology. Size means SVL in mm.

Taxon	Family	# specimens/ stages	Ordering criterium	Reproductive mode	Cranium	Postcranium
Acrochordus granulatus	Acrochordidae	10/?	stage/size	ovivivipar ous	Y	N
Calotes versicolor	Agamidae	?/11	stage/egg size/age	oviparous	N	Y
Chamaeleo hoehnelii	Chamaeleontidae	25/5	stage/size	ovivivipar ous	Y	Y
Cyrtodactylus pubisulcus	Gekkonidae	20/ca.20	size	oviparous	Y	Y
Gehyra oceanica	Gekkonidae	37/?	size	oviparous	N	Y
Lepidodactylus lugubris	Gekkonidae	16/?	size	oviparous	N	Y
Bachia bicolor	Gymnopthalmidae	at least 5/?	size	?oviparous	N	Y
Liolaemus scapularis	Iguanidae	5/4	stage/?	oviparous	Y	Y
Liolaemus quilmes	Iguanidae	9/ca. 3	stage/age	oviparous	Y	Y
Lacerta agilis exigua	Lacertidae	18/7	stage/size/ext. morph.	oviparous	Y	Y
Zootoca vivipara	Lacertidae	23/?	stage/size	viviparous	Y	Y
Callisaurus draconoides	Phrynosomatidae	43/ca. 22	size	oviparous	Y	Y
Uta stansburiana	Phrynosomatidae	33/ca. 22	size	oviparous	Y	Y
Chalcides ocellatus	Scincidae	?/7	stage/size	viviparous	N	Y
Chalcides sepoides	Scincidae	?/?	size	viviparous	N	Y
Eumeces schneideri	Scincidae	?/?	size	oviparous	N	Y
Hemiergis initialis	Scincidae	27/9	stage/size	oviparous	N	Y
Hemiergis peronii	Scincidae	43/9	stage/size	oviparous	N	Y
Hemiergis quadrilineata	Scincidae	15/5	stage/size	oviparous	N	Y
Liopholis whitii	Scincidae	8/8	stage/size	viviparous	Y	Y
Mabuya capensis	Scincidae	42/7	age/size	viviparous	Y	N
Mabuya quinquetaeniata	Scincidae	?/?	size	oviparous	N	Y
Scincus scincus	Scincidae	?/?	size	viviparous	N	Y
Tupinambis merianae	Teiidae	13/5	stage/size	oviparous	Y	Y
Tubinambis rufescens	Teiidae	11/5	stage/size	oviparous	Y	Y

Table 1. (continued)

Taxon	Family	Limbs	Chondrogenesis	Prenatal-hachting	Postnatal-hatching	References
Acrochordus granulatus	Acrochordidae	N	N	Y	Y	Rieppel & Zaher 2001
Calotes versicolor	Agamidae	Y	Y	Y	Y	Mathur & Goel 1976
Chamaeleo hoehnelii	Chamaeleontidae	Y/N	N	Y	Y	Rieppel 1993
Bachia bicolor	Gymnopthalmidae	Y	N	N	Y	Jerez & Tarazona 2008
Cyrtodactylus pubisulcus	Gekkonidae	Y/N	N	N	Y	Rieppel 1992b
Gehyra oceanica	Gekkonidae	Y	N	N	Y	Rieppel 1994a
Lepidodactylus lugubris	Gekkonidae	Y	N	N	Y	Rieppel 1994a
Liolaemus scapularis	Iguanidae	Y/N	N	Y	Y	Lobo et al. 1995
Liolaemus quilmes	Iguanidae	Y/N	N	Y	Y	Abdala et al. 1997
Lacerta agilis exigua	Lacertidae	Y/N	N	Y	Y	Rieppel 1994b
Zootoca vivipara	Lacertidae	N	Y	Y	Y	Rieppel 1992a
Callisaurus draconoides	Phrynosomatidae	Y/N	N	N	Y	Maisano 2002
Uta stansburiana	Phrynosomatidae	Y/N	N	N	Y	Maisano 2002
Chalcides ocellatus	Scincidae	Y/N	Y	Y	Y	Mohammed 1991; Mohammed et al. 1995
Chalcides sepoides	Scincidae	Y	N	Y	Y	Mohammed et al. 1995
Eumeces schneideri	Scincidae	Y/N	N	Y	Y	Mohammed et al. 1995
Hemiergis initialis	Scincidae	Y	Y	Y	Y	Shapiro 2002
Hemiergis peronii	Scincidae	Y	Y	Y	Y	Shapiro 2002
Hemiergis quadrilineata	Scincidae	Y	Y	Y	Y	Shapiro 2002
Liopholis whitii	Scincidae	Y	Y	Y	N	This work
Mabuya capensis	Scincidae	N	Y	Y	Y	Skinner 1973
Mabuya quinquetaeniata	Scincidae	Y/N	N	Y	Y	Mohammed et al. 1995
Scincus scincus	Scincidae	Y/N	N	Y	Y	Mohammed et al. 1995
Tupinambis merianae	Teiidae	Y/N	N	Y	N	Federico & Lobo 2006
Tubinambis rufescens	Teiidae	Y/N	N	Y	N	Federico & Lobo 2006

each specimen, a more fine-grained sequence order is given in the description. The fine-grained sequence is based on differently progressed ossification states of every skeletal element within each specimen. Table 3 lists the relative sequence of onset of ossification of *Liopholis whitii*.

Maisano (2001, 2002a, b) provided a standardized usage of skeletal terms in earlier studies, which is followed here. No distinction is made between onset of calcification and onset of ossification as both are part of a continuous fluent process. "Advanced chondrogenesis" and "advanced ossification" are descriptions used in this study. "Advanced" ossification is used for describing the condition of an element that already began ossification but is not yet completely ossified. "Advanced" chondrogenesis is used for describing the condition of an element that already began chondrogenesis but is not completely chondrified yet.

Symphyses in the pectoral girdle, symphyses and processes in the pelvic girdle (iliac process, epi- and prepubis, ischial symphysis and metaischial process) and epiphyses of long bones only ossify postnatally within secondary ossification centers (e.g., Rieppel 1992b; Maisano 2001, 2002a, b; Jerez & Tarazona 2008). Processes of the pectoral girdle (suprascapula and epicoracoid) never ossify (Mohammed et al. 1995). Thus all these events are not described in the current series of *Liopholis whitii*. Furthermore, the elements in the skull do neither fuse (i.e. interdigitating along their margins) nor fully ossify (e.g., there is still a parietal fontanelle in the largest embryo) in this series. Neural arches do not fuse to their centra in the embryological series.

Results

Patterns and sequences of chondrogenesis and ossification of *Liopholis whitii*

Cranium (Figs 1, 2q–u; Tab. 3). In specimen 102 (SVL 13.4 mm), the quadrate, articular, epipterygoid and all neurocranial elements are fully chondrified.

The first cranial ossification starts in the neurocranium in specimen 103 (SVL 15.7 mm). The supraoccipital is the first cranial element to start ossification (Fig. 1). In specimen 104 (18.6 mm) parts of the dermatocranium are next to begin ossification. Structures of the mandibles (splenial, squamosal, supratemporal, angular, surangular, dentary), the palate (pterygoid, maxilla) and the orbital region (jugal) show sequestering of calcium in their tissues. So far, the sequence of onset of ossification is supraoccipital > pterygoid > surangular > angular > dentary, maxilla, jugal > squamosal, supratemporal, splenial. Tooth crowns are visible, but the teeth are not yet embedded into the premaxilla, maxilla and dentary. Splanchnocranial elements (quadrate, articular, epipterygoid) start ossification in specimen 106

Table 2. Timing of onset of ossification in the elements and taxa analyzed with event pairing in this study.[1]

	Liopholis whitii	*Zootoca vivipara*	*Lacerta agilis exigua*	*Liolaemus scapularis*	*Liolaemus quilmes*
Dermatocranium	18.6 mm	<7 mm	34+	33	34A
Neurocranium	15.7 mm	7 mm	35	34B	34
Splanchnocranium	22 mm	7 mm	35	34A	35
Cervic. v.	22 mm	7 mm	35	34A	35
Dorsal v.	22 mm	15 mm	35	34A	35
Sacral v.	26.5 mm	?	36	34A	35
Caudal v.	26.5 mm	17.5 mm	36	34A	35
Ribs	22 mm	9 mm	34+	34B	35
Interclavicle	22 mm	9 mm	35–	34A	33
Clavicle	22 mm	7 mm	34+	33	32
Scapula	26.5 mm	9 mm	35	34B	34
Coracoid	26.5 mm	19 mm	36	34B	34
Humerus	22 mm	7 mm	34–	33	32
Radius/Ulna	22 mm	7 mm	34–	34B	34
Ulnare	31.4 mm	20 mm	posthatching	posthatching	37
Dist. Carp. 4	31.4 mm	24.5 mm	posthatching	posthatching	37
Metacarp. 1, 2	26.5 mm	9 mm	35–	34B	33
Metacarp. 3	22 mm	9 mm	35–	34B	33
Metacarp. 4	26.5 mm	9 mm	35–	34B	33
Metacarp. 5	26.5 mm	15 mm	35–	34B	33
Phal. Manus	26.5 mm	9 mm	37+	34B	34
Ilium	26.5 mm	15 mm	36	34B	34
Pubis	26.5 mm	17.5 mm	36	34B	34
Ischium	26.5 mm	20.5 mm	37+	34B	34
Femur	22 mm	7 mm	34–	34A	33
Tibia/Fibula	22 mm	7 mm	34–	34B	34
Astragalus	28.8 mm	17.5 mm	40–	35	36
Calcaneum	31.4 mm	20 mm	posthatching	posthatching	37
Dist. Tars. 3	31.4 mm	24.5 mm	posthatching	posthatching	37
Dist. Tars. 4	31.4 mm	20 mm	posthatching	posthatching	37
Metatars. 1–4	22 mm	7 mm	35–	34B	33
Metatars. 5	28.8 mm	16.5 mm	35–	35	33
Phal. Pes	22 mm	9 mm	35	34B	34

[1] Either size (in mm) or stages (after Lemus 1967 in *Liolaemus scapularis* and *L. quilmes*; after Peter 1904 in *Lacerta agilis exigua*) identify the timing for each (Tab. 1). Missing data (i.e.: ?) reflect either absence of an element or lack of information in the original source. The onset of ossification in the first element of a subgroup (dermatocranium, neurocranium, splanchnocranium, vertebrae, phalanges) is accounted for the sequence order of the whole group. Several squamates from the Table 1 are not included in the analysis due to little resolution available for them; v. – vertebrates; phal. – phalanges.

(SVL 22 mm) with the onset of ossification in the clavicle and interclavicle. By specimen 106 (SVL 22 mm) all cranial structures, except for the basipterygoid process, basioccipital, exoccipital, opisthotic, parasphenoid and the prootic, have at least begun ossification, and those showing advanced ossification become more clearly defined in form. The quadrate begins to ossify endochondrally at its mid portion. The articular is still cartilaginous at its posterior margin. The parietal shows ossification only along its lateral margin. The postorbital starts ossification at its anterior margin. The prefrontal is well recognizable as triangular red bone anterior to the orbit. The ventral margin of the maxilla shows irregularly shaped unossified lacunae. The dorsally situated ascending process of the maxilla is calcified. The dorsal roof of the cranium consisting of the nasal, prefrontal, frontal and parietal, is marked by an anteroposteriorly decreasing gradient in intensity of uptake of Alizarin Red. In specimen 107 (SVL 26.5 mm) all neurocranial elements started ossification, most of them already showing advanced ossification. The scleral ring starts ossification and the teeth are embedded into the premaxilla, maxilla and dentary. The nasal and frontal show advanced ossification at their

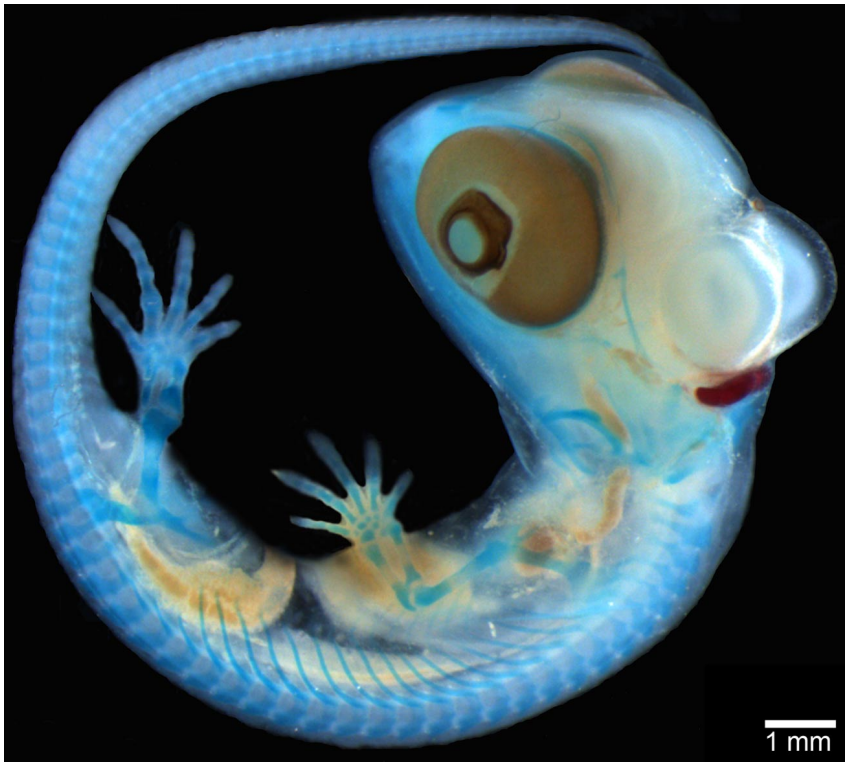

Figure 1. Cleared and double-stained specimen (103) of *Liopholis whitii*. The supraoccipital located ventroposteriorly of the cranium is the first bone that retains Alizarin Red.

medial areas, whereas the parietal is still only ossified along its lateral margin. The overall sequence of onset of ossification in the cranium is neurocranium > dermatocranium > splanchnocranium. This gradient is based on the onset of ossification of the first element of each cranial subgroup.

Vertebral column (Tab. 3). The ossification of the vertebral column repeats chondrogenic patterns and sequences. Both proceed in an overall anteroposterior direction. Chondrogenesis and ossification begins first in the centra, subsequently in the neural arches and at last in the ribs. The centra show first perichondral ossification at their ventral sides. Ossification then spreads dorsally over the centra, reaching the ventral parts of the neural arches. The ribs start endochondrally at midshaft. Ossification of sacral centra begins simultaneously with the onset of the pubis and the coracoid.

In the second largest specimen (108; SVL 28.8 mm) the last vertebral components which still are cartilaginous are the proximal tips of the ribs, the pre- and postzygapophyses of the neural arches and the dorsal tips of the neural arches. The two former skeletal parts show already advanced ossification in the largest available specimen (109; SVL 31.4 mm), whereas the dorsal tips of the neural arches display only early onset of ossification.

Pectoral and Pelvic Girdles (Tab. 3). In specimen 102 (13.4 mm) the scapula and coracoid started chondrogenesis whereas the rest of the endochondral elements of the pectoral girdle still are precartilaginous (scapula, suprascapula, coracoid, epicoracoid and sternum). Dermal bones (clavicles, interclavicles) are not yet visible in specimen 102 (13.4 mm). All elements of the pelvic girdle have begun to chondrify. Ossification of the ilium and pubis precede that of the ischium. In specimen 104 (SVL 18.6 mm) all endochondral pectoral girdle elements (scapula, suprascapula, coracoid, epicoracoid) are fully chondrified, except for the sternum which still shows only advanced chondrogenesis.

The clavicles are the first girdle elements to start ossification (specimen 105; SVL 20.4 mm). In the next larger specimen (106; SVL 22 mm), interclavicle, scapula as well as the ilium display onset of ossification. The scapula shows perichondral ossification around its mid-portion. The ilium begins to sequester calcium perichondrally as an anteroposterior band at its mid-height. The sequence of onset of ossification of the girdle elements is: clavicle > interclavicle > scapula, ilium > coracoid, pubis > ischium.

Forelimb and Hind Limb (Figs 2a–p; Tab. 3). The manus and pes of the embryos slightly differ in their composition from that seen in the adult specimen. Thus, before proceeding with the results of the patterns and sequences of chondrogenesis and ossification in the limbs, a short morphological description of the manus and pes of the adult specimen is given (Fig. 3). The adult carpal region consists of five distal carpals, a centrale, a proximal row formed by the ulnare and radiale and one small intermedium at the distal end of the zeugopodial region. The palmar view reveals the wedge like pisiforme that lies just distolateral to the

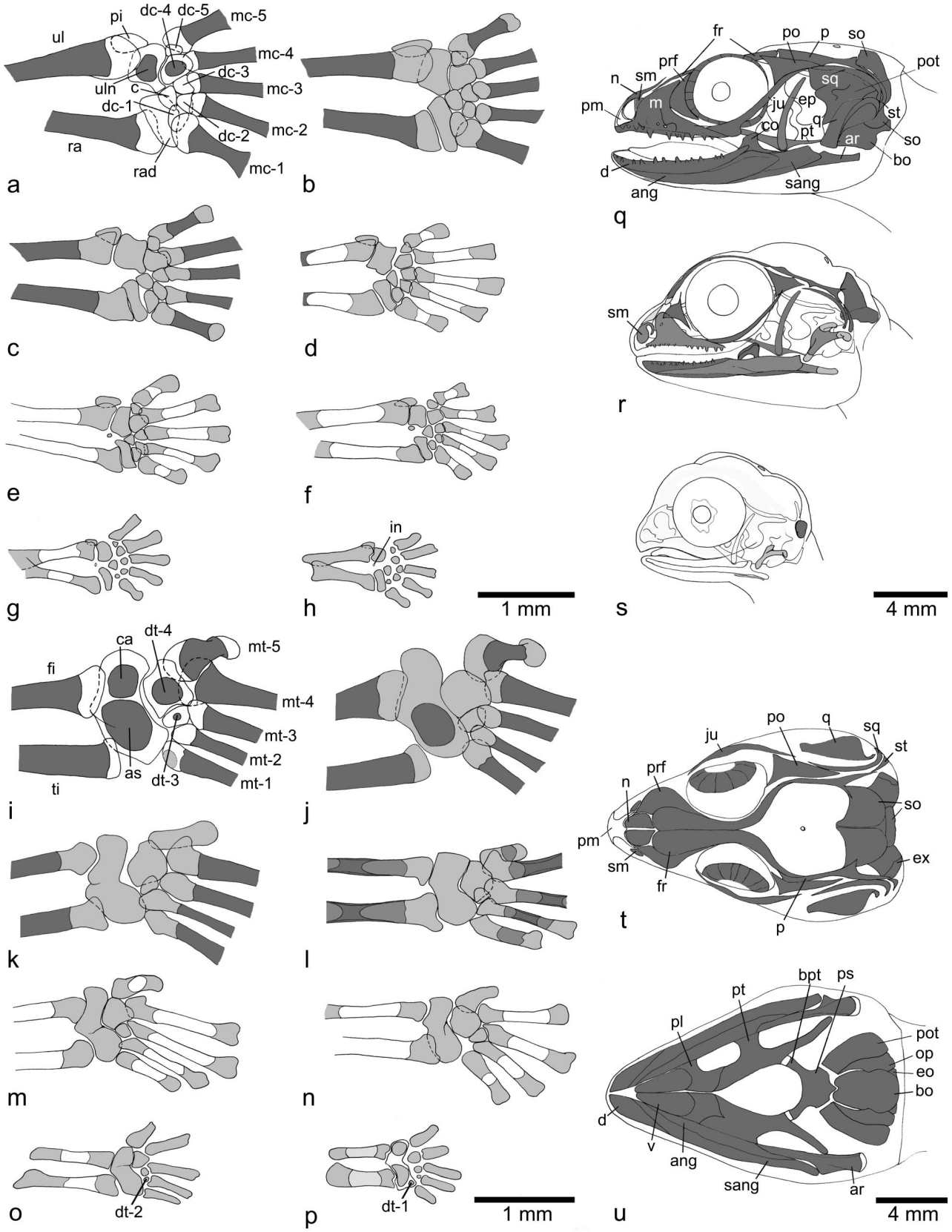
pi
dc-4
dc-5
mc-5
ul
mc-4
dc-3
uln
c
mc-3
dc-1
dc-2
mc-2
ra
rad
mc-1
a
b
fr
po
p
so
pot
prf
n
sm
sq
pm
m
ju
ep
st
co
q
pt
ar
so
bo
d
ang
sang
q
c
d
sm
r
e
f
in
g
h
1 mm
s
4 mm
ca
dt-4
mt-5
fi
mt-4
mt-3
mt-2
as
dt-3
mt-1
ti
i
j
po
q
sq
ju
st
prf
n
so
pm
ex
sm
fr
p
t
k
l
m
n
bpt
ps
pt
pl
pot
op
eo
bo
d
v
ang
sang
ar
o
dt-2
p
dt-1
1 mm
u
4 mm

Table 3. Timing of onset of ossification in all the skeletal elements of *Liopholis whitii* recorded. Elements that are not listed (sternum, epicoracoid, suprascapula) start either ossification postnatally or never ossify. The first figure in brackets is the SVL in mm, the second is the rank in the fine-grained sequence (a relative onset of ossification order based on the progress of ossification of each element compared within one specimen).

Sequence of onset of ossification of *Liopholis whitii*

Skeletal region	Skeletal elements
Dermatocranium	Angular (18.6; 4), Coronoid (22; 12), Dentary (18.6; 5), Frontal (22; 12), Jugal (18.6; 5), Maxilla (18.6; 5), Nasal (22; 12), Palatine (22; 12), Parietal (22; 12), Postorbitofrontal (22; 12), Prefrontal (22; 12), Premaxilla (22; 12), Pterygoid (18.6; 2), Surangular (18.6; 3), Septomaxilla (26.5; 13), Splenial (18.6; 6), Squamosal (18.6; 6), Supratemporal (18.6; 6), Vomer (22; 12), Scleral ring (26.5; 14)
Neurocranium	Basioccipital (26.5; 14), Basipterygoid process (22; 12), Basisphenoid (26.5; 14), Exoccipital (26.5; 14), Opisthotic (26.5; 14), Parasphenoid (26.5; 14), Prootic (26.5; 14), Supraoccipital (15.7; 1)
Splanchnocranium	Articular (22; 11), Epipteryoid (22; 12), Quadrate (22; 9)
Cervical vertebrae	Centra (22; 9), Neural arches (22; 10), Ribs (22; 11)
Dorsal vertebrae	Centra (22; 10), Neural arches (26.5; 14), Ribs (26.5; 15)
Sacral vertebrae	Centra (26.5; 15), Neural arches (26.5; 16), Ribs (26.5; 17)
Caudal vertebrae	Centra (26.5; 16), Neural arches (26.5; 17), Ribs (26.5; 18)
Shoulder girdle	Interclavicle (22; 10), Clavicle (22; 9), Coracoid (26.5; 15), Scapula (26.5; 14)
Forelimb	Humerus (20.4; 8), Radius (22; 12), Ulna (22; 11), Metacarpal-1 (26.5; 16), Metacarpal-2 (26.5; 15), Metacarpal-3 (22; 12), Metacarpal-4 (26.5; 14), Metacarpal-5 (26.5; 17), Digit 1 phalange 1 (26.5; 16), Digit 1 phalange 2 (26.5; 16), Digit 2 phalange 1 (26.5; 16), Digit 2 phalange 2 (26.5; 16), Digit 2 phalange 3 (26.5; 16), Digit 3 phalange 1 (22; 14), Digit 3 phalange 2 (22; 14), Digit 3 phalange 3 (26.5; 16), Digit 3 phalange 4 (26.5; 16), Digit 4 phalange 1 (26.5; 16), Digit 4 phalange 2 (26.5; 16), Digit 4 phalange 3 (26.5; 16), Digit 4 phalange 4 (26.5; 16), Digit 4 phalange 5 (26.5; 16), Digit 5 phalange 1 (26.5; 16), Digit 5 phalange 2 (26.5; 16), Digit 5 phalange 3 (26.5; 16), Centrale (postnatal; 21), Distal carpal-1 (postnatal; 21), Distal carpal-2 (postnatal; 21), Distal carpal-3 (postnatal; 21), Distal carpal-4 (31.4; 19), Distal carpal-5 (postnatal; 21),Intermedium (postnatal; 21), Pisiforme (postnatal; 21), Ulnare (31.4; 19), Radiale (postnatal; 21)
Pelvic girdle	Ilium (26.5; 14), Pubis (26.5; 15), Ischium (26.5; 16)
Hind limb	Femur (20.4; 7), Tibia (20.4; 8), Fibula (20.4; 8), Metatarsal-1 (22; 14), Metatarsal-2 (22; 13), Metatarsal-3 (22; 12), Metatarsal-4 (22; 11), Metatarsal-5 (28.8; 18), Digit 1 phalange 1 (26.5; 15), Digit 1 phalange 2 (26.5; 15), Digit 2 phalange 1 (26.5; 15), Digit 2 phalange 2 (26.5; 15), Digit 2 phalange 3 (26.5; 15), Digit 3 phalange 1 (22; 14), Digit 3 phalange 2 (22; 14), Digit 3 phalange 3 (26.5; 15), Digit 3 phalange 4 (26.5; 15), Digit 4 phalange 1 (22; 13), Digit 4 phalange 2 (22; 13), Digit 4 phalange 3 (26.5; 15), Digit 4 phalange 4 (26.5; 15), Digit 4 phalange 5 (26.5; 15) , Digit 5 phalange 1 (26.5; 15), Digit 5 phalange 2 (26.5; 15), Digit 5 phalange 3 (26.5; 15), Digit 5 phalange 4 (26.5; 15), Astragalus (28.8; 18), Calcaneum (31.4; 19), Distal tarsal-3 (31.4; 20), Distal tarsal-4 (31.4; 19)

ulna, and three larger ventral sesamoids beneath the proximal and the distal row of carpals. The phalangeal formula of the manus is 2–3–4–5–3. The adult tarsus consists of one large proximal element, representing the fused astragalus and calcaneum; its distal margin is articulating to one tarsal here referred to as distal tarsal-4 that in turn articulates to distal tarsal-3. Metatarsal-5 is proximodistally short and hook-shaped as typical of lepidosaurs (Romer 1956; Robinson 1975; Camp 1988; Rieppel & Grande 2007; Conrad 2008). The pes shows

◄

Figure 2. Drawings of the chondrogenesis (very light grey: prechondrogenic; light grey: chondrogenic) and ossification (grey: beginning to ossify; dark grey: advanced to completely ossified) sequence patterns in *Liopholis whitii*. **a**–**h**. Carpus dorsal view (**a.** specimen 109; **b.** specimen 108; **c.** specimen 107; **d.** specimen 106; **e.** specimen 105; **f.** specimen 104; **g.** specimen 103; **h.** specimen 102); **i**–**p.** Tarsus dorsal view (**i.** specimen 109; **j.** specimen 108; **k.** specimen 107; **l.** specimen 106; **m.** specimen 105; **n.** specimen 104; **o.** specimen 103; **p.** specimen 102); **q**–**s.** Cranium lateral view (**q.** specimen 108; **r.** specimen 106, **s.** specimen 103); **t**–**u. t.** Cranium dorsal view specimen 108 (superficial cranial elements are shown, dermatocranium and quadrate); **u.** Cranium ventral view specimen 108 (superficial cranial elements are shown). Abbreviations: **ang** – angular; **ar** – articular; **as** – astragalus; **bo** – basioccipital; **bpt** – basipterygoid process; **c** – centrale; **ca** – calcaneum; **cor** – coronoid; **d** – dentary; **dc** – distal carpal; **dt** – distal tarsal; **ep** – epipterygoid; **ex** – exoccipital; **f** – frontal; **fi** – fibula; **hu** – humerus; **in** – intermedium; **ju** – jugal; **m** – maxilla; **mc** – metacarpal; **mt** – metatarsal; **n** – nasal; **op** – opisthotic; **p** – parietal; **pfr** – prefrontal; **pi** – pisiforme; **pl** – palatine; **po** – postorbitofrontal; **pot** – prootic; **ps** – parasphenoid; **pt** – pterygoid; **q** – quadrate; **ra** – radius; **rad** – radiale; **sang** – surangular; **sm** – septomaxilla; **so** – supraoccipital; **sq** – squamosal; **st** – supratemporal; **ti** – tibia; **ul** – ulna; **uln** – ulnare; **v** – vomer.

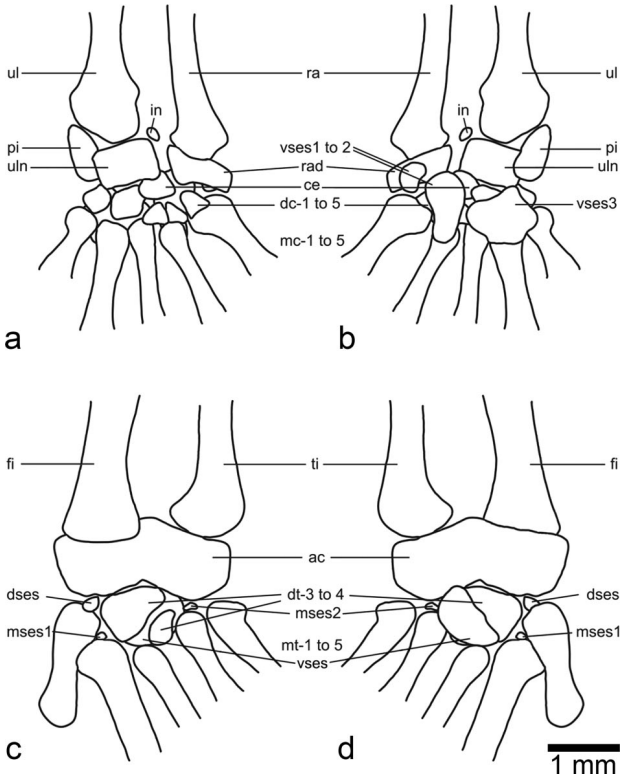

Figure 3. Adult proximal region of the autopodial skeleton in *Liopholis whitii*. **a.** Dorsal and **b.** ventral aspect of manus; **c.** Dorsal and **d.** ventral aspect of pes. Abbreviations: **ac** – astragalocalcaneum-complex; **ce** – centrale; **dc** – distal carpal; **dses** – dorsal sesamoid; **dt** – distal tarsal; **fi** – fibula; **in** – intermedium; **mc** – metacarpal; **mses** – medial sesamoid; **mt** – metatarsal; **pi** – pisiforme; **ul** – ulna; **uln** – ulnare; **ra** – radius; **rad** – radiale; **ti** – tibia; **vses** – ventral sesamoid.

one small sesamoid located dorsally at the proximal margin of mt-5, and two even smaller medial sesamoids lying at the proximal ends of the shaft of mt-2 and mt-4. In addition, there is a ventral sesamoid on the plantar face of the pes; its medial side lies upon dt-3 and -4, whereas its distal portion is positioned adjacent to the proximal shaft end of mt-3 and its proximal margin matches the preaxial side of the astragalocalcaneum-complex. The phalangeal formula of the pes is 2–3–4–5–4.

In specimen 102 (SVL 13.4 mm) the long bones are elongated and well developed. Chondrogenesis can be seen at diaphyseal and metaphysial regions in all long bones except for the terminal phalanges. Epiphyses are still precartilaginous. The femur, tibia and fibula are more advanced in the extent of chondrogenesis than are the corresponding elements of the forelimb. In addition, there is also a difference between the preaxial and postaxial element of the zeugopodial region: the postaxial ulna and fibula are more advanced in chondrogenesis than are the preaxial radius and tibia. The chondrogenic sequence of both the manus and pes is digit IV > digit III > digit II > digit I > digit V. The chondrogenic sequence of the carpals is radiale, ulnare, centrale, dc-4 > dc-2, -3 > dc-5 > dc-1. Distal carpal-1 is of precartilaginous state and the smallest of all distal carpals. The tarsals are all completely cartilaginous. However, specimen 102 (SVL 13.4 mm) shows two more, very small, distal tarsals (dt-1 and -2) compared to the pattern encountered in the adult. The proximal tarsals are fused into an astragalocalcaneum-complex showing separate chondrifying centers. There is still a superficial suture visible at their juncture. In the forelimb and hind limb the intermediate and ungual phalanges are still precartilaginous, indicating that chondrogenesis occurs from proximal to distal in the phalanges. The pisiforme, a small and thin cartilaginous wedge, shows as the intermedium beginning chondrogenesis.

In the next two larger specimens, 103 (SVL 15.7 mm) and 104 (SVL 18.6 mm), there is a reduction in the number of the distal tarsals. Reduction starts in specimen 103 with the absence of dt-1. The next reduction is evident in specimen 104, which has additionally lost dt-2. The decreased complement of two distal tarsals, namely dt-3 and dt-4, is the condition as seen in the adult. In specimen 104, chondrogenesis is evident in the most distal tips of the phalanges as well as the epiphyses of the long bones of the hind limb.

In specimen 105 (SVL 20.4 mm) the humerus shows beginning perichondral ossification at mid diaphyseal region whereas the femur, the tibia and fibula exhibit early peripheral ossification at the shaft region.

In the next specimen (106; SVL 22 mm) ossification is evident perichondrally in the ulna, metatarsals-1 to -4, but is scarcely visible in metacarpal-3 and the proximal and intermediate phalanges of digit III of the manus and IV of the pes. Metatarsal-4 and -3 are more advanced in ossification compared to metatarsal-1, -2 and metacarpal-3. Furthermore, metatarsal-4 and its proximal and intermediate phalanges are even more progressed in ossification than are corresponding members of digit III of the pes. The intermedium is not visible anymore.

In specimen 107 (SVL 26.5 mm), all remaining metacarpals (metacarpals-1, -2, -4, -5), all remaining phalanges of the manus and pes as well as the metatarsal-5 display onset of ossification.

In specimen 108 (SVL 28.8 mm) the preaxial area of the cartilaginous astragalocalcaneum-complex shows one endochondral ossification center. A second, postaxial endochondral center is displayed in the next specimen (109; SVL 31.4 mm) with the onset of endochondral ossification in two carpals, the ulnare and dc-4. The shape of metatarsal-5 is now recognizably 'hooked'.

The sequence of timing in the onset of ossification in the forelimb is: humerus > ulna > radius > metacarpal-3 > metacarpal-4 > metacarpal-2 > metacarpal-1 > phalanges > metacarpal-5 > ulnare, distal carpal-4, distal carpal-3. In the hind limb the sequence is: femur > fibula > tibia > metatarsal-4 > metatarsal-3 > metatarsal-2 > metatarsal-1 > phalanges > astragalus, metatarsal-5 > calcaneum, distal tarsal-3, distal tarsal-4. In the manus, the centrale, distal carpal-1 to -3, intermedium, pisiforme and the radiale start ossification postnatally. Every single element of the hind limb preceeds its fore-

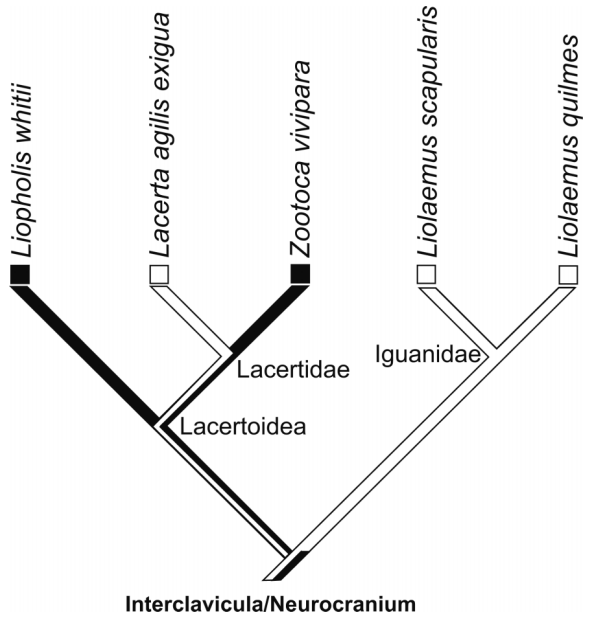

Figure 4. Phylogeny of the species examined and the taxonomic groups mentioned in the text (after Estes & Pregill 1988). Distribution of one event-pair. Black and white lines represent character states 2 and 0, respectively.

limb counterpart regarding timing of onset and progression of ossification.

Event Pairing

Figure 4, Tables 2 and 4

Of the 741 event-pairs (characters) examined, 265 (35.8 %) show the same state in all taxa. For 229 (30.9 %) of the event-pairs, all except ties are uniform. These two groups of uninformative characters constitute 66.7 % of the total. In 159 event pairs, there are states 0 and 2, but also ties, so that there are no phylogenetically informative characters, as resolution of the ties may then imply no heterochronies. In 88 event pairs there are no ties but they are also phylogenetically uninformative, in that only autapomorphies in one or more species are shown.

There is no change that indicates an unequivocal autapomorphy for a clade of two or more taxa. For example of an event pair showing alternative reconstructions see Figure 4. The event pairing method revealed no feature of unequivocal phylogenetic information. Future studies could examine squamate taxa with a close phylogenetic relationship and different habitats (Richardson et al. 2009). Besides, intraspecific variation (polymorphism or phenotypic plasticity) is also worth considering (e.g., digits in *Zootoca vivipara* (*Lacerta vivipara* Jacquin), Rieppel 1992a).

Discussion

Here, mostly the ossification pattern is discussed, because, in contrast to the chondrogenic events, ossification sequences have been documented in many squamates (see Tab. 1).

Cranium. The onset of ossification in structures of the head precedes that of all other skeletal elements in all squamates studied to date (Rieppel 1992a, b, 1993, 1994b; Lobo, Abdala & Scrocchi 1995; Abdala, Lobo & Scrocchi 1997; Rieppel & Zaher 2001; Maisano 2002a; Federico & Lobo 2006). Dermal bones situated around Meckel's cartilage are the first to undergo ossification in *Zootoca vivipara* (*Lacerta vivipara* Jacquin) (Rieppel 1992a), *Lacerta agilis exigua* (Rieppel 1994), *Tupinambis merianae, T. rufescens* (Federico & Lobo 2006) as well as in *Liolaemus quilmes* (Abdala et al. 1997) and *L. scapularis* (Lobo et al. 1995); the pterygoid is in all these taxa the first structure to sequester calcium (in *Liolaemus quilmes* it does so simultaneously with the dentary and surangular). After ossification has begun in the dermatocranium in these lizards, parts of the splanchnocranium undergo calcification (i.e. quadrate), either before or synchronously with regions of the neurocranium (i.e. exoccipital) (Rieppel 1992a, 1994; Lobo et al. 1995; Abdala et al. 1997; Federico & Lobo 2006). In contrast, *Liopholis whitii* shows the following ossification gradient: neurocranium (first: supraoccipital) > dermatocranium (first: pterygoid) > splanchnocranium (first: quadrate). In this skink it is the supraoccipital which begins ossification before all other cranial elements. The pterygoid ossifies shortly after the supraoccipital and slightly before the surangular. The splanchocranium starts ossification later. The quadrate seems to start before the articular that, on the other hand, seems to start before the epipterygoid based on their intensity of uptake of Alizarin Red.

Table 4. Distribution of character states, expressed as actual numbers, and percentage of the 741 total event pairs examined.[1]

Taxon	State 0	State 1	State 2	Missing data
Lacerta agilis exigua	291 (39.3 %)	109 (14.7 %)	341 (46 %)	0
Zootoca vivipara	234 (31.6 %)	137 (18.5 %)	332 (44.8 %)	38 (5.1 %)
Liolaemus scapularis	102 (13.8 %)	266 (35.9 %)	373 (50.3 %)	0
Liolaemus quilmes	322 (43.5 %)	158 (21.3 %)	261 (35.2 %)	0
Liopholis whitii	183 (24.7 %)	230 (31 %)	328 (44.3 %)	0

[1] Missing data reflect either absence of an element or lack of information in the original source.

Vertebrae and ribs. Regarding vertebrae and ribs, there are not only differences in the timing of the onset of ossification, but also within the ossification gradient of the subgroups of vertebrae (centra, neural arches and ribs) among the studied squamates. In *Liopholis whitii*, *Zootoca vivipara* (*Lacerta vivipara* Jacquin), *L. agilis exigua*, *Tupinambis merianae* and *T. rufescens*, the ossification of the vertebrae proceeds along distinct anteroposterior and ventrodorsal gradients (Rieppel 1992a, 1994; Federico & Lobo 2006). Thus, first the ventral part of the centrum is affected, with the pattern then spreading dorsally over its lateral sides to the neural arches in a strict anteroposterior temporal sequence. Following the beginning of ossification of the centra and neural arches, the ribs take up Alizarin Red also along this distinct anteroposterior gradient. In the cervical, dorsal and caudal vertebrae of *Liolaemus quilmes*, the neural arches, vertebral centra, and the mid-shaft of the ribs begin ossification at the same time (Abdala et al. 1997). Although the vertebral centra start to sequester calcium before the neural arches and ribs in *Liolaemus scapularis* (Lobo et al. 1995), it happens in the absence of an anteroposterior gradient. The centra begin to ossify simultaneously, followed by the neural arches and then the ribs.

Appendicular Skeleton

Pectoral and pelvic girdle. The sequence in the anterior and posterior appendicular skeleton represents the only one that seems to be constant in all lizards studied to date (Rieppel 1992a, b, 1993, 1994; Mohammed et al. 1995; Lobo et al. 1995; Abdala et al. 1997; Maisano 2002 a, b; Federico & Lobo 2006). In all squamates examined, the clavicles represent the first of the pectoral and pelvic girdle structures to take up Alizarin Red. Furthermore, the overall ossification gradient displays little variation: clavicle > interclavicle > ilium, scapula > pubis, coracoid > ischium.

Forelimb and hind limb. In the long bones, the ossification process follows detailed steps described by Mathur & Goel (1976: p. 405) for chondrogenesis and calcification in *Calotes versicolor*: "(I) only peripheral calcification in the mid-diaphyseal region; (II) peripheral calcification in the entire diaphysis accompanied with central calcification in the mid-diaphyseal region; and (III) peripheral and central calcification of the entire diaphysis along with a deeply stained plate near either of the distal ends of the diaphysis."

For chondrogenesis, the pattern of the digital arch and primary axis (Burke & Alberch 1985; Fabrezi et al. 2007) was observed in the zeugopods. There is a strict postaxial dominance of ossification in the zeugopods and autopods. This postaxial dominance is characteristic for anurans and amniotes as stated by Fröbisch (2008). The postaxial dominance varies among the studied squamates only in the ossification order of metapodials 3 and 4 among the studied taxa. The ossification gradient in the autopodial region is either metapodial-3 > metapodial-4 > metapodial-2 > metapodial-1 > metapodial-5 or metapodial-4 > metapodial-3 > metapodial-2 > metapodial-1 > metapodial-5. All published accounts for lizards indicate a delay of ossification of metacarpal-5 and -tarsal-5 (Rieppel 1992a, 1994; Lobo et al. 1995; Abdala et al. 1997; Shapiro 2002; Federico & Lobo 2006). In *Liopholis whitii*, *Lacerta agilis exigua* (Rieppel 1994) and *Tupinambis merianae* (Federico & Lobo 2006) there is a predominance in ossification of digit III before digit IV in the manus and a predominance in digit IV before digit III in the pes. In *Zootoca vivipara* (*Lacerta vivipara* Jacquin) (Rieppel 1992a) and *Gehyra oceanica* (Rieppel 1994a), digit III precedes digit IV in both the hind limbs and forelimbs. The ossification gradient of all *Hemiergis* spp. (Shapiro 2002) as well as *Chalcides ocellatus* (Mohammed 1991) strictly reflect the digital arch pattern theory with a predominance of digit IV in both manus and pes.

For every structure of the hind limb, corresponding elements of the forelimb ossify relatively later in all examined lizards. The ossification gradient occurs proximodistally in stylo- and zeugopodial regions, as well as in the phalanges (Fabrezi et al. 2007). In the hind limb, the astragalus (or the astragalar portion in the case of a compound element) is often the first of all carpals and tarsals to show ossification (Rieppel 1992a, 1992b, 1993, 1994; Mohammed et al. 1995; Lobo et al. 1995; Abdala et al. 1997; Maisano 2002 a, b; Shapiro 2002; Federico & Lobo 2006). In all *Hemiergis* spp. the calcaneum and distal tarsal-4 ossify before the astragalus (Shapiro 2002). The usual tarsal gradient is reported as: astragalus > calcaneum > dt-4 > dt-3. The order of the carpal elements is stated as follows: ulnare > dc-4 > dc-3, centrale > dc-2 > radiale > dc-5 > pisiforme > dc-1 > intermedium. The time of onset of calcification is highly variable among the studied species. *Liopholis whitii* shows rather advanced development of the beginning of Alizarin Red uptake in the carpals and tarsals. Many other squamates show ossification of these structures only postnatally, and not prenatally.

The autopodial region not only varies in its dominance order but shows also differences in its composition: elements often appear during chondrogenesis and fuse or are resorbed afterwards (Romer 1956; Mathur & Goel 1976; Shubin & Alberch 1986). The adult of the last common ancestor of recent lizards is hypothesized to have had two proximal carpals, one centrale, one intermedium, one pisiforme, and five distal carpals in the manus; one large and fused proximal complex and two distal tarsals (dt-3 and dt-4) in the pes (Romer 1956; Rieppel 1992b). In *Chalcides ocellatus*, no other distal tarsals besides dt-3 and dt-4 are observed (Mohammed 1991). In contrast, *Calotes versicolor* exhibits three elements in the distal tarsal row in adult individuals, tarsals 1, 3 and 4 which increase in size in that order (Mathur & Goel 1976). In embryos of *Calotes* each of these elements appears separately and there is no evidence of tarsals-2 and -5. It is noteworthy that all

the reptiles in which metatarsal-5 is hooked, tarsal-5 is always missing, although the reverse is not true (Mathur & Goel 1976). As described above, in *Liopholis whitii* there is an early appearance of dt-1, dt-2 and an intermedium, but these vanish after a short period. In the adult of *Liopholis whitii* a bony intermedium between the distal heads of the radius and ulna is visible. In the agamid *Calotes versicolor* and the skink *Chalcides ocellatus*, the only intermedium described is a transient cartilage in early embryonic stage (before stage 34), fusing or disappearing later in ontogeny (Mathur & Goel 1976; Mohammed 1991). Fabrezi et al. (2007) found neither an embryonic nor a bony intermedium in *Liolaemus multicolor*, *L. quilmes*, *L. zullyi* and *Tubinambis merianae*.

When focusing on morphogenesis of the astragalus and calcaneum, Mohammed (1991) described a third element in *Chalcides ocellatus* (stage 34) which he claimed to be the distal centrale. This structure was not observed in *Liopholis whitii*, perhaps due to limited sampling. At stage 35 of *Chalcides ocellatus*, Mohammed (1991) reported the cartilaginous fusion of the astragalus and calcaneum.

Conclusions

In general terms, the sequence of ossification regarding the whole skeleton of *Liopholis whitii* corresponds to that of *Lacerta agilis exigua* (Rieppel 1994) and *Tupinambis merianae* (Federico & Lobo 2006). However, *Liopholis whitii* still differs in the ossification gradient of the cranium, which shows parts of the neurocranium ossifying first, unlike the situation in the remainder of studied lizards in which ossification occurs first in the dermatocranium.

The squamate ossification sequence of the vertebral column seems to be stable (centra, neural arches, ribs), as is that of the pectoral and pelvic girdle. The onset of calcification of the clavicle precedes that of the chondral elements of both girdles. The ilium is the first element to show ossification in the pelvic girdle, more or less simultaneously with the scapula and interclavicle. Uptake of Alizarin Red starts in the ischium, pubis and coracoid at a time when ossification is already advanced in the sacral vertebral region. *Liolaemus scapularis* displays a separate sequence of ossification in the centra, neural arches and ribs, but without an anteroposterior ossification gradient. Each element starts as groups synchronously (centra, neural arches, ribs) (Lobo et al. 1995).

The outcomes of the current study of ossification sequence pattern adds further evidence to the concept of decoupling of ossification from chondrogenesis, as shown by Rieppel (1994b) for *Lacerta agilis exigua* and by Federico & Lobo (2006) for *Tupinambis merianae*. For ossification, *Lacerta agilis exigua*, *Tupinambis merianae* and *Liopholis whitii* show a predominance of the fourth digit in the pes but a predominance of the third digit in the manus. In *Zootoca vivipara* (*Lacerta vivipara* Jacquin), Rieppel (1992a) detected intraspecific heterochronic shifts in the onset of ossification of digit III and IV in the manus. A few specimens of *Zootoca vivipara* (*Lacerta vivipara* Jacquin) showed a predominance of digit III in the forelimb whereas the majority displayed predominance of the fourth one.

Acknowledgements

This work would not have been possible without the generous help of Mark Hutchinson from the South Australian Museum in Adelaide, who provided the specimens on which this study is based and made important suggestions for comparative literature. We also thank the Paleontological Institute and Museum of the University of Zürich, members of our group T. Scheyer, I. Werneburg and L. Wilson, for advice and help. Additionally, we are thankful to Johannes Müller and on anonymous reviewer for helpful comments to improve the manuscript. At last, we thank Peter Giere of the Natural History Museum in Berlin for curation of the skink series studied here. This project was funded by Swiss National Science Foundation (3100A0–116013 to MRS-V).

References

Abdala, F., Lobo, F. & Scrocchi, G. 1997. Patterns of ossification in the skeleton of *Liolaemus quilmes* (Iguania: Tropiduridae). – Amphibia-Reptilia 18: 75–83.

Avery, D. F. & Tanner, W. W. 1964. The osteology and mycology of the head and thorax regions of the obesus group of the genus *Sauromalus* Dumeril (Iguanidae). – Brigham Young University Science Bulletin, Biology Series 5: 1–30.

Bellairs, A. d'A. & Kamal, A. M. 1981. The chondrocranium and the development of the skull in recent reptiles. *In* Gans, C. & Parsons T. S. (eds). Biology of the Reptilia, Morphology F. Academic Press, New York 11: pp. 1–263.

Burke, A. C. & Alberch, P. 1985. The development and homologies of the chelonian carpus and tarsus. – Journal of Morphology 186: 119–131.

Camp, C. 1923. Classification of lizards. – Bulletin of the American Museum of Natural History 48: 289–481.

Chapple, D. G. & Keogh, J. S. 2005. Complex mating system and dispersal patterns in a social lizard, *Egernia whitii*. – Molecular Ecology 14: 1215–1227.

Chapple, D. G. & Keogh, J. S. 2004. Parallel adaptive radiations in arid and temperate Australia: molecular phylogeography and systematics of the *Egernia whitii* (Lacertilia: Scincidae) species group. – Biological Journal of the Linnean Society 83: 157–173.

Conrad, J. L. 2008. Phylogeny and systematics of Squamata (Reptilia) based on morphology. – Bulletin of the American Museum of Natural History 310: 1–182.

Dingerkus, G. & Uhler, L. D. 1977. Enzyme clearing of Alcian Blue stained whole small vertebrates for demonstration of cartilage. – Stain Technology 52: 229–232.

Estes, R. & Pregill, G. 1988. Phylogenetic relationships of the lizard families. Stanford University Press, Stanford, California: pp. 1–631.

Fabrezi, M., Abdala, V. & Martinez Oliver, M. I. 2007. Development basis of limb homology in lizards. – Anatomical Record 290: 900–912.

Federico, A. & Lobo, F. 2006. Patrones de osificacion en *Tupinambis merianae* y *Tupinambis rufescens* (Squamata: Teiidae) y patrones generales en Squamata. – Cuadernos de Herpetología 20 (1): 3–23.

Fischer, D. L. & Tanner, W. W. 1970. Osteological and mycological comparisons of the head and thorax regions of *Cnemidophorus tigris septentrionalis* Burger and *Ameiva undulate parva* Barbour and Noble (Family Teiidae). – Brigham Young University Science Bulletin, Biology Series 11: 1–39.

Fröbisch, N. 2008. Ossification patterns in the tetrapod limb – conservation and divergence from morphogenetic events. – Biological Reviews 83: 571–600.

Gardner, M. G., Bull, C. M. & Cooper, S. J. B. 2002. High levels of genetic monogamy in the group-living Australian lizard *Egernia stokesii*. – Molecular Ecology 11: 1787–1794.

Gardner, M. G., Hugall, A. F., Donnellan, S. C., Hutchinson, M. N. & Foster, R. 2008. Molecular systematics of social skinks: phylogeny and taxonomy of the *Egernia* group (Reptilia: Scincidae). – Zoological Journal of the Linnean Society 154: 781–794.

Good, D. A. 1995. Cranial ossification in the northern alligator lizard, *Elgaria coerulea* (Squamata: Anguidae). – Amphibia-Reptilia 16: 157–166.

Greer, A. E. 1991. Limb reduction in Squamates: identification of the lineages and discussion of the trends. – Journal of Herpetology 25 (2): 166–173.

Greer, A. E., Caputo, V., Lanza, B. & Palmieri, R. 1998. Observations on limb reduction in the scincid lizard genus *Chalcides*. – Journal of Herpetology 32 (2): 244–252.

Jerez, A. & Tarazona, O. A. 2008. Appendicular skeleton in *Bachia bicolor* (Squamata: Gymnophthalmidae): osteology, limb reduction and postnatal skeletal ontogeny. – Acta Zoologica 90 (1): 42–50.

Lemus, D. A. 1967. Contribución al studio de la embriología de reptiles chilenos II. Tabla de desarrollo de la lagartija vivípara *Liolaemus gravenhorti* (Reptilia: Squamata: Iguanidae). – Biologica 40: 39–61.

Lobo, F., Abdala, F. & Scrocchi, G. 1995. Desarrollo del esqueleto de *Liolaemus scapularis* (Iguania: Tropiduridae). – Bollettino del Museo Regionale di Scienze Naturali, Torino 13 (1): 77–104.

Liem, K. F., Walker, W., Bemis, W. E. & Grande, L. 2001. Functional anatomy of the vertebrates: an evolutionary perspective. Harcourt College Publishers, Philadelphia, 3rd edition: pp. 1–784.

Maisano, J. A. 2001. A survey of state of ossification in neonatal squamates. – Herpetological Monographs 15: 135–157.

Maisano, J. A. 2002a. Postnatal skeletal ontogeny in *Callisaurus draconoides* and *Uta stansburiana* (Iguania: Phrynosomatidae). – Journal of Morphology 251: 114–139.

Maisano, J. A. 2002b. Postnatal skeletal ontogeny in five xantusiids (Squamata: Scleroglossa). – Journal of Morphology 254: 1–38.

Mathur, J. K. & Goel, S. C. 1976. Patterns of chondrogenesis and calcification in the developing limb of the lizard, *Calotes versicolor*. – Journal of Morphology 149: 401–420.

Mohammed, B. H. M., Khalifa, S. A., El-Sayad, F. I. & Ibrahim, S. A. 1995. Comparative analysis of ossification in the appendicular skeleton in some scincid lizards (Scincidae: Reptilia). – Journal of Egyptian-German Society for Zoology 17 B: 93–119.

Mohammed, B. H. M. 1991. Morphogenesis of the carpus and tarsus in the skink *Chalcides ocellatus* (Scincidae, Reptilia). – Journal of Egyptian-German Society for Zoology 4: 357–373.

Peter, K. 1904. Normentafel zur Entwicklungsgeschichte der Zauneidechse (*Lacerta agilis*). *In* Keibel, F. (ed.). Normentafeln zur Entwicklungsgeschichte der Wirbeltiere. Gustav Fischer, Jena: pp. 1–165.

Renous-Lécuru, S. 1973. Morphologie comparée du carpe chez les Lepidosauriens actuels (Rynchocéphales, Lacertiliens, Amphisbéniens). – Gegenbaurs Morphogisches Jahrbbuch Leipzig 119: 727–766.

Richardson, M. K., Gobes, S., Leeuwen, A. van, Poelman, A., Pieau, C. & Sánchez-Villagra, M. R. 2009. Heterochrony in Limb Evolution: Developmental Mechanisms and Natural Selection. – Journal of Experimental Zoology, Molecular Development and Evolution 312 B: 639–664.

Rieppel, O. 1992a. Studies on skeleton formations in reptiles. III. Patterns of ossification in the skeleton of *Lacerta vivipara* Jacquin (Reptilia: Squamata). – Fieldiana Zoology, N.S. 68: 1–25.

Rieppel, O. 1992b. Studies on skeleton formation in reptiles. I. The postembryonic development of the skeleton in *Cyrtodactylus pubisulcus* (Reptilia: Gekkonidae). – Journal of Zoology, London 227: 87–100.

Rieppel, O. 1993. Studies on skeleton formation in reptiles. II. *Chamaeleo hoehnelii* (Squamata: Chamaeleoninae), with comments on the homology of carpal and tarsal bones. – Herpetologica 49 (1): 66–78.

Rieppel, O. 1994a. Studies in skeleton formation in reptiles. Patterns of ossification in the limb skeleton of *Gehyra oceanica* (Lesson) and *Lepidodactylus lugubris* (Duméril & Bibron). – Annales des Sciences Naturelles Zoologie, Paris 13 (15): 83–91.

Rieppel, O. 1994b. Studies on skeleton formation in reptiles l. Patterns of ossification of *Lacerta agilis exigua* Eichwald (Reptilia, Squamata). – Journal of Herpetology 28 (2): 145–153.

Rieppel, O. & Zaher, H. 2001. The development of the skull in *Acrochordus granulatus* (Schneider) (Reptilia: Serpentes), with special consideration of the otico-occipital complex. – Journal of Morphology 249: 252–266.

Rieppel, O. & Grande, L. 2007. The anatomy of the fossil varanid lizard *Saniwa ensidens* Leidy, 1870, based on a new discovered complete skeleton. – Journal of Paleontology 81 (4): 643–665.

Robinson, P. L. 1975. The functions of the hooked fifth metatarsal in lepidosaurian reptiles. Colloques Internationaux C.N.R.S. 218: 461–483.

Romer, A. S. 1956. Osteology of the reptiles. University of Chicago Press, Chicago.

Shapiro, M. D. 2002. Development morphology of limb reduction in *Hemiergis* (Squamata: Scincidae): Chondrogenesis, osteogenesis, and heterochrony. – Journal of Morphology 254: 211–231.

Shapiro, M. D., Hanken, J. & Rosenthal, N. 2003. Developmental basis of evolutionary digit loss in the Australian lizard *Hemiergis*. – Journal of Experimental Zoololgy (Molecular and Developmental Evolution) 297 B: 48–56.

Shapiro, M. D., Shubin, N. H. & Downs, J. P. 2008. Limb diversity and digit reduction in reptilian evolution. *In* Hall, B. K. (ed.). Fins and Limbs: Evolution, Development, and Transformation. University of Chicago Press, Chicago: pp. 225–244.

Shubin, N. H. & Alberch, P. 1986. A morphogenetic approach to the origin and basic organization of the tetrapod limb. – Evolutionary Biology 20: 319–387.

Skinner, M. M. 1973. Ontogeny and adult morphology of the skull of the South African skink, *Mabuya capensis* (Gray). – Annale Universiteit Stellenbosch 48, Series A (3): 1–116.

Velhagen, W. A. 1997. Analyzing developmental sequences using sequence units. – Systems Biology 46: 204–210.

Character matrix of the event pairing analysis of the osteogenetic sequences in the terrestrial surface dwelling lacertilian squamates

Liopholis whitii

0222212211 2222222222 1221110022 1110012211 1001122222 1122222222
1122212211 1001110022 1110011100 1221110011 1001122222 2222222222
2222222222 2222212222 2112221122 2002222211 2221122200 1221110011
1001110000 2222211222 1122200112 2222211222 1122200112 1222221122
2112220011 2112222211 2221122200 1121112222 2112221122 2001121111
2222211222 1122200112 1111122111 0011100111 0000100000 0221110011
1001110000 1000000122 1110011100 1110000100 0000112222 2222222222
2002222222 2222222222 2222222222 1122222222 2222222222 2222222222
1122222222 2222212222 2222222222 2112222222 2222221122 1110011100
1110000100 0000111000 0221110011 1001110000 1000000111 0000122111
0011100111 0000100000 0111000011 2211100111 0011100001 0000001110
0001112222 2222222222 2002222222 2222210002 2222211100 1110011100
0010000001 1100001111 0

Lacerta vivipara

2212112222 ?????22222 ?22220?022 220?012111 0?00022220 ?011222222
?222222111 0?00010021 110?000100 121110?000 1001122222 ?222222222
22222?2222 2222222222 0?01121022 2002222O?0 1121022200 122220?011
2102220011 22220?0112 1022200111 22221?0222 2022200222 222220?011
2102220011 1102222l?0 2222022200 2222122222 2?12222022 2002222222
22222?2222 2222220222 2222221110 ?000100111 0000000000 021110?000
1001110000 0000000121 110?000100 1110000000 0000112222 2?12222022
2002222222 1022222222 ?222222222 1022222222 0222222222 ?222222222
2122222222 2222222222 2?22222222 2102222222 2022221021 110?000100
1110000000 0000111000 021110?000 1001110000 0000000111 0000121110
?000100111 0000000000 0111000011 21110?0001 0011100000 0000001110
0001112222 2?02222022 2002222222 0022200002 2222222O?0 1121022200
1111010002 2200002222 0

Lacerta agilis exigua

2212112111 2222222222 1100000020 0000021000 0001021111 0022222222
1122220000 0000000000 0000000000 1000000000 0001122222 2222222222
2222222222 2222212000 0002120022 2002000000 2120022200 1200000021
2002220011 2000000212 0022200111 2000000212 0022200111 1222222222
2222220022 2222222211 2222122200 2222202222 2112222122 2002222201
2222222222 2222200222 2212200000 0000000111 0000000000 0000000000

0001110000 0000000100 0000000000 1110000000 0000112222 2222222222
2002222222 2222222222 2222222222 1122222222 2222222222 2222222222
1122222222 2222212222 2222222222 2112222222 2222221120 0000021200
2220011111 0000222000 0200000021 2002220011 1110000222 0000120000
0021200222 0011111000 0222000011 2000000212 0022200111 1100002220
0001112000 0002120022 2001111100 0022200001 1112111100 2221022200
2222200002 2200002222 2

Liolaemus scapularis

2202012011 2011120111 1212222220 1111101000 0000021222 2212221222
2212211000 0000010021 2222212211 2212222212 2112122222 2222222222
2222222222 2222212122 2221221121 1002122222 1221121100 1212222212
2112110011 2122222122 1121100111 2122222122 1121100111 1212222212
2112110011 1112122222 1221121100 1111112122 2221221121 1001111111
2122222122 1121100111 1111120111 1101200200 0000000000 0212222212
2112110011 1111111221 2222212211 2110011111 1111212222 2222222222
2002222222 2222222222 2222222222 1122222222 2222222222 2222222222
1122222222 2222212222 2222222222 2112222222 2222221121 2222212211
2110011111 1111211000 0212222212 2112110011 1111111211 0000121222
2212211211 0011111111 1211000011 2122222122 1121100111 1111112110
0001112222 2222222222 2002222222 2222210002 2222122222 1221121100
1111111112 1100001111 0

Liolaemus quilmes

2222212211 2211122111 1221111100 0000000000 0000021000 0002221000
0002210000 0000010021 0000002211 2210000002 2112122222 2222222222
2222222222 2222210000 0000120020 0000000000 0120020000 1000000001
2002000011 0000000012 0020000111 0000000012 0020000111 1210000002
2112110022 2222100000 0221121100 2222212100 0000221121 1002222211
2100000022 1121100222 2211100000 0001200200 0011111000 0210000002
2112110022 2221111221 0000002211 2110022222 1111212222 2222222222
2002222222 2222222222 2222222222 1122222222 2222222222 2222222222
1122222222 2222212222 2222222222 2112222222 2222221100 0000001200
2000011111 0000100000 0000000001 2002000011 1110000100 0000100000
0001200200 0011111000 0100000011 0000000012 0020000111 1100001000
0001110000 0000120020 0001111100 0010000001 1112100000 0221121100
2222211112 1100002222 2

Chapter 3:

Heterochronic shifts in the ossification sequences of surface and subsurface-dwelling skinks are correlated with the degree of limb reduction

Jasmina Hugi, Mark N. Hutchinson and Marcelo R. Sánchez-Villagra

Submitted to *Zoology*

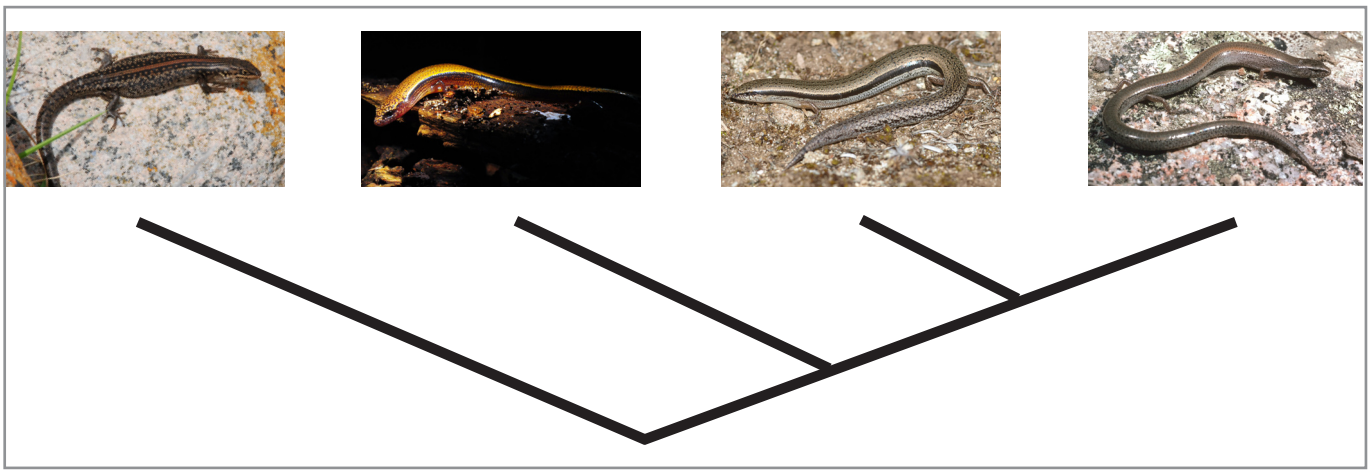

Photographies: M. Hutchinson, Ian Williams, Nadav Pezaro

Heterochronic shifts in the ossification sequences of surface and subsurface-dwelling skinks are correlated with the degree of limb reduction

Jasmina Hugi[1*], Mark N. Hutchinson[2] and Marcelo R. Sánchez-Villagra[1]

[1]Palaeontological Institute and Museum, University of Zurich, Karl Schmid-Straße 4, 8006 Zurich, Switzerland
[2]South Australian Museum, North Terrace, Adelaide SA 5000, Australia

*corresponding author: jasmina.hugi@pim.uzh.ch, Tel. +41-44 634 23 47, Fax +41-44 634 49 23

Abstract

Scincid lizards exhibit a variety of limb anatomies which reflect the functional requirements of different modes of life. Besides surface-dwellers which show neither body elongation nor limb reduction, there are numerous examples that can be arranged as increasingly serpentiform taxa that move in sand, humus or leaf-litter. We explored the question of whether limb reduction and body elongation in skinks with attenuate body plans are linked to heterochronic shifts in the ossification sequences. Ossification sequences were studied and compared in skinks showing four different stages of limb reduction: *Liopholis whitii*, *Lerista bougainvillii*, *Hemiergis peronii* and *Saiphos equalis*. Results showed that: 1) scincid lizards with limb reductions show an earlier onset of ossification in the cervical vertebrae, and 2) ossification starts earlier in the proximal parts of the pectoral girdle (scapula and coracoid) and pelvic girdle (ilium, ischium and pubis) relative to the timing of the onset in elements of the forelimbs and hind limbs. Furthermore, the morphotypes with body elongation and/or limb reduction show 3) an earlier strengthening of the premaxilla, which first completes the anterior part of the dorsal cranial roof, and 4) an earlier onset in the forelimb elements than in the equivalent elements of the hind limbs. Among the taxa showing elongation and limb reduction, the species showing the least limb reduction (*L. bougainvillii*) had the greatest developmental similarity to the normally-proportioned surface-dwelling species (*L. whitii*). *S. equalis*, as the morphotype with the greatest deviations from the normally proportioned, pentadactyle form, varies the most from *L. whitii*. The heterochronic shifts in the ossification sequences are linked to a shift in the emphasis from limbed locomotion to trunk locomotion (lateral undulation) in the species with body elongation and/or limb reduction.

Introduction

The phenomenon of limb reduction and its underlying developmental processes is a classic topic in evolutionary biology and tetrapod morphology. The squamates have undergone numerous limb reduction events, sometimes with multiple events occurring within single evolutionary lineages. In some cases sets of morphological character states can be arranged as an evolutionary series of morphotypes in related taxa (e.g., Gans, 1975; Siler and Brown, in press). Such lineages therefore include a variety of morphotypes, ranging from some that show neither body elongation nor limb reduction to forms with a moderately to strongly serpentiform body shape (Greer, 1991; Caputo et al., 1995; Wiens et al., 2006; Skinner et al., 2008; Brandley et al., 2008). Scincid lizards are a diverse group of lacertilian squamates which are widely distributed in all continents except Antarctica (e.g., Mattison, 1989; Hutchinson, 1993). Various different morphotypes are recognised, each broadly related to their ecology, including surface-dwellers, "sand-swimmers" and forms that move in humus or leaf-litter. The two latter groups show body elongation and/or limb reduction, but use their limbs to a varying degree when on the surface and shift to lateral undulation with adpressed limbs when moving below the surface (e.g., Choquenot and Greer, 1989; Caputo et al., 1995). Limb reduction in skinks can vary from reduction in relative limb size, to the loss of single phalangeal elements, entire digits and ultimately the entire limb. Elements are always lost along the long axis, i.e., digit IV, or the distal expanses of the foot, i.e., digit I and V (Greer, 1987, 1990, 1991; Wiens et al., 2006; Wiens, 2009). If there were any functional reasons to reduce the region of the foot along either of these major axes, i.e., to shorten the reach of the foot or to narrow its span, the digits most likely involved would be the ones which are actually affected. Skeletal elements that get lost entirely are among the last to condense and chondrify in the developmental sequence in many cases (e.g., Shapiro et al., 2007).

The early development of skeletal elements comprises the mesenchymal condensation and chondrification events that follow two conserved pathways in tetrapods: anurans and amniotes show a proximodistal direction across the limb compartments (after Rieppel, 1993a) with a postaxial dominance in the autopodium (e.g., Shubin and Alberch, 1986). Urodeles, in contrast, show a preaxial dominance in both the zeugopodial and autopodial region with a proximodistal direction across the entire limb (e.g., Erdmann, 1933; Shubin and Alberch, 1986; Nye et al., 2003). The subsequent ossification sequences are often not simple recapitulations of the preceding developmental program of condensation and chondrification (e.g., Rieppel, 1992a; Rieppel, 1994a, b) and show plasticities in the timing, which are influenced by functional requirements in both amniotes and anamniotes. The terrestrial surface dwelling lacertilian squamates with non-reduced limbs and no body elongation form one group within the Amniota that shows rather conserved ossification sequences. For them, only minor heterochronic shifts regarding for example the position of the first digit that starts ossification at the postaxial side of the autopodial region have been reported (Rieppel, 1993a; Mohammed et al., 1995; Federico and Lobo, 2006; Fröbisch, 2008; Hugi et al., 2010). There is less information available for elongate, limb-reduced species, although the studies of

Shapiro (2002, 2003) have been an important contribution to this area of research.

Here we describe the ossification sequences and parts of the chondrification in a set of four scincid lizard species that show a trend towards increasing limb reduction and elongation, from fully surface-dwelling and pentadactyle species, to elongate, fossorial and tridactyle forms. The phylogenetic breadth and the methods employed address the question: how conserved are ossification sequences among lizards with different lifestyles? Event-pairing analysis is used as a comparative approach to study the extent of possible heterochronic shifts in the ossification data (Velhagen, 1997).

Material and Methods

The study is based on the ontogenetic series of four scincid lizard species from Australia. *Liopholis whitii* is a surface-active, pentadactyle species with robust limbs and the plesiomorphic presacral vertebral count of 26. *Lerista bougainvillii* is a semifossorial species with an elongate body (35-38 presacral vertebrae) but it retains a pentadactyle forelimb and hind limb. *Hemiergis peronii* and *Saiphos equalis* are both markedly elongate and fossorial in habits (according to Greer 1987, 1989 presacral vertebral counts range between 34-38 and 38-40 respectively) and show pronounced reduction in limb size accompanied by loss of phalanges (digital formula 4-4 in *H. peronii*, 3-3 in *S. equalis*). Embryos of *L. whitii* and *H. peronii* were obtained from specimens in the collection of the South Australian Museum, Adelaide, those of *S. equalis* from material collected by Prof. M. B. Thompson, University of Sydney, and those of *L. bougainvillii* from females collected near Burra, South Australia, during November 2009. Specimens examined were as follows: *Liopholis whitii* (snout-vent length SVL 13.4–31.4 mm; Naturkundemuseum Berlin; Hugi et al., 2010), *Hermiergis peronii* (SVL 3.4–26.5 mm), *Saiphos equalis* (SVL 6.1–30.0 mm) and *Lerista bougainvillii* (SVL 6.0–30.3 mm). The latter three series are deposited in the collection of the Paleontological Institute and Museum of the University of Zurich (PIMUZ).

Embryos were dissected out of female specimens (*L. whitii, H. peronii*, most *S. equalis*) or from shelled eggs (all *L. bougainvillii* and two *S. equalis*) and subsequently fixed in 4% neutral buffered formaldehyde for the first 24 hours and then placed into 70% ethanol. Morphological description is based on observations with a Leica MZ-16 dissection microscope; pictures were taken with a DFC 420C digital camera and IM 50 software, the drawings were processed with Adobe Illustrator CS3. The embryos were ordered based on body length, which was measured using digital callipers to the nearest 0.1 mm. Body length is defined as the distance between the tip of the snout and the end of the cloaca, a standard measurement in squamate research (Maisano 2001, 2002a, b). Specimens were subject to a clearing and double-staining procedure (Dingerkus and Uhler, 1977), with modifications by Hiroshi Nagashima, Kobe (pers. comm. 2007). This procedure visualises the onset of chondrogenesis and ossification. The chondrogenic sequences are only preserved in the autopodial regions of both the forelimbs and hind limbs of all four skinks. No distinction is made between onset of calcification and onset of ossification as both are part of a continuous fluent process. The first visible uptake of Alizarin red, i.e., as red stained areas in the bones, is interpreted as the onset of ossification (Table 1). The data on the timing

of the onset of ossification relative to the size of the embryo is complemented with data on the first appearance of red staining, relative to its first appearance in all of the other elements. (Table 1: numbers in brackets). To further visualize heterochronic shifts in the ossification sequences of the four scincid lizard species, data of four surface dwelling lizard species with non-reduced limbs were included for performing the event-pairing method (Velhagen, 1997; Table 2). Some elements of Table 2 are treated as compartments of skeletal groups as defined in terms of function and/or topographical region and/or members of a metameric series (Hugi et al., 2010). The first structure that ossifies within each compartment is taken to represent the onset of ossification of the group as a whole (e.g., jugal in the dermatocranium). Besides grouping of elements, some skeletal elements are neither included in groups nor listed separately in Table 2 (e.g., pisiform, radiale, phalanges) due to invariable timing of onset of ossification (postnatal ossification/never ossified) or a lack in resolution in all examined squamates (e.g., no further division within the phalanges). The 35 characters of the eight lizard species included result in 595 event-pairs. Three character states reflect the timing of one event relative to another (Table 3): before (0), simultaneously (1), or after (2) (Velhagen, 1997). Simultaneous events, which are ties, probably result from a lack in resolution, since it is unlikely that ossification of two or several bones occurs at exactly the same time.

Maisano (2001, 2002a, b) provided a standardized usage of skeletal terms in earlier studies, which is followed here. Symphyses in the pectoral girdle, as well as symphyses and processes in the pelvic girdle (iliac process, epi- and prepubis, ischial symphysis and metaischial process) only ossify in neonates within secondary ossification centres (e.g., Rieppel, 1992b; Maisano, 2001, 2002a, b; Jerez and Tarazona, 2008). Processes of the pectoral girdle (suprascapula and epicoracoid), as well as the sternum calcify but never ossify (Mohammed et al., 1995). Furthermore, the elements in the skull neither fuse, nor, in some cases, do they completely ossify (e.g., there is still a parietal fontanelle in the largest embryo) in embryos. The neural arches do not fuse to the corresponding centra in the embryological series.

We revise some of the results reported by Hugi et al. (2010) on *L. whitii*. Corrected data comprise: 1) the timing of the beginning of chondrogenesis can be documented in the autopodial regions of the smallest specimen of the series (nr. 102), where it shows a proximodistal gradient with a postaxial dominance. The data on the rest of the skeletal elements refer to the first visible resorption of cartilaginous tissue, therefore to a process which is involved in the process of early ossification. Hugi et al. (2010, Figs. 1 and 2) confused the onset of ossification of the supraoccipital with the appearance of calcified endolymph in the endolymphatic sacs as these elements in the posteroventral cranial region are already stained in very small embryos. The plate that borders the calcified endolymphatic sacs along their ventral margin is now recognized as the supraoccipital in Figure 2 of Hugi et al. (2010). The revision also showed that the exoccipital is the first neurocranial element that starts ossification, a condition common in other lizards as well (e.g., Rieppel, 1993b; Mohammed et al., 1995; Maisano, 2002; Federico and Lobo, 2006). As a result, this is further evidence that there are no unequivocal phylogenetic differences in the

ossification sequences between *L. whitii* and the other surface-dwelling lizards included in the event-pairing and Paup analysis of Hugi et al. (2010). In this study, we added the corrected data of *L. whitii* in Table 1 and Table 2 and performed an event-pairing analysis including the available data.

Results

Cranium

The endolymph in the endolymphatic sacs is the first element that starts to store calcium in early ontogenetic stages in all species (Table 1). Common trends in the onset of ossification between the four scincid species are: 1) regions of the dermatocranium are first to ossify, starting with the palate (first: pterygoid), 2) followed by regions of the mandible (e.g., angular, coronoid, dentary, surangular, splenial), 3) the rest of the palate (e.g., palatine, vomer) and 4) orbital region (first: jugal). The first ossification in the neurocranium occurs in the exoccipital in all scincid species, shortly followed by the onset of ossification in the splanchnocranium (first: quadrate). The rest of the braincase starts ossification synchronously with the ceratobranchial II of the hyoid apparatus among the last cranial elements. One unambiguous difference between the order of ossification within the cranium between *Liopholis whitii* and the three skinks with body elongation and/or limb reduction is the timing of the onset of ossification in the premaxilla. In *L. whitii* this starts relatively late, at a time when ossification of the vertebrae, as well as the forelimbs and hind limbs, has begun. In the limb-reduced species, the premaxilla begins to ossify shortly after the first onset of ossification in the humerus. The whole of the cranium of the three lizard species with body elongation and/or limb reduction starts ossification somewhat earlier than the postcranial skeleton when compared to *L. whitii*.

Vertebral column

In all scincid lizards, the ossification pattern shows an anteroposterior gradient along the central body axis in all vertebral parts (centra, neural arches and ribs) (Table 1). The order is as follows: elements of the cervical vertebrae > dorsal vertebrae > sacral vertebrae > caudal vertebrae. The first retention of Alizarin red is always displayed in the centra, followed by the neural arches which themselves precede the ribs. Ossification generally starts at the proximal shaft region in the ribs and subsequently expands to the distal shaft end. The resorption of the cartilage, in contrast, starts first at mid-shaft area. Ossification starts at the ventral base of the neural arches and expands dorsally. The dorsal-most tips of the spinal processes are the last parts of the vertebrae that start ossification, lagging behind the articulation facets of the centra (pre- and postzygapophyses, diapophysis and parapophysis), as well as of the ribs (tubercle and capitulum; distal shaft end). The transverse processes start ossification before the articulation areas between the centra, followed by the articulation surfaces of the ribs which precede the dorsalmost tip of the neural arches. The cervical vertebrae start ossification simultaneously with the humerus in *H. peronii* and *S. equalis*, whereas they lag behind the humerus in *L. whitii* and *L. bougainvillii*. The difference in the timing of the onset of

Table 1, next page. Timing of the Onset of the Ossification in the studied skinks.

Onset of Ossification Embryo No.(rel. sequence)					**Region**
Element\Species	*L. whitii*	*L. bougainvillii*	*H. peronii*	*S. equalis*	
Angular	18.6(2)	16.8(2)	12.4(3)	18.8(4)	D
Articular	22(14)	20.3(12)	12.4(6)	26.0(20)	S
Basioccipital	22(13)	20.3 (12)	18.1(12)	26.0(20)	N
Basisphenoid	22(12)	20.3 (12)	18.1(12)	23.4(18)	N
Endolymph calcified	Present 15.7	Present 1	Present 3	Present 2	
Ceratobranchial I	nn(26)	nn(28)	nn(23)	nn(36)	S
Ceratobranchial II	<22(9)	20.3(12)	12.4(6)	26.0(22)	S
Coronoid	18.6(2)	16.8(5)	12.4(4)	23.4(15)	D
Dentary	18.6(3)	16.8(4)	12.4(4)	18.8(7)	D
Epipterygoid	<22(9)	16.8(11)	12.4(5)	23.4(18)	D
Exoccipital	<22(9)	16.8(3)	12.4(3)	23.4(17)	N
Frontal	<22(9)	16.8(6)	12.4(5)	23.4(14)	D
Hyoid corpus	nn(26)	nn(28)	nn(23)	nn(36)	S
Jugal	18.6(5)	16.8(3)	17.0(9)	17.1(10)	D
Maxilla	18.6(4)	16.8(4)	12.4(4)	18.8(7)	D
Nasal	<22(9)	16.8(6)	12.4(4)	23.4(16)	D
Opisthotic	<22(9)	20.3(12)	18.1(12)	23.4(18)	N
Palatine	<22(9)	16.8(5)	12.4(4)	23.4(15)	D
Parietal	18.6(5)	16.8(4)	17.0(9)	18.8(5)	D
Postorbital	<22(12)	16.8(6)	17.0(10)	17.1(12)	D
Prefrontal	<22(10)	16.8(6)	12.4(6)	18.8(5)	D
Premaxilla	22(14)	16.8(5)	12.4(3)	17.1(13)	D
Prootic	<22(12)	20.3(12)	18.1(12)	23.4(17)	D
Pterygoid	15.7(1)	16.8(1)	12.4(1)	18.8(1)	D
Surangular	18.6(2)	16.8(2)	12.4(2)	18.8(2)	D
Septomaxilla	26.5(17)	nn(28)	nn(23)	nn(36)	D
Splenial	18.6(3)	16.8(3)	12.4(3)	18.8(6)	D
Squamosal	18.6(4)	16.8(4)	12.4(3)	17.1(11)	D
Columella	26.5(18)	20.3(12)	18.1(18)	23.4 (17)	S
Supraoccipital	26.5(17)	20.3(12)	18.1(12)	23.4(17)	N
Supratemporal	18.6(4)	16.8(4)	12.4(3)	17.1(12)	D
Quadrate	<22(9)	16.8(6)	12.4(5)	23.4(18)	S
Vomer	<22(9)	16.8(6)	12.4(4)	23.4(15)	D
Clavicula	20.4(6)	16.8(3)	12.4(2)	18.8(3)	Pe
Coracoid	26.5(19)	20.3(16)	18.1(15)	26.0(26)	Pe
Interclavicula	<22(11)	16.8(7)	12.4(4)	23.4(18)	Pe
Scapula	26.5(18)	20.3(15)	17.0(10)	26.0(21)	Pe
Humerus	20.4(8)	16.8(5)	12.4(3)	18.8(8)	Pe

Radius	<22(13)	16.8(6)	12.4(4)	26.0(23)	Pe
Ulna	<22(12)	16.8(6)	12.4(4)	26.0(27)	Pe
Centrale	nn(26)	nn(28)	nn(23)	nn(36)	Pe
Intermedium	nn(26)	nn(28)	nn(23)	nn(36)	Pe
Radiale	nn(26)	nn(28)	nn(23)	nn(36)	Pe
Ulnare	31.4(24)	nn:30.3(24)	nn(23)	30.0(34)	Pe
Pisiform	nn(26)	nn:30.3(26)	nn(23)	nn(36)	Pe
Dc-1	nn(26)	nn(28)	nn(23)	/	Pe
Dc-2	nn(26)	nn(28)	nn(23)	nn(36)	Pe
Dc-3	nn(26)	nn(28)	nn(23)	nn(36)	Pe
Dc-4	31.4(24)	nn:30.3(25)	nn(23)	nn(36)	Pe
Dc-5	nn(26)	nn(28)	nn(23)	nn(36)	Pe
Mc-1	26.5(20)	20.3(12)	/	/	Pe
Mc-2	26.5(19)	20.3(12)	18.1(13)	30.0(32)	Pe
Mc-3	22(14)	16.8(10)	12.4(8)	26.0(30)	Pe
Mc-4	26.5(18)	16.8(11)	17.0(11)	30.0(32)	Pe
Mc-5	26.5(21)	20.3(14)	18.1(15)	/	Pe
Prox. Phal. I	26.5(20)	20.3(14)	/	/	Pe
Prox. Phal. II	26.5(19)	20.3(13)	18.1(14)	30.0(32)	Pe
Prox. Phal. III	22(16)	20.3(12)	18.1(14)	26.0(31)	Pe
Prox. Phal. IV	26.5(20)	20.3(12)	18.1(14)	30.0(32)	Pe
Prox. Phal. V	26.5(20)	20.3(14)	18.1(14)	/	Pe
Int. Phal. I	/	/	/	/	Pe
Int. Phal. II	26.5(20)	20.3(14)	18.1(14)	/	Pe
Int. Phal. III	22(16)	20.3(14)	18.1(14)	30.0(32)	Pe
Int. Phal. IV	26.5(20)	20.3(14)	18.1(14)	30.0(32)	Pe
Int. Phal. V	26.5(20)	20.3(14)	18.1(14)	/	Pe
Term. Phal. I	26.5(20)	22.5(19)	/	/	Pe
Term. Phal. II	26.5(20)	22.5(19)	18.1(15)	30.0(32)	Pe
Term. Phal. III	26.5(20)	22.5(19)	18.1(14)	30.0(32)	Pe
Term. Phal. IV	26.5(20)	22.5(19)	18.1(15)	30.0(32)	Pe
Term. Phal. V	26.5(20)	22.5(19)	18.1(15)	/	Pe
Ilium	26.5(18)	20.3(16)	18.1(14)	23.4(19)	Pl
Ischium	26.5(20)	22.5(19)	18.1(15)	30.0(32)	Pl
Pubis	26.5(19)	20.3(16)	17.0(11)	23.4(19)	Pl
Femur	20.4(7)	16.8(6)	12.4(4)	23.4(19)	Pl
Tibia	20.4(8)	16.8(7)	12.4(5)	26.0(25)	Pl
Fibula	20.4(8)	16.8(7)	12.4(5)	26.0(28)	Pl
Astragalus	28.8(23)	21.9(21)	22.3(20)	30.0(33)	Pl
Calcaneum	31.4(24)	28.0(23)	26.5(22)	nn(36)	Pl

Dt-3	31.4(25)	nn:30.3(27)	nn(23)	nn(36)	Pl
Dt-4	31.4(24)	28.0(22)	nn(23)	30.0(34)	Pl
Mt-1	22(16)	20.3(12)	/	/	Pl
Mt-2	22(15)	20.3(10)	18.1(14)	30.0(32)	Pl
Mt-3	22(14)	20.3(8)	12.4(7)	26.0(30)	Pl
Mt-4	<22(12)	20.3(9)	12.4(7)	30.0(32)	Pl
Mt-5	28.8(23)	22.5(20)	22.3(20)	30.0(32)	Pl
Prox. Phal. I	26.5(19)	20.3(14)	/	/	Pl
Prox. Phal. II	26.5(19)	20.3(13)	18.1(14)	30.0(32)	Pl
Prox. Phal. III	22(16)	20.3(11)	18.1(14)	26.0(31)	Pl
Prox. Phal. IV	22(15)	20.3(12)	18.1(14)	30.0(32)	Pl
Prox. Phal. V	26.5(19)	20.3(14)	18.1(14)	/	Pl
Int. Phal. I	/	/	/	/	Pl
Int. Phal. II	26.5(19)	20.3(14)	18.1(14)	/	Pl
Int. Phal. III	22(16)	20.3(14)	18.1(14)	30.0(32)	Pl
Int. Phal. IV	22(15)	20.3(14)	18.1(14)	30.0(32)	Pl
Int. Phal. V	26.5(19)	20.3(14)	18.1(14)	/	Pl
Term. Phal. I	26.5(19)	22.5(19)	/	/	Pl
Term. Phal. II	26.5(19)	22.5(19)	18.1(15)	30.0(32)	Pl
Term. Phal. III	26.5(19)	22.5(19)	18.1(14)	30.0(32)	Pl
Term. Phal. IV	26.5(19)	22.5(19)	18.1(15)	30.0(32)	Pl
Term. Phal. V	26.5(19)	22.5(19)	18.1(15)	/	Pl
Cervical	<22(10)	20.3(12)	12.4(3)	18.8(9)	Vc
Dorsal	<22(11)	20.3(12)	12.4(5)	26.0(24)	Vc
Sacral	26.5(19)	20.3(12)	18.1(16)	26.0(27)	Vc
Caudal	26.5(20)	20.3(17)	18.1(18)	26.0(29)	Vc
Cervical	<22(11)	20.3(12)	18.1(12)	23.4(17)	Vna
Dorsal	26.5(18)	20.3(15)	18.1(15)	26.0(25)	Vna
Sacral	26.5(20)	20.3(16)	18.1(17)	26.0(29)	Vna
Caudal	26.5(21)	20.3(18)	18.1(19)	26.0(31)	Vna
Dorsal	26.5(19)	20.3(15)	18.1(14)	26.0(26)	Vr
Sacral	26.5(21)	20.3(17)	18.1(17)	26.0(30)	Vr
Caudal	26.5(22)	22.5(19)	22.3(21)	30.0(35)	Vr

Table 1. Timing in the onset of ossification in the skeletal elements. The number in front of the brackets marks the first uptake of red staining in an element, whereas the numbers in brackets represent the relative order of ossification based on the timing of appearance, as well as on the extent of the staining in relation to the progression in another element within one embryo. Abbreviations: D: dermatocranium; N: neurocranium; Pe: pectoral girdle; Pl: pelvic girdle; S: splanchnocranium; Vc: vertebral centrum; Vna: vertebral neural arch; Vr: vertebral rib.

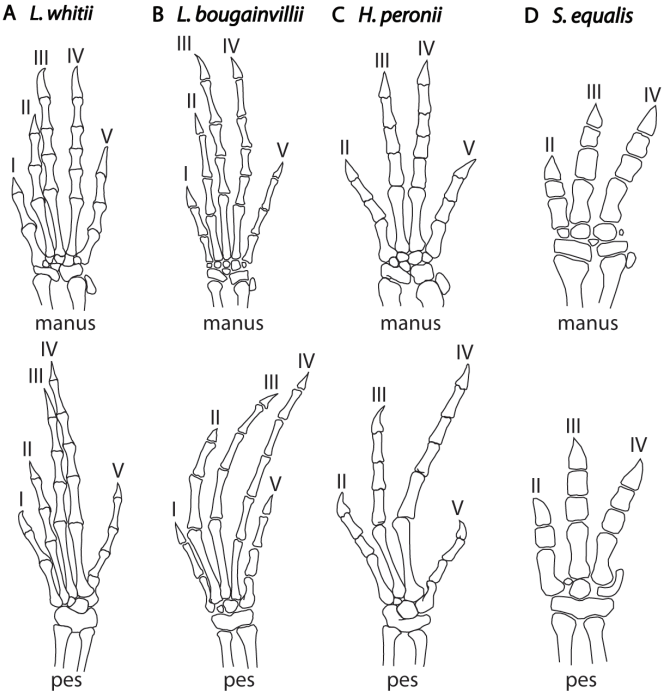

Fig. 1. Drawings of the manus and pes of A*) Liopholis whitii,* B) *Lerista bougainvillii*, C) *Hemiergis peronii* after Choquenot and Greer (1989) and D) *Saiphos equalis*. The lack of a single phalange first occurs in digit V of *L. bougainvillii*, whereas entire digits are lost in digit I before digit V. Abbreviations: D-I to D-V: digit I to digit V.

ossification of the cervical and dorsal vertebrae is well resolved, i.e., in different specimens of *S. equalis*, whereas it is based on the relative extent of the staining in ossification in the other skinks.

Pectoral and pelvic girdle

Shoulder. The clavicula is among the first elements of the entire skeleton that starts ossification in all four scincid lizards. It shows the first retention of Alizarin red directly after the first onset of ossification in the palate in *L. bougainvillii*, *H. peronii* and *S. equalis*. In *L. whitii*, the clavicula retains red staining after the ossification is advanced in the palate, i.e., affecting more elements than only the pterygoid (Table 1). Ossification of the interclavicula starts very early in *L. bougainvillii* and *H. peronii* and, based on the relative extent of the staining, shortly after the humerus, whereas the timing of the onset of ossification is observed in differently sized embryos in *L. whitii* and *S. equalis* (Table 1). *H. peronii*, *L. bougainvillii* and *S. equalis* show a relatively earlier strengthening of the entire proximal part of the pectoral girdle compared to *L. whitii*. The order in the ossification sequence based on the relative extent of the staining, as well as on the timing of the first visible onset of this process is common to all four skinks examined, showing the order: clavicula > interclavicula > scapula > coracoid.

Pelvis. The pelvic girdle shows variation in the order and timing of the ossification sequences between the four scincid lizards, with the ilium starting ossification first in *L. whitii*, and with synchronous onset in the ilium and in the pubis in *S. equalis* and *L. bougainvillii*. *H. peronii* shows the pubis as the first element of the proximal part of the pelvic girdle that starts ossification (Table 1). The entire strengthening of the pelvic girdle occurs relatively earlier in the skinks with body elongation and/or limb reduction in comparison to the data in *L. whitii*. Alizarin red is generally retained first at the mid-shaft areas and then expands to the dorsal and ventral direction.

Forelimb and hind limb. The four scincid species show variation in the number of the skeletal elements in the metapodial and phalangeal region and therefore, a short morphological description of the manus and pes is given for each species (Fig. 1). *L. whitii* shows the phalangeal count of 2-3-4-5-3 in the forelimb and 2-3-4-5-4 in the hind limb (Hugi et al., 2010). Furthermore, it shows no reduction in the mesopodial region of the forelimb

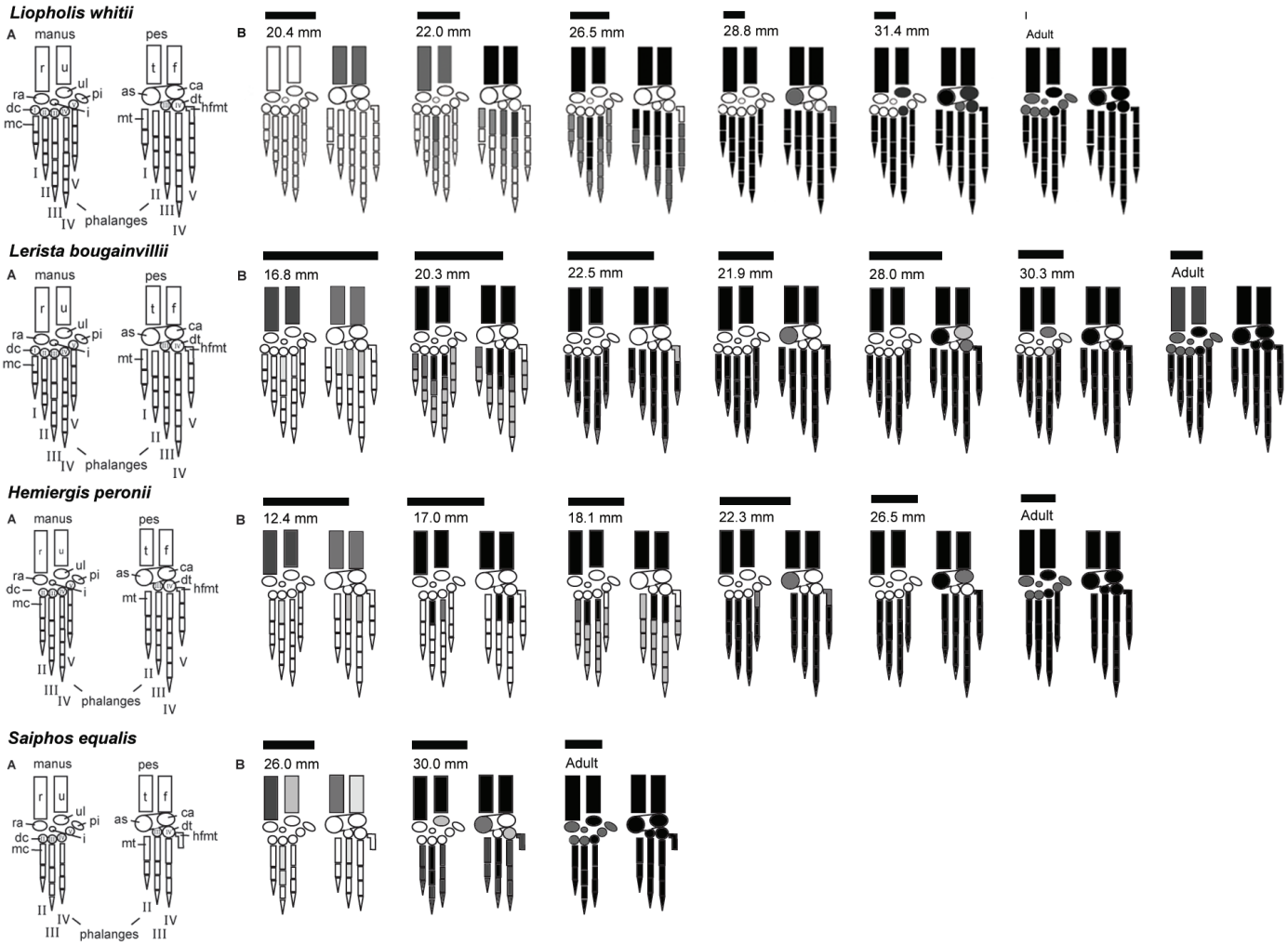

Fig. 2. Sketches of the timing in the ossification sequences of all four skinks studied. Greyscales refer to the relative extent of red staining in each skeletal element. In *L. whitii*, the black coloured elements mark the timing when ossification is completed, whereas in the other skinks the black elements refer to elements that already started in embryos of younger ontogenetic age. Scale bar: 1 mm.

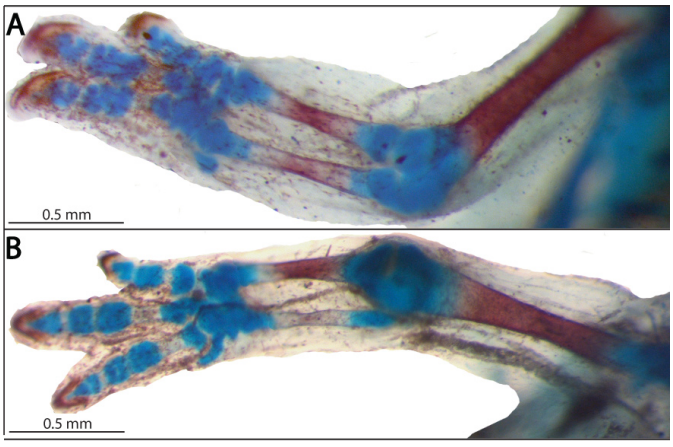

Fig. 3. Photography of the forelimb (A) and hind limb (B) of *Saiphos equalis* (SVL 26.0 mm). The ossification sequence is proximodistally directed with a preaxial dominance in the zeugopodial region, whereas the autopodial region shows only slight perichondral staining in metacarpal-3 and metatarsal-3 together with the proximal phalanges of the same digits.

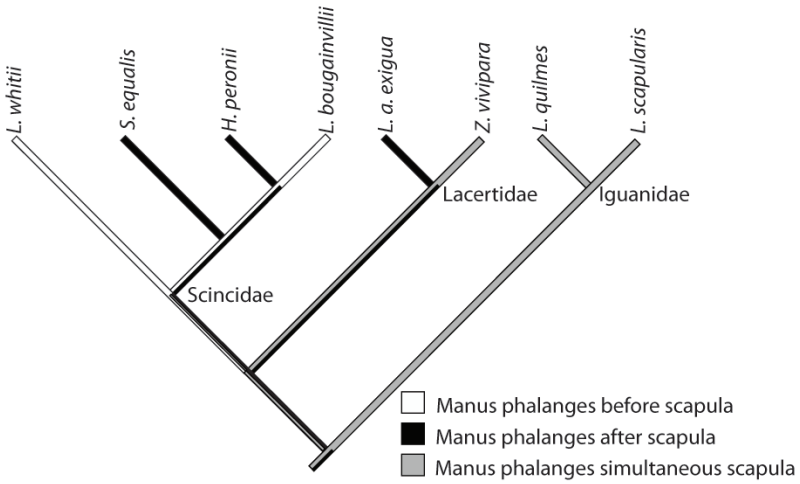

Fig. 4. Example of one heterochronic shift of the 124 characters that are resolved within the Scincidae, comprising the timing of the onset in the phalanges of the manus compared to the timing of the scapula. White colour signifies character state (0), black colour state (2) and grey ones ties (1). *S. equalis* and *H. peronii* share most of the characters, whereas *L. bougainvillii,* the form with body elongation but not yet limb reduction, reveals more similarities to the data of *L. whitii* (no limb reduction, no body elongation). This data on the ossification sequences support the fact that forms with limb reduction are linked to differences in habits rather than to phylogeny.

with the ulnare, radiale, intermedium, distal carpal-1 to -5 in the forelimb and astragalus, calcaneum, distal tarsals-3 and -4 in the hind limb (Hugi et al., 2010). *L. bougainvilii* shows a phalangeal count of 2-3-4-5-3 in the forelimb and 2-3-4-5-3 in the hind limb, as well as a mesopodial composition as seen in *L. whitii*. *H. peronii* shows reductions in the autopodial region, with a phalangeal formula of X-3-4-5-3 in the forelimb and X-3-4-5-3 in the hind limb (Choquenot and Greer, 1989; Greer, 1991; Shapiro et al., 2002; this study). The forelimb shows distal-carpals-2, -3, -4, -5, as well as the intermedium, ulnare, radiale and pisiform, whereas the hind limb exhibits distal tarsals-3 and -4, as well as a fused astagalocalcaneum complex. *S. equalis* shows a phalangeal count of X-2-3-3-X in the forelimb and hind limb. The mesopodial region of the forelimb also only lacks distal carpal-1, whereas the hind limb has a complete count in the mesopodial region, therefore showing the astragalus, calcaneum, distal tarsal-3 and distal tarsal-4. Furthermore, the hooked metatarsal-5 is present but reduced in size.

The humerus is the first element in *H. peronii*, *L. bougainvillii* and *S. equalis* that starts ossification in the limbs, synchronously with the first elements of the dermatocranium. The first onset of ossification in the limbs of *L. whitii* is displayed in the diaphyseal region of the femur, followed simultaneously by the tibia, fibula and humerus (Table 1; Fig. 2). The relative intensity and extent of the red staining indicate that the femur starts ossification slightly before the tibia, fibula and humerus. The hind limb elements of *L. whitii* start ossification before the equivalent forelimb elements, whereas the inverse condition is preserved in the three skinks with either body elongation and/or limb reduction. The zeugopodial elements of the forelimbs and hind limbs of *L. whitii, H. peronii,* and *L. bougainvillii* show no axis preference, hence a synchronous onset of ossification (Figs. 2, 3). The zeugopods of the forelimbs and hind limbs of *S. equalis* vary in the timing based on strong differences in the relative extent of the staining, with the preaxial zeugopodial elements always being more advanced (Table 1; Figs. 2-3). The metapodial regions of the forelimb and hind limb of *S. equalis, H. peronii,* and *L. bougainvillii* start ossification in the third element, whereas *L. whitii* displays the first uptake of red staining in the metacarpal-3 and metatarsal-4. In all skinks, the hooked metatarsal-5 is delayed and among the last skeletal elements to start ossification. The

relative extent of staining shows a proximodistal direction with a postaxial gradient in the autopodial region. The ossification sequence of the phalanges is not well resolved, indicating that this process occurs within a small timeframe. The smallest specimens of each ontogenetic series of the skinks furthermore reveal data on the chondrogenic sequence which are also proximodistally directed with a postaxial gradient. The ulnare, astragalus, calcaneum and in some cases the distal carpal-4, as well as the distal tarsals-3 and -4, start ossification already in embryonic stages (Table 1), with the order as follows in the forelimb: ulnare > distal carpal-4 and astragalus > calcaneum, distal tarsal-4 > distal tarsal-3 in the hind limb. The rest of the mesopodial region starts ossification in neonatal stages. The astragalus or the preaxial part of the fused astragalocalcaneum-process retains red staining before any other mesopodial element in *L. whitii*, *H. peronii* and *L. bougainvillii*, but ossifies simultaneously with the ulnare in *S. equalis*. Therefore, although the ossification always starts first in the forelimb elements compared to the timing in equivalent hind limb elements, it is the reverse order in the mesopodial region in all skinks, except for *S. equalis*.

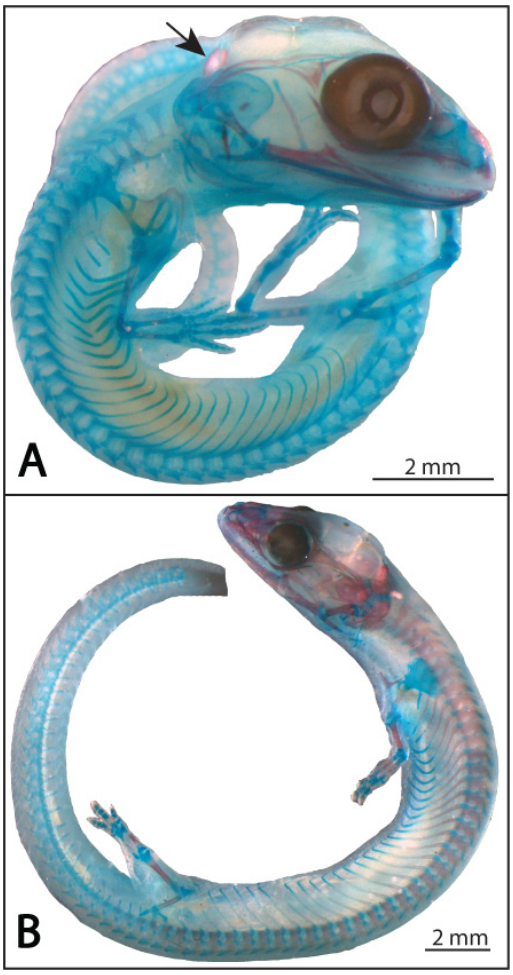

Fig. 5. Late embryo of *Hemiergis peronii* (A; SVL 17 mm) and *Saiphos equalis* (B; SVL 26.0 mm) at a time when the zeugopodial regions show the first uptake of red staining. In *S. equalis*, the ossification is advanced in the vertebral column, in all cranial components, as well as in the shoulder girdle and pelvis, whereas *H. peronii* shows the onset of ossification earlier in the limbs compared to the rest of the postcranium. However, *H. peronii* still shares more similarities with *S. equalis* than with the other skinks studied. In *H. peronii*, the calcified endolymph in the endolympatic sacs (marked by arrow) can be seen between the parietals and the supraoccipital.

Event-pairing

Of all characters (595) of the event-pairing analysis, 119 (20.0 %) show the same state in all taxa. 148 (24.9 %) of the event-pairs are uniform with ties. These two groups of uninformative characters constitute 44.9 % of the total. 93 characters (15.6 %) have only states 0 and 2, but still are not informative as they offer no resolution within the Scincidae. In 235 event-pairs (39.5 %), there are states 0 and 2, but also ties, hence in general only some of them may be phylogenetically informative characters, because resolution of the ties may imply no heterochronies. However, 124 of 235 characters are the most informative regarding the distribution within the Scincidae. Results support observations on the proximal part of the pectoral girdle (i.e., scapula, coracoid, clavicula, interclavicula), as well as the pelvis (ilium, ischium, pubis) of *L. bougainvillii*, *H. peronii* and *S. equalis* that start ossification earlier in

Element/Species	*L. quilmes*	*L. scapularis*	*L. a. exigua*	*Z. vivipara*	*L. whitii*	*L. bougainvilli*	*H. peronii*	*S. equalis*
Dermatocranium	3	1	2	1	1	1	1	1
Neurocranium	4	3	4	2	5	2	3	6
Splanchnocranium	5	2	4	2	5	4	5	5
Clavicula	1	1	2	2	2	2	2	2
Interclavicula	2	2	3	3	7	5	4	7
Scapula	4	3	4	3	12	13	8	9
Coracoid	4	3	5	7	13	14	13	13
Humerus	1	1	1	2	4	3	3	3
Radius	4	3	1	2	8	4	4	10
Ulna	4	3	1	2	8	4	4	14
Carpals	7	5	8	8	18	22	20	21
Metacarpal-1	2	3	3	3	14	10	/	/
Metacarpal-2	2	3	3	3	13	10	11	19
Metacarpal-3	2	3	3	3	9	8	7	17
Metacarpal-4	2	3	3	3	12	9	9	19
Metacarpal-5	2	3	3	4	15	12	13	/
Manus phalanges	4	3	6	3	11	10	12	18
Ilium	4	3	5	4	12	14	12	8
Ischium	4	3	6	9	14	17	13	18
Pubis	4	3	5	6	13	14	9	8
Femur	2	2	1	2	3	4	4	8
Tibia	4	3	1	2	4	5	5	12
Fibula	4	3	1	2	4	5	5	15
Tarsals	6	4	7	6	17	19	18	20
Metatarsal-1	2	3	3	2	11	10	/	/
Metatarsal-2	2	3	3	2	10	8	12	19
Metatarsal-3	2	3	3	2	9	6	6	17
Metatarsal-4	2	3	3	2	8	7	6	19
Metatarsal-5	2	4	3	5	17	18	18	19
Pes phalanges	4	3	4	3	10	11	12	18
Cervical vertebrae	5	2	4	2	6	10	3	4
Dorsal vertebrae	5	2	4	4	7	10	5	11
Sacral vertebrae	5	2	5	?	13	10	14	14
Caudal vertebrae	5	2	5	6	14	15	16	16
Ribs	5	3	2	3	13	13	12	13

Table 2. The relative sequence of onset of ossification based on the data of Table 1 for each lizard species included in the event-pairing analysis.

relation to their other skeletal elements, but also in comparison to equivalent data of *L. whitii* and other lizards. *S. equalis* is the only skink, which is separated by the majority of characters from the other skinks studied. The dorsal centra of *S. equalis* start ossification before the fibula, tibia, and the dorsal ribs precede the onset in metacarpal-3 and -4. The ilium of *S. equalis* shows the onset of ossification before the ulna, contrary to the timing in any other lizard (Table 2). Furthermore, the pubis of *S. equalis* starts ossification very early. The ischium, which is rather delayed in the other lizards, starts ossification before the metacarpals in *S. equalis* (Table 2). In *S. equalis* the interclavicula starts ossification after the onset in the femur, with all other skinks and lizards showing the inverse or no resolution. Some event-pairs shared by *H.*

peronii and *S. equalis* separate them from *L. bougainvillii* and *L. whitii,* that is for example the timing of the onset of ossification in the scapula and the metacarpals or the pubis compared to the phalanges of the manus (Fig. 4). The cervical vertebrae start ossification simultaneously with the humerus in *H. peronii* and *S. equalis*, whereas they lag behind the humerus in *L. whitii* and *L. bougainvillii. H. peronii* and *S. equalis* show simultaneous onset of the cervical centra compared to the first onset of ossification in the elements of the splanchnocranium, as well as of the stylopodium and zeugopodium of the hind limbs, in contrast to all other lizards. The pubis of *S. equalis* and *H. peronii* starts ossification before the first onset in the sacral centra which is the inverse condition of other three skink species. In some cases, *L. whitii* is separated from the other skinks and lizards studied based on the early onset of the hind limb elements compared to the neurocranium and the interclavicula. A few characters show all skinks to be separated from the other lizards with the humerus starting ossification after the clavicula, but this difference may result from a lack in resolution in the ossification sequences of all studied lizards (Table 2). The earlier timing of the radius compared to the first onset in the neurocranium might be a result of the same bias.

Discussion

Hemiergis peronii, Lerista bougainvillii and *Saiphos equalis* show similar trends in the timing and order of the ossification in the dermatocranium, shoulder, pelvis and limbs, which vary from those seen in *Liopholis whitii* and from other lacertilians (Hugi et al., 2010). *H. peronii, L. bougainvillii* and *S. equalis* show that: 1) the dermatocranium (including the premaxilla) is well developed in early embryos; 2) elements of the forelimb start ossification earlier than equivalent elements of the hind limb; the ossification starts early in 3) the cervical centra, 4) the shoulder elements and 5) the pelvis. Differences among these three species are: 1) in contrast to *L. bougainvillii* and *H. peronii, S. equalis* shows no synchronous onset in the zeugopodial region, but a preaxial gradient in both the forelimb and hind limb (Figs. 2-3); 2) in *H. peronii* the pubis is the first element of the pelvis that starts ossification; 3) *L. bougainvillii*, which is elongate but shows only mild limb reduction, shares more similarities in the timing in ossification with *L. whitii* than with the two skinks with more pronounced limb reduction; 4) *S. equalis*, which shows the greatest degree of limb reduction and body elongation, also shows greatest number of heterochronic shifts compared to *L. whitii*. Although *S. equalis* and *H. peronii* share the most characters with each other, the former shows the onset of ossification in the limbs only in larger embryos of older ontogenetic age, at a time when ossification in the cranial and axial skeleton is well advanced (Fig. 5).

In surface-dwelling lizards with non-reduced limbs and lack of body elongation, forelimb and hind limb elements often start ossification within a small timeframe which is interpreted as a simultaneous onset (e.g., Rieppel, 1992a, 1994b, 1994a; Shapiro, 2002; Federico and Lobo, 2006). In *L. whitii,* the femur starts ossification as the first element of the limbs based on the relative intensity and extent of the red staining, and the zeugopodial region of the hind limb clearly starts ossification before the equivalent region of the forelimbs. The

Taxon	State 0	State 1	State 2	Missing data or absent elements (?)
Liolaemus quilmes	169 (28.4 %)	148 (24.9 %)	278 (46.7 %)	0
Liolaemus scapularis	147 (24.7 %)	256 (43.0 %)	192 (32.3 %)	0
Lacerta agilis exigua	214 (36.0 %)	99 (16.6 %)	282 (47.4 %)	0
Zootoca vivipara	173 (29.0 %)	133 (22.4 %)	255 (42.9 %)	34 (5.7 %) Missing data
Liopholis whitii	224 (37.6 %)	28 (4.7 %)	343 (57.7 %)	0
Lerista bougainvillii	180 (30.3 %)	36 (6.0 %)	379 (63.7 %)	0
Hemiergis peronii	165 (27.7 %)	31 (5.2 %)	332 (55.8 %)	67 (11.3 %) elements absent
Saiphos equalis	164 (27.6 %)	19 (3.2 %)	313 (52.6 %)	99 (16.6 %) elements absent

Table 3. Proportions of the relative timing in the species analysed (see Table 2). The missing data in *Hemiergis peronii* and *Saiphos equalis* result from the reduction in the autopodial regions of both the forelimbs and hind limbs.

iguanids, *L. scapularis* and *L. quilmes*, show red staining first in the humerus, which is followed by a synchronous onset of ossification in the zeugopods of both the forelimbs and hind limbs (Lobo et al., 1995; Abdala et al., 1997). In contrast, the studied lizards with limb reduction start ossification in the stylo- and zeugopodial regions of the forelimbs, preceding equivalent elements of the hind limbs. These observations are based on the relative extent of the staining in *H. peronii* and *L. bougainvilli*, but are visible in two separate specimens of *S. equalis*. In addition, *S. equalis* shows a clear preaxial gradient in the zeugopodial region of both the forelimbs and hind limbs.

The earlier uptake of Alizarin red in the forelimbs of all skinks with body elongation and/or limb reduction, as well as the preaxial gradient of the zeugopodial regions in *S. equalis* is similar to data of the ossification sequences for urodeles (e.g., Erdmann, 1933; Nye et al., 2003), whereas the postaxial gradient in the metapodials is common in anurans (e.g., Erdmann, 1933; Haas, 1999) and plesiomorphic for amniotes (e.g., Rieppel, 1993c; Sánchez-Villagra et al., 2009; Sheil and Greenbaum, 2005). Lacertilians show the most conserved order with a proximodistal gradient and a postaxial dominance in the autopodial region (e.g., Rieppel, 1993a; Mohammed et al., 1995; Maisano, 2002; Federico and Lobo, 2006; Hugi et al., 2010).

The sequence in which digits are lost completely in the adult morphology has been

studied in several lizard taxa and in most cases follows the order digit I > digit V > digit II > digit III > digit IV (e.g., Greer, 1991; Caputo et al., 1995; Greer et al., 1998; Shapiro et al., 2003; Shapiro et al., 2007) – a sequence that is not observed in the developmental sequence of any lacertilian studied to date (e.g., Shapiro, 2002; Shapiro et al., 2003). The loss of single phalanges, in contrast, always occurs first in digit IV in the manus and in the fifth digit in the pes of squamates (e.g., Greer, 1987, 1991; Greer et al., 1998; Wiens et al., 2006, Shapiro et al., 2007), which is also not reflected in the developmental sequence. In contrast, the data on the subsurface-dwellers in the present study show the first reduction of the phalangeal formula in digit V, whereas digit I is completely lost before any other digit, which fits the data on other limb reduced lizards. Furthermore, no reduction occurs in any digit simultaneously with or before digit IV in both the manus and pes (Fig. 1). The order of how digits are reduced differs between metapodials and phalanges. The hooked metatarsal-5 persists in rudimentary form in the tridactyle *S. equalis,* the general condition of other tri- and didactyle lizard species (Caputo et al., 1995), linked to the fact that this element is an insertion point for the extensor muscles of the hind limbs (e.g., Robinson, 1975; Russel and Rewcastle, 1979).

The same morphological trends are shared by other skinks and lizards of similar ecology (e.g., *Agama* in Moody 1980; *Chalcides* in Caputo et al. 1995, Greer et al. 1998; *Coleonyx* in Haacke 1976; *Hemiergis* in Choquenot and Greer 1989, Shapiro et al., 2002; and *Lerista* species in Greer 1987, 1990, 1991). The lack of a phylogenetic signal (e.g., Fig. 4) suggests an adaptive significance for the heterochronies observed (Gans, 1975; Greer, 1991; Caputo et al., 1995). Even so, our pentadactyle reference species is phylogenetically distant from our set of limb-reduced species (*Liopholis* belongs to the *Egernia* Group, the others belong to the *Sphenomorphus* Group; Greer 1989, Skinner et al. 2011). Further studies including non-attenuate, pentadactyle members of the Australian *Sphenomorphus* group (e.g., *Ctenotus*, *Eulamprus*) would be illuminating.

Conclusion

The differences in the ossification pattern of the subsurface moving skinks compared to all other lacertilians concern the earlier strengthening that includes earlier onset of ossification and a more rapid development of parts of the dermatocranium, the vertebral column, the pubis, as well as the accelerated development of the forelimbs. Ossification of the limbs, girdles and the head develops earlier but also more rapidly in limb reduced skink species, which is reflected by the timing in the onset of ossification in embryos of a smaller absolute size. In the case of the head, the front of the snout is well ossified at the time of hatching or birth. The timing of the ossification sequence is more similar in *L. whitii* and *L. bougainvillii* than in *S. equalis* and *H. peronii*. The detected heterochronic shifts in the developmental timing of the ossification sequences of *H. peronii, L. bougainvillii* and *S. equalis* compared to the data of *L. whitii* are most likely coupled with changes in the functionality of muscle insertion areas and applied forces (cf. Rot-Nikcevic et al. 2006).

In summary, the heterochronic shifts in the ossification sequences might be linked to a shift in the emphasis from limbed locomotion to

trunk locomotion (lateral undulation) – a mode of locomotion found in both the leaf litter and sand swimming species, *H. peronii*, *L. bougainvillii* and *S. equalis* and therefore, strongly indicate adaptive significance to different habitat types.

Acknowledgements

We thank C. Mitgutsch, T. Scheyer and J. Neenan. Collection of *Lerista bougainvillii* was enabled by a South Australian Department of Environment and Natural Resources scientific permit to M. Hutchinson. We thank M. B. Thompson and J. Herbert, University of Sydney, for the provision of the *Saiphos* embryos, and K. de Baets, A. Fenner and I. Williams for their assistance in the field. The contribution of S. Dewdney and the Australian Reptile Breeding Facility, Echunga, South Australia, is gratefully acknowledged. The Swiss National Science Foundation supported this project (grant No. 31003A-133032/1 to MRS-V).

Literature

Abdala, F., Lobo, F, Scrocchi, G. 1997. Patterns of ossification in the skeleton of *Liolaemus quilmes* (Iguania: Tropiduridae). Amphibia-Reptilia 18:75-83.

Brandely, M.C., Huelsenbeck, J.P., Wiens, J.J. 2008. Rates and patterns in the evolution of snake-like body form in squamate reptiles: evidence for repeated re-evolution of lost digits and long-term persistence of intermediate body forms. Evolution 62:2042-2064.

Caputo V., Lanza, B., Palmieri R. 1995. Body elongation and limb reduction in the genus *Chalcides* Laurenti 1768 (Squamata Scincidae): a comparative study. Tropical Zoology 8:95-152.

Choquenot, D., Greer, A.E. 1989. Intrapopulational and Interspecific Variation in Digital Limb Bones and Presacral Vertebrae of the Genus *Hemiergis* (Lacertilia, Scincidae). Journal of Herpetology 23(3):274-281.

Dingerkus, G., Uhler, L.D. 1977. Enzyme clearing of Alcian Blue stained whole small vertebrates for demonstration of cartilage. Stain Technology 52: 229-23.

Erdmann, K. 1933. Zur Entwicklung des knöchernen Skelets von *Triton* und *Rana* unter besonderer Berücksichtigung der Zeitfolge der Ossifikationen. Zeitschrift für die gesamte Anatomie, I. Abt. 101:566-649.

Federico, A., Lobo, F. 2006. Patrones de osificación en *Tupinambis merianae* y *Tupinambis rufescens* (Squamata: Teiidae) y patrones generales en Squamata. Cuadernos de Herpetologia 20 (1):3-23.

Fröbisch, N. 2008. Ossification patterns in the tetrapod limb; conservation and divergence from morphogenetic events. Biological Reviews 83(4):571-600.

Greer, A.E. 1987. Limb reduction in the lizard genus *Lerista*. 1. Variation in the number of phalanges and presacral vertebrae. Journal of Herpetology 21(4):267-276.

Greer, A.E. 1989. Biology and evolution of Australian lizards. Surrey Beatty & Sons, Sydney, Australia.

Greer, A.E. 1990. Limb reduction in the scincid lizard genus *Lerista*. 2. Variation in the bone complements of the front and rear limbs and the number of postsacral vertebrae. Journal of Herpetology 24(2):142-150.

Greer, A.E. 1991. Limb reduction in Squamates: identification of the lineages and discussion of the trends. Journal of Herpetology 25 (2):166-173.

Greer, A., Caputo, V., Lanza, B., Palmieri, R. 1998. Observations on limb reduction in the scincid lizard genus *Chalcides*. Journal of Herpetology 32(2):244-252.

Haacke, W. 1976. The burrowing gekkos of southern Africa, 2 (Reptilia: Gekkonidae). Annals of theTransvaal Museum 30(6):71-89.

Hugi, J., C. Mitgutsch, Sánchez-Villagra, M.R. 2010. Chondrogenic and ossification patterns in White's skink *Liopholis whitii* (Scincidae, Reptilia). Zoosystematics and Evolution 86:21-32.

Hutchinson, M.N. 1993. Family Scincidae. In Fauna of Australia. Vol. 2A, Amphibia and Reptilia, edited by C. J. Gasby, C. J. Ross, and P. L. Beesly. Canberra: Australian Biological and Environmental Survey, 1993.

Jerez, A., Tarazona, O.A. 2008. Appendicular skeleton in *Bachia bicolor* (Squamata: Gymnophthalmidae): osteology, limb reduction and postnatal skeletal ontogeny. Acta Zoologica 90(1):42-50.

Maisano, J.A. 2001. A survey of state of ossification in neonatal squamates. Herpetological Monograph 15:135-157.

Maisano, J.A. 2002a. Postnatal ontogeny in *Callisaurus draconoides* and *Uta stansburiana* (Iguania: Phrynosomatidae). Journal of Morphology 251:114-139.

Maisano, J.A. 2002b. Postnatal skeletal ontogeny in five xantusiids (Squamata: Scleroglossa). Journal of Morphology 254:1-38.

Mattison, C. 1989. Lizards of the World. New York, NY: Facts on File.

Moody, S.M. 1980. Phylogenetic and historical biogeographical relationships of the genera in the family Agamidae (Reptilia: Lacertilia). Unpublished Ph.D. Thesis. University of Michigan. Ann Arbor. 373 pp.

Mohammed, B.H.M., Khalifa, S.A., El-Sayad, F.I., Ibrahim, S.A. 1995. Comparative analysis of ossification in the appendicular skeleton in some scincid lizards (Scincidae: Reptilia). Journal of Egyptian-German Society for Zoology 17 B:93-119.

Nye, H.L.D., Cameron, J.A., Chernoff, E.A.G., Stocum, D.L. 2003. Extending the table of stages of normal development in the axolotl: Limb development. Developmental Dynamics 226:555-560.

Rieppel, O. 1992a. Studies on skeleton formation in Reptiles. I. The postembryonic development of the skeleton in *Cyrtodactylus pubisulcus* (Reptilia: Gekkonidae). Journal of Zoology, London 227:87-100.

Rieppel, O. 1992b. Studies on skeletal formation in reptiles III: Patterns of ossification in the skeleton of *Lacerta vivipara* Jacquin (Reptilia, Squamata). Fieldiana (Zoology) 1437:1-25.

Rieppel, O. 1993a. Die Gliedmassen der Tetrapoden – ein aktuelles Problem der Evolutionsforschung. Naturwissenschaften 80: 295-301.

Rieppel, O. 1993b. Studies on skeleton formation in reptiles. V. Patterns of ossification in the skeleton of *Alligator mississipiensis* Daudin (Reptilia, Crocodylia). Zoological Journal of the Linnean Society 109:301-325.

Rieppel, O. 1993c. Studies on skeleton formation in reptiles - patterns of ossification in the skeleton of *Chelydra serpentina* (Reptilia, Testudines). Journal of Zoology, London 231:487-509.

Rieppel, O. 1994a. Studies on skeletal formation in reptiles. Patterns of ossifcation in the skeleton of *Lacerta agilis exigua* Eichwald (Reptilia, Squamata). Journal of Herpetology 28:145-153.

Rieppel, O. 1994b. Studies on skeleton formation in reptiles. Patterns of ossification in the limb skeleton of *Gehyra oceanica* (Lesson) and *Lepidodactylus lugubris* (Duméril & Bibron). Annales des Sciences Naturelles, Zoologie, Paris 15:83-91.

Robinson, P.L. 1975. The functions of the hooked fifth metatarsal in lepidosaurian reptiles, pp. 461-483. In: Colloque International C.N.R.S., no. 218: Problèmes actuels de paléontologie-évolution des Vertébrés. Paris: C.N.R.S.

Rot-Nikcevic, I., Reddy, T., Downing, K.J., Belliveau, A.C., Hallgrímsson, B., Hall, B.K., Kablar, B. 2006. Myf5/: MyoD/ amyogenic fetuses reveal the importance of early contraction and static loading by striated muscle in mouse skeletogenesis. Development, Genes & Evolution 216:1-9.

Russel, A.P., Rewcastle, S.C. 1979. Digital reduction in Sitana (Reptilia: Agamidae) and the dual role of the fifth metatarsal in lizards. Canadian Journal of Zoology 57:1129-1135.

Sánchez-Villagra, M.R., Müller, H., Sheil, C.A., Scheyer, T.M., Nagashima, H., Kuratani, S. 2009. Skeletal Development in the Chinese soft-shelled turtle *Pelodiscus sinensis* (Testudines: Trionychidae). Journal of Morphology:270:1381-1399.

Schoch, R.R. 2004. Skeleton formation in the Branchiosauridae: A Case study in comparing ontogenetic trajectories. Journal of Vertebrate Paleontology 24:309-319.

Shapiro, M.D. 2002. Development morphology of limb reduction in *Hemiergis* (Squamata: Scincidae): Chondrogenesis, osteogenesis, and heterochrony. Journal of Morphology 254:211-231.

Shapiro, M.D., Hanken, J., Rosenthal, N. 2003. Developmental basis of evolutionary digit loss in the Australian lizard *Hemiergis*. Journal of Experimental Zoology (Molecular and Developmental Evolution) 297 B:48-56.

Shapiro, M.D., Shubin, N.H., Downs, J.P. 2007. Limb diversity and digit reduction in reptilian evolution. In Fins into Limbs, B. K. Hall (ed.), The University of Chicago Press, Chicago 433 pp.

Sheil, C.A., Greenbaum, E. 2005. Reconsideration of skeletal development of *Chelydra serpentina* (Reptilia: Testudinata: Chelydridae): evidence for intraspecific variation. Journal of Zoology, London 265:235-267.

Shubin, N.H., Alberch, P. 1986. A morphogenetic approach to the origin and basic organization of the tetrapod limb. Evolutionary Biology:319-387.

Siler, C.D., Brown, R.M. in press. Evidence for repeated acquisition and loss of complex body form characters in an insular clade of Southeast Asian semi-fossorial skinks. Evolution, doi: 10.1111/j.1558-5646.2011.01315.x.

Skinner, A., Lee, M.Y., Hutchinson, M.N. 2008. Rapid and repeated limb loss in a clade of scincid lizards. BMC Evolutionary Biology 8:310.

Velhagen, W.A. 1997. Analyzing developmental sequences using sequence units. Systems Biology 46:204-210.

Werneburg, I., Hugi, J., Müller, J., Sánchez-Villagra, M.R. 2009. Embryogenesis and ossification of *Emydura subglobosa* (Testudines, Pleurodira, Chelidae) and patterns of turtle development. Developmental Dynamics 238:2770-2786.

Wiens, J.J., Brandley M.C., Reeder, T.W. 2006. Why does a trait evolve multiple times within a clade? Repeated evolution of snake-like body form in squamate reptiles. Evolution

55:2303-2318.

Wiens, J.J. 2009. Estimating rates and patterns of morphological evolution from phylogenies: lessons in limb lability from Australian *Lerista* lizards. Journal of Biology 8:19

Wiens, J.J., Brandley, M.C., Reeder, T.W. 2006. Why does a trait evolve multiple times within a clade? Repeated evolution of snake-like body form in squamate reptiles. Evolution 60:123-141.

Character matrix of the event pairing analysis of the osteogenetic sequences in the lacertilian squamates in comparison to subsurface dwelling morphoclines

Liolaemus quilmes

2220000002 2102221022 1000100021 0221122102 2112122222 2222200021
0020000002 1002000100 0210020001 1000210020 0011100021 0020001111
2102211211 0222222102 2112110222 2212102211 2110222221 1210221121
1022222111 0002100200 0111110000 2102211211 0222221111 2210221121
1022222111 1212222222 2220222222 2222220002 1002000111 1100001000
000210020 0011111000 0100010002 1002000111 1100001000 1100021002
0001111100 0010001110 0021002000 1111100001 0001111210 2211211022
2221111211 0222222212 2222220222 2222222220 2222222212 2222220222
2222222220 2222221221 2222222022 2222222222 0222222112 2122222220
2222222222 2202222221 1122122222 2202222222 2222202222 221111

Liolaemus scapularis

2201002012 2122221222 1100100021 2221122122 2112122222 2222221222
1121102122 2112110121 2221121101 1212221121 1011121222 1121101111
2122211211 0111112122 2112110111 1112122211 2110111111 1212221121
1011111111 2012100200 0000000000 2122211211 0111111111 2212221121
1011111111 1212222222 2220222222 2222222122 2112110111 1111112110
2122211211 0111111111 2110121222 1121101111 1111121101 1212221121
1011111111 1211011122 2222222202 2222222222 2122222122 2112110111
1111112110 1111020121 0020000000 0000010000 0000020121 0020000000
0000010000 0000012012 1002000000 0000001000 0000001120 1210020000
0000000010 0000000011 1212221121 1011111111 1211011110 12222

Lacerta agilis exigua

2211002002 2112222222 2000000000 0000010000 0001122222 2222220021
0022202002 1002220120 0210022201 1200210022 2011120021 0022201111
2222222222 0222222222 2212220222 2202222222 2220222221 2222222122
2022222010 0000000111 0000000000 0000000111 0000000000 1000000011
1000000000 0112222222 2220222222 2222222002 1002220111 1100002220
2002100222 0111110000 2220120021 0022201111 1000022201 1200210022
2011111000 0222011120 0210022201 1111000022 2011112112 2102220222
2200002220 2222221122 1022202222 2000022202 2222121122 1022202222
2000022202 2222112222 2212220222 2201012220 2222222222 2222122202
2222010122 2022222222 1100100022 2000000000 0222000000 00000

Zootoca vivipara

2212112222 2222122222 2211100021 1100012111 0001122222 2222222221
1022202222 1102220122 2211022201 1222211022 2011122222 2022202222
2222110222 0111102222 2202220222 2122222222 2222222222 2222222022
2022222220 2111000111 0000000000 2111000111 0000000000 1211100011
1000000000 0112222220 2220222222 2012222111 0001110000 0000001110
2111000111 0000000000 1110121110 0011100000 0000011101 1211100011
1000000000 0111011122 2222022202 2222220022 2022222222 1102220111
1010002220 2222021110 0011100000 0000011101 1110022222 2022202222
1210022202 222022???? ?????????? ?????????? ????????22 2222022202
2222220122 2122222222 ?222211022 2011110100 0222022220 120?0

Liopholis whitii

2212002222 2222222222 2200200022 2220022222 2002122222 2222222222
2222202222 2212220022 2220022200 0222221022 2000222222 2222202222
2222200222 0002002222 2102220002 1022222222 2220122202 2222222122
2001220220 2002000000 0000000000 2002000100 0000000000 2200200010
0000000000 0212222222 2220222222 2222222222 2002220002 0010002220
2222200222 0002000000 2220022222 0022200010 0000022200 0222220021
1000000000 0222000022 2222222202 2222222222 2122222222 2002220002

0000002220 0122022220 0020000000 0000022200 0000022221 0020000000
0000022200 0000022222 2212220012 2022012220 2222022222 2222222201
2220221222 2022220222 2222222122 2001220220 1222022220 22210

Lerista bougainvillii
2222102222 2222222222 2220200022 1200022212 0002122222 2222222222
0022202222 2002220122 2220022200 0222220022 2000222222 0022202222
2222200222 0112202222 2212220222 2222222222 2220222222 2222222122
2022222210 2212000211 0000000000 2222100222 0000000000 2222210022
2000000000 0212222222 2220222222 2222222222 2002220112 2010002220
2222200222 0001000000 2220022222 0022200000 0000022200 0222220022
2000000000 0222000222 2222222202 2222222222 2022222222 2002220222
2020002220 2222022222 0022201122 0100022201 2220022222 0022201122
0100022201 2220012222 2002220112 2010002220 1222001122 2222222202
2222220222 2022220222 2222221022 2022222200 0222022220 22220

Hemiergis peronii
2222002202 2222222222 2210200022 0210022202 1002122222 22222?????
??????2222 2202220?22 222002220? 0222222022 20?0222222 212220?222
2222220222 0?22202222 2202220?22 2012222221 2220?22212 2222222022
20?0210000 2202100211 0?00000000 2212200222 0?00000000 2221220022
20?0000000 0212222222 2220?22222 2222222??? ?????????? ??????????
2222220222 0?22201102 2220?22222 002220?000 000002220? 0222220022
20?0000000 02220?0122 222222220? 2222222222 21?2222222 2202220?22
2011022220 ?122021020 001000?000 000000000? 0000022122 002220?000
000002110? 0000022222 2222220?22 2222222220 ?222022222 222222220?
2222222222 20?2220222 2222222022 20?2220110 22220?1220 12200

Saiphos equalis
2202002222 2222222222 2200200022 2222022222 2222222222 22222?????
??????2222 2222220?22 222222220? 0222222222 20?12????? ??????????
2222222222 0?020?2222 2002000?00 0?02222222 2220?020?1 2222220020
00?000?010 2222200200 0?000?0101 2222220220 0?000?0202 2222222222
20?000?020 2222222222 2220?222?2 2222222??? ?????????? ??????????
2222222222 0?121?2222 2220?22222 222220?010 ?02022220? 0222222222
20?121?222 22220?1222 222222220? 121?222222 20?1212222 2222220?02
0?12122220 ?020020020 002000?000 ?00000000? 0000022222 202200?000
?02022000? 0000022222 2222210?00 0?02022200 ?000002222 222222220?
000?020222 20?0000022 2222222122 00?000?020 22200?0000 02200

Lerista bougainvillii
2222102222 2222222222 2220200022 1200022212 0002122222 2222222222
0022202222 2002220122 2220022200 0222220022 2000222222 0022202222
2222200222 0112202222 2212220222 2222222222 2220222222 2222222122
2022222210 2212000211 0000000000 2222100222 0000000000 2222210022
2000000000 0212222222 2220222222 2222222222 2002220112 2010002220
2222200222 0001000000 2220022222 0022200000 0000022200 0222220022
2000000000 0222000222 2222222202 2222222222 2022222222 2002220222
2020002220 2222022222 0022201122 0100022201 2220022222 0022201122
0100022201 2220012222 2002220112 2010002220 1222001122 2222222202
2222220222 2022220222 2222221022 2022222200 0222022220 22220

Hemiergis peronii

2222002202	2222222222	2210200022	0210022202	1002122222	22222?????
??????2222	2202220?22	222002220?	0222222022	20?0222222	212220?222
2222220222	0?22202222	2202220?22	2012222221	2220?22212	2222222022
20?0210000	2202100211	0?00000000	2212200222	0?00000000	2221220022
20?0000000	0212222222	2220?22222	222222????	??????????	??????????
2222220222	0?22201102	2220?22222	002220?000	000002220?	0222220022
20?0000000	02220?0122	222222220?	2222222222	21?2222222	2202220?22
2011022220	?122021020	001000?000	000000000?	0000022122	002220?000
000002110?	0000022222	2222220?22	2222222220	?222022222	222222220?
2222222222	20?2220222	2222222022	20?2220110	22220?1220	12200

Saiphos equalis

2202002222	2222222222	2200200022	2222022222	2222222222	22222?????
??????2222	2222220?22	222222220?	0222222222	20?12?????	??????????
2222222222	0?020?2222	2002000?00	0?02222222	2220?020?1	2222220020
00?000?010	2222200200	0?000?0101	2222220220	0?000?0202	2222222222
20?000?020	2222222222	2220?222?2	222222????	??????????	??????????
2222222222	0?121?2222	2220?22222	222220?010	?02022220?	0222222222
20?121?222	22220?1222	222222220?	121?222222	20?1212222	2222220?02
0?12122220	?020020020	002000?000	?00000000?	0000022222	202200?000
?02022000?	0000022222	2222210?00	0?02022200	?000002222	222222220?
000?020222	20?0000022	2222222122	00?000?020	22200?0000	02200

Chapter 4:

Ossification Sequences and associated ontogenetic changes in the bone histology of pachypleurosaurids from Monte San Giorgio (Switzerland/Italy)

Jasmina Hugi and Torsten M. Scheyer

In Review, *Journal of Vertebrate Paleontology*

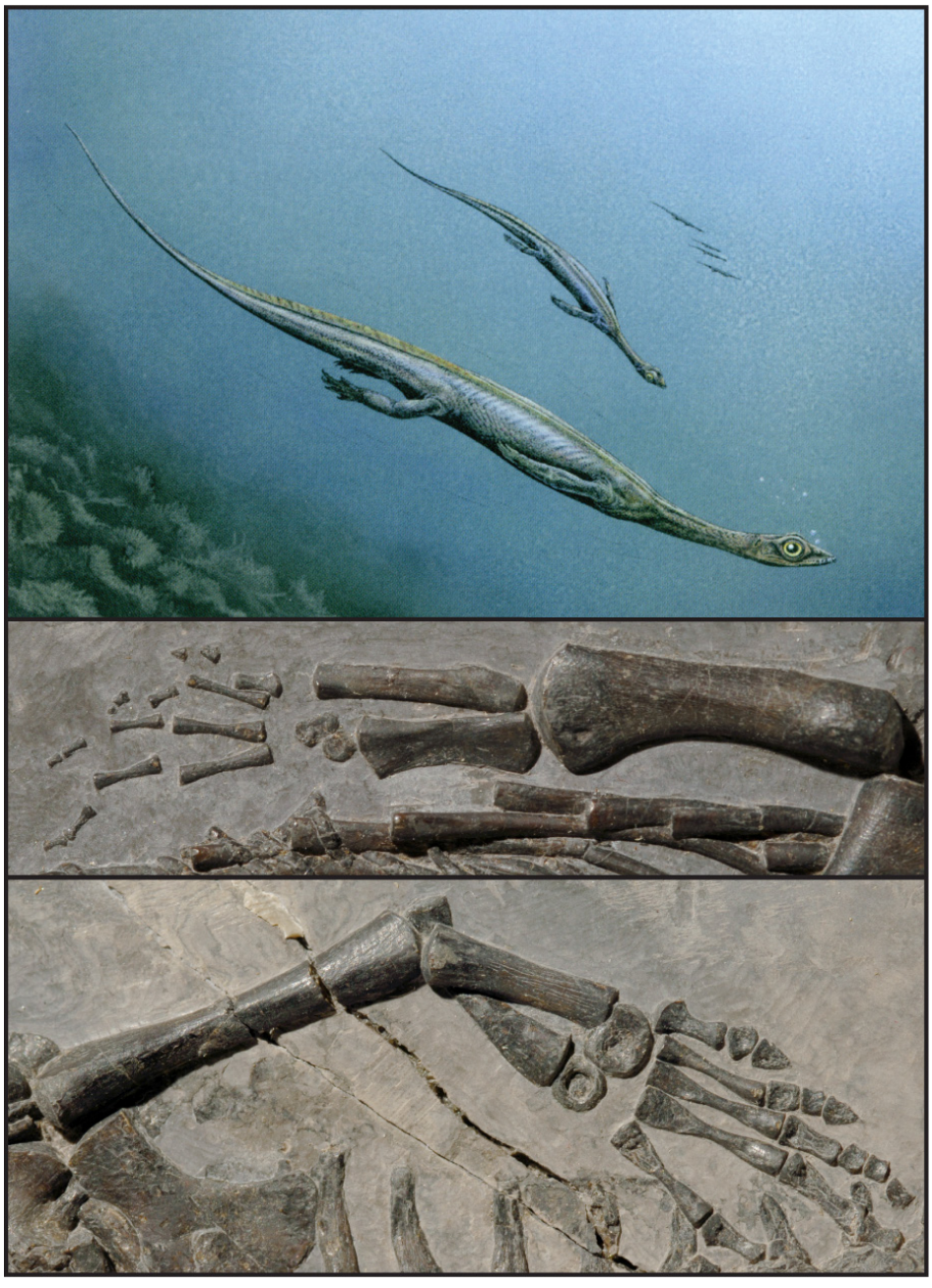

Drawing: B. Scheffold
Photograph: J. Hugi

Ossification sequences and associated ontogenetic changes in the bone histology of pachypleurosaurids from Monte San Giorgio (Switzerland/Italy)

JASMINA HUGI* and TORSTEN M. SCHEYER

Paleontological Institute and Museum, University of Zürich, Karl Schmid-Strasse 4, Zürich 8006, Switzerland, jasmina.hugi@pim.uzh.ch; tscheyer@pim.uzh.ch

* Corresponding author.

ABSTRACT—Evolutionary changes in lifestyle (e.g., terrestrial vs. aquatic modes of life) within tetrapod vertebrate clades are known to influence limb morphology. Modified limb morphotypes can reveal changes in the osteogenetic sequences (order in bone formation) and bone histology (microstructure of bone) in comparison to the plesiomorphic ancestral condition. Osteogenetic sequences of the limbs are conservative in Recent terrestrial surface dwelling lacertilian squamates and are hypothesized to represent the plesiomorphic ancestral condition for terrestrial eureptilians. In contrast, osteogenetic sequences are more variable in the rest of the tetrapods. However, similar evolutionary trends in the order of osteogenesis and in bone microstructure are often shared in tetrapods with similar habit preferences. Such data are in some cases also preserved in fossil tetrapods for which the lifestyle is often unknown. The pachypleurosaurids (Sauropterygia, Eureptilia, Reptilia) from Monte San Giorgio (Switzerland, Italy) are fossil marine eureptiles that represent an excellent case study for the exploration of osteogenesis based on their high abundance and high quality of complete ontogenetic series. We studied the osteogenesis and bone histology of all four pachypleurosaurid species from this locality, *Neusticosaurus edwardsii, N. peyeri, N. pusillus* and *Serpianosaurus mirigiolensis,* in comparison to data of Recent terrestrial lizards and Recent secondarily aquatic reptiles. The goals of the study are to explore 1) whether the osteogenetic sequences of the pachypleurosaurids reveal more similarities to the hypothesized plesiomorphic ancestral condition for terrestrial surface dwelling eureptilians, or 2) whether they show more similarities with Recent aquatic reptiles. Results show that the osteogenesis of the pachypleurosaurian limbs is divided into two steps: (1) developmental sequences of ossification during embryology and/or in early neonates, (2a) additional primary periosteal compaction processes, and (2b) additional primary and secondary endosteal compaction processes of the bones during the neonate ontogeny. Specific external taphonomic patterns reveal detailed information on the order of the initiation and termination of these two steps, that are described as: (A) onset of ossification, (B) onset of additional compaction processes (early phase of compaction); and (C) termination of the additional compaction processes (final phase of compaction). An event pairing analysis was performed to detect heterochronic shifts in the osteogenetic sequences of the

four pachypleurosaurids in comparison to the hypothesized plesiomorphic ancestral eureptilian condition. Results showed that elements of the forelimb of all pachypleurosaurids precede their serial homologues of the hind limb in all osteogenetic stages except for initiation of ossification (A). The order of the early phase of the compaction processes is similar to the hypothesized plesiomorphic ancestral eureptilian condition, whereas the final phase of the compaction processes reveals similar trends of other aquatic reptiles. The order in the final phase of the compaction processes varies interspecifically in pachypleurosaurid taxa with *S. mirigiolensis* showing minor heterochronic shifts and *N. edwardsii* showing most heterochronic shifts relative to the data on the osteogenesis of the hypothesized plesiomorphic ancestral eureptilian condition . Therefore, pachypleurosaurids from Monte San Giorgio increase the number of heterochronic shifts with decreasing stratigraphical age and show a transition from more “terrestrial” to more variable “aquatic” data in comparison to Recent reptiles.

INTRODUCTION

Sediments of the UNESCO World Heritage site of Monte San Giorgio (Switzerland/Italy) have yielded several hundred pachypleurosaurid specimens since excavations started in 1924. Four distinct horizons of Middle Triassic bituminous limestones and shales ranging from the Anisian-Ladinian boundary to early Ladinian age have yielded two genera and four species of pachypleurosaurids: *Neusticosaurus edwardsii, N. peyeri, N. pusillus* and *Serpianosaurus mirigiolensis. S. mirigiolensis* is the oldest taxon and is known only from the basal Besano Formation (Rieppel, 1989). The three *Neusticosaurus* species were all found in the younger strata, the Lower Meride Limestone. *N. pusillus* originates from the Cava Inferiore horizon, *N. peyeri* from the Cava Superiore horizon (Sander, 1989), and *N. edwardsii* from the Alla Cascina horizon (Carroll and Gaskill, 1985). *N. pusillus* has also been found in the Germanic Triassic (Sander, 1989).

Pachypleurosaurids are sauropterygians which are extinct eureptiles found in marine sediments. Facies analyses indicate a habitat with more open sea influences for *S. mirigiolensis* and more lagoonal environments with an increasing restriction to the open sea for *Neusticosaurus* spp. (e.g., Furrer, 1995; Sander, 1989). Their degree of aquatic adaptation has been discussed in several morphological and histological studies during the last seven decades (Peyer, 1932; Nopsca and Heidsieck, 1934; Zangerl, 1935; Rothschild and Storrs, 2003; Carroll and Gaskill, 1985; Buffrénil and Mazin, 1989; Sander, 1989; Germain and Laurin, 2005; Canoville and Laurin, 2010). This study describes the order of the timing of limb formation in all four pachypleurosaurids in comparison to Recent terrestrial and aquatic reptiles. The aims of the study are to explore 1) whether the osteogenetic sequences of the pachypleurosaurids reveal more similarities to their hypothesized plesiomorphic ancestral eureptilian condition, and 2) whether the stratigraphically well separated pachypleurosaurids show an increasing trend of similarities, with decreasing stratigraphical age, towards data of Recent aquatic reptiles. The evolutionary changes in the morphology and the stratigraphical distribution of the pachypleurosaurid taxa from Monte San Giorgio indicate that it is more likely that the oldest pachypleurosaurid, *Serpianosaurus mirigiolensis*, shows more ancestral terrestrial features in its osteogenesis than the younger *Neusticosaurus* spp.: the morphological and histological changes from the stratigraphically older *S. mirigiolensis* to the stratigraphically younger *Neusticosaurus* spp. would leave evidence for the transition from less to more aquatic lifestyles (or other habitat preferences) (Carroll and Gaskill, 1985; Rieppel, 1989; Sander, 1989; Hugi et al., 2011).

Ossification sequences in Recent vertebrates have been extensively studied during the last decades (e.g., Keller, 1946; Mohammed, 1991; Rieppel, 1992, Caldwell, 1994, 1997; Abdala et al., 1997; Haas, 1999; Fröbisch, 2008; Werneburg et al., 2009). Fröbisch (2008) summarized the existing data on the timing of the beginning of ossification in tetrapods and showed that most of them in general show plasticity in the order within the single limb compartments, in contrast to the conserved sequence of terrestrial surface dwelling lizards with non-reduced limbs. The osteogenetic sequences in the limbs of Recent terrestrial surface dwelling lizards are always

proximodistally directed with a postaxial dominance in the autopodial region (e.g., Rieppel, 1992, 1993a, 1993b, 1994a, 1994b; Fröbisch, 2008; Hugi et al., 2010). However, similar trends in the ossification sequence data are generally indicated in tetrapods which share the same lifestyle: secondarily aquatic reptiles, for example, more often tend to show a preaxial gradient in the autopodial region in relation to tetrapods with other lifestyles. Furthermore, aquatic tetrapods more often show a delayed ossification in the proximal phalanges in relation to more distally located phalanges (e.g., Werneburg et al., 2009; Rieppel 1993a; Fröbisch, 2008) – a gradient that is even more generally preserved in the ossification sequences of urodeles (Fröbisch, 2008). Urodeles show more variation in the ossification sequences, but some common trends often are: a preaxial gradient in the zeugopodial region with a delayed overall development of the forelimb elements compared to equivalent regions of the hind limb (e.g., Erdmann, 1933; Keller, 1946; Haas, 1999; Nye et al., 2003; Fröbisch, 2008).

The clearing and double-staining procedure is a common tool to visualize the timing of the osteogenetic sequences in Recent vertebrates (Dingerkus and Uhler, 1977). The cartilaginous precursors of the limb bones are stained blue, whereas the onset of the ossification (i.e. primary endosteal and periosteal calcification of cartilaginous tissue) is stained red. The first recognition of red stained areas in a skeletal element is taken as the timing of initiation of ossification process to which we refer to as 'beginning of ossification' (Figs. 1, 2A). This early process of ossification is also indicated in the autopodial region of the pachypleurosaurids by the absence, or small size and shape of the phalanges (Appendix 2).

Immature pachypleurosaurids reveal additional osteogenetic processes that lead to their characteristically pachyosteosclerotic long bones (Peyer, 1932; Nopsca and Heidsieck, 1934; Zangerl, 1935; Ricqlès, 1976; Buffrénil and Mazin, 1989; Sander, 1989; Hugi et al., 2011). The term pachyosteosclerosis combines

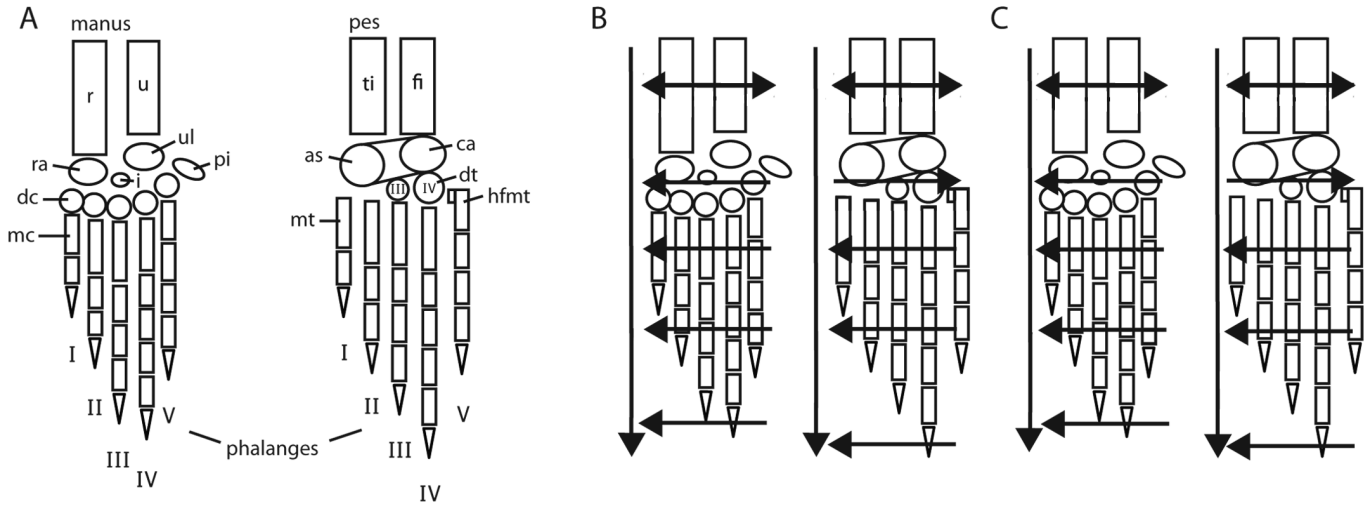

Fig. 1. Ossification sequences of the hypothesized terrestrial eureptilian model with *Liopholis whitii* as representative of other terrestrial surface dwelling lizards with non-reduced limbs (Hugi et al., 2010). **A**, skeletal composition of the zeugo- and autopodial region of the forelimb and hind limb of *Liopholis whitii*; **B**, arrows indicate the direction in the order of the initiation of ossification; **C**, arrows indicate the direction of the order of the termination of ossification. The termination sequence recapitulates the order of the initiation sequence.

pachyostosis and osteosclerosis (after Ricqlès and Buffrénil, 2001) and is achieved by the retention of a calcified cartilaginous core in the medullary region that is subsequently remodelled in neonates (osteosclerosis). In addition, the cortex appears to be swollen from external view based on no or only minor resorption processes that occur along the inner wall of the cortex in combination with an elongated phase of bone deposition along its outer wall (pachyostosis; Hugi et al., 2011). These osteogenetic processes that lead to pachyosteosclerotic long bones are here referred to as 'additional processes of compaction' to illustrate the fact that they increase the compactness parameters (after Girondot and Laurin, 2003) of the bone during the ontogeny, hence, producing more compact bones (Hugi et al., 2011). These additional processes of compaction are divided into an 'early phase of compaction sequence' and a 'final or end phase of compaction sequence' which are based on the preservation of a specific external taphonomic pattern in the limb bones of each pachypleurosaurids (Figs. 2B, 3). Neonate pachypleurosaurids for example show completely compressed bones (i.e., taphonomic, dorsoventral flattening), whereas juvenile specimens display different taphonomic patterns that can be arranged in a progressive order. Completely compact long bones are achieved in pachypleurosaurids that reached their final sizes, therefore, reveal no external depression patterns (Fig. 2B).

MATERIAL AND METHODS

The study is based on 40 specimens of *Serpianosaurus mirigiolensis* (30 specimens for the morphological description plus ten for histological description), 116 *Neusticosaurus pusillus* (all morphology), 58 *Neusticosaurus peyeri* (all morphology) and 31 *Neusticosaurus edwardsii* (21 specimens for morphology plus ten for histology) (Appendices 2–3), all housed in the Palaeontological Institute of the University of Zürich (PIMUZ). All pachypleurosaurid specimens are dorsoventrally embedded and prepared from one side. Rarely, both sides are available for study. Preparation was accomplished with a fine steel needle under a binocular microscope (magnifications: 16x, 40x); only a few specimens were prepared by air abrasive and phosphatic acid treatment (Sander, 1989). Petrographic thin-sections, both of longitudinal and transverse bone sections, were used for studying osteogenetic growth patterns (Hugi et al., 2011). Processing of thin-sections followed the protocol of Scheyer and Sánchez-Villagra (2007). Bone samples were first embedded into synthetic resin (Araldite-2020), before grinding with SiC powder (220, 500, 800) to approximately 80 µm thickness, depending on the natural colour of the bones. Histological description is based on observations with a binocular microscope (magnifications: 16x and 32x) and a Leica DM2500 compound polarizing microscope (magnifications: 1.25x, 2.5x, 5x, 10x, 20x, normal transmitted and polarized light), the latter being equipped with a wide-field lens (1.6x) and a DFC 420C digital camera. The extinct specimens were ordered based on their standard lengths (Sander 1989: st = length of the four posteriormost dorsal centra) using digital calipers to the nearest 0.1 mm. In this study, the st ranges from 5.4 mm (size class <A) to 38.5 mm (size class H) in *S. mirigiolensis,* from 3.7 mm (size class B) to 23.2 mm (size class M) in *N. pusillus*, 2.4 mm (size class A) to 34.6 mm (size class Q) in *N. peyeri*, 23.2 mm (size class B) to 64.1 mm (size

class F) in *N. edwardsii* (see Appendices 2-3; size classes after Sander, 1989). Specimens used for histological sectioning were generally incomplete and estimated size classes are assigned based on growth analysis from Sander (1989). Sander gave detailed parameters for several morphometric ratios (e.g., humerus/st; humerus/femur, etc.) for each of the four pachypleurosaurids (Sander, 1989:table 9, page 631). The estimation of the size classes is achieved by retro-calculation of the given ratios and requires either the preservation of the st, the length of humerus, third metacarpal or femur.

The information about the osteogenetic sequences in extinct and extant reptiles is either derived from literature (e.g., Mohammed, 1991; Rieppel, 1992, 1993b, 1994a, B; Caldwell, 1994, 1997; Lobo et al., 1995; Abdala et al., 1997; Federico and Lobo, 2006; Fröbisch, 2008) or is based on personal observations (Werneburg et al., 2009; Hugi et al., 2010). The ossification studies of extant reptiles are mainly based on cleared and double-stained ontogenetic series (Dingerkus and Uhler, 1977). The osteogenetic sequences in the limbs of Recent terrestrial surface dwelling lizards with well developed limbs are hypothesized to represent the plesiomorphic ancestral condition for terrestrial eureptiles – an assumption which is indicated by several features: (1) Recent terrestrial lizards often show the same limb morphology as the hypothesized plesiomorphic ancestral reptilian condition (except for the number of mesopodial or sesamoid bones; Romer, 1956; Mathur and Goel, 1976; Rieppel, 1992, 1994a; Mohammed, 1991; Lobo et al., 1995); (2) A terrestrial mode of life is also indicated for the plesiomorphic ancestral eureptile (e.g., Canoville and Laurin, 2010); (3) The known osteogenesis of early diapsids conforms to the pattern of Recent terrestrial lizards (Rieppel, 1992; Caldwell, 1994); (4) Recent terrestrial lizards are the only tetrapods whose osteogenetic data closely resemble the order of the condensation and chondrogenesis processes (exception: mesopodial region and fifth digit; e.g., Mathur and Goel, 1976; Rieppel, 1992; Fröbisch, 2008). In contrast to the large variety of osteogenetic sequences in other tetrapods, condensation and chondrogenesis strictly follow two conserved pathways, one shared by all amniotes and anurans and one shared by all urodeles (Shubin and Alberch, 1986; Oster et al., 1988; Rieppel, 1992, 1994a, 1994b; Fröbisch, 2008).

An event pairing analysis was performed separately for the sequence order in the early and final phase of the additional compaction processes for all four pachypleurosaurid species for detecting heterochronic shifts in the osteogenetic sequences. More recent studies for estimating evolution of temporal changes in the ossification sequences were not applied (Harrison and Larsson, 2008; Germain and Laurin, 2009), because these methods are out of the scope of this study which focuses mainly on the description of the osteogenesis in pachypleurosaurids.

The event pairing analysis includes osteogenetic data of Recent terrestrial surface dwelling lizards as the hypothesized plesiomorphic ancestral condition for terrestrial eureptilians (Table 1 of Appendix 4; Supplementary Data 1; Hugi et al. (2010). The existing data on the osteogenetic sequences of other semi-aquatic or aquatic reptiles reveal similar trends in the order, but often lack enough resolution for inclusion in the analysis. For each of the five eureptilian species included in the event pairing (Velhagen, 1997), a character

matrix was constructed in which the sequence order of the early and end phase of the additional compaction processes among the 26 elements listed in Table 1 of Appendix 4 is related to every other event. This resulted in a total of 325 event pairs for each species (Supplementary Data 1) which were plotted in a parsimony optimization using the program Mesquite version 2.74 (Maddison and Maddison, 2010; Appendix 5). The distribution of the character states of the event pairs are given as numerical values and percentages in Table 2 and Appendix 4. Three ordered character states—before 0), simultaneously (1), or after (2)—reflect the timing of one event relative to another (Table 2, Appendix 4). Simultaneous events, so called ties, are regarded to result from a lack in resolution.

Anatomical Abbreviations—**as**, astragalus; **be**, band of lamellar bone in the calcified cartilaginous core of the medullary region; **c**., cartilage; **ca**, calcaneum; **c.c.,** calcified cartilage; **co, cortex; dia. meta. dep**., dia-, metaphyseal depression; **dia. elev**., diaphyseal elevation; **dc**, distal carpal; **dt**, distal tarsal; **e. calc**., endochrondral calcification; **en. dep**., endosteal bone depositional infillings; **ep. acc**., epiphyseal bone accretion; **ep. rd**., epiphyseal ridge; **f**, fibula; **gm**, growth mark; **hfmt**, hooked fifth metatarsal; **i**, intermedium; **mc**, metacarpal; **meta. dep**., metaphyseal depression; **mt**, metatarsal; **lzb**, lamellar-zonal bone type; **p. calc**., perichondral calcification; **pi**, pisiforme; **po. acc**., periosteal accretion at the outer wall of the cortex; **prim. if**., primary infilling of vascular canals; **prim. ost**., primary osteon; **r**, radius; **ra**, radiale; res., resorption; **sb**, sharp border between cortex and medullary region; **sec. if**., secondary infillings of vascular canals; **sec. tra**, secondary trabeculae; **srvc**, simple radial vascular canals; **t**, tibia; **u**, ulna; **ul**, ulnare; **wp**, woven-fibered bone tissue grading into parallel-fibered bone tissue.

RESULTS

The osteogenesis of the pachypleurosaurian limbs is divided into two steps: (1) developmental sequences of ossification during embryology and/or in early neonates, (2a) additional primary periosteal compaction processes, and (2b) additional primary and secondary endosteal compaction processes of the bones during the neonate ontogeny. The pattern and sequences of the developmental and additional compaction processes are described in more detail in the following result sections.

Developmental Sequences of Ossification

Ossification in the mesopodial and phalangeal region occurs during the neonate ontogeny in pachypleurosaurids, and as a result these elements are often absent or not completely preserved (small size and shape) (Appendix 1) due to the weak fossilisation potential of their cartilaginous precursors. Results show that in all four pachypleurosaurid taxa, the pes completes phalangeal ossification prior to manus (Appendix 2). The manus initiates beginning of ossification as follows in *Serpianosaurus mirigiolensis*, *Neusticosaurus pusillus* and *N. peyeri*: digit I > digit II > digit III > digit IV > digit V. The order in the beginning of ossification in the manus of *N. edwardsii* is digit I > digit II > digit III > digit V > digit IV. The same observation was made in the pes of *N. pusillus* and *S. mirigiolensis*. The other pachypleurosaurid taxa, *N. peyeri* and *N. edwardsii* show ossification initiation sequences of the pes as follows: digit I > digit

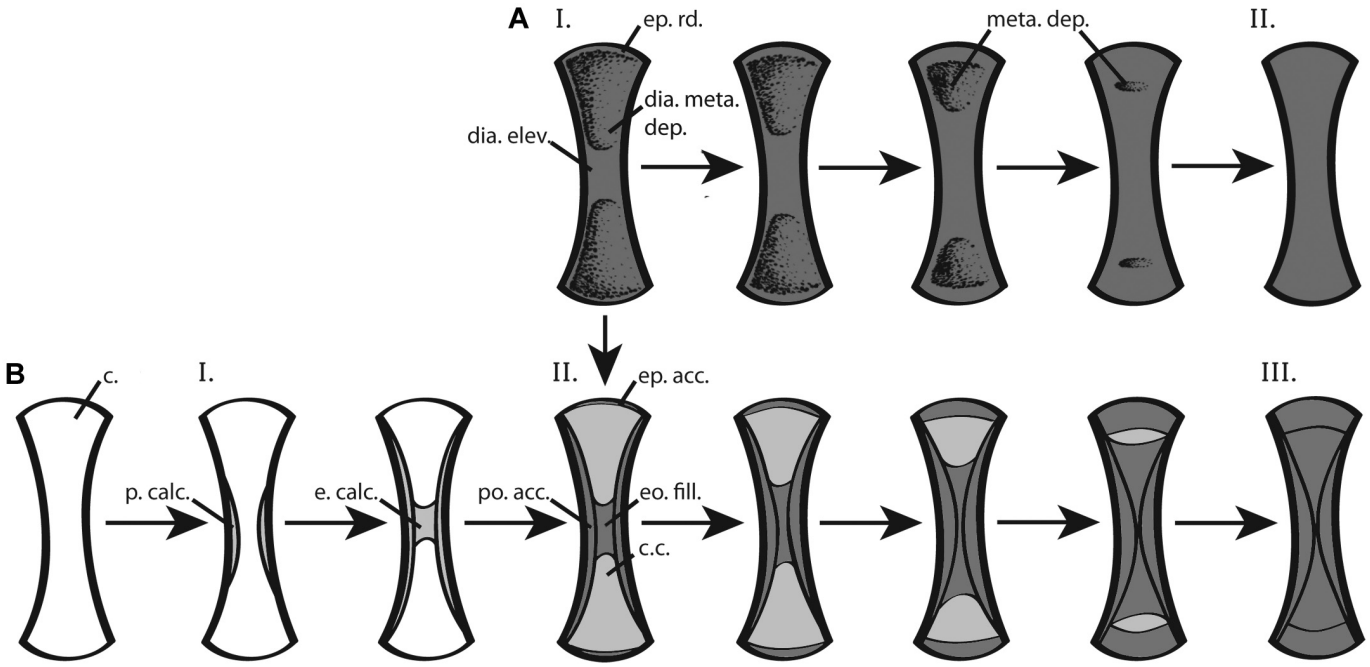

Fig. 2. Summary of the osteogenesis in pachypleurosaurid long bones as revealed by bone histology and morphology. **A**, sketch of the external taphonomic patterns. External depression patterns correspond to the internal bone histology. I, Series of subsequent reduction of the depression patterns in the diaphyseal and metaphyseal areas. II, Completely compact long bone that shows no external taphonomic depressions. **B**, sketch of the internal histological view of longitudinally sectioned long bones. I, Ossification first starts perichondrally in the diaphysis in late embryos forming the mid-shaft periosteal collar, proceeding to the meta- and subsequently to the epiphyseal regions. Endochondral calcification starts in the diaphyseal region. II, Early phase of the additional compaction processes with increasing progression of pachyosteosclerosis. III. Final phase of additional compaction processes that is marked by completely compact bones, therefore with no external taphonomic depression patterns (see AII).

II > digit III > digit IV > digit V (Appendix 2). All four pachypleurosaurid taxa show delayed initiation of ossification mesopodial ossification in relation to other limb bones.

Primary Periosteal and Secondary Primary and Endosteal Compaction

External Taphonomic Sequences of Compaction—External taphonomic patterns reveal subsequent compaction series in postembryonic ontogenetic stages in all pachypleurosaurid taxa (Figs. 2 and 3; Appendix 3). In very small pachypleurosaurid specimen, the limb bones are entirely dorsolaterally compressed prior to additional compaction processes. Later in ontogeny, a non-depressed diaphyseal area is recognized (Fig. 2A), accompanied by a slightly thickened rim which 'frames' the complete outline of the bone (Fig. 2A). The occurrence of these two characters marks the early phase of the additional compaction processes (Fig. 2A). The diaphyseal non-depressed area continuously expands to both shaft ends in limb bones throughout ontogeny. Whereas the outline of the dorsoventrally embedded limb bones broadens slightly along the mediolateral margins, both the epiphyseal ridges appear to grow in thickness more rapidly. The limb bones are regarded as fully compact bones as soon as the diaphyseal elevation and epiphyseal ridge reach each other, resulting in a compact bone with no depression patterns (Fig. 2A). To summarize, the order of the compaction sequences is based on the

ratio of the non-depressed area to the entire bone area. Results of the external compaction sequences show slight variation between the four pachypleurosaurid species studied. Common trends in compaction sequences are (Fig. 4: e.g., *Neusticosaurus pusillus*; Appendix 3):

(1) the early phase of the additional compaction processes takes place from proximal to distal across the whole limb; (2) the preaxial and postaxial zeugopodial bones of both the forelimbs and hind limbs start the early phase of the additional compaction processes simultaneously (when available); (3) the early phase of the additional compaction processes of mesopodial bones is delayed and shows a postaxial gradient in the manus and a preaxial gradient in the equivalent region of the pes (when available); (4) the early phase of the additional compaction processes in the phalanges proceeds in proximodistal direction, when available with a postaxial dominance; (5) the end phase of the additional compaction processes displays a preaxial dominance in the zeugopodial region; (6) the end phase of the additional compaction processes is delayed in the mesopodial bones and shows a preaxial gradient; (7) the end phase of the additional compaction processes proceeds with a preaxial dominance within the phalanges (when available); (8) in cases where the metapodials show a postaxial gradient in the early phase and/or in the end phase of the additional compaction processes, the order is as follows: metapodial-4 > metapodial-3 > metapodial-2 > metapodial-1 > metapodial-5; (9) in cases where the metapodials show a preaxial gradient in the early phase and/or in the end phase of the additional compaction processes, the order is as follows: metapodial-1 > metapodial-2 > metapodial-3 > metapodial-4 > metapodial-5; (10) every forelimb bone precedes its equivalent hind limb element in the early phase of the additional compaction processes; and (11) the final phase of compaction processes is also first completed in the forelimb.

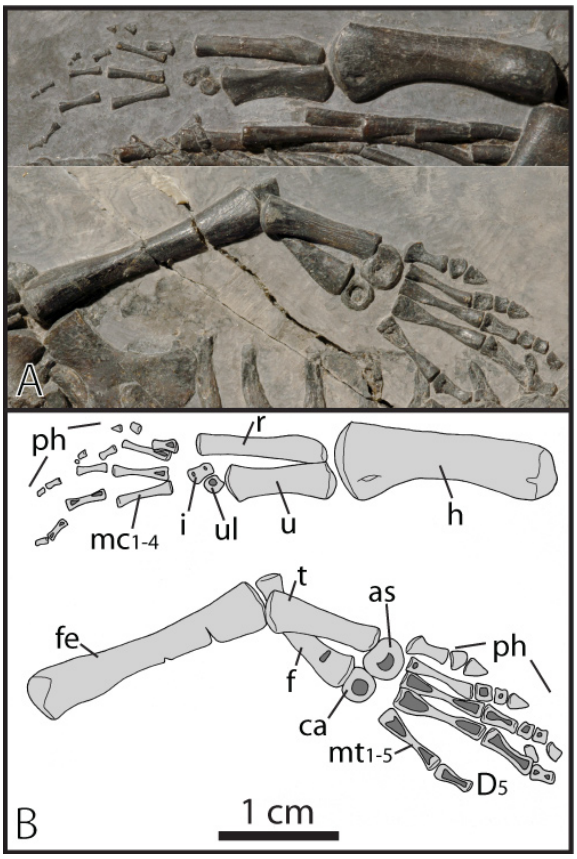

Fig.3. An example of the osteogenetic order of one pachypleurosaurid taxon. The images and the redrawing show an intermediate stage of compaction in T3639 of *Neusticosaurus pusillus*. Compaction ended already in the stylo- and zeugopodial region as well as in the terminal phalanges of the forelimb (upper part of image **A** and **B**), whereas depression patterns are still discernable in the intermediate and proximal phalanges of the fourth digit. Therefore, a distoproximal gradient in the phalanges and a post- to preaxial gradient in the metacarpals is indicated in this case. The metatarsals (lower part of image **A** and **B**) show a pre- to postaxial gradient, whereas compaction mainly ended already in the terminal phalanges of the hind limb (preaxial distoproximal gradient). A proximodistal gradient is indicated in the stylo- and zeugopodial region.

To summarize, in all pachypleurosaurid taxa, compaction processes are accelerated in individual elements of the forelimb relative to the hind limb. Variation in the timing of the sequence

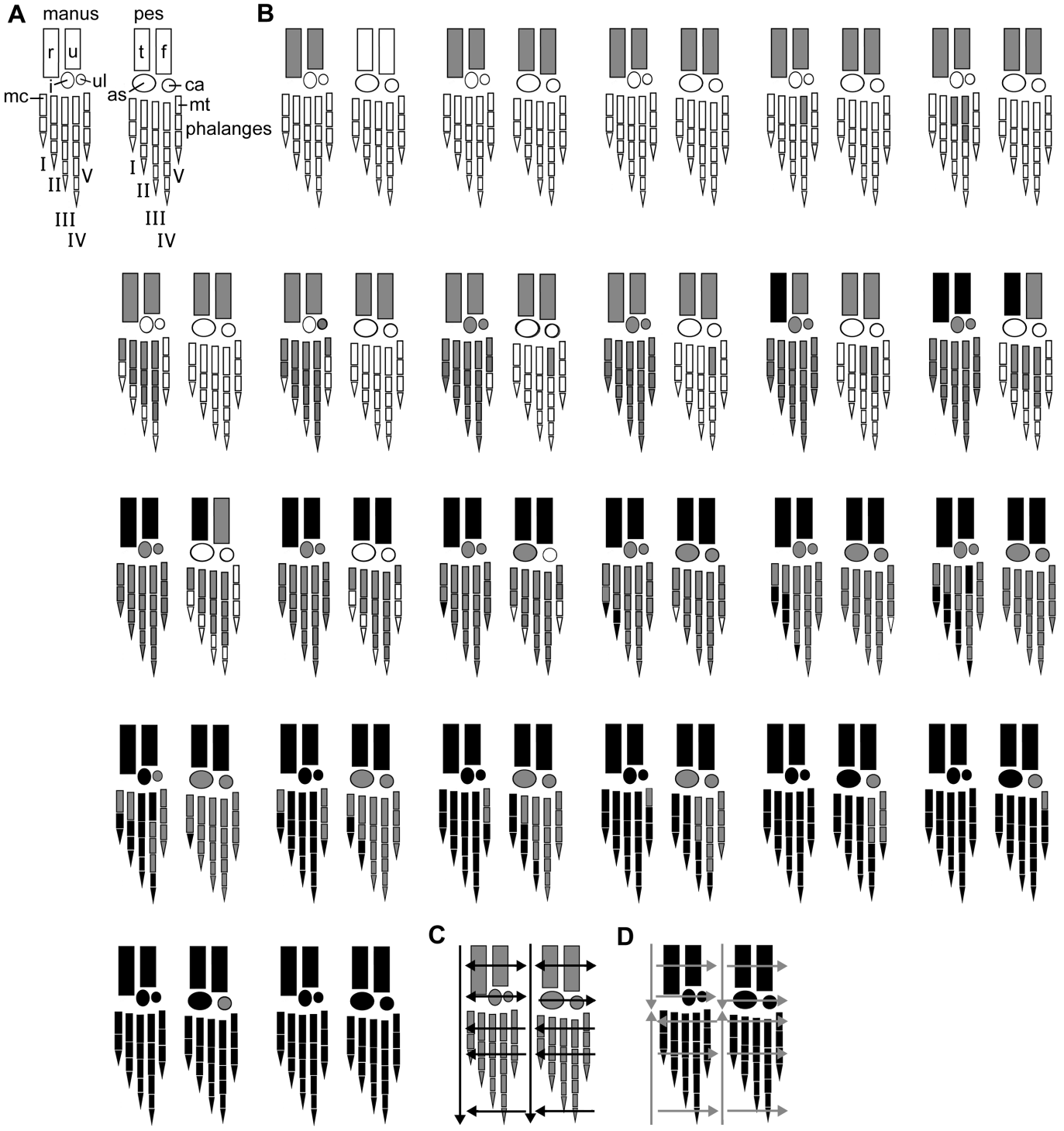

Fig. 4. Osteogenetic sequences of *Neusticosaurus pusillus* as an example for the pachypleurosaurid taxa from Monte San Giorgio. **A**, sketch of the skeletal composition of the zeugo- and autopodial region of the forelimb and hind limb. **B**, different greyscales indicate the relative progression in osteogenesis with black representing entirely compact bones. **C**, arrows indicate the direction of the early phase of the additional compaction processes showing an overall proximodistal gradient with a postaxial dominance in the zeugopodial region as well as in the metapodials, and proximal and intermediate phalanges. Mesopodial bones of the pes and terminal phalanges display a preaxial dominance. **D**, arrows indicate the direction of the order during the final phase of the additional compaction processes. Every single structural element of the zeugo- and autopodial regions (except for the metacarpals) now changed into preaxial dominance. The osteogenesis is now distoproximally directed across the autopodial region.

order of the early and final phase of compaction is preserved in the order within and among the single limb compartments, and therefore, in the gradient of the zeugopodial region, as well as in the dominance of the metapodial and the phalangeal regions (Appendices 3–4). In the phalanges of *Serpianosaurus mirigiolensis*, both the early and final phase of the additional compaction processes maintain a proximodistal direction, whereas the autopodial regions of *Neusticosaurus* spp. reveal a proximodistal direction in their early phase of the additional compaction, but a distoproximal gradient when these compaction processes end (exception: metapodials of *N. edwardsii* start and end compaction processes after the proximal phalanges). The metacarpals of *S. mirigiolensis, N. pusillus* and *N. edwardsii* show a postaxial gradient in both the early and final phase of the additional compaction processes. *N. peyeri* shows a postaxial gradient in the metapodials of the forelimbs and hind limbs when the additional compaction processes start, whereas a preaxial gradient is observed when the additional compaction processes end. The same pattern is also visible in the metatarsals in *S. mirigiolensis* and in showing more frequent postaxial than preaxial dominance. Furthermore, in most cases the fibula of *N. edwardsii* ends the additional compaction processes simultaneously with the terminal phalanges of the pes–a sequence that sometimes occurs in *N. peyeri,* as well as in rare cases in *N. pusillus* (Appendix 3).

Internal Compaction Patterns—Postembryonic specimen of all pachypleurosaurid taxa from Monte San Giorgio reach maximal compaction (pachyosteosclerosis) in their bones by retaining a calcified cartilaginous core in the medullary region, which is subsequently modified by remodelling processes (i.e., resorption, as well as primary and secondary endosteal depositional infillings [osteosclerosis sensu Ricqlès and Buffrénil, 2001]). In addition, the accretion of primary periosteal bone, which is cyclically deposited at the outer wall of the cortex combined with no or minor resorption of the inner wall of the cortex, leads to a pachyostotic condition (sensu Ricqlès and Buffrénil, 2001). The three dominant causes leading to pachyosteosclerosis are listed in more detail (modified and emended from Buffrénil and Mazin, 1989):

(1) The calcified cartilaginous core is not resorbed during embryology, neither in the dia-, meta- nor in the epiphyseal region. Therefore, no medullary cavity is formed. (2) Bone depositional processes start simultaneously at different localities within the well-vascularized, cartilaginous core. In the diaphysis, secondary trabeculae, as well as primary and secondary infillings of vascular canals, are deposited (Figs. 5A–F). In the epiphyseal regions, bands of lamellar bone are deposited subparallel to the epiphyseal articular surface (Fig. 5F). (3) Synchronously with (2), circular periosteal bone accretion along the outer wall of the cortex associated with minor or no resorption of the inner wall of the cortex leads to the pachyostotic condition of the bone.

During early embryonic stages (T3705, Sander, 1988, 1989), the cartilaginous precursor of the bone is mineralized and the endochrondral tissue remains as a calcified cartilaginous core. In the diaphysis, the medullary region remains the same in width whereas circular cortical layers continue to cyclically accrete postembryonically. Cross sections of the diaphyseal regions of small pachypleurosaurid specimen reveal a very

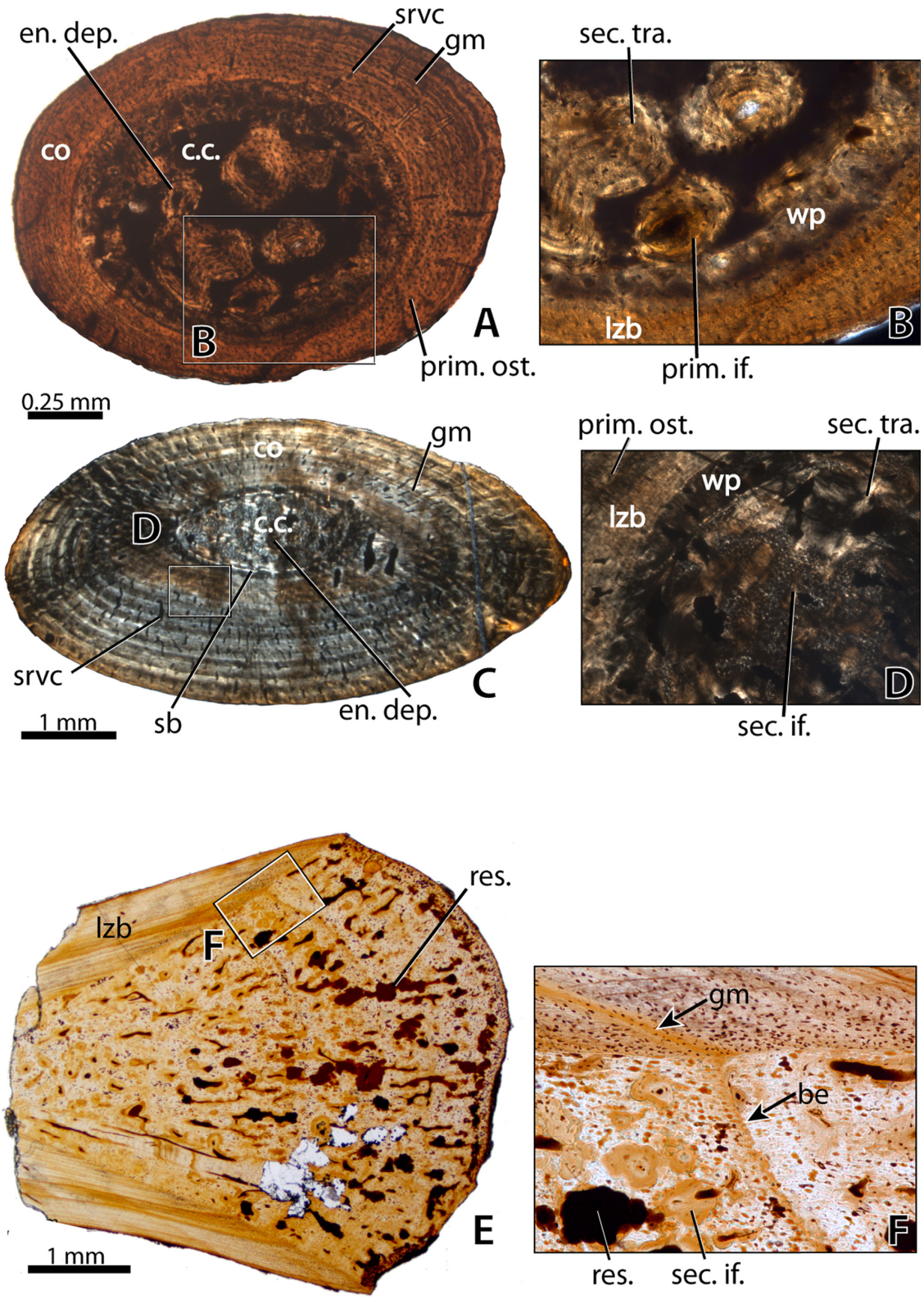

Fig. 5. Long bone histology of *Serpianosaurus mirigiolensis* and *Neusticosaurus peyeri* as examples for all pachypleurosaurid taxa of Monte San Giorgio from Switzerland/Italy. **A**, **C** and **E** show the general view of the sections, whereas **B**, **D**, **F** display a part in higher magnification. **A** and **B**, cross section of the diaphyseal area of the femur of a juvenile *S. mirigiolensis* (T131; normally transmitted light). Bone accretion along the outer wall of the cortex constitutes of four growth cycles. A few secondary infillings of the vascular canals and a single secondary trabeculae are housed in the calcified cartilage in the medullary region; **C** and **D**, cross section of the diaphyseal area of the humerus of an adult specimen of *S. mirigiolensis* (T4510; polarized light). A minimum number of 11 annuli and lags (i.e., lines of arrested growth after Castanet et al., 1993) are counted in the cortex. The medullary region shows more secondary infillings of the vascular canals as well as an extensive scaffold of secondary trabeculae; **E** and **F**, longitudinal section of the humerus of *N. peyeri* (T4258; normally transmitted light; thin section kindly provided by P. Martin Sander). In the epiphyseal area of the calcified cartilaginous core, bands of lamellar bone are visible. Higher magnification reveals the correspondence between these bands and the growth marks in the cortex.

thin cortex and a comparatively large medullary region (Fig. 5A). The bone tissue of the bone type varies in the growth and vascularisation pattern of the cortical region within the four pachypleurosaurid taxa. The long bones of all pachypleurosaurid taxa show slower deposited lamellar-zonal bone type (except for the innermost periosteal bone layer of embryonic bone). *S. mirigiolensis* only shows lamellar bone, *N. pusillus* and *N. peyeri* display parallel-fibered and lamellar bone (Hugi et al., 2011), and *N. edwardsii* shows a varying growth pattern of lamellar bone and poorly organised parallel-fibered bone with higher vascularisation (Hugi et al., 2011). The cortex of all pachypleurosaurid taxa shows a varying number of simple radial and longitudinal vascular canals, as well as a few primary osteons (Fig. 5C). The number of cortical bone layers increases with the size of the animal. Cortical bone deposition rates may decline with progressing age when sexual maturity is reached or remain constant (Hugi et al., 2011). The Castanet et al., 1993) along the periphery of the cortex called external fundamental system (EFS after Horner et al., 2001).

The additional compaction processes that occur as endosteal depositional infillings in the inner calcified cartilaginous core start simultaneously with the periosteal bone accretion along the outer wall of the cortex. An increase in the compactness values of the medullary region, which start in the mid-shaft area, is produced by deposition of secondary trabeculae and bony infillings of simple vascular canals which are later widened by resorption and secondarily filled with centrifugally deposited lamellar bone (Hugi et al., 2011). Secondary trabeculae continuously build up a bony scaffold within the medullary region. In longitudinal sections of the bones, smooth lamellar bone bands, which correspond to the annuli preserved in the cortex, are accreted in the epiphyseal areas of the calcified cartilaginous core (Fig. 5F). The bone infillings of the vascular canals and the trabeculae are continuously deposited, starting from mid-shaft and expanding to both shaft ends, whereas the lamellar bone bands are deposited cyclically in the shaft ends (Fig. 2B; Fig. 5E). The quantity of the secondary trabeculae, as well as the widened and infilled vascular canals, increases with the age of the pachypleurosaurids, but also with the total adult size in the specimens of the *Neusticosaurus* spp. (Hugi et al., 2011) Therefore, *N. edwardsii* shows a higher amount of bony deposits in the calcified cartilaginous core of the medullary region (Hugi et al., 2011).

Event pairing

Variation in the Timing in the Early Phase of Additional Compaction Processes—The data for the event pairing analysis are based on 26 long bone elements listed in Table 1 of Appendix 4. Of all event pairs found in the event pairing analysis for the detection of heterochronic shifts in the early phase of compaction processes, 212 (65.2 %) show the same state in all taxa. For 27 (8.3 %) of the event pairs, all except ties are uniform. These two groups of uninformative characters constitute 73.5 % of the total analysis. In 22 event pairs, there are states 0 and 2, but also ties. 5 of these 22 event pairs indicate a separation of *Neusticosaurus* spp. from the hypothesized terrestrial eureptilian model with *Serpianosaurus mirigiolensis* showing a lack of resolution. In 64 event pairs there are no ties and 32 of them are informative showing a distinction between the hypothesized terrestrial eureptilian model and pachypleurosaurid taxa, which is

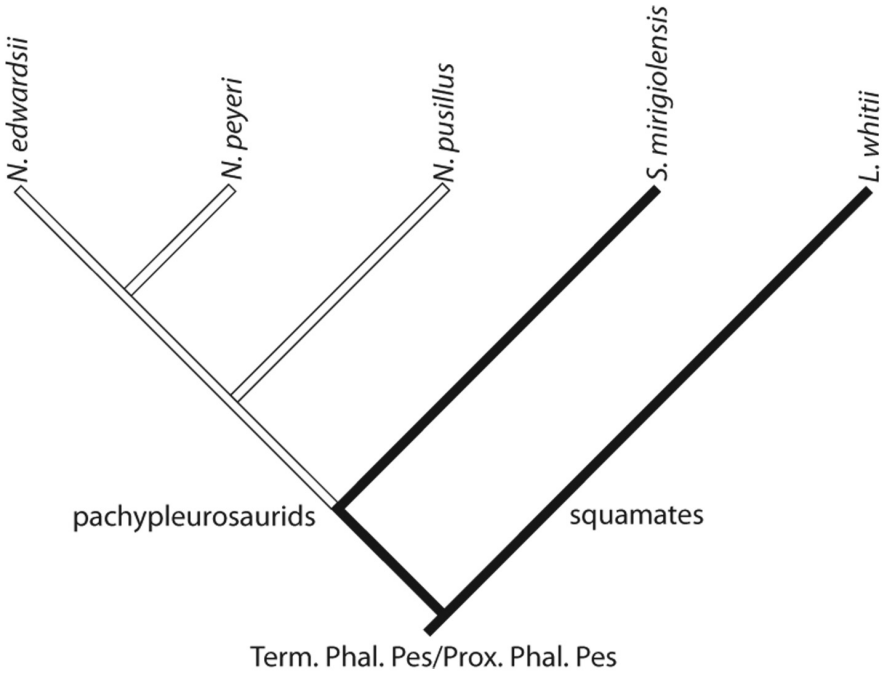

Fig. 6. Parsimony optimization of the results of the event pairing analysis, using the order of the 'terminal phalanges pes/ proximal phalanges pes' during ending of ossification in the outgroup and during the final phase of the additional compaction processes in the pachypleurosaurid taxa as an example. For this event pair, *Neusticosaurus* species show state 0, whereas *Serpianosaurus mirigiolensis* and the outgroup show state 2, indicating that in the stratigraphically oldest pachypleurosaurid (*Serpianosaurus*), the terminal phalanges of the pes develop later than the proximal phalanges, as in the outgroup.

based on the difference in the timing of the onset of ossification in the forelimb elements compared to the equivalent elements of the hind limbs. 4 of 64 event pairs support a separation of *N. edwardsii* from the rest of the pachypleurosaurid taxa and from the hypothesized terrestrial eureptilian model based on the variation in the timing of the first onset in the metapodials and the proximal phalanges. The rest of the 64 event pairs displays differences in the timing of single subunits of the forelimbs in relation to the other subunits of the hind limbs, therefore, supports the observation of a delayed onset of compaction processes in the hind limbs of the pachypleurosaurids.

Variation in the Timing in the Final Phase of Additional Compaction Processes—No heterochronic shifts were detected in 186 (57.2 %) of the 325 event pairs as they show the same state in all eureptilian taxa. For 23 (7.1%) of the event pairs, all except ties are uniform. These two groups of uninformative characters constitute 64.3 % of the total. In 22 event pairs, there are states 0 and 2, but also ties, so that only a few of them are informative characters, as resolution of the ties may then imply no heterochronies. 16 of 22 indicate a separation of the hypothesized terrestrial eureptilian model from the pachypleurosaurid taxa but with one or two ties in the latter. In 94 event pairs there are no ties and 55 of them are informative clearly separating the hypothesized terrestrial eureptilian model from the pachypleurosaurid taxa. This separation is based on the difference in the timing of the forelimb and hind limb elements, as well as based on the variation in the osteogenetic gradient in the autopodial region. 6 of 94 show the hypothesized terrestrial eureptilian model and *N. edwardsii* to be separated from the rest of the pachypleurosaurids, based on similar postaxial osteogenetic gradient in the metatarsals of the two former taxa. 7 of 94 show a separation of *Serpianosaurus mirigiolensis* and the hypothesized terrestrial eureptilian model from the pachypleurosaurid taxa, based on the proximodistal gradient in the autopodial region (e.g., Fig. 6). The rest of the 94 event pairs reflect differences in the timing of single

subunits of the forelimbs compared to the other subunits of the hindlimbs that are delayed in the development of maximal compaction.

DISCUSSION

The pachypleurosaurid taxa from Monte San Giorgio provide snapshots of various stages of ontogeny and reveal detailed information about the osteogenetic sequences and associated histology. The timing of the order of the early phase of the additional compaction processes in the pachypleurosaurid taxa from Monte San Giorgio follows the major trends of the ossification sequences of terrestrial surface dwelling lizards, whereas the timing of the end phase of the additional compaction processes displays major heterochronic shifts compared to their early phase, as well as compared to the ossification gradients of the hypothesized terrestrial ancestor. The results of the event pairing analysis show that the differences are based mainly on three variations in osteogenetic sequences: (1) differences based on the relative timing of the elements of the forelimb compared to equivalent elements of the hind limb; (2) differences in the proximodistal and distoproximal direction in the manus and pes in the end phase of the additional compaction processes; and (3) differences in the preaxial and postaxial dominance of the metapodials in the end phase of the additional compaction processes.

A comparison of ossification sequences in the limbs of Recent semi-aquatic or aquatic reptiles (e.g., pleurodire [Werneburg et al., 2009], cryptodire turtles [e.g., Sheil, 2003, 2005; Sánchez-Villagra et al., 2009], as well as crocodiles [e.g., Rieppel 1993b]) shows variation in the two major gradients of the autopodial region compared to the conserved ossification sequences of Recent terrestrial surface dwelling lizards. However, similar trends in the ossification sequences of secondarily semi-aquatic or aquatic reptiles are often displayed in a change from a postaxial to a preaxial gradient and/or a change from proximodistally to distoproximally directed osteogenesis in the phalanges (e.g., Rieppel, 1993b, 1993c; Sheil and Greenbaum, 2005; Sánchez-Villagra et al., 2009). The order of the end phase of the additional compaction processes of the *Neusticosaurus* spp. is similar to trends in extant semi-aquatic or aquatic reptiles. A clear preaxial dominance in the zeugopodial region has, at least to our knowledge, only been preserved in Urodela and not in any amniote reptile (e.g., Keller, 1946; Nye et al., 2003; Fröbisch, 2008).

The osteogenetic sequences of the pachypleurosaurids reveal more ancestral terrestrial features for *Serpianosaurus mirigiolensis*, and more aquatic features for the younger *Neusticosaurus* spp. These data therefore, support previously results on the morphology and histology of the pachypleurosaurid taxa from Monte San Giorgio. *S. mirigiolensis* shows a proximodistal direction in the early and end phase of the compaction processes in the phalanges, whereas the younger *Neusticosaurus* spp. show this region to end the additional compaction process inversely. Therefore, the interspecific variation in the osteogenetic gradient of the phalanges could indicate an adaptive change in the *Neusticosaurus* spp.. In contrast, the interspecific variation in the metapodials does not give any information about the transition of an adaption among the pachypleurosaurid taxa. The order of the final phase of the additional compaction processes in the metatarsals, for

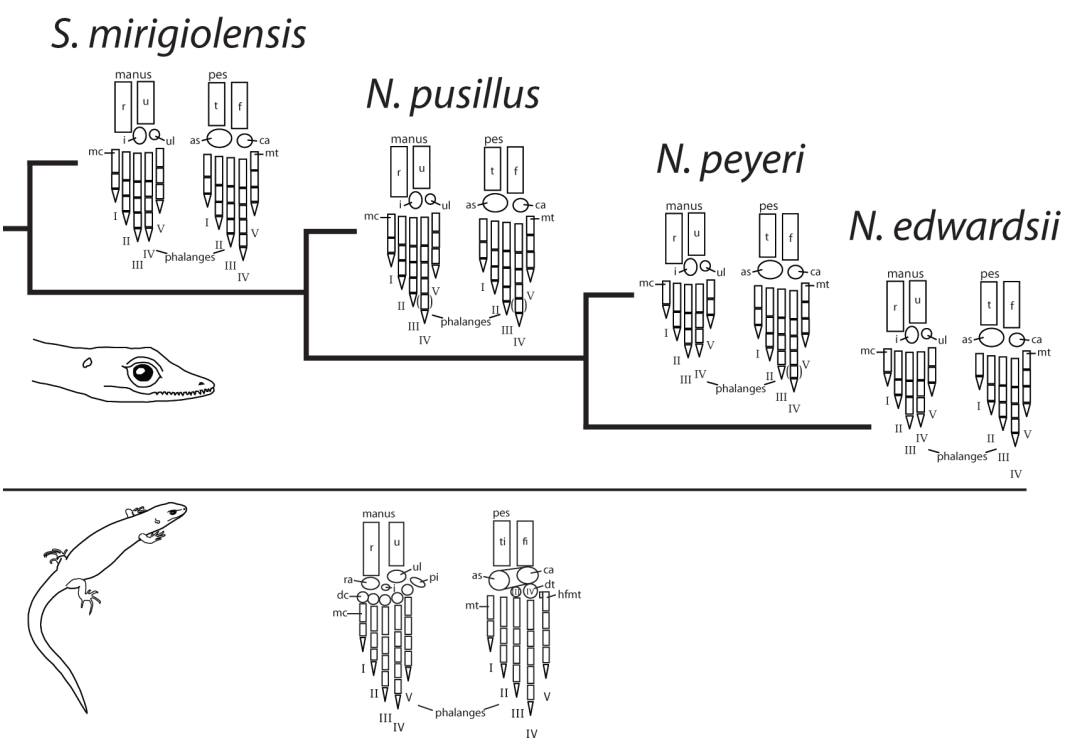

Fig. 7. Skeletal composition of the forelimb and hind limb of all four pachypleurosaurid taxa from Monte San Giorgio, in relation to the plesiomorphic ancestral condition of terrestrial eureptiles. Pachypleurosaurids tend to decrease the number of the phalanges with decreasing stratigraphical age.

example, changes from a preaxial gradient in *S. mirigiolensis* to a postaxial one in *N. pusillus*, to preaxial in *N. peyeri*, and to postaxial in *N. edwardsii* again. Intraspecific variation is preserved in the dominance of the end phase of the compaction processes in the hind limbs (metatarsals of *N. edwardsii*, fibula of *N. pusillus*, *N. peyeri* and *N. edwardsii*; Appendix 3), without obvious functional reasons.

Reduced phalangeal formulae of *Neusticosaurus* spp. conform to snapshots of the end phase of the compaction sequences of *S. mirigiolensis* (Fig. 7; Appendix 3)–a general trend in the ossification sequences in limb reduced species and their relatives with no limb reduction (Morse, 1872; Alberch and Gale, 1985; Shapiro et al., 2007). Greer (1987, 1990), for example, studied this phenomenon in the forelimbs and hind limbs of extant squamates and documented that the ontogenetic stages of the manus and pes of squamates with non-reduced pentadactyl limbs are reflected by the adult limb morphology of related squamates with limb reduction.

O'Keefe et al. (1999) demonstrated that the ontogenetic trajectory between the transitions from *N. peyeri* to *N. edwardsii* were more highly conserved than the transition from *Serpianosaurus* to *Neusticosaurus*. Main differences between *N. peyeri* and *N. pusillus* in relation to *N. edwardsii* were found in the adult body sizes, vertebral growth and number as well as in skeletal growth rings of the long bones indicating conserved growth with respect to chronological age, size and shape (O'Keefe et al., 1999). Similarly, in the present study, the osteogenetic sequences separate *S. mirigiolensis* from *Neusticosaurus* spp., but the bone histology of the former is similar to *N. edwardsii* (Hugi et al., 2011).

In conclusion, the results of sequence analysis and the comparison with extinct and extant reptiles show that the pachypleurosaurid

taxa from Monte San Giorgio exhibit heterochronic shifts in the osteogenetic sequences of their limbs in comparison to the hypothesized plesiomorphic ancestral condition for terrestrial eureptilians. The order of the osteogenetic sequences varies interspecifically in pachypleurosaurid taxa with *S. mirigiolensis* showing less heterochronic shifts and *N. edwardsii* showing the most heterochronic shifts relative to the data of the hypothesized plesiomorphic ancestral eureptilian condition. Therefore, pachypleurosaurids from Monte San Giorgio increase the number of heterochronic shifts with decreasing stratigraphical age. Data further indicate a correlation between the ontogenetic changes in the bone histology and the taphonomic external depression patterns of the bones (Figs. 2A–B).

The reoccurrence of these patterns in the ontogenetic series of all four pachypleurosaurid taxa whose extremities are entirely preserved by large sample sizes (30 *Serpianosaurus mirigiolensis*, 116 *Neusticosaurus pusillus,* 58 *Neusticosaurus peyeri* and 21 *Neusticosaurus edwardsii*) demonstrates that these observed patterns can be regarded as biological features that are revealed by taphonomy. The same diagenesis is applied to at least the bones within a single specimen as the same patterns are preserved in all pachypleurosaurids originating from four different horizons and different localities. Hence, at least the bones of each specimen can be compared to each other by their external pattern and can be ordered by their relative progress of compaction.

ACKNOWLEDGMENT

This work would not have been possible without the generous help of H. Furrer, PIMUZ, who kindly provided the specimens on which this study is based. We thank M. Sánchez-Villagra and the whole PIMUZ for support. We thank especially M. Hebeisen for technical advice and help. We also thank P.M. Sander (Bonn), N. Klein (Bonn), M. Laurin (Paris), R. O'Keefe (West Virginia) and N. Fröbisch (Chicago) whose helpful comments certainly improved the quality of the manuscript. Swiss National Science Foundation No. 31003A_127053 to TMS and 31003A_133032 to MRS-V.

LITERATURE CITED

Abdala, F., F. Lobo, and G. Scrocchi. 1997. Patterns of ossification in the skeleton of *Liolaemus quilmes* (Iguania: Tropiduridae). Amphibia-Reptilia 18:75–83.

Alberch P., and E. A. Gale. 1985. A developmental analysis of an evolutionary trend: digital reduction in amphibians. Evolution 39:8–23.

Buffrénil, de V., and J. M. Mazin. 1989. Bone histology of *Claudiosaurus germaini* (Reptilia, Claudiosauridae) and the problem of pachyostosis in aquatic tetrapods. Historical Biology 2:311–322.

Canoville, A., and M. Laurin. 2010. Evolution of humeral microanatomy and lifestyle in amniotes, and some comments on paleobiological inferences. Biological Journal of the Linnean Society 100:384–406.

Caldwell, M. W. 1994. Developmental constraints and limb evolution in Permian and extant lepidosauromorph diapsids. Journal of Vertebrate Paleontology 14:459–471.

Caldwell, M. W. 1997. Limb osteology and

ossification patterns in *Cryptoclidus* (Reptilia: Plesiosauria) with a review of sauropterygian limbs. Journal of Vertebrate Paleontology 17:295–307.

Carroll, R., and P. Gaskill. 1985. The nothosaur *Pachypleurosaurus* and the origin of plesiosaurs. Philosophical Transactions of the Royal Society of London. B, Biological Sciences 309:343–393.

Castanet, J., H. Francillon-Vieillot, F. J. Meunier, and A. de Ricqlès. 1993. Bone Growth - Bone and individual aging; pp. 245–283 in B. K. Hall (ed.), Bone, CRC Press, Boca Raton.

Dingerkus, G., and L. D. Uhler. 1977. Enzyme clearing of Alcian Blue stained whole small vertebrates for demonstration of cartilage. Stain Technology 52:229–232.

Erdmann, K. 1933. Zur Entwicklung des knöchernen Skeletts von *Triton* und *Rana* unter besonderer Berücksichtigung der Zeitfolge der Ossifikationen. The Anatomical Record 290:900–912.

Federico, A., and F. Lobo. 2006. Patrones de osificacion en *Tupinambis merianae* y *Tupinambis rufescens* (Squamata: Teiidae) y patrones generales en Squamata. Cuendos de herpetologica 20:3–23.

Fröbisch, N. B. 2008. Ossification patterns in the tetrapod limb - conservation and divergence from morphogenetic events. Biological Reviews 83:571–600.

Furrer, H. 1995. The Kalkschieferzone (Upper Meride Limestone) near Meride (Canton Ticino, Southern Switzerland) and the evolution of a Middle Triassic intraplatform basin. Eclogae Geologicae Helvetiae 88(3):827–852.

Germain, D., and M. Laurin. 2005. Microanatomy of the radius and lifestyle in amniotes (Vertebrata, Tetrapoda). Zoologica Scripta 34:335–350.

Germain, D., and M. Laurin. 2009. Evolution of ossification sequences in salamanders and urodele origins assessed through event-pairing and new methods. Evolution & Development 11:170–190.

Girondot, M., and M. Laurin. 2003. Bone profiler: a tool to quantify, model, and statistically compare bone-section compactness profiles. Journal of Vertebrate Paleontology 23(2):458–461.

Greer, A. 1987. Limb reduction in the lizard genus *Lerista*. 1. Variation in the number of phalanges and presacral vertebrae. Journal of Herpetology 21:267–276.

Greer, A. 1990. Limb reduction in the scincid lizard genus *Lerista*. 2. Variation in the bone complements of the front and rear limbs and the number of postsacral vertebrae. Journal of Herpetology 24:142–150.

Haas, A. 1999. Larval and metamorphic skeletal development in the fast-developing frog *Pyxicephalus adspersus* (Anura, Ranidae). Zoomorphology 119:23–35.

Harrison, L. B., and H. C. E. Larsson. 2008. Estimating evolution of temporal sequence changes: a practical approach to inferring ancestral developmental sequences and sequence heterochrony. Systematic Biology 57:378–387.

Horner, J. R., K. Padian, and A. de Ricqlès. 2001. Comparative osteohistology of some embryonic and perinatal archosaurs: developmental and behavioral implications for dinosaurs. Paleobiology 27(1):39–58.

Hugi, J., C. Mitgutsch, and M. R. Sánchez-Villagra.

2010. Chondrogenic and ossification patterns in White's skink *Liopholis whitii* (Scincidae, Reptilia). Zoosystematics and Evolution 86:21–32.

Hugi, J., T. M. Scheyer, P. M. Sander, N. Klein, and M. R. Sánchez-Villagra. 2011. Long bone microstructure gives new insights into the life history data of pachypleurosaurids from the Middle Triassic of Monte San Giorgio, Switzerland/Italy. Comptes Rendues Palevol.

Keller, R. 1946. Morphogenetische Untersuchungen am Skelett von *Sirenodon mexicanus* Shaw mit besonderer Berücksichtigung des Ossifikationsmodus beim neotenen Axolotl. Revue Suisse de Zoologie 53:329–426.

Lee, M. S. Y., T. W. Reeder, J. B. Slowinski, and R. Lawson. 2008. Resolving reptile relationships: molecular and morphological markers. In: Assembling the Tree of Life, J. Cracraft and M. J. Donoghue (Eds.), Oxford University Press, New York, pp. 451–467.

Lobo, F., F. Abdala, and G. Scrocchi. 1995. Desarrollo del esqueleto de *Liolaemus scapularis* (Iguania: Tropiduridae) Bollettino del Museo Regionale di Scienze Naturali, Torino 13:77–104.

Maddison, W. P., and D. R. Maddison. 2010. Mesquite: a modular system for evolutionary analysis. Version 2.74. http://mesquiteproject.org

Mathur, J. K., and S. C. Goel. 1976. Patterns of chondrogenesis and calcification in the developing limb of the lizard *Calotes versicolor*. Journal of Morphology 149:401–420.

Mohammed, M. B. H. 1991. Morphogenesis of the carpus and tarsus in the skink *Chalcides ocellatus* (Scincidae, Reptilia). Journal of the Egyptian and German Society of Zoology 4:357–373.

Morse, E. 1872. On the tarsus and carpus of birds. Annals of the Lyceum of the Natural History New York 10:141–158.

Nopcsa, F., and E. Heidsieck. 1934. Über eine pachyostotische Rippe aus der Kreide Rügens. Acta Zoologica 15:431–455.

Nye, H. L. D., J. A. Cameron, E. A. G. Chernoff, and D. L. Stocum. 2003. Extending the table of stages of normal development in the axolotl: Limb development. Developmental Dynamics 226:555–560.

O›Keefe, F. R., O. Rieppel, and P. M. Sander. 1999. Shape disassocation and inferred heterochrony in a clade of pachypleurosaurs (Reptilia, Sauropterygia). Paleobiology 25:504–517.

Oster, G. F., N. H. Shubin, J. D. Murray, and P. Alberch. 1988. Evolution and morphogenetic rules: the shape of the vertebrate limb in ontogeny and phylogeny. Evolution 42:862–884.

Peyer, B. 1932. B. Peyer, die Triasfauna der Tessiner Kalkalpen. V. *Pachypleurosaurus edwardsii* Corn. spec. Abhandlungen der Schweizerischen Palaeontologischen Gesellschaft Band 52:3–18.

Ricqlès, de A. 1976. Recherches paléohistologiques sur les os longs des tétrapodes. VII. Sur le classification, la signification fonctionnelle et l'histoire des tissus osseux des tétrapodes. Annales de Paléontologie 62:71–126.

Ricqlès, de A., and V. de Buffrénil. 2001. Bone histology, heterochronies and the return

of tetrapods to life in water: w[h]ere are we?; pp. 289–310 in J. M. Mazin & V. de Buffrénil (eds.), Secondary Adaptation of Tetrapods to Life in Water, Verlag Dr. Friedrich Pfeil, München, Germany.

Rieppel, O. 1989. A new pachypleurosaur (Reptilia, Sauropterygia) from the Middle Triassic of Monte San Giorgio, Switzerland. Philosophical Transations of the Royal Society London Series B 323:1–73.

Rieppel, O. 1992. Studies on skeleton formations in reptiles. III. Patterns of ossification in the skeleton of *Lacerta vivipara* Jacquin (Reptilia: Squamata). Fieldiana, Zoology, N.S. 68:1–25.

Rieppel, O. 1993a. Die Gliedmassen der Tetrapoden – ein aktuelles Problem der Evolutionsforschung. Naturwissenschaften 80:295–301.

Rieppel, O. 1993b. Studies on skeleton formation in reptiles, V. Patterns of ossification in the skeleton of *Alligator mississippiensis* DAUDIN (Reptilia, Crocodylia). Zoological Journal of the Linnean Society 109:301–325.

Rieppel, O. 1993c. Studies on skeleton formation in reptiles: Patterns of ossification in the skeleton of *Chelydra serpentina* (Reptilia, Testudines). Journal of Zoology 231:487–509.

Rieppel, O. 1994a. Studies on skeleton formation in reptiles. Patterns of ossification in the skeleton of *Lacerta agilis exigua* Eichwald (Reptilia, Squamata). Journal of Herpetology 28:145–153.

Rieppel, O. 1994b. Studies on the skeleton formation in reptiles. Patterns of ossification in the limb skeleton of *Gehyra oceanica* (Lesson) and *Lepidodactylus lugubris* (Duméril and Bibron). Annales des Sciences Nouvelles, Zoologie, Paris 13:83–91.

Romer, S. 1956. Osteology of the Reptiles. The University of Chicago Press, Chicago & London, pp. 3-772.

Rothschild, B. M., and G. W. Storrs. 2003. Decompression syndrome in plesiosaurs (Sauropterygia: Reptilia). Journal of Vertebrate Paleontology 23:324–328.

Sánchez-Villagra, M. R., H. Müller, C. A. Sheil, T. M. Scheyer, H. Nagashima, and S. Kuratani. 2009. Skeletal Development in the Chinese soft-shelled turtle *Pelodiscus sinensis* (Testudines: Trionychidae). Journal of Morphology 270:1381–1399.

Sander, P. M. 1988. A fossil reptile embryo from the Middle Triassic of the Alps. Science, New Series 239:780–783.

Sander, P. M. 1989. The pachypleurosaurids (Reptilia: Nothosauria) from the Middle Triassic of Monte San Giorgio (Switzerland) with the description of a new species. Philosophical Transactions of the Royal Society of London. B, Biological Sciences 325:561–666.

Scheyer, T. M. and M. R. Sanchez-Villagra. 2007. Carapace bone histology in the giant pleurodiran turtle *Stupendemys geographicus*: phylogeny and function. Acta Palaeontologica Polonica 52:137–154.

Shapiro, M. D., Shubin, N. H., and J. P. Downs. 2007. Limb diversity and digit reduction in reptilian evolution.;pp. in B. K. Hall (ed.) Fins into limbs, University of Chicago Press.

Sheil, C. 2003. Osteology and skeletal development of Apalone spinifera, Chelydra serpentina (Reptilia: Testudines:

Trionychidae). Journal of Morphology 256:42–78.

Sheil, C. 2005. Skeletal development of *Macrochelys temminckii* (Reptilia: Testudines: Chelydridae). Journal of Morphology 263:71–106.

Sheil, C. A., and E. Greenbaum. 2005. Reconsideration of skeletal development of *Chelydra serpentina* (Reptilia: Testudinata: Chelydridae): evidence for intraspecific variation. Journal of Zoology, London 265:235–267.

Shubin, N. H., and P. Alberch. 1986. A morphogenetic approach to the origin and basic organisation of the tetrapod limb. Evolutionary Biology 20:319–387.

Velhagen, W. A. 1997. Analyzing developmental sequences using sequence units. Systematic Biology 46:204–210.

Werneburg, I., J. Hugi, J. Müller, and M. R. Sánchez-Villagra. 2009. Embryogenesis and ossification of *Emydura subglobosa* (Testudines, Pleurodira, Chelidae) and patterns of turtle development. Developmental Dynamics 238:2770–2786.

Zangerl, R. 1935. B. Peyer, die Triasfauna der Tessiner Kalkalpen. IX. *Pachypleurosaurus edwardsi*, Cornalia sp. Abhandlungen der Schweizerischen Palaeontologischen Gesellschaft 56:1–80.

Appendix 1. Conserved ossification pattern of terrestrial surface dwelling lizards with non-reduced pentadactyl limbs as model for the hypothesized plesiomorphic ancestral condition of terrestrial surface dwelling eureptilians

Hugi et al. (2010) studied ossification sequences in Liopholis whitii (Scincidae, Lepidosauria, Reptilia) and compared the data to the main groups of terrestrial surface dwelling squamates with non-reduced pentadactyl limbs from literature. Sequence analysis showed minor difference in the degree of heterochrony of all studied squamates regarding the position of the third and fourth digit in both the beginning and ending of ossification sequences. The results of the event pairing analysis therefore, support previous observations on the ossification sequences in terrestrial squamates with non-reduced limbs as a group of tetrapods which show highly conserved ossification sequences. The ossification sequences with the two major gradients for L. whitii as a representative of this group is shown in Figure 1 of Appendix 1. Results showed that every single element of the hind limb slightly precedes its forelimb counterpart regarding the timing of the onset and ending of ossification. Beginning and ending of ossification sequences show either a simultaneous onset or a postaxial predominance in the zeugopodial elements with a postaxial dominance in all sub-regions of the autopodium. Beginning and ending of ossification show the same order and proceed from proximal to distal across the whole limb. The ossification of digit V is delayed in both manus and pes.

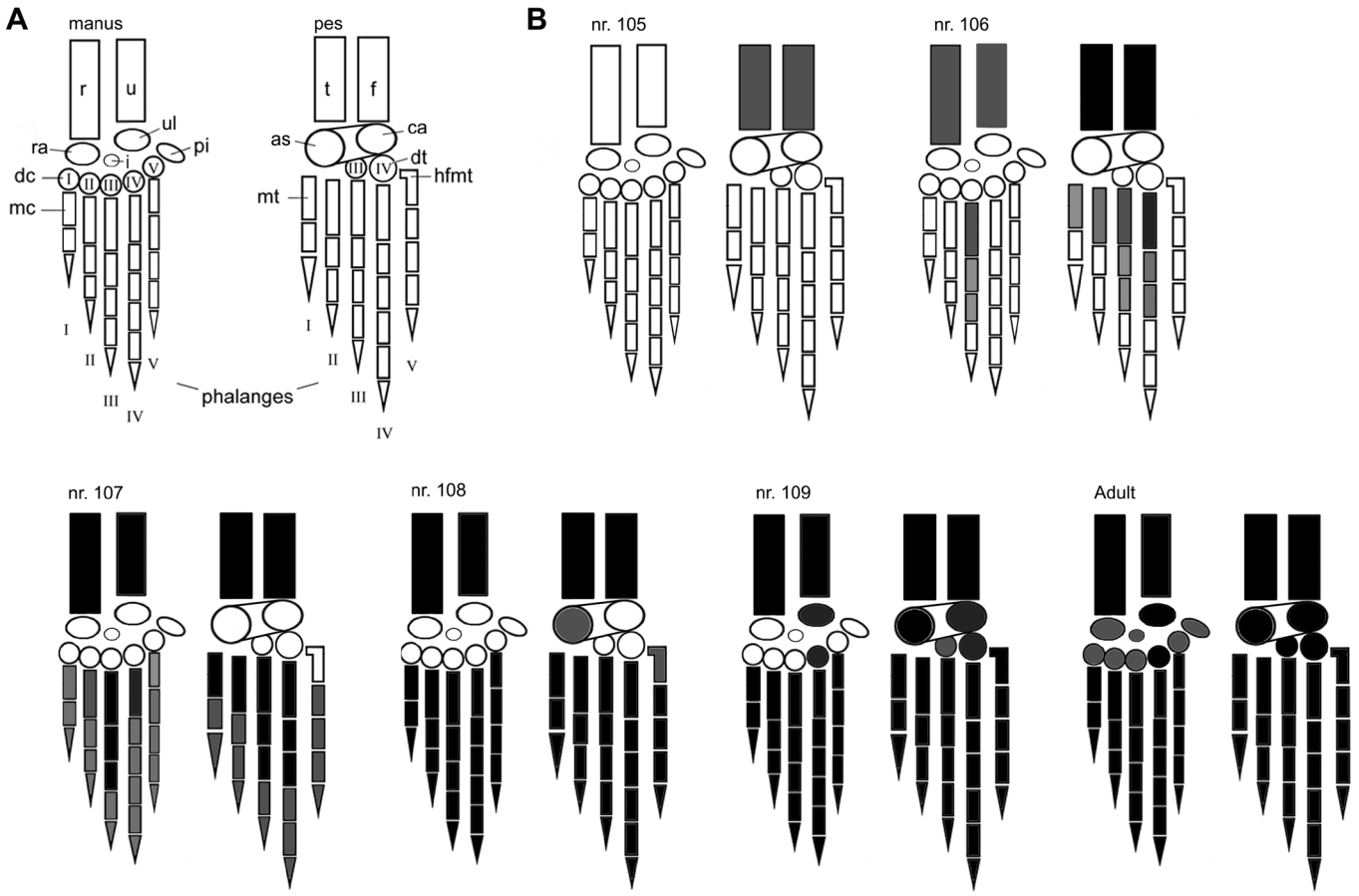

Fig. 1, Appendix 1. Schematic drawing of the ossification sequence in the surface dwelling skink Liopholis whitii. Sketches in **A** show the skeletal composition of the manus and pes. Sketches in **B** show the progress in ossification in the series of cleared and double stained specimens. Greyscales represent the different extent of the red staining in relation to another element. Black marks that the elements ended the ossification process.

Appendix 2. Detailed information on the phalangeal count in immature individuals of all four pachypleurosaurids.

Serpianosaurus mirgiolensis		**phalangeal count**		
Museum no	**size class**	**manus**	**pes**	**st**
T3810	A	2-?-?-4-2	not visible	7.8
T0132	A	2-2-3-4-2	2-2-4-4-3	9.1
T4507	A	not visible	2-3-4-3-2	10.0
C74/21	B	not visible	2-3-4-4-4	15.0
T90	B	not visible	2-3-4-4-3	15.8
T3684	B	not visible	2-3-4-5-3	16.9
C73/7	C	2-3-3-4-3	2-3-?-?-2	17.5
T1071	C	not visible	2-3-4-4-3	17.6
T3685	C	2-3-4-4-2	not visible	18.0
T0951	C	not visible	2-3-4-?-?	18.8
T3933	C	?-2-3-4-3	2-3-4-4-3	19.9
T0097	C	2-3-?-?-?	bedeckt	20.0
T3676	D	2-3-4-4-3	2-3-4-5-4	21.2
T3448	D	2-3-3-3-2	not visible	21.2
T3681	D	2-3-4-4-3	2-3-4-5-4	21.2
T3677	D	not visible	2-3-4-5-?	21.7
T3406	D	not visible	1-2-4-4-3	22.4
T3679	D	not visible	2-3-4-?-?	ca. 23.9
T3675	D	not visible	?-?-?-?-4	24.1
T3678	E	2-2-?-?-?	2-3-4-?-?	ca. 25.7
T3931	F	not visible	2-3-4-3-1	29.0
T1834a	F	not visible	2-3-3-2-2	32.5
T1834b	G	not visible	2-3-4-?-?	ca. 35.7

Neusticosaurus pusillus		phalangeal count		
Museum no	**size class**	**manus**	**pes**	**st**
T3409	B	1-2-3-4-?	2-3-3-3-2	3.7
T4296	C	1-2-3-3-2	2-3-4-4-2	6.6
T4293	C	1-?-?-?-2	2-3-4-4-2	6.6
T3714	D	1-2-3-3-1	2-3-4-4-2	7.2
T3571	D	not visible	?-?-3-4-2	8.2
T3387	F	not visible	2-3-4-4-2	10.3
T3775	F	2-2-3-4-3	2-3-4-4-2	10.4
T3535b	F	not visible	1-2-3-4-2	10.6
T3853	F	1-2-3-3-2	2-3-3-3-2	11.0
T3767	F	2-3-3-3-2	not visible	11.1
T3562	F	not visible	2-?-?-?-2	11.2
T3603	G	2-2-3-4-2	2-3-4-4-3	12.0
T3541	G	2-2-3-4-2	2-3-4-4-2	12.3
T3564	G	not visible	not visible	12.6
T3547 a	H	2-2-3-5-3	2-3-4-?-?	12.7
T3517	G	not visible	not visible	12.9
T3795	G	not visible	2-3-4-4-2	12.9
T3585	G	2-?-?-4-?	2-3-?-?-?	12.9
T3390	G	?-2-3-?-?	not visible	13.1
T3601	G	2-3-4-4-2	2-3-4-5-2	13.3
T3672	G	not visible	not visible	13.4
T3622	G	2-3-3-?-?	not visible	13.5
T4289	G	not visible	2-2-3-5-3	13.5
T3572	G	2-2-2-3-2	2-3-4-5-?	13.5
T3618	H	2-2-3-?-?	2-3-4-?-3	13.6
T3515	H	2-3-?-?-?	not visible	13.7
T3612	H	not visible	2-3-4-4-3	13.7
T3623	H	not visible	2-3-4-4-1	13.7
T3553a	H	2-2-?-3-?	2-3-4-?-?	13.8

T3651	H	not visible	2-3-4-5-3	13.8
T3551	H	not visible	2-3-4-4-2	13.9
T3599	H	not visible	2-3-4-4-3	13.9
T4311	H	not visible	2-3-3-4-2	13.9
T3516	H	not visible	2-?-?-?-?	14.0
T3660	H	not visible	2-3-4-4-3	14.0
T3555	H	1-2-3-3-X	2-3-3-3-2	14.1
T3670	H	2-2-4-5-2	not visible	14.1
T3514	H	2-2-3-4-2	not visible	14.2
T3597	H	2-2-3-4-2	2-2-?-?-?	14.3
T3533	H	not visible	not visible	14.4
T3545	H	1-2-3-4-2	not visible	14.4
T3604	H	2-2-3-4-1	2-3-4-4-2	14.4
T3790	H	2-3-3-4-2	not visible	14.4
T3421	H	not visible	?-3-3-4-2	14.4
T3530	H	2-3-4-4-2	2-3-4-4-3	14.5
T3556	H	2-3-4-4-2	not visible	14.5
T3643	H	2-2-3-4-?	2-3-4-5-?	14.5
T3509	H	?-?-?-?-2	2-3-3-4-?	14.6
T3525	H	2-3-3->3-2	not visible	14.6
T3405	H	2-3-?-?-?	not visible	14.6
T3535 a	H	not visible	2-3-?-?-?	14.7
T3580	H	1-2-3-4-2	not visible	14.7
T3627	H	not visible	2-3-4-5-3	14.8
T3637	H	2-3-4-5-2	2-3-4-5-3	14.9
T3654	H	2-3-4-5-2	not visible	14.9
T3671	H	not visible	2-3-4-5-3	14.9
T3518	H	2-2-3-4-2	not visible	15.0
T3519	H	2-2-4-?-?	not visible	15.0
T3529	H	not visible	2-3-?-4-3	15.1
T3620	H	2-3-4-5-3	not visible	15.1

T3576	H	2-3-3-4-2	2-3-4-5-3	15.1
T3643	I	2-3-4-5-?	2-3-4-?-3	15.2
T3673	I	2-3-4-5-3	not visible	15.3
T3626	I	2-2-4-4-2	not visible	15.6
T3645	I	2-3-?-?-?	2-3-4-4-2	15.7
T3629	I	2-2-?-?-?	2-3-4-4-3	15.9
T3661	I	2-2-3-5-2	2-3-4-?-?	16.1
T3606	I	not visible	2-3-4-5-3	16.2
T3740	I	2-3-4-4-2	2-3-4-5-3	16.6
T3598	I	not visible	2-3-4-5-3	16.6
T3625	I	1-2-3-3-2	not visible	16.7
T3631	I	2-3-3-4-?	2-3-4-?-3	16.7
T3602	I	not visible	2-3-?-?-?	16.8
T3442	I	1-2-3-4-2	2-3-4-4-?	16.9
T3639	J	2-3-3-4-?	2-3-4-5-3	17.1
T3400	J	2-2-3-4-2	not visible	17.1
T3481	J	2-3-3-?-?	2-3-4-5-3	17.3
T3639	J	2-3-?-?-?	2-3-4-5-?	17.5
T3750	J	not visible	2-3-4-5-3	18.0
T3528	J	2-3-4-5-3	2-3-4-4-3	18.4
T3527	M	not visible	?-2-4-4-?	23.2

Neusticosaurus peyeri		**phalangeal count**		
Museum no	**size class**	**manus**	**pes**	**st**
T3705	A	?-?-?-?-?	?-?-1-1-?	2.4
T3408	B	1-2-2-3-1	2-3-3-3-1	5.1
T4292	C	1-2-2-2-1	2-3-3-4-2	ca. 5.7
T4290	D	1-2-3-2-1	not visible	9.1
T3586	D	X-1-1-1-X	1-3-2-3-1	9.4
T3389	E	not visible	2-3-4-4-2	10.5
T3615	E	not visible	1-2-3-4-2	11.3
T3607	F	1-2-2-3-1	2-3-4-4-2	12.9

T3394	F	not visible	2-2-4-4-3	13.8
T3716	F	not visible	2-3-4-4-2	13.9
T3422	G	1-2-3-4-?	2-3-4-4-2	14.0
T3411	G	not visible	2-3-?-?-2	ca. 14.4
T3410	G	1-2-3-3-2	2-3-4-4-2	14.8
T3431	G	1-2-3-3-2	2-3-4-4-3	15.3
T3444	E	1-2-3-3-1	2-3-4-4-3	15.9
T3755	H	1-2-3-3-2	2-3-4-4-3	16.2
T3449	H	1-2-3-3-2	2-3-3-4-2	16.3
T4295	H	2-3-?-?-?	not visible	ca. 16.4
T3395	H	not visible	2-3-3-4-2	16.9
T3588	H	1-2-3-3-1	2-3-4-5-2	17.0
T3534	H	1-2-3-?-?	2-3-4-4-3	17.3
T3511	H	not visible	2-3-3-4-2	17.5
T3510	H	not visible	2-3-4-5-3	17.6
T3902	H	not visible	2-3-3-4-2	17.6
T3482	H	1-2-3-4-2	not visible	17.7
T3710	I	1-2-3-3-1	2-3-4-4-2	18.2
T3474	I	1-2-3-?-2	not visible	18.3
T3479	I	1-2-2-2-2	2-3-4-?-?	18.4
T3396	I	1-2-3-3-2	2-3-4-5-3	18.4
T3412	I	not visible	2-3-3-4-2	18.5
T3423	I	not visible	2-3-3-4-3	18.7
T3476	J	not visible	2-3-?-4-?	20.1
T3393	J	1-2-3-3-2	2-3-4-4-3	20.1
T3788	J	not visible	2-3-4-4-3	21.4
T3744	K	not visible	2-3-4-5-3	22.3
T3764	M	1-2-2-1-1	not visible	26.2
T3584	M	not visible	2-X-4-5-3	26.6
T3445	Q	1-2-3-3-2	2-3-4-4-3	34.5
T3345	Q	1-2-3-3-2	2-3-4-4-3	34.6

N. edwardsii		**phalangeal count**		
Museum no	**size class**	**manus**	**pes**	**st**
T3759	B	not visible	1-2-3-4-2	23.2
T461?	B	not visible	1-2-3-4-2	24.6
T3407	B	1-2-2-1-1	1-2-3-3-2	24.8
T3708	B	not visible	1-2-3-4-2	25.1
T3425	B	not visible	1-2-3-3-2	ca. 25.5
T3775	B	1-2-?-?-?	not visible	ca. 27.8
T3453	B	not visible	1-2-4-4-2?	28.3
T3758	B	not visible	1-2-3-?-?	28.9
T3776	B	not visible	1-2-3-4-3	ca. 29.6
T3749	B	1-2-3-3-2	not visible	29.9
T3438	D	not visible	1-2-3-4-3	42.3
T3711	E	not visible	1-2-3-4-3	ca. 51.5
T3460	E	1-2-3-4-2	1-2-3-4-3	53.3
T3935	F	not visible	1-2-3-4-2	64.1

Appendix 2. Data used for the reconstruction of the developmental sequence in the manus and pes of each pachypleurosaurid species. Museum number (no), size class, phalangeal formula, and standard length (st) (after Sander, 1989, for conducting the size classes) of all pachypleurosaurids used in this study are given where possible. Measurements are all given in millimetres. The term "not visible" is used in cases where the bones are covered, adpressed to the body, disarticulated or not preserved. Grey numbers in the phalangeal formula refer to the most distal phalanx which are of relatively small size and therefore, are regarded as elements which have just started ossification. These elements are smaller and different in form than in adult forms, being regarded as less progressed in the beginning ossification process than the other phalanges. Abbreviations: st: standard length; ?: unknown; >: minimum number; X: not yet ossified, therefore not preserved.

Appendix 3. Summary of the compaction patterns based on Table Appendix 3. The common trends are listed for all four pachypleurosaurids from Monte San Giorgio.

Serpianosaurus mirigiolensis – The sequence of the early and final phase of additional compaction processes is proximodistally directed all across the limbs. Information of the early phase of compaction processes of the stylo- and zeugopodial region in the forelimb and hind limb of S. mirigiolensis is not available. metacarpals > proximal phalanges > intermediate phalanges > terminal phalanges > ulnare > intermedium. Hind limb: metatarsals > proximal phalange > intermediate phalange, terminal phalanges > astragalus > calcaneum. The overall sequence of the early phase of compaction processes is as follows: metacarpals > proximal phalanges manus, metatarsals > intermediate phalanges manus > proximal phalanges pes > intermediate phalanges pes > terminal phalanges manus > ulnare > intermedium > terminal phalanges pes > astragalus > calcaneum. The order of the final phase of compaction processes in the forelimb: humerus > radius > ulna > metacarpals > proximal phalanges >intermediate phalanges, terminal phalanges > intermedium, ulnare. Hind limb: femur > tibia > fibula > proximal phalanges > intermediate phalanges, terminal phalanges > metatarsals > astragalus > calcaneum. The overall order of the final phase of compaction processes is: humerus > radius, femur > ulna, tibia > metacarpals, fibula > proximal phalanges manus > intermediate phalanges manus, terminal phalanges manus > ulnare, intermedium > proximal phalanges pes > intermediate phalanges pes, terminal phalanges pes > metatarsals > astragalus > calcaneum. Metacarpals start and end compaction processes with a postaxial dominance: metacarpal-4 > metacarpal-3 > metacarpal-2 > metacarpal-1, metacarpal-5. The same postaxial dominance is also preserved in the order of the early phase of the compaction processes of the metatarsals. Metatarsals end this process in a preaxial order: metapodial-1 > metapodial-2 > metapodial-3 > metapodial-4 > metapodial-5. Phalanges of the forelimb and hind limb start and end compaction in a proximodistal direction with an unknown axial dominance. Limb bones of *S. mirigiolensis* tend to end compaction earlier, i.e. in smaller individuals than *Neusticosaurus* spp.

Neusticosaurus pusillus (Fig. 5) - The early phase of compaction processes shows a proximodistal gradient all across the limbs, but the final phase of compaction processes is first completed from distally to proximally in the phalanges in both the manus and pes. The early phase of compaction processes: forelimb: humerus > ulna, radius > metacarpals > proximal phalanges > intermediate phalanges > terminal phalanges > intermedium, ulnare; hind limb: femur > fibula, tibia > metatarsals > proximal phalanges > intermediate phalanges > terminal phalanges > astragalus > calcaneum. The overall sequence of the early phase of compaction processes in the forelimb and hind limb is as follows: humerus > femur, ulna, radius> fibula, tibia, metacarpals > proximal phalanges manus > intermediate phalanges manus > terminal phalanges manus > metatarsals > intermedium, ulnare > proximal phalanges pes > intermediate phalanges pes > terminal phalanges pes > astragalus > calcaneum. The order of the final phase of compaction processes in the forelimb: humerus > radius > ulna > terminal phalanges, intermediate phalanges > proximal phalanges > metacarpals > intermedium > ulnare; the order of the final phase in the hind limb is: femur > tibia > fibula >

terminal phalanges > intermediate phalanges > proximal phalanges > metatarsals > astragalus > calcaneum. The overall order of the final phase of compaction processes of the forelimb and hind limb is: humerus > femur, radius > ulna, tibia > fibula > terminal phalanges manus, intermediate phalanges manus > proximal phalanges manus > metacarpals > intermedium > ulnare, terminal phalanges pes > intermediate phalanges pes > proximal phalanges pes > metatarsals > astragalus > calcaneum. Metacarpals show a postaxial dominance in both the order of the early and final phase of compaction processes: metacarpal-4> metacarpal-3 > metacarpal-2 > metacarpal-1 > metacarpal-5. Metatarsals show the early phase of the compaction process with a postaxial dominance: metatarsal-4> metatarsal-3 > metatarsal-2> metatarsal-1> metatarsal-5; whereas the final phase of compaction processes shows a preaxial dominance: metatarsal-1 > metatarsal-2 > metatarsal-3> metatarsal-4 > metatarsal-5. Phalanges of the forelimb and hind limb display the early phase of compaction processes with a postaxial predominance, and complete it in a preaxial direction.

Neusticosaurus peyeri - The early phase of compaction processes shows a proximodistal gradient all across the limbs, whereas the final phase of compaction processes first completes from distally to proximally in the phalanges in both the manus and pes. The order of the early phase of compaction processes: forelimb: humerus > ulna, radius > metacarpals, proximal phalanges > intermediate phalanges, terminal phalanges, ulnare > intermedium; hind limb: femur > fibula, tibia > metatarsals > proximal phalanges > intermediate phalanges > terminal phalanges > astragalus > calcaneum. The overall order of the early phase of compaction processes is: humerus > femur > ulna, radius > fibula, tibia > metacarpals > proximal phalanges manus > intermediate phalanges manus, terminal phalanges manus, ulnare> intermedium, metatarsals > proximal phalanges pes > intermediate phalanges pes > terminal phalanges pes > astragalus > calcaneum. The order of the final phase of compaction processes: forelimb: humerus > radius > ulna > terminal phalanges, intermediate phalanges > proximal phalanges > metacarpals > intermedium > ulnare; hind limb: femur > tibia > fibula > terminal phalanges > intermediate phalanges > metatarsals, proximal phalanges > astragalus > calcaneum. The overall sequence of the final phase of compaction processes is: humerus > radius, femur > ulna > tibia > fibula > terminal phalanges manus, intermediate phalanges manus > proximal phalanges manus > metacarpals, intermedium > terminal phalanges pes, ulnare > intermediate phalanges pes > proximal phalanges pes, metatarsals > astragalus > calcaneum. Metacarpals and –tarsals show a postaxial dominance in the early phase of compaction processes: metapodial-4> metapodial-3 > metapodial-2 > metapodial-1 > metapodial-5, which is the same sequence of the final phase of compaction processes in the metacarpals as well. In contrast, the final phase of compaction processes of the metatarsals show a preaxial dominance: metapodial-1 > metapodial-2 > metapodial-3 > metapodial-4 > metapodial-5. The phalanges of both manus and pes start compaction processes sequence from proximal to distal, but end in distal to proximal direction. In addition, phalanges of the pes show first postaxial dominance starting in digit IV > III > II > I > V, but they complete their compaction processes in a preaxial sequence order (digit I > digit II > digit III > digit IV > digit V). The phalanges of the manus

also show a preaxial order in the early phase of compaction processes, whereas the beginning sequence of ossification is not preserved.

Neusticosaurus edwardsii - The early phase of compaction processes shows a proximodistal gradient all across the limbs, but the final phase of compaction processes first completes from distally to proximally in the phalanges in both manus and pes. No data is available on order of the early phase of compaction processes in the stylo- and zeugopodial region of the forelimbs and hind limbs. The order of the early phase of compaction processes in the forelimb is as follows: proximal phalanges > intermediate phalanges, metacarpals > terminal phalanges > ulnare > intermedium; the order of the early phase of compaction processes in the hind limb is: proximal phalanges > metatarsals > intermediate phalanges > terminal phalanges > astragalus > calcaneum. The overall sequence of the early phase of compaction processes is: proximal phalanges manus > metacarpals, intermediate phalanges manus > ulnare, proximal phalanges pes > intermedium, metatarsals > terminal phalanges manus > intermediate phalanges pes > terminal phalanges pes > astragalus > calcaneum.

The order of the final phase of compaction processes: forelimb: humerus > radius > ulna > terminal phalanges > intermediate phalanges > proximal phalanges > metacarpals > intermedium > ulnare; hind limb: femur > tibia > fibula, terminal phalanges > intermediate phalanges > proximal phalanges, metatarsals > astragalus > calcaneum. The overall sequence of the final phase of compaction processes is: humerus > radius > femur > ulna > tibia > terminal phalanges manus > intermediate phalanges manus, fibula, terminal phalanges pes > proximal phalanges manus > metacarpals > intermediate phalanges pes > proximal phalanges pes, metatarsals > intermedium > ulnare > astragalus > calcaneum. Metacarpals start the compaction processes with a postaxial dominance metacarpal-4 > metacarpal-3 > metacarpal-2 > metacarpal-1, metacarpal-5 and end in a similar postaxial gradient: metacarpal-4, metacarpal-5 > metacarpal-3 > metacarpal-2 > metacarpal-1. Metatarsals start the compaction processes with a postaxial dominance: metatarsal-4 > metatarsal-3 > metatarsal-2 > metatarsal-1, metatarsal-5 and end this process slightly different order: metatarsal-4 > metatarsal-3 > metatarsal-2 > metatarsal-1, metatarsal-5. In some cases, metatarsals also show a preaxial dominance in the order of the final phase of compaction processes. Phalanges start first compaction in digit V showing a subsequently postaxial dominance (digit V> digit V > digit III > digit II > digit I). The final phase of compaction processes displays reverse order: digit I > II > III > IV >V. *N. edwardsii* completes compaction processes of its limbs very late compared to all other pachypleurosaurids. *N. edwardsii* shows weak compaction in the carpus still at large sizes.

Next page, Table 1 of Appendix 3: The detailed information of the compaction patterns is listed for all four pachypleurosaurids. The early and final phase of compaction processes are a continuous process. The sequences are mainly based on the relative progress within the exact timing of early and final phase. The onset of these secondary compaction processes appears to start in a small timeframe and, therefore is only preserved in a few specimens. These cases are additionally labelled with “beg.” for marking the early phase of the compaction processes. In specimens in which both the early and final phase of compaction processes are visible, sequences are also marked with “beg.” And “end.”. Additionally, grey numbers standing in the front of a sequence represent elements which are not yet completely compact. Abbreviations: as: astragalus; ca: calcaneum; fe: femur; f: fibula; h: humerus; i: intermedium; int. phal. manus: intermediate phalanges manus; int. phal. pes; intermediate phalanges pes; mc: metacarpals; meso: mesopodial bones; mt: metatarsals; M. no.: museum collection number; prox. phal. manus: proximal phalanges manus; prox. phal. pes: proximal phalanges pes; r: radius; sc: size class; term. phal. manus: terminal phalanges manus; term. phal. pes: terminal phalanges pes; t: tibia; u: ulna; uln: ulnare; >: before.

Serpianosaurus mirigiolensis

M. no.	sc	Compaction patterns	st
T3522	<A	beginning ossification; only mesopodial bones are not yet visible	5.4
T3810	<A	forelimb:completely preserved; not yet compact: int., term.phal.manus; hind limb: only fe preserved, not yet compact	7.8
T0132	A	h>r,fe>u,t>mc,f>phal.manus,mt>phal.pes; mc4>mc3>mc2>mc1>5;mt1>mt2>mt3>mt4,5	9.1
T3683	B	Present and entirely compact: stylo, zeugo and mesopodial	14.9
T3680	B	only hind limb: completely compact	16.2
T3684	B	only hind limb: prox.phal.pes>int. phal.>term.phal.pes; mt1>mt2>mt3>mt4>mt5	16.9
T1071	C	h,r,u,manus>fe>t,prox.phal.pes>f, int.phal.pes>term.phal.pes>mt>as>ca;mt1,2>mt3>mt5>mt4	17.6
T3685	C	h,r,fe,t>u,f>mc>prox.phal.manus>term.phal.manus,int.phal.manus>i,uln; mc4>mc3>mc2>mc1,5 (beg.)	18.0
T3933	C	h,r,fe,t>manus,u,f>mt>prox.phal.pes, int.phal.pes>term.phal.pes>as,ca;mt1>mt2>mt3,4>mt5	19.9
T0097	C	forelimb:only phal.and mc not compact; hind limb: fe,t>f>phal,mt,meso; mt1>mt2>mt3>mt4>mt5	20.0
T3448	D	all: compact	21.2
T3681	D	h>u,r,fe>t,f>term.phal.pes>mt> int..phal.pes,prox.phal.pes>as,ca; mt1>mt2>mt3>mt4>mt5	21.2
T3676	D	h,r,u,fe,t,f>mc>prox.phal.manus,prox.phal.pes,mt> int.phal.manus> int.phal.pes>term.phal.manus>term.phal.pes>meso; mc4>mc3,2>mc1>mc5; mt1>mt2>mt3>mt4>mt5	21.2
T3677	D	forelimb: only stylo-,zeugopods preserved & compact; hind limb: fe,t,f>prox.phal.> int.phal.>mt>term.phal.>as>ca; mt1>mt2>mt3,5>mt4	21.7
T3682	D	forelimb: only stylo-,zeugo-,mesopods preserved, sequence indicated: h>r>u>meso; hind limb completely preserved: fe>t>f>prox.phal.>int.phal.>term.phal.>mt >as>ca; mt1>mt2>mt3,5>mt4	22.0
T3406	D	mt>prox., int., term. phal pes; all other limb bones: compact	22.4
T3679	D	only stylo-,zeugopods hind limb & forelimb; completely compact	ca. 23.9
T3675	D	Present and entirely compact: forelimb complete, only fe, t and f in hind limb	24.1
T3709	D	forelimb: only stylo-, zeugopods preserved, compact	24.8
T3678	E	forelimb: only stylo-,zeugopod;hind limb: almost completely preserved; phal.pes, and mt not yet completely compact	ca. 25.7
T3931	F	h,r,u,fe,t,f>uln,i,phal.manus,mc,prox.phal.pes>mt>int.phal.pes,term.phal.pes, as,ca;mc4,3,2,>1>5;mt2,3,4>mt5>mt1	29.0
T1045	H	h,r,fe,t>u,f>mc>phal.manus>uln>i>mt>phal.pes>as>ca;mc(end.):mc4>mc3>mc2>mc1>mc5;mt(beg.):mt4>mt3>mt2>mt1>mt5	38.5

Neusticosaurus pusillus

M. no.	sc	Compaction patterns	st
T3409	B	beginning compaction: h>u, ra,fe>f,t>mt,mc>phal.	3.7
T4296	C	h,r>fe>u,t>f>term.phal.manus,mc, >int.phal.manus,prox.phal.manus>i,uln>term.phal.pes>int.phal.pes,prox.phal.pes>mt>as,ca;mc1,2>mc3>mc4>mc5;mt1>mt2>mt5 >mt3,4	6.6
T4293	C	h,r,fe,t>f,u>phal.manus,mc> i,uln,term.phal.pes>int.phal.pes>prox.phal.pes,mt>as,ca;mt1>mt2>mt3>mt4>mt5	6.6
T3714	D	beginning compaction:h>u,r>mc>prox.phal.manus>int.phal.manus>term.phal.manus>i,uln; prox.phal.pes,int.phal.pes>fe>mt>t,f,as>ca;mc4>mc3>mc2>mc1>mc5;mt4>mt3>mt2>mt1>mt5	7.2
T3571	D	h,r,fe>u,f,uln,i,f>mc>phal.manus,as,ca>mt>prox.phal.pes,int.phal.pes>term.phal.pes;mc(beg.):mc4>mc5,mt(beg.):mt4>mt2,3>mt1 >mt5	8.2
T3387	F	beginning compaction:h>r,u,fe>t,f>rest of manus>term.phal.pes,int. phal.pes>prox.phal.pes,mt>as>ca;mt4>mt3>mt2>mt1>mt5	10.3

T3535b	F	completely preserved & compact;except pes not yet completely compact:meso,mt,prox.phal.	10.6
T3547	F	forelimb:completely preserved & compact;hind limb: fe,t>r>term.phal.>int. phal.,prox.phal.>mt;mt1>mt2,3>mt4,5	11.1
T3767	F	h,r,fe>u,t>phal.manus,f>term.phal.pes,mc>i,uln>int.phal.pes,prox.phal.pes,mt>as,ca;mc4>mc3>mc2>mc1,5;mt1>mt2>mt3>mt4>mt5	11.1
T3562	F	h,r,u,phal.manus,fe,t,f>mc,phal.pes>mt,as>ca;mc4>mc3>mc2>mc1>mc5;mt1>mt2>mt3>mt4>mt5	11.2
T3756	F	h,r,fe,t>u>f,phal.manus>mc>i,uln,phal.pes>mt>as>ca;mc4>mc3>mc2>mc1>5;mt1>mt2>mt3>mt4>mt5	11.3
T3738	F	h,r,fe,t>u,f>phal.manus>mc,mt,term.phal.pes>i,uln,int.phal.pes>prox.phal.pes>as,ca;mt1>mt2>mt3>mt4>mt5	11.3
T3603	G	h>r>u>fe>term.phal.manus,int.phal.manus,prox.phal.manus,meso manus,f>t,mc>term.phal.pes,int.phal.pes>prox.phal.pes>mt>meso pes;mc4>mc3>mc2>mc1>mc5;mt1>mt2>mt3>mt4>mt5;phal:D1>D2>D3>D4>D	12.0
T3653	G	h,r,fe,u>phal.manus,t>f,mc,term.phal.pes,int.phal.pes,uln,i>prox.phal.pes,>mt>as>ca;mc4>mc3>mc2>mc1>mc5;mt1>mt2>mt3>mt4>mt5	12.1
T3852	G	h,r,fe,t>u,term.phal.manus>int.phal.manus,prox.phal.manus,term.phal.pes>mc,int.phal.pes,prox.phal.pes>i>uln,mt>as,ca;mc4,3>mc2>mc1,5;mt1,5>mt2>mt3>mt4	12.4
T3607	G	h>r,fe>u>manus,f>t>term.phal.>int.phal.>mt,prox.phal.>as,ca;phal:D1>D2>D3>D4>D5	12.5
T3721	G	h,r>u,fe>phal.manus,mc>i,uln,t>f,phal.pes>mt>as,ca;mc4>mc3>mc2>mc1>mc5;mt2>mt3>mt4>mt1,5	12.8
T3664	G	completely preserved & compact	12.8
T3585	G	h,r,fe>u,t>f>term.phal.manus>int.phal.manus>prox.phal.manus,mc,term.phal.pes>meso manus,mt,int.phal.pes>as,ca;mc1>mc4>mc3>mc2>mc5;mt1>mt2>mt3>mt4>mt5	12.9
T3795	G	h,r,fe>u,t,f>mc,phal.manus,term.phal.pes>int.phal.pes>uln,i,prox.phal.pes>mt>as>ca;mt1>mt2>mt3>mt4>mt5;indicated:mc4>mc3>mc2>mc1>mc5	12.9
T3614	G	forelimb & hind limb compact	12.1
T3577	G	h,r,fe>u,t>f	12.1
T3541	G	forelimb:completely preserved & compact;hind limb:fe,t,f>phal.,mt,as,ca	12.3
T3426	G	h,r,fe>u,t>f>phal.manus>mc,phal.pes>mt,uln,i>as>ca;mc4>mc3>mc2>mc1>mc5;mt1>mt2>mt3>mt4>mt5	12.9
T3630	G	h,fe>r>u>t>f>phal.manus,mc,meso manus>term.phal.pes>int. phal.pes>prox.phal.pes,mt>as,ca;mt1>mt2>mt3>mt4>mt5:phal.pes:D1>D2>D3>D4>D5	ca.13.2
T3644	G	h,r,u,fe,t>f,phal.manus,mc,i,uln>term.phal.pes,int.phal.pes>prox.phal.pes,mt,as>ca;mt1>mt2>mt3>mt4>mt5,r,fe,t>u,f>phal.manus, mc,term.phal.pes>i,uln>int. phal.pes,prox.phal.pes>mt>as>ca;mc4>mc3>mc2>mc1>mc5;mt1>mt2>mt3>mt4>mt5;phal.pes(end.):D1>D2>D3>D4>D5	13.2
T3601	G	h,r,u,fe>t>f>phal.manus,mc>phal.pes>i>uln,mt>as>ca;mc4>mc3>mc2>mc1>mc5;mt1>mt2>mt3>mt4>mt5	13.3
T3672	G	completely preserved; as & ca not yet compact	13.4
T4289	H	h,r,u,fe,mc,phal.manus>t,uln,i,phal.pes,as>f,mt,ca;mt1,5>mt2>mt3>mt4	13.5
T3618	H	forelimb compact;hind limb:fe>t>f>phal.,mt>as>ca;mt1>mt2>mt3>mt4>mt5;phal:D1>D2>D3>D4>D5	13.6
T3623	H	h,r,u,fe,t,f,term.phal.pes>int.phal.pes>mt>prox.phal.pes>as>ca	13.7
T3612	H	forelimb & hind limb compact except ca	13.7
T3651	H	completely preserved & compact	13.8
T3553a	H	completely preserved;meso manus not yet compact; mt>as>ca	13.8
T3551	H	completely preserved & compact; except:ca	13.9
T3599	H	h,r,u,fe,t>f,mc>term.phal.pes>int.phal.pes>meso manus,prox.phal.pes>mt>ca,as;mt1>mt2>mt3>mt4>mt5;phal:D1>D2>D3>D4>D5	13.9
T3611	H	h,r,fe,t>u,f>meso manus,term.phal.pes>int.phal.pes>mt>prox.phal.pes>as,ca;mt1>mt2>mt3>mt4>mt5;phal:D1>D2>D3>D4>D5	14.0

T3600a	H	h,r,u,fe,t>mc>f>phal.pes,mt>as,ca;mt1>mt2>mt3>mt4>mt5	ca.14.0
T3555	H	h,r,u>phal.manus,mc,fe>t,uln,i>f,term.phal.pes,int. phal.pes>prox.phal.pes>mt>ca>as;mt4>mt3>mt2>mt5>mt1	14.1
T3418	H	forelimb:only h preserved, compact; hind limb: completely preserved and compact	14.1
T3670	H	h,r,u,fe,t,f,term.phal.manus,int.phal.manus>prox.phal.manus,uln,i,mc>term.phal.pes>int.phal.pes>prox.phal.pes>mt>as,ca;mc(end.):mc4>mc3>mc2>mc1>mc5;mt(end.):mt1>mt2>mt3>mt4>mt5;phal.pes(end.):D1>D2>D3>D4>D5	14.1
T3597	H	forelimb & hind limb compact except ca	14.3
T3948	H	forelimb & hind limb compact except ca	14.4
T3790	H	forelimb,stylo-,zeugopods in hind limb:preserved & compact	14.4
T3717	H	h,fe>t,r>u>f>term.phal.manus,int.phal.manus>mc>i,uln,mt,term.phal.pes>int.phal.pes>prox.phal.pes>as>ca;mc4>mc3>mc2>mc1>mc5;mt1>mt2>mt3>mt4>mt5	ca.14.4
T3533	H	forelimb:completely preserved & compact; hind limb:mt>prox.phal.>as>ca	14.4
T3421	H	completely preserved; mt,as,phal.pes not yet compact, sequence not preserved	14.4
T3545	H	forelimb:completely preserved & compact; hind limb: mt,prox.phal.>as>ca	14.4
T3604	H	forelimb compact except i>uln;fe>t>f,prox.phal.pes>mt>as>ca	14.4
T3643	H	h,r,fe>t,u,phal.manus>mc>i>uln>f,mt>as>ca;mc4>mc3>mc2>mc1>mc5;mt1>mt2>mt3>mt4>mt5;phal.pes(end.):D1>D2>D3>D4>D5	14.5
T3530	H	completely preserved & compact	14.5
T3556	H	completely preserved; mt,phal.pes,meso pes not yet compact	14.5
T3509	H	completely preserved; forelimb:compact; hind limb:mt>as>ca	14.6
T3739	H	h,r,fe>u>t>phal.manus,mc>i,uln,term.phal.pes,int.phal.pes>prox.phal.pes,mt>as>ca;mt1>mt2>mt3>mt4>mt5	14.8
T3570	H	forelimb compact except phal.,meso,mc:mc4>mc3>mc2>mc1>mc5;hind limb:compact except phal.,meso,mt	14.8
T3627	H	h,fe>r,t>u,f>phal.manus>term.phal.pes>mc>int.phal.pes>prox.phal.pes>mt>uln,i>as>ca;mt1>mt2>mt3,5>mt4	14.8
T3671	H	h,r>fe>t,u>f,phal.manus>mc,term.phal.pes,int.phal.pes>prox.phal.pes,i,uln>mt,as>ca;mc(end.):mc4>mc3>mc2>mc1>mc5;mt(beg.):mt4>mt3>mt2>mt1>mt5;phal.pes(end.):D1>D2>D3>D4>D5	14.9
T3654	H	h,r,fe,t>u,term.phal.manus,int.phal.manus,f>prox.phal.manus>mc>i,uln;mc(end.):mc4>mc3>mc2>mc1>mc5	14.9
T3637	H	forelimb:compact; hind limb:fe,t>f>term.phal.,int. phal.>prox.phal.>mt>as,ca;mt1,2>mt3,5>4	14.9
T3518	H	forelimb:completely preserved & compact; hind limb:fe,t>f>term.phal.,int. phal.>prox.phal.>mt>as>ca;mt1>mt2>mt3>mt4>mt5	15.0
T3576	H	forelimb:compact except prox.phal,meso and mc;mc4>mc3>mc2>mc1>mc5;hind limb:fe,t>f>term.phal.>prox.phal.,int. phal.,mt>as>ca;mt1>mt2>mt3>mt4>mt5;phal:D1>D2>D3>D4>D5	15.1
T3620	H	forelimb compact except i>uln;hind limb:only stylo-,zeugopods preserved:compact	15.1
T3529	H	completely preserved & compact, except ca	15.1
T3673	I	h,r,fe>t>u>f>mc,phal.pes,i,uln;rest covered	15.3
T3642	I	h,r,fe>t,u>phal.pes>mt,as>ca;manus:not preserved	15.3
T3574	I	forelimb:only stylo-,zeugopod preserved,compact;hind limb:fe,t>f>mt>meso	15.5
T3652	I	forelimb,hind limb compact except:uln,mc1,prox.phal.pes>mt,as>ca;mc1,2,3,4,>mc5;mt1>mt2>mt3>mt4>mt5	15.6
T3645	I	h,r,fe,t>u,f>phal.manus,mc,term.phal.pes>i,uln>int.phal.pes,prox.phal.pes>mt>as>ca;mc4>mc3>mc2>mc1>mc5;mt1>mt2>mt3>mt4>mt5	15.7
T3725	I	h,r,u,fe,t>phal.manus>mc,i,uln>phal.pes>mt>as>ca;mt1>mt2>mt3>mt4>mt5	15.9
T3626	I	h,r,u,phal.manus,fe,t,f>mc2,3,4,5>mc1> >pahl.pes,mt,meso manus and pes	15.6
T3629	I	forelimb:complete & compact;hind limb:fe,t,f>term.phal.,int. phal.>mt>prox.phal.>as,ca;mt2>mt3>mt4>mt1,5	15.9
T3559	I	forelimb: only stylo-,zeugopods & compact;hind limb:fe>t>f>term.phal,int. phal.>prox.phal>mt>as,ca	16.8
T3661	I	h,r>u,fe,term.phal.manus,int.phal.manus>prox.phal.manus>mc>t>uln,i,,f,term.phal.pes>int.phal.pes>prox.phal.pes>mt>as>ca;mc3	16.1

		>mc4>mc5>mc2>mc1;mt(beg.):mt4>mt3>mt2>mt1>mt5	
T3606	I	forelimb:compact;hind limb:fe>t>fr>term.phal.,int.phal.>prox.phal.>mt>as>ca;mt1>mt2>mt3>mt4>mt5;phal:D1>D2>D3>D4>D5	16.2
T3468	I	h,r,fe>u,t>f>phal.manus,mc>mt> uln,i,phal.pes;mt1>mt2>mt3>mt4>mt5	16.5
T3781	I	h,r,f>u,phal.manus,mc>phal.pes>t,i>f,mt>as,ca	16.5
T3598	I	h,r,u,fe,t>f>term.phal.manus,int.phal.manus>meso	16.6
		manus>prox.phal.pes>mt>as,ca;mc4>mc3>mc2>mc1>mc5;mt1>mt2>mt3>mt4>mt5;phal:D1>D2>D3>D4>D5	
T3740	I	h,r,fe>u,t,int.phal.manus,term.phal.manus>f>prox.phal.manus,mc>i,uln,term.phal.pes>int.phal.pes>prox.phal.pes>mt,as>ca;mc	16.6
		(end.):mc5>mc1>mc2,3,4;mt (beg.):mt4>mt3>mt2>mt1>mt5;phal.pes:D1>D2>D3>D4>D5	
T3631	I	forelimb: compact; hind limb:fe,t>f>term.phal.,int. phal.>prox.phal.,mt>as>ca;mt1>mt2>mt3,5>mt4	16.7
T3625	I	forelimb:compact except i>uln;hind limb:fe,t,f>term.phal.>int.phal.,prox.phal.,mt>as,ca;mt2>mt3>mt4>mt1,5	16.7
T3602	I	h,r,u,fe>phal.manus>mc,t,f>meso	16.8
		manus>term.phal.pes>int.phal.pes,prox.phal.pes>mt>as>ca;mc4>mc3>mc2>mc1>mc5;mt3>mt4>mt5>mt1,2;phal:D1>D2>D3>D4	
		>D5	
T3442	I	forelimb:preserved & compact except mc2,3; hind limb sequence: fe>mc>t>f>term.phal.pes>int.	16.9
		phal.pes>prox.phal.pes>mt>as>ca;mt1>mt2>mt3>mt4>mt5	
T3400	J	completely preserved & compact	17.1
T3639	J	forelimb:completely preserved & compact;hind limb:fe>t>f>term.phal.>int. phal.>mt>prox.phal.>as>ca;mt4>mt3>mt2,5>mt1	17.1
T3610	J	forelimb & hind limb compact except ca	17.1
T3745	J	forelimb & hind limb compact	17.1
T3934	J	all preserved & compact except:i>uln,as>ca	17.5
T3750	J	forelimb preserved & compact;fe,t,f,term.phal.pes,int.phal.pesprox.phal.pes,as>mt,ca;mt1,2>mt3>mt4,5	18
T3741	K	forelimb only:stylo-,zeugopods:compact;fe,t>f,int.phal.pes,term.phal.pes>prox.phal.pes,as>mt>ca;mt1>mt2>mt3>mt4>mt5	18.2
T3528	J	forelimb:completely preserved & compact, except: i>uln;hind limb:fe>t,f>term.phal.,int.	18.4
		phal.,prox.phal.>mt>as>ca;mt2>mt5>mt1,4>mt3	
T3636a	K	forelimb:compact;hind limb:fe>t>f>term.phal.>int. phal.,prox.phal.,mt>meso;mt1>mt2>mt3>mt4>mt5	18.7
T3638	K	forelimb:compact;hind limb compact except:mt,phal.,meso	19.5
T3634	L	forelimb:compact;hind limb:compact except: ca	20.4
T3635	L	forelimb:compact;hind limb:fe>t>f>term.phal.>int. phal.>prox.phal, mt>meso;mt1>mt2>mt3>mt4>mt5	21.1
T3527	M	only hind limb preserved, completely compact	23.2

Neusticosaurus peyeri

M. no.	sc	Compaction patterns	st
T3705	A	beginning compaction:h,fe>u,r>f,t>mt>uln>I,phal.pes>as,ca	2.4
T3408	B	h,u,r,fe>f(beg.)>t(beg.)>phal.pes,mt,mc,meso(beg.)o	5.1
T3789	B	h,fe>r,t>u>f>term.phal.pes>int.phal.pes>prox.phal.pes,mt,as>ca;mt(beg.):mt4>mt3>mt2>mt1>mt5	5.5
T4292	C	beginning compaction:h>u,r,fe>f,t>mc>prox.phal.manus>int.phal.manus,term.phal.manus,uln>i,mt>prox.phal.pes>int.	ca. 5.7
		phal.pes>term.phal.pes>as>ca;phal.manus(beg.):D1>D2>D3>D4>D5;phal.pes(beg.):D4>D3>D2>D1>D5;mc(beg.):mc4>mc3>m	
		c2>mc1>mc5;mt(beg.):mt4>mt3>mt2>mt1>mt5	
T3932	B	h,fe>r>u,t>f,phal.manus>mc,uln,i,term.phal.pes,int.phal.pes>prox.phal.pes,mt,as>ca;mc(end.):mc1>mc2>mc3>mc4>mc5;mt(en	8.6
		d.):mt1>mt2>mt3>mt4>mt5	
T4290	D	h,r,fe>u>t,f,phal.manus>mc>uln,i	9.1
T3586	D	h>r,t>u>f,mc,phal.manus>phal.pes>mt>as,ca;mc4>m3>mc2>mc1>mc5;mt1>mt2>mt3>mt4>mt5	9.4

T3389	E	h,r,u,i,uln,phal.manus,fe,t>f,phal.pes>mt,as>ca:mt1>mt2>mt3>mt4>mt5;phal.pes:D1>D2>D3>D4>D5	10.5
T4299	E	h,fe>r,u>t>f,mc,i,uln,phal.pes>mt>as,ca;phal.manus not informative;mc(end.):mc4>m3>mc2>mc1>mc5;mt(beg.):mt4>mt3>mt2>mt1>mt5	10.9
T3615	E	h,fe,r>t,u>f,manus,term.phal.pes>int.phal.pes,prox.phal.pes>mt,as>ca;mt1>mt2>mt3>mt4>mt5	11.3
T3754	F	h,r,fe>u,t>phal.manus,mc,f>phal.pes>mt,as>ca;mt(beg.):mt4>mt3>mt2>mt1>mt5	12.9
T3583	F	h,re>r,u,t>term.phal.manus,int.phal.manus,f>term.phal.pes>prox.phal.manus,int.phal.pes>mc,prox.phal.pes>i,uln,mt,as>ca;mc1>mc2>mc3>mc4>mc5;mt1>mt2>mt3>mt4>mt5;phal.manus:D1>D2>D3>D4>D5	13.3
T3394	F	h not preserved; zeugopods and pes completely compact; fe, t> term.phal.pes>int.phal.pes>f,prox.phal.pes>mt,; mt1>mt2>mt3>mt4>mt5; phal.pes:D1>D2>D3>D4>D5	13.8
T3716	F	h,fe>r>t,u>f,phal.manus>mc,term.phal.pes>int.phal.pes>prox.phal.pes>mt>ca(beg.)>as(beg.);phal.pes:D1>D2>D3>D4>D5;mt1>mt2>mt3>mt4>mt5	13.9
T3422	G	completely preserved, not all yet compact: int.phal.pes>prox.phal.pes	14.0
T3715	G	h,r,fe,t>u>f>phal.manus,uln,mc,term.phal.pes>prox.phal.pes,int.phal.pes,mt>as>ca;mc4>m3>mc2>mc1>mc5;mt1>mt2>mt3>mt	14.0
T3665	G	h,r,fe>u,t>f,phal.manus,i,uln,phal.pes>mt>as>ca	14.1
T3410	G	completely preserved, completely compact	14.8
T3542	G	h,re>t,r>u,f,mc,i>uln,phal.pes>mt>as>ca;mt1>mt2>mt3>mt4>mt5	15.1
T3431	G	h,r,fe>u,t>phal.manus>mc>f> uln,i>phal.pes>mt>as>ca	15.3
T3444	E	completely preserved, completely compact	15.9
T3755	H	h,r,fe,u,t>f>phal.manus>mc,term.phal.pes>i>uln>int.phal.pes>mt>prox.phal.pes>as>ca;mt(beg.):mc(end.):mc4>m3>mc2>mc1>mc5;mt(beg.):mt4>mt3>mt2>mt1>mt5;phal.pes:D1>D2>D3>D4>D5	16.2
T3523	H	h,r,u,i,phal.manus,fe,t,term.phal.pes,int.phal.pes>f,as,prox.phal.pes>mt,ca;mt1>mt2>mt3>mt4>mt5;phal.pes:D1>D2>D3>D4>D5	16.2
T3449	H	h,r,fe,t>u>phal.manus>f,mc,phal.pes,i>uln,mt>as,ca	16.3
T3663	H	h,r,fe>phal.manus,t>mc,f,term.phal.pes>int.phal.pes,prox.phal.pes,i,uln>mt>as,ca;mc(end.):mc4>m3>mc2>mc1>mc5;mt(beg.):mt4>mt3>mt2>mt1>mt5;phal.manus(end.):D1>D2>D3>D4>D5	16.4
T3395	H ;sex y	h,fe>r,t,phal.manus>mc>phal.pes>f,mt>as,ca	16.9
T3588	H	h,r,fe>u,t,f>phal.manus>mc>uln,i,term.phal.pes,int.phal.pes>prox.phal.pes,mt,as>ca;mc4>m3>mc2>mc1>mc5;mt1>mt2>mt3>mt4>mt5;phal.pes (end.):D1>D2>D3>D4>D5	17.0
T3534	H	r>fe>t,phal.manus>u,mc,term.phal.pes,int.phal.pes>f,uln,i,prox.phal.pes>mt,as>ca;mc(beg.):mc4>mc3>mc2>mc1>mc5;mc(end.):mc4>mc3>mc2>mc1>mc5;mt(beg.):mt4>mt3>mt2>mt1>mt5;mt(end.):mt1>mt2>mt3>mt4>mt53>D4>D5	17.3
T3902	H	h,r,fe>u,t,f>term.phal.pes,int.phal.pes>prox.phal.pes>mt,as>ca;mt4>mt3>mt2,5>mt1;phal.pes:D1>D2>D3>D4>D5	17.6
T3510	H	h,r,u,fe,t>term.phal.pes,int.phal.pes>prox.phal.pes,f,mt;mt1>mt2>mt3>mt4>mt5	17.6
T3467	H	h>r,u,fe>t,f>prox.phal.pes 1,2,3>prox.phal.pes 4,5>mt4,5(beg.)>mt3,2(beg.)>mt1(beg.)>as,ca	17.9
T3710	I	h,r,fe>t>u,phal.manus>f,i>uln,term.phal.pes,int.phal.pes>prox.phal.pes>mt>as,ca;mc(end.):mc1>m2>mc3>mc4>mc5;mt(beg.):mt4>mt3>mt2>mt1>mt5;phal.pes(beg.):D4>D3>D2>D1>D5	18.2
T3474	I	manus:mc not yet compact; pes:prox.phal., ca, as: not yet compact	18.3
T3479	I	h,r,u,term.phal.manus,int.phal.manus, prox.phal.manus,i,uln,fe,t>f,term.phal.pes,int.phal.pes>prox.phal.pes>mt	18.4
T3396	I	completely preserved, not all yet compact:mt,phal.pes	18.4
T3412	I	h,fe,t>f>phal.,mt>as,ca;mt1,mt2,mt3,mt4>mt5; prox.phal.D1,D2>D3,D5>D4	18.5
T3423	I; sex y	completely preserved, not all yet compact: int.phal.pes>prox.phal.pes>mt>as>ca;mt1>mt2>mt3,mt4,mt5	18.7

T3662	I	h,r,fe,t,f,u,phal.manus,i,uln,mc,term.phal.pes,int.phal.pes>mt>as>ca;mt1>mt2>mt3>mt4>mt5	18.9
T3531	I	h,fe>t>f,int.phal.pes,term.phal.pes>prox.phal.pes,as>mt,ca;mt1>mt2>mt3>mt4>mt5;phal.pes:D1>D2>D3>D4>D5	19.0
T3471	I	all preserved.as,ca>int.,prox.phal.pes	19.4
T3476	J	pes:prox.phal.pes>as>ca	20.1
T3393	J	h,u,r,manus,fe,t,f,term.phal.pes,int.phal.pes>prox.phal.pes,i,uln>mt>as>ca;mt1>mt2>mt3>mt4>mt5 mt4>mt5;phal.manus&pes:D1>D2>D3>D4>D5	20.1
T3788	J	h,r,fe,t>f,u>phal.manus,term.phal.pes>mc,int.phal.pes,uln,i>as,prox.phal.pes>mt,ca;phal.pes:D1>D2>D3>D4>D5;mt1>mt2,5>mt3>mt4	21.4
T3497	J	h,r,u,fe,t,f>manus,int.phal.pes,term.phal.pes>prox.phal.pes,mt,as>ca;mt1>mt2>mt3>mt4>mt5;phal.pes:D1>D2>D3>D4>D5	21.8
T3744	K	h,r,fe>u,t>f,phal.manus>mc,term.phal.pes>int.phal.pes,uln,i>prox.phal.pes,mt>as>ca;mt(beg.):mt4>mt3>mt2>mt1>mt5;phal.pes: D1>D2>D3>D4>D5	22.3
T3712	L	h,r,fe,t>u>phal.manus>f,mc,phal.pes>mt,as,uln,i>ca;mc(end.):mc4>m3>mc2>mc1>mc5;mt2,3,4>mt5>mt1;	25.4
T3764	M	h,r,fe>u>t,f,phal.manus>mc>i>uln>term.phal.pes>int.phal.pes>prox.phal.pes,mt>as,ca;mc4>m3>mc2>mc1>mc5;mt1>mt2>mt3>mt4>mt5	26.2
T3584	M	h,r,u,fe,t,f,term.phal.pes,int.phal.pes>prox.phal.pes>mt,as>ca;mt1>mt2>mt3>mt4>mt5	26.6
T3445	Q	completely preserved, completely compact	34.5

Neusticosaurus edwardsii

M. no.	sc	Compaction patterns	st
T3454	B	h,r,u>prox.phal.manus,fe>mc,t>u,i,f,phal.pes>mt>as,ca;beg.:mt4>mt3>mt2,5>mt1;phal.pes(end.):D4>D5>D3>D2>D1	ca.26.5
T2466	D	hind limb:preserved & compact	ca.46.4
T3425	B	fe>t>f,term.phal.pes>int.phal.pes>prox.phal.pes,mt,as,ca;mt3,4,5>2>1	ca.25.7
T3456	B	h>r,u,fe,t>phal.manus>mc,f,phal.pes>mt>i>u>as>ca	24.0
T3452	B	h,r,u,fe,t>f,phal.pes>mt;beg.:mt4>mt3>mt2	24.42
T3407	B	h,fe,r,t>u>f>prox.phal.manus(beg.)>mc(beg.),int.phal.manus(beg.)>uln,prox.phal.pes(beg.)>i,mt(beg.)>as>ca;mt4>3,5>mt2>mt1	24.8
T3708	B	h,fe>r>u,t>int.phal.manus,term.phal.manus>prox.phal.manus>mc>i>uln>f,term.phal.pes>int.phal.pes>prox.phal.pes>mt>as>ca; mc4>mc3>mc2;mt5>mt4>mt3>mt2>mt1	25.1
T3778	B	h,fe,r>u,mc,t>f,uln,i>mt>prox.phal.pes>as,ca	25.4
T3719	B	forelimb preserved:h,r>u	25.4
T3775	B	h,r>u>mc>uln>i	ca. 27.8
T3453	B	h,fe,r>u,t>term.phal.manus>f,mc,int.phal.manus,term.phal.pes>uln,i>prox.phal.manus,int.phal.pes>as,ca> prox.phal.pes>mt;mt4>3,5>mt2>mt1	28.3
T3758	B	h>r,fe>u,t>phal.manus>mc>f,term.phal.pes>int.phal.pes>prox.phal.pes>mt>as>ca;beg.:mc4,5>mc3>mc2>mc1;beg.:mt4>mt5>mt2>mt1	28.9
T3776	B	h,r,u,uln,i,mc,term.phal.manus,int.phal.manus,fe,t,f,mt2-5,as,ca,term.phal.pes,int.phal.pres>prox.phal.manus>mt1,prox.phal.pes	a. 29.6
T3749	B	h>r>u>int.phal.manus>prox.phal.manus,mc>uln>i	29.9
T3438	D	h,r,fe>u,t>f,term.phal.pes>int.phal.pes>mt>prox.phal.pes>as>ca;mt1>mt2,5>mt3>mt4;phal.pes:D1,3,5>4>2	47.4
T3711	E	fe>t>f,term.phal.pes>int.phal.pes>mt>prox.phal.pes>as>ca;mt4>mt3>mt2>mt1>mt5;phal.pes:D1>D2>D3>D4>D5	ca. 51.5
T3460	E	h,r,u,fe,t,f,uln,i,phal.manus,term.phal.pes,int.phal.pes>mc,prox.phal.pes>mt>as,ca;mt1,2>mt3>mt4>mt5;phal.pes:D1>D2>D3>D4>D5	53.3

Appendix 4, Table 1. Data for the Event pairing analysis. The tables show the relative sequences of the early and final phase of compaction processes for all four pachypleurosaurids and beginning and ending of ossification of the outgroup, *Liopholis whitii*.

Order of the early phase of compaction processes

Elements\Species	***S. mirigiolensis***	***N. pusillus***	***N. peyeri***	***N. edwardsii***	***L. whitii***
Humerus	?	1	1	?	2
Radius	?	2	3	?	3
Ulna	?	2	3	?	3
preax. carpal	9	10	9	5	13
postax. carpal	8	10	8	4	12
Metacarpal-1	4	6	8	5	9
Metacarpal-2	3	5	7	4	8
Metacarpal-3	2	4	6	3	4
Metacarpal-4	1	3	5	2	7
Metacarpal-5	5	7	9	6	10
Prox. phal. manus	3	5	7	1	6
Int. phal. manus	4	6	8	2	7
Term. phal. manus	7	7	8	6	9
Femur	?	2	2	?	1
Tibia	?	3	4	?	2
Fibula	?	3	4	?	2
preax. tarsal	11	14	17	9	11
postax. tarsal	12	15	18	10	12
Metatarsal-1	6	11	12	8	6
Metatarsal-2	5	10	11	7	5
Metatarsal-3	4	9	10	6	4
Metatarsal-4	3	8	9	5	3
Metatarsal-5	7	12	13	9	11
Prox. phal. pes	5	11	14	4	5
Int. phal. pes	6	12	15	7	6
Term. phal. pes	10	13	16	8	8

Order of the final phase of the compaction processes

Elements\Species	***S. mirigiolensis***	***N. pusillus***	***N. peyeri***	***N. edwardsii***	***L. whitii***
Humerus	1	1	1	1	2
Radius	2	2	2	2	3
Ulna	3	3	3	4	3
preax. carpal	7	9	10	14	13
postax. carpal	7	10	11	15	12
Metacarpal-1	7	10	11	12	9
Metacarpal-2	6	9	10	11	8
Metacarpal-3	5	8	9	10	4
Metacarpal-4	4	7	8	9	7
Metacarpal-5	8	11	12	9	10
Prox. phal. manus	5	6	7	8	6
Int. phal. manus	6	5	6	7	7
Term. phal. manus	6	5	6	6	9
Femur	2	2	2	3	1
Tibia	3	3	4	5	2
Fibula	4	4	5	7	2
preax. tarsal	11	14	18	16	11
postax. tarsal	12	15	19	17	12
Metatarsal-1	10	13	13	15	6
Metatarsal-2	11	14	14	14	5
Metatarsal-3	12	15	15	13	4
Metatarsal-4	13	16	16	12	3
Metatarsal-5	14	17	17	16	11
Prox. phal. pes	8	12	13	12	5
Int. phal. pes	9	11	12	11	6
Term. phal. pes	9	10	11	7	8

Appendix 4, Table 2. Distribution and percentage of character states of the total event pairs (n=325) examined. Character states reflecting the timing of one event relative to another: 0) before; 1) simultaneously; 2) after.

Early phase compaction	**State 0 (%)**	**State 1 (%)**	**State 2 (%)**	**Missing data (%)**
Liopholis whitii	155 (47.7 %)	16 (4.9 %)	154 (47.4 %)	0
Serpianosaurus mirigiolensis	75 (23.1 %)	11 (3.4 %)	104 (32.0 %)	135 (41.5 %)
Neusticosaurus pusillus	80 (24.6 %)	14 (4.3 %)	231 (71.1 %)	0
Neusticosaurus peyeri	76 (23.4 %)	12 (3.7 %)	237 (72.9 %)	0
Neusticosaurus edwardsii	60 (18.5 %)	13 (4.0 %)	117 (36.0 %)	135 (41.5 %)
Final phase compaction	**State 0 (%)**	**State 1 (%)**	**State 2 (%)**	**Missing data (%)**
Liopholis whitii	155 (47.7 %)	16 (4.9 %)	154 (47.4 %)	0
Serpianosaurus mirigiolensis	79 (24.3 %)	14 (4.3 %)	232 (71.4 %)	0
Neusticosaurus pusillus	93 (28.6 %)	10 (3.1 %)	222 (68.3 %)	0
Neusticosaurus peyeri	99 (30.5 %)	8 (2.5 %)	218 (67.0 %)	0
Neusticosaurus edwardsii	128 (39.4 %)	11 (3.4 %)	186 (57.2 %)	0

Appendix 5: Character matrix of the event pairing analysis of the osteogenetic sequences in the four pachypleurosaurids from Monte San Giorgio.

Sequences of the early phase of compaction processes

Serpianosaurus mirigiolensis
??????????0 ???00???00 0???0000?? ?00000???0 02222???00 01220???00
122202???0 0222222?? ?????????? ?????????? ?????????? ??????????
????222222 222???????2 2222222?? ??????0022 222220???0 0???002222
1220???000 ???0012220 210???0000 ???0001220 100???0000 0???002222
2221???002 222???0022 221220???0 001220???0 022222220? ??00122202
???2222222 222???0022 22222

Neusticosaurus pusillus
2212222221 2220022200 0222000022 2000002220 0222222200 0122022200
1222022220 0222212221 1000000000 0222000001 0000222200 0001000021
2222222222 2222222222 2222222222 2222222222 2222222220 0222112222
2222222000 2220022222 2222220000 2220022222 2222220000 0222222222
2222222002 2222222222 2222222220 0122202222 2222222222 2200222212
2222222222 2222220022 22222

Neusticosaurus peyeri
2212222220 2220122200 0222000022 2000002221 2222222200 0122022201
1222022220 1122202120 0000000000 0222000000 0000222200 0000000021
2222222222 2222222222 2222222222 2222222222 2222222220 0222222222
2222222000 2222222222 2222220000 2221222221 2222220000 0222222222
2222222002 2222222222 2222222220 0222222222 2222222222 2200222222
2222222222 2222220022 22222

Neusticosaurus edwardsii
??????????0 ???12???01 0???0000?? ?00000???2 2222???00 00000???00
000102???2 222221222? ?????????? ?????????? ?????????? ??????????
????222222 222???????2 222222222? ???2???222 222222???0 0???222222
2222???000 ???2222221 221???0000 ???1212220 220???0000 0???222222
2222???102 222???0101 220220???0 000000???2 222222222? ??00012202
???2222222 222???0012 22022

Liopholis whitii
2212222220 2220022200 0222000022 2000022220 0222222200 0020022200
0021022220 0122202200 0000000000 0100000000 0000210000 0000000021
2220022222 2222222220 1222222222 2222220000 2001002220 0222000020
0000222000 2220000100 0002220000 2110000000 0002220000 0222002222
2222222102 2222220000 2000002220 0012202220 0002001002 2200122202
2220001220 2202220022 22022

Sequences of the final phase of compaction processes

Serpianosaurus mirigiolensis
2222222221 2221122200 0222000022 2000002222 2222222200 0012022200
0122022220 0012202121 0000000000 0221000000 0000222200 0001000022
2222222222 2222222222 2222222222 2222222222 2222222220 0222222222
2222222102 2222222222 2222222122 2222222222 2222222222 2222222222
2222222222 2222222222 2212222220 0000002222 2222222222 2200000002
2222222222 2222220000 00021

Neusticosaurus pusillus
2222222222 2222122210 0222000022 2000002222 2222222200 0000022200
0000002220 0000000121 0000000000 0221000000 0000222200 0000000022
2222222222 2222222222 2222222222 2222222222 2222222220 0222222222
2222222102 2222222222 2222222122 2222222222 2222222222 2222222222
2222222222 2222222222 2222222220 0000002222 2222212222 2200000000
2222112220 2222220000 00000

Neusticosaurus peyeri
2222222222 2222122210 0222000022 2000002222 2222222200 0000022200
0000002220 0000000121 0000000000 0222000000 0000222200 0000000022
2222222222 2222222222 2222222222 2222222222 2222222220 0222222222
2222222002 2222222222 2222220022 2222222222 2222220022 2222222222
2222222002 2222222222 2222222220 0100002222 2222212222 2200000000
2222112220 2222220000 00000

Neusticosaurus edwardsii
2222222222 2220022200 0222000022 2000002220 0000122200 0000022200
0000002220 0000000022 0000000000 0222000000 0000222200 0000001222
2222222222 2222222222 2222222222 2222222122 2222222220 0222102222
2222222000 2220022222 2222220000 2220012222 2222220000 0222222222
2222222102 2222220012 2222222220 0000102220 0012222222 2200000000
2220000000 0122210000 00000

Liopholis whitii
2212222220 2220022200 0222000022 2000022220 0222222200 0020022200
0021022220 0122202200 0000000000 0100000000 0000210000 0000000021
2220022222 2222222220 1222222222 2222220000 2001002220 0222000020
0000222000 2220000100 0002220000 2110000000 0002220000 0222002222
2222222102 2222220000 2000002220 0012202220 0002001002 2200122202
2220001220 2202220022 22022

Chapter 5:

Long bone microstructure gives new insights into the life of pachypleurosaurids from the Middle Triassic of Monte San Giorgio, Switzerland/Italy

Jasmina Hugi, Torsten M. Scheyer, P. Martin Sander, Nicole Klein,
and Marcelo R. Sánchez-Villagra

Published in *C. R. Palevol* xxx (2011) xxx–xxx

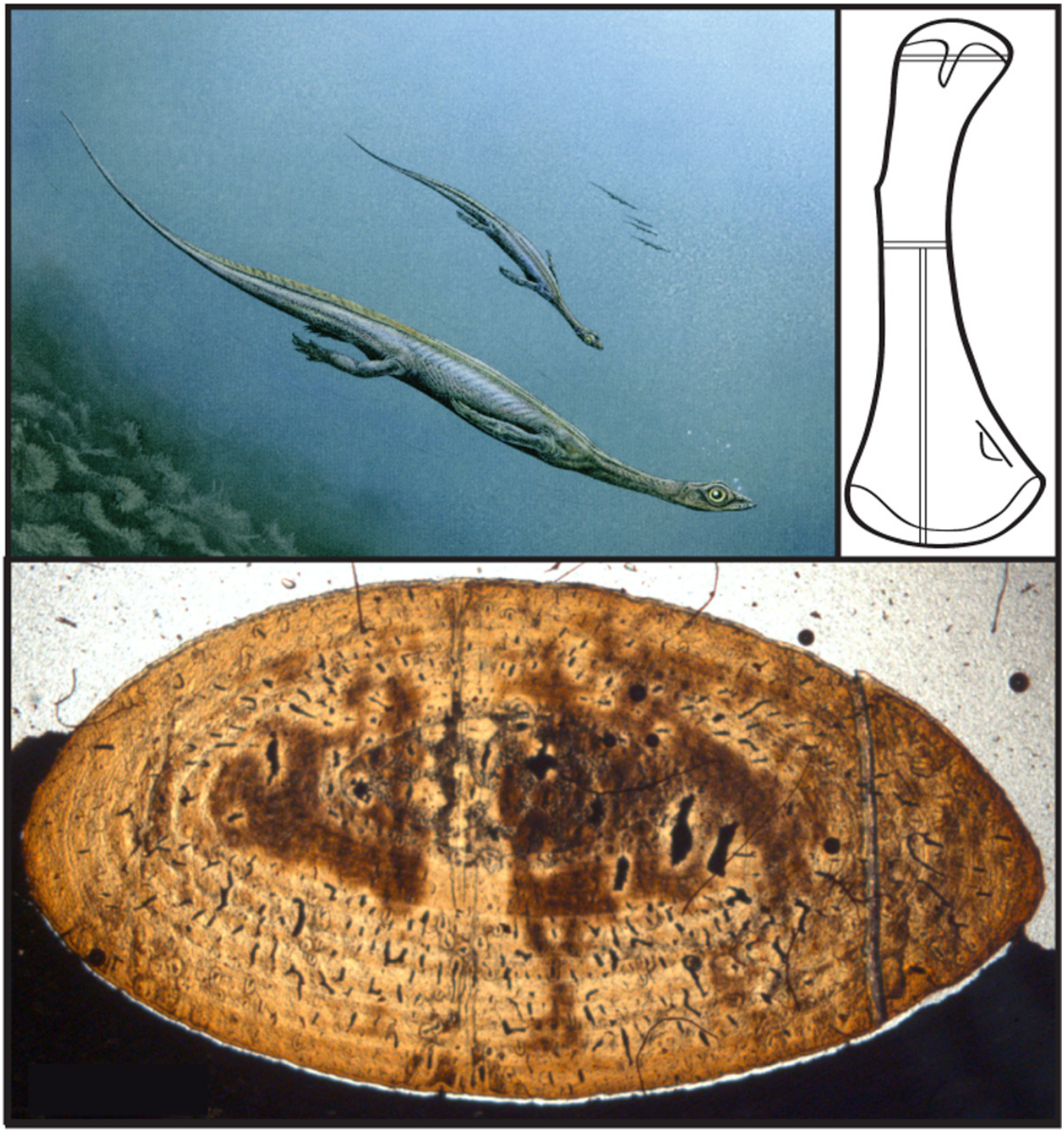

Drawing upper left: B. Scheffold
Drawing upper right drawing and lower photograph: J. Hugi

Contents lists available at ScienceDirect

Comptes Rendus Palevol

www.sciencedirect.com

General palaeontology, systematics and evolution (Vertebrate palaeontology)

Long bone microstructure gives new insights into the life of pachypleurosaurids from the Middle Triassic of Monte San Giorgio, Switzerland/Italy

La microstructure des os longs donne un nouveau regard sur la vie des pachypleurosauridés du Trias moyen de Monte San Giorgio, Suisse/Italie

Jasmina Hugi[a,*], Torsten M. Scheyer[a], P. Martin Sander[b], Nicole Klein[b], Marcelo R. Sánchez-Villagra[a]

[a] Paläontologisches Institut und Museum, Universität Zürich, Karl Schmid-Strasse 4, 8006 Zürich, Switzerland
[b] Steinmann-Institut für Geologie, Mineralogie und Paläontologie, Universität Bonn, Bonn, Germany

ARTICLE INFO

Article history:
Received 8 October 2010
Accepted after revision 14 March 2011
Available online xxx

Written on invitation of the Editorial Board

Keywords:
Sauropterygia
Bone histology
Biostratigraphy
Ecology
Life history
Switzerland
Italy

ABSTRACT

The long bone microstructure of four pachypleurosaurid taxa from Monte San Giorgio (Switzerland/Italy) was studied. Pachypleurosaurids are secondarily aquatic reptiles that lived during the Middle Triassic in varying marine environments of the Tethys. All four pachypleurosaurids show high compactness values in their long bones based on a thick cortex and a calcified cartilaginous core, which is evident for the osteohistology throughout the ontogeny. Parts or even the entire endosteal bone layer composed of a mixture of woven-fibered bone tissue and parallel-fibered bone tissue is preserved in both pachypleurosaurid genera. The rest of the cortex consists of lamellar-zonal bone tissue type. Differences in the microstructure of the bones between the pachypleurosaurids are reflected in the occurrence of remodelling processes, which, if present, affect the innermost growth marks of the cortex or the calcified cartilaginous core. Further variation is present in the spacing pattern of the growth cycles, as well as in the degree of vascularization of the lamellar-zonal bone tissue type. Our data on the microstructure of the long bones support previous studies on morphology and facies distribution, which indicated different habitats and adaptations to a secondary aquatic lifestyle for each pachypleurosaurid taxon. Life history data further corroborate different lineage-styles and ages at sexual maturity. The bone histological data of the stratigraphically youngest and oldest pachypleurosaurid species might indicate possible climate-dependent reproductive seasons similar to Recent lissamphibian aquatopes.

© 2011 Académie des sciences. Published by Elsevier Masson SAS. All rights reserved.

Mots clés :
Sauropterygia
Histologie d'os
Squelette humanologie
Écologie
Histoire de vie
Suisse
Italie

RÉSUMÉ

La microstructure des os longs de quatre taxa de pachypleurosauridés de Monte San Giorgio (Suisse/Italie) a été étudiée. Les pachypleurosauridés sont des reptiles secondairement aquatiques qui ont vécu au Trias moyen, dans des environnements proches des rivages de la Téthys. Les quatre pachypleurosauridés présentent des valeurs de compacité élevées dans les os longs, basées sur un cortex épais et un cœur cartilagineux calcifié, qui persiste dans la région ostéohistologique tout au long de l'ontogénèse. Des parties ou même la totalité du feuillet

* Corresponding author.
E-mail address: jasmina.hugi@pim.uzh.ch (J. Hugi).

1631-0683/$ – see front matter
doi:10.1016/j.crpv.2011.03.004

...

1. Introduction

Pachypleurosaurids are small secondarily aquatic reptiles which belong to the Triassic ensuropterygians (Klein, 2010; Rieppel, 2000). The UNESCO World Heritage site of Monte San Giorgio (Switzerland/Italy) has yielded pachypleurosaurids in great quantity and quality since excavations started in 1924. Two genera and four species of pachypleurosaurids, *Serpianosaurus mirigiolensis*, *Neusticosaurus pusillus*, *N. peyeri* and *N. edwardsii*, are recognized from four distinct horizons of Middle Triassic Ladinian carbonates (Peyer, 1932; Fig. 1). *S. mirigiolensis* is the stratigraphically oldest taxon and is known only from the Besano Formation (Furrer, 1995; Bürgi et al., 2001; Sander, 1989; Fig. 1). The stratigraphically younger genus *Neusticosaurus* is found in the Lower Meride Limestone (Carroll and Gaskill, 1985; Sander, 1989; Fig. 1). *N. pusillus* is found in the beds of the Cava Inferiore horizon, whereas the beds of the Cava Superiore horizon exclusively yielded specimens of *N. peyeri* (Fig. 1). The stratigraphically youngest taxon, *N. edwardsii*, is preserved only in the Alla Cascina horizon (Sander, 1989; Fig. 1).

The Monte San Giorgio pachypleurosaurids lived in more or less near-shore environments in the Tethys (Sander, 1989) during a subtropical monsoonal climate (Bürgi et al., 2001). Pachypleurosaurids clearly exhibit aquatic adaptations such as the loss of ossified carpal and tarsal elements, the ventral expansion of the girdles, the flattening of the forelimbs and hind limbs, and an isodont dentition that is typical for carnivorous animals (Carroll and Gaskill, 1985; Sander, 1989). However, the four species from Monte San Giorgio also show certain morphological variation which might be linked to different habitat preferences. *N. pusillus*, *N. peyeri* and *N. edwardsii* lived in a lagoonal environment with increasing restriction based on the evidence of facies and fossil distribution (Furrer, 1995). In contrast, *S. mirigiolensis* lived in a basin with more open marine influences (Furrer, 1995; Carroll and Gaskill, 1985; Rieppel, 1989). *N. pusillus* and *N. peyeri* differ morphologically from *S. mirigiolensis* and *N. edwardsii* by exhibiting anatomically pachyostotic vertebral centra and ribs (sensu Francillon-Viellot et al., 1990), as well as elongated transverse processes of the caudal vertebrae (Sander, 1988). In contrast, *S. mirigiolensis* and *N. edwardsii* show less anatomically pachyostotic bones, but prominent insertion areas for strong muscles along the vertebral column, as well as higher dorsal spines of their caudal vertebrae (Carroll and Gaskill, 1985; Rieppel, 1989). Pachypleurosaurids also differ between each other by an advanced reduction of phalangeal formulae and body lengthening by increasing the vertebral count of the dorsals in the stratigraphically younger taxa compared to the stratigraphically older ones (Carroll and Gaskill, 1985; Nopcsa and Heidsieck, 1934; Rieppel, 1989; Sander, 1989). Histological studies of the limb bones and ribs of the pachypleurosaurids (Buffrénil and Mazin, 1989; Nopcsa and Heidsieck, 1934; de Ricqlès, 1975; de Ricqlès and Buffrénil, 2001; Sander, 1989; Zangerl, 1935) revealed that all four species exhibit pachyostosclerotic bones in thin-section (sensu Francillon-Viellot et al., 1990). Such dense and heavy bones are typically found in secondarily aquatic amniotes and are generally thought to

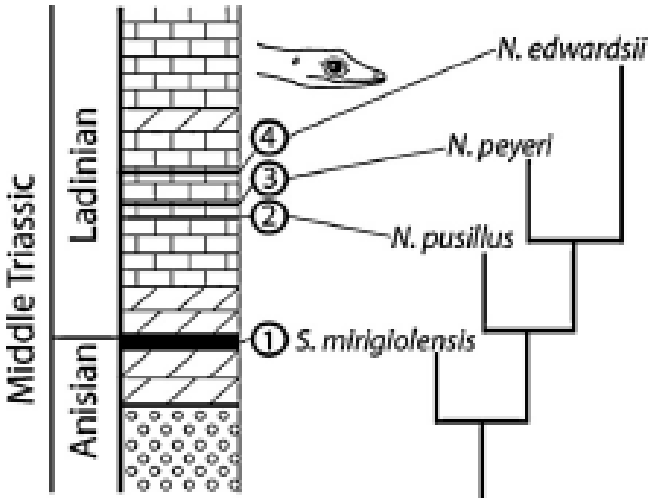

Fig. 1. Stratigraphic range of the four pachypleurosaurids from Monte San Giorgio (after Furrer, 1995; D'Orazi et al., 1988; modified). 1: Besano Formation; 2: Cava Inferiore horizon; 3: Cava Superiore horizon; 4: Alla Cascina horizon.

Fig. 1. Stratigraphie range des quatre pachypleurosaurides du Monte San Giorgio (d'après Furrer, 1995; D'Orazi et al., 1988; modifié). 1 : Formation Besano ; 2 : Horizon Cava Inferiore ; 3 : Horizon Cava Superior ; 4 : Horizon Alla Cascina.

increase ballast, allowing a hydrostatic control of body density and body trim in water (Canoville and Laurin, 2010; Germain and Laurin, 2005; de Ricqlès and Buffrénil, 2001). Rothschild and Storrs (2003) suggested that Nothosaurus spp. routinely dived into great depths or changed diving depths rapidly based on a few cases of avascular necrosis in the epiphyseal regions of the long bones, which was hypothesized to be caused by decompression syndrome. Avascular necrosis is also rarely indicated at the proximal epiphyseal regions of the humerus of *S. wirtgeiensis* (Hugi and Scheyer, unpublished). New results obtained from the ontogenetic sequences in *S. wirtgeiensis* show that it shares slightly more similarities with data from terrestrial reptiles, whereas the Nothosaurus spp. resemble slightly more closely extant semi-aquatic and aquatic reptiles (Hugi and Scheyer, unpublished; Rieppel, 1993; Wermeburg et al., 2008).

The aim of this study is to reveal further "terrestrial"- and "aquatic-like" features among the pachypleurosaurids from Monte San Giorgio based on new histological data. Questions include whether these new data show a gradual variation from stratigraphically older to younger specimens as seen in the reduction of the phalangeal formula and the elongation of the vertebral count, or whether new results reflect possible adaptations to different marine environments. Zangerl (1935) described the bone microstructure of Nothosaurus spp. and de Ricqlès (1976) summarized his results in a comparative study of the histology of fossil and living reptiles. Sander (1989) then studied the skeletochronology of several specimens of *N. pusillus* and *N. peyeri* by counting the minimum number of lines of arrested growth (LAGs) (Castanet et al., 1993) in polished sections, as well as describing the spacing pattern of the growth cycles (Buffrénil and Castanet, 2000). This study is focused on the histological changes during the ontogeny of all four pachypleurosaurid taxa. It further expands the database, especially for *S. wirtgeiensis* and *N. edwardsii*, and describes new histological and skeletochronological data for all pachypleurosaurids from Monte San Giorgio. The results are discussed in comparison to published accounts of fossil osteosclerotic and Recent lacertilian squamates.

2. Material and methods

We examined 11 specimens of *S. wirtgeiensis*, nine of *N. edwardsii* (Table 1), 18 specimens of *N. pusillus* and nine of *N. peyeri*, all housed in the Paläontological Institute of the University of Zurich (PIMUZ). These new data complement previous results of the bone histological studies of Sander (1989), where polished sections of *N. pusillus* and *N. peyeri* were used. Size classes of *S. wirtgeiensis* and *N. edwardsii* were adopted from Sander (1989) (Rieppel, 1989). Diaphyseal thin-sections of the growth series of the bones of forelimb and hind limb (humerus, radius, ulna, femur, tibia, fibula, metacarpals, metatarsals; note that not all bones were available for each specimen) were processed and documented at the PIMUZ, following standard petrographic preparation techniques (Scheyer and Sánchez-Villagra, 2007). The diaphyseal region of the long bones is known to yield the strongest ecological signal

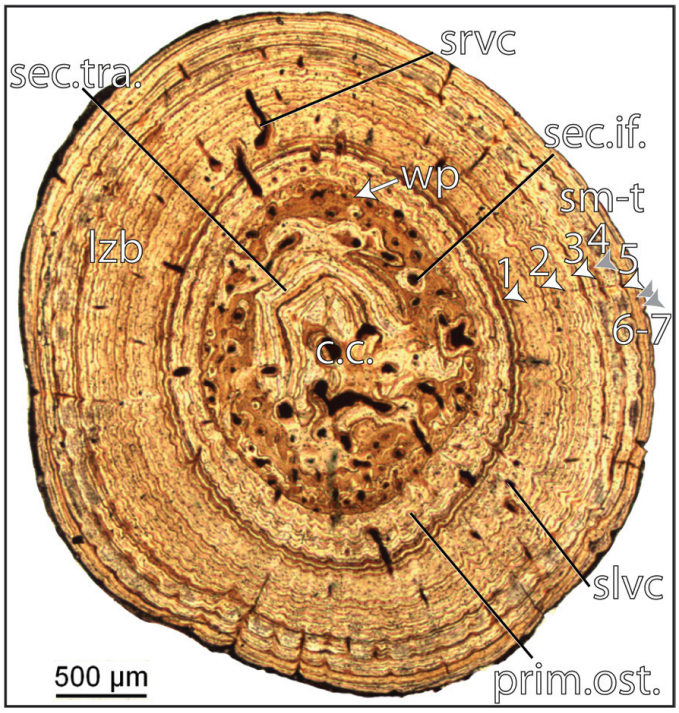

Fig. 2. Metaphyseal transverse section of the humerus of an adult *Neusticosaurus pusillus* (PIMUZ T 4778) in normal transmitted light. The specimen shows seven LAGs (arrow heads). The annual maturity (sm-t) is estimated at age three to four years due to the abrupt decline in thickness of growth cycle four (grey arrow head; Sander, 1989). The inner periosteal bone layers at the cortex are only partly affected by resorption processes and therefore, still reveal large parts of the first growth cycle which is composed of woven-fibered grading into parallel-fibered bone tissue type (wp). An extensive Haversian system (HS) is developed in the outer cortex. The cortex shows lamellar-zonal bone tissue type (lzb) which is vascularized by simple longitudinal and cortical vascular canals (slvc, srvc) and primary osteons (prim.ost.). The medullary region is filled with a calcified cartilage core (c.c.) and shows remodeling trabeculae (sec.tra.), as well as widened and secondarily filled simple vascular canals (sec.if.).

Fig. 2. Section transversale de métaphyse de l'humérus d'un adulte de *Neusticosaurus pusillus* (PIMUZ T 4778) en lumière transmise normale. L'échantillon montre sept LAGs (flèches de tête). La maturité annuelle (sm-t) est estimée à trois à quatre ans, en raison de la diminution abrupte de l'épaisseur du cycle de croissance quatre (flèche de tête grise ; Sander, 1989). Les tissus internes d'os périostique du cortex ne sont qu'en partie affectés par les processus de résorption et, de ce fait, révèlent encore de grandes parties du premier cycle de croissance qui est composé d'un tissu osseux de type entrelacé-fibreux passant à un type de tissu parallèle (wp). Un système fondamental externe (HS) se développe dans la partie la plus externe du cortex. Le cortex montre un tissu osseux de type lamellaire-zonal (lzb) qui est vascularisé par des canaux vasculaires simples, longitudinaux et corticaux (slvc, srvc) et des ostéones primaires (prim.ost.). La région médullaire est occupée par un cœur cartilagineux calcifié (c.c.), et montre des trabécules remodelées (sec.tra.), ainsi que des canaux vasculaires simples, élargis et remplis secondairement (sec.if.).

(Canoville and Laurin, 2010) and generally preserves the most complete growth record of the bones among vertebrates (Francillon-Vieillot et al., 1990). The amount of vascularization of the long bones, as well as the age of sexual maturity and the ontogenetic age of each individual (Table 1) was assessed qualitatively through the analysis of bone types and tissues, spacing patterns, as well as through the counting of LAGs. The bone compactness of one adult *S. wirtgeiensis* and one adult *N. edwardsii* was also quantitatively analysed (Table 2) using the PC version of the program Bone Profiler (Girondot and Laurin, 2003). Paired t-tests were performed to report the probability (p) of the

Table 1.
Skeletal chronology of *Anarosaurus heterolepidotus* and *Neusticosaurus edwardsii*.
Tableau 1.
Âge squelettochronologique d'*Anarosaurus heterolepidotus* et *Neusticosaurus edwardsii*.

	Museum #	sc (ld)	Element	Length	Proximal width	Distal width	# LAGs (ann-c)
A. heterolepidotus	T131	A (1,88)	Humerus	12,7	2,8	4	2 (j)
			Ischium	8,7	2,1	2,3	
			Ulna	7,1	1,8	2,5	
			Femur	11,3	3,3	2,3	
			Tibia	7,8	2,6	2,4	
			Fibula	8	1,7	2,9	
A. heterolepidotus	T8015a	A	Ulna	7,8	2,4	2,7	2 (j)
			Metacarpal-1	2,2	0,3	0,3	
			Metacarpal-2	3,4	0,4	0,4	
			Metacarpal-3	3,9	0,4	0,4	
			Metacarpal-4	4,1	0,4	0,4	
			Metacarpal-5	2,7	0,3	0,3	
A. heterolepidotus	T8015b	A	Ischium	8,8	0,9	0,9	3 (j)
A. heterolepidotus	T1568	B	Humerus (right)	18,7	4,5	6,3	4 (2,-3)
			Humerus (left)	18,3	4,3	6,3	
A. heterolepidotus	T1114	B	Ulna	12,4	4,22	3,8	4 (2,-3)
A. heterolepidotus	T1585	B (2,28)	Humerus	18,8	3,6	6,3	4 (2,-3)
			Femur	17,1	4,8	2,8	
			Tibia	11,3	3,2	2,9	
			Fibula	11,2	3,5	2,7	
A. heterolepidotus	T1110	C (1,54)	Humerus	21,3	4,8	5,4	5 (2,-3)
A. heterolepidotus	T1584	C	Femur	18,8	4,2	2,8	8 (3,-4)
			Tibia	18	3,8	2,2	
			Fibula	18,5	2	2,3	
A. heterolepidotus	T1115	C	Humerus	ca. 23,5	5,3	7	7 (2,-3)
A. heterolepidotus	T1105	D	Femur	24,1	5,3	2,8	8 (2,-3)
A. heterolepidotus	T8510	D (1,88)	Humerus	38	5,2	8,9	13 (2,-3)
			Ischium	17	3,3	3,1	
			Ulna	15,5	5,2	3,1	
N. edwardsii	T8748	B (2,8)	Humerus	28,8	8,5	8,4	4 (j)
			Ischium	15,8	2,9	3,7	
			Ulna	ca. 13,5			
N. edwardsii	Ln/3412	B	Femur	18,9	4,9	2	8 (4,-6)
N. edwardsii	Ln/3411	B	Humerus	35,8	5,7	7	8 (5,-8)
N. edwardsii	T8752	B (1,98)	Humerus	28,7	8,3	6,9	5 (4,-6)
			Ischium	17,5	3,4	3,1	
			Ulna	13,5	5,2	4,1	
			Femur	ca. 18,1	8,9	3,3	
			Tibia	18,1	3,8	2,5	
			Fibula	18,3	2,8	3,8	
N. edwardsii	T8757	C (2,58)	Humerus	38,2	8	10	8 (4,-6)
			Femur	28,5	7,2	3,9	
			Tibia	12,8	4,2	2,9	
			Fibula	11,3	2,8	4,8	
			Metatarsal-5	7,8	1,3	1,3	
N. edwardsii	Schlicht L	C (2,81)	Humerus	38,7	8,3	15,4	8 (5,-8)
N. edwardsii	T8752	D	Femur	47,8	18,1	10,5	18 (5,-8)
			Tibia	28,4	7,3	6,1	
			Fibula	23,9	5,3	2,8	
			Rib (bone)	34,3	2,08		
N. edwardsii	T8037	B (3,21)	Humerus	82,8	15,4	27,9	22 (8,-7)
			Ischium	38,9	11,2	8	
			Ulna	35,7	13,1	10,9	
			Femur	45,5	18,9	10,1	
			Tibia	27,3	18	8,9	
			Fibula	28,1	7,2	10,1	

Question marks indicate non-preserved regions of bone. In those cases where the humerus was completely preserved, the ratio between maximum distal width (minimum width of humerus (sensu Sander, 1990)) is given (hr). sc: size class (after Sander, 1990); LAGs: lines of arrested growth (after Castanet et al., 1993); ann-c: growth cycle at which sexual maturity is first reached; #: specimen number.

Les points d'interrogation (?) indiquent les régions non préservées de l'os. Dans les cas où l'humérus est resté entièrement conservé, le rapport entre la largeur distale maximale et la largeur minimale de l'humérus (sensu Sander, 1990) est donné (hr). sc : classe de taille (d'après Sander, 1990) ; LAGs : lignes d'arrêt de croissance (selon Castanet et al., 1993) ; ann-c : cycle de croissance auquel la maturité sexuelle est atteinte pour la première fois ; # : numéro de l'échantillon.

Table 2
Observed individual variation of comparison profile parameter values in several limb elements for two adult specimens of *Neusticosaurus edwardsii* and *Serpianosaurus arlbergensis*, as retrieved from Bone Profiler (Chevalier and Laurin, 2005). O.c.: observed comparisons; n.a.: not available.

Tableau 2
Variation individuelle observée dans les valeurs paramétriques du profil de compacité, pour différents éléments de membre de deux spécimens adultes de *Neusticosaurus edwardsii* et de *Serpianosaurus arlbergensis*, estimés à l'aide du logiciel Bone Profiler (Chevalier et Laurin, 2005). O.c. : compacité observée ; n.a. : non disponible.

Specimen	Element	O.c.	S (SD)	P (SD)	Min (SD)	Max (SD)	R^2
N. edwardsii							
T3037	Humerus	0.935	0.9785578 (0.00825)	−0.3385335 (0.08381)	0.8529833 (0.07188)	0.9719088 (0.08117)	0.2103421
T3037	Radius	0.888	0.8977001 (0.00748)	0.8757331 (0.08113)	0.8000008 (0)	0.9598535 (0.08823)	0.3718287
T3037	Ulna	0.880	0.8748288 (0)	−0.8885388 (0)	0.2883865 (0)	0.9775581 (0)	0.8004791
T3037	Femur	0.858	0.287714 (n.a.)	−38.88885 (n.a.)	0.8858478 (n.a.)	0.8577488 (n.a.)	4.101188e-11
T3037	Tibia	0.898	0.8988878 (n.a.)	−1.537819 (n.a.)	0.8000008 (n.a.)	0.8981052 (n.a.)	2.820138e-12
T3037	Fibula	0.918	0.1111582 (n.a.)	−105.1377 (n.a.)	0.8000008 (n.a.)	0.9184818 (n.a.)	2.277175e-13 (n.a.)
S. arlbergensis							
T1046	Humerus	0.859	0.8535038 (0.00081)	0.848583 (0.00888)	0.8488888 (0.00882)	0.8000008 (0)	0.2715581
T1046	Radius	0.887	0.8170708 (0.00081)	0.7183157 (0.00883)	0.8828888 (0.00887)	0.8974881 (0.00885)	0.8357777
T1046	Ulna	0.885	0.8127315 (0.00081)	−0.8480758 (0.00782)	0.8800888 (0.00884)	0.8000008 (0.00887)	0.8552888
T1015	Femur	0.884	0.8887788 (0.00088)	0.1780578 (0.00783)	0.8154585 (0.00788)	0.8988858 (0.00888)	0.3842788

two null hypotheses, which state that: (1) the limb bones of the sampled pachypleurosaurids all show an equal mean compactness value; and (2) *N. edwardsii* shows no statistically significant difference in the mean compactness values between the preaxial and postaxial elements of the zeugopodial region of both the forelimbs and hind limbs. The black and white sketches were prepared using Adobe Photoshop CS3.

3. Results

3.1. Bone histology, bone compactness and skeletochronology

The medullary region is entirely filled with a calcified cartilaginous core throughout the ontogeny of all pachypleurosaurids. In ontogenetically young pachypleurosaurids, primary endosteal bony infillings of the vascular canals and a few secondary trabeculae are preserved in the calcified cartilaginous core. Throughout ontogeny, secondary endosteal bony deposits progressively increase in all pachypleurosaurids (i.e. increased remodelling). Accordingly, the vascular canals are secondarily widened by resorption of the primary infillings, as well as of parts of the surrounding calcified cartilage. Subsequently, secondary deposition takes place (Fig. 2). These secondary endosteal infillings of vascular canals are similar to secondary osteons, which are usually found in bone tissue (Francillon-Vieillot et al., 1990), but are here surrounded by the calcified cartilage matrix. These remodelling processes (i.e. secondary endosteal infillings of the vascular canals and secondary trabeculae) are found only in the diaphyseal regions of the long bones in younger individuals, but progressively increase in abundance towards the epiphyseal regions in older specimens.

In both pachypleurosaurid genera, the LAGs are distinct in contrast to the growth zones and annuli, which in some cases change in thickness throughout the ontogeny of an individual (Fig. 3B–E, Fig. 4E–F'). All the pachypleurosaurids show minor or no remodelling of the innermost wall of the cortex. The highest grades of remodelling occur within *N. pusillus* and *N. peyeri*, but even in these species only parts of the innermost periosteal bone layer are affected and therefore, the growth record can be entirely reconstructed.

The studied pachypleurosaurids show two bone tissue types in the cortex of their long bones; each is differently vascularized, contains a different quantity and shape of osteocyte lacunae, as well as shows a different birefringence based on the alignment of the crystallites (Ghiasher and Muir, 1994). The innermost bone layers are composed of a mixture of woven-fibered bone tissue and parallel-fibered bone tissue (wp; Figs. 2, 3C–D, 4G–H), whereas a lamellar-zonal bone tissue type is found in the outer, more peripheral part of the cortex. The innermost bone layer (wp) is visible as an opaque zone in polarized light showing a high quantity of round osteocyte lacunae (Fig. 3D).

The stylopodial elements of both the forelimbs and hind limbs of pachypleurosaurids show constant and high compactness, as shown by compactness profiles (Table 2). The zeugopodial elements of all pachypleurosaurids, in contrast, show more and also larger erosion cavities in the medullary region. The amount of vascularization appears

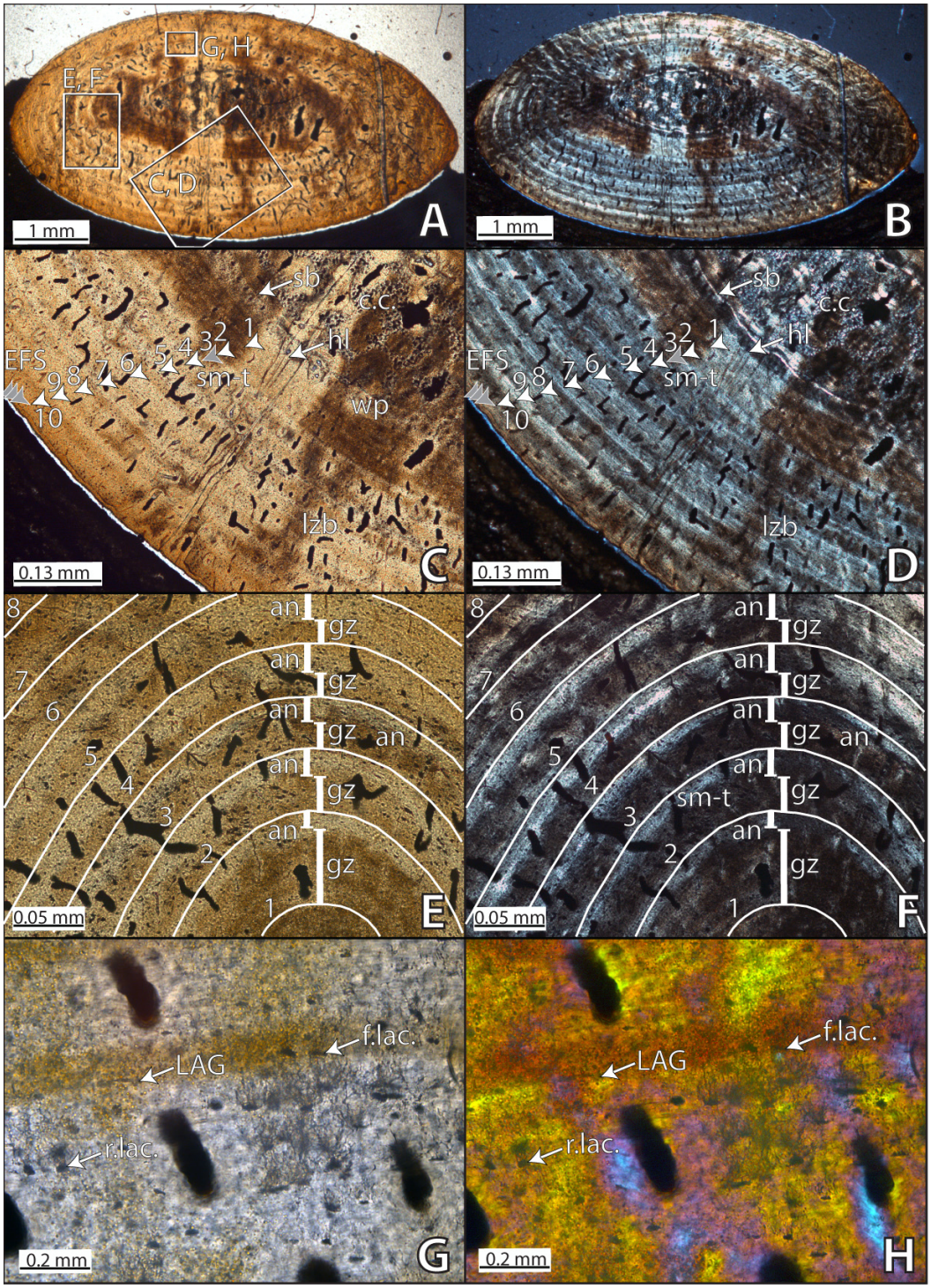

Fig. 5. Histological transverse section within humerus of a large *Serpianosaurus arigiolensis* (TE510). A, C, E, G in normal transmitted light; B, D, F in polarized light; H in polarized light and Lambda compensator. Images C and D show the sharp border (sb) between the cortex and the medullary region, the hatching line (hl) which bears the endosteal bone layer (wp), the growth cycle at second maturation (No. 3, grey arrow head) and 13 LAGs (lines of arrested growth; arrow heads). The EFS is composed of three LAGs (grey arrow heads in adjacent circles). Images E and F give a detailed look at the light and extinction pattern based on the different characteristics of the growth zones (gz) and annuli (an) within each growth cycle (enclosed by white lines). Images G and H show the different characteristics of the growth zones and annuli (birefringence, opacity and shapes of the osteocyte lacunae; flattened osteocyte lacunae; f.lac., round osteocyte lacunae; r.lac.). c.c.: calcified cartilage; wp: woven-like and grading into parallel-fibered bone.

Fig. 5. Section transversale de diaphyse de l'humérus d'un grand *Serpianosaurus arigiolensis* (TE510). A, C, E, G sont en lumière transmise normale, B, D, F en lumière polarisée, H en lumière polarisée et compensateur Lambda. Les images C et D montrent une limite nette (sb) entre le cortex et la région médullaire, la ligne hachurée (hl) qui borde le feuillet osseux endosté (wp), le cycle de croissance effectué l'année 3 maturité sexuelle (No. 3, extrémité de flèche grise) et 13 LAGs (lignes de croissance arrêtée, flèches de flèches). L'EFS est composé de trois LAGs (flèches de flèches grises dans la partie la plus extérieure du cortex). Les images E et F donnent le détail du schéma d'extinction caractéristique exhibant les caractéristiques des zones (gz) et anneaux (an) de croissance, au sein de chaque cycle de croissance, entourés de lignes blanches. Les images G et H montrent les différentes caractéristiques des zones et des anneaux de croissance (biréfringence, opacité et formes des lacunes d'ostéocyte ; lacunes d'ostéocyte aplaties ; f.lac., lacunes d'ostéocyte rondes, r.lac.). c.c. : cartilage calcifié ; wp : os à cellules dispersé passant au type 3 fibres parallèles.

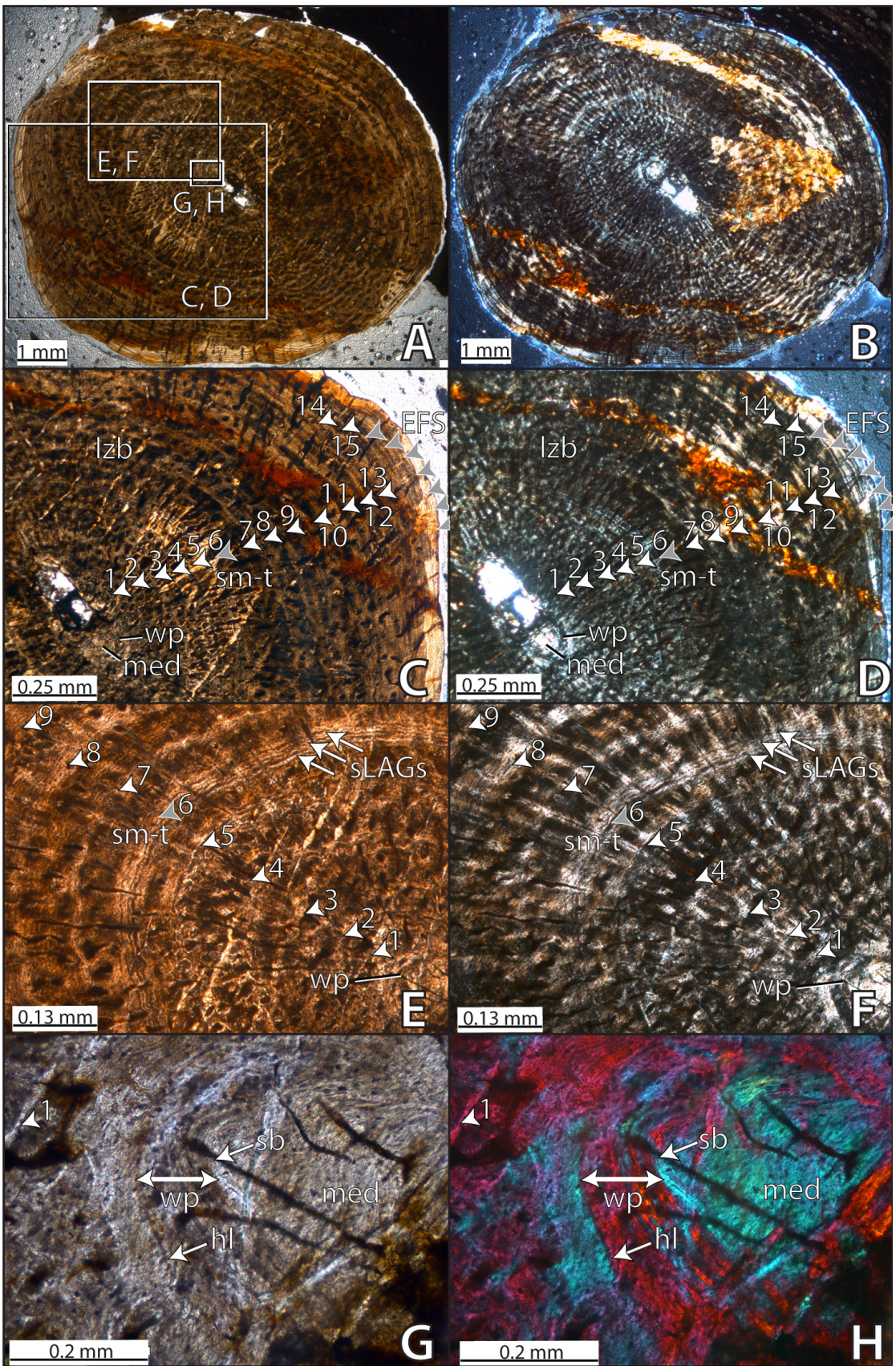

Fig. 4. Diagonal transverse sections of the humerus of a large Neanderthal male from Arbreda cave (D4077). A, C, E, G in normal transmitted light; B, D, F, H in polarized light; H is polarized light and Gamdia compensator. The calcified cartilaginous core of the medullary region (med), which is entirely replaced by secondary trabeculae, is visible in all the figure pairs, whereas the sharp border (sb) between the medullary region is shown in more detail in images G and H. Images C and D show the number of LAGs (numbered, arrow heads). Images E and F give a detailed look at the growth cycle at external periphery (No. 9, grey arrow head) which shows supernumerary LAGs (sLAGs) and no decrease in the growth cycle thickness. Images G and H show the lacunocanalicular system

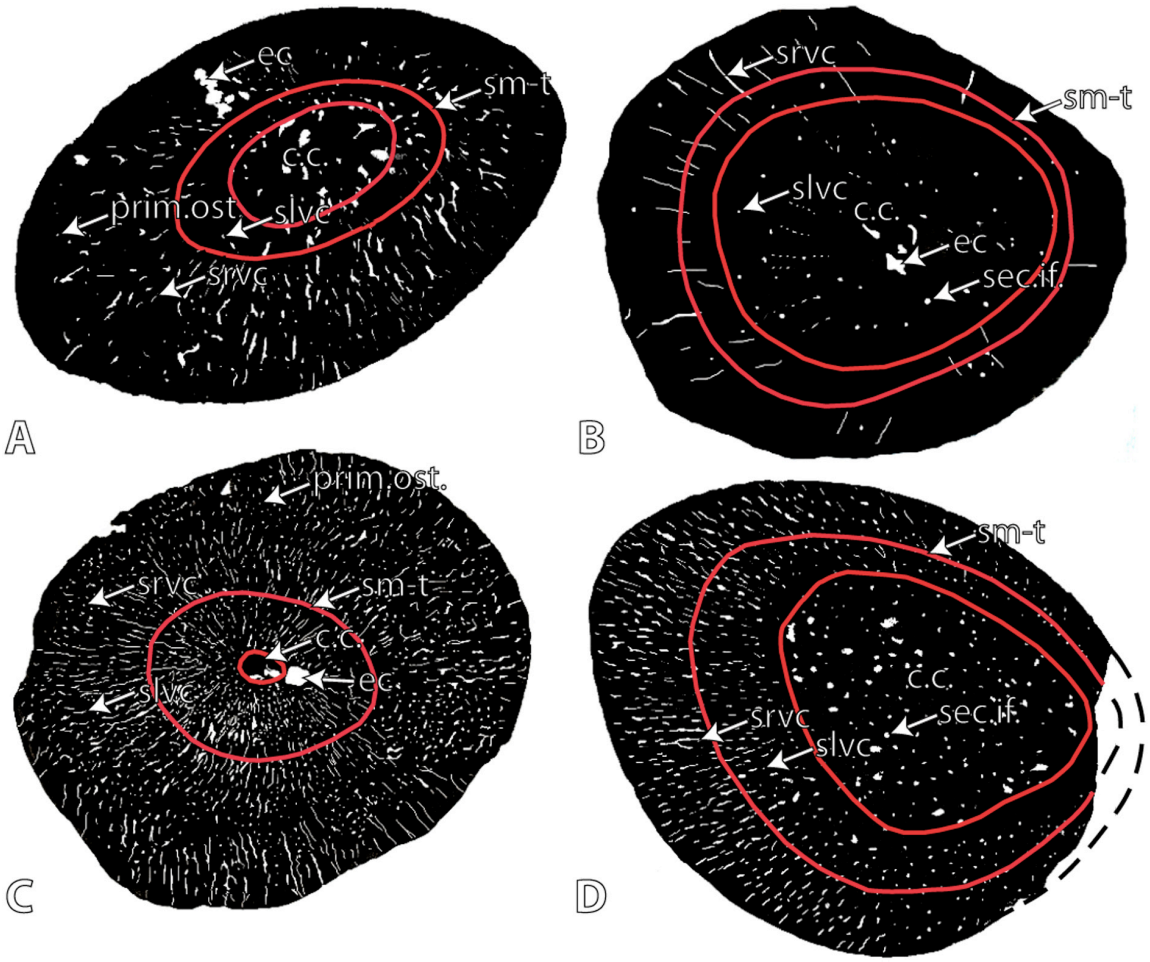

Fig. 5. Black and white sketches of the displayed transverse sections through the humerus and femur of a large-sized *Neusticosaurus edwardsii* (A: humerus, B: femur) and of a large-sized *Neusticosaurus edwardsii* (C: humerus, D: femur) for which compactness values were established with the program Inner Position (Girondot and Laurin, 2003; Table 2). Although *N. edwardsii* generally shows higher vascularization and more canal-in cavities (ec), as well as slightly lower observed compactness values, compactness curves are still close to 1.0 and remain constant at least throughout the cortex. c.c.: calcified cartilage; wpc: woven-fibered grading into parallel-fibered bone.

Fig. 5. Schémas en noir et blanc de sections transversales de diaphyse de l'humérus et du fémur d'un grand *Neusticosaurus edwardsii* (A: humérus, B: fémur) et d'un grand *Neusticosaurus edwardsii* (C: humérus, D: fémur), pour lesquelles les valeurs de compacité ont été établies à l'aide du programme Inner Position (Girondot et Laurin, 2003; Tableau 2). Bien que *N. edwardsii* présente une vascularisation plus élevée et plus de cavités d'invasion (ec), ainsi que des valeurs de compacité observées légèrement plus faibles, les courbes de compacité sont encore proches de 1,0 et restent constantes au moins au travers du cortex. c.c.: cartilage calcifié; wpc: os à cellules tissant passant au type 3 fibres parallèles.

to increase with stratigraphic age with *N. edwardsii* showing long bones with the highest degree of vascularization (Fig. 5C–D), as is also indicated by the compactness profiles (Table 2). The humerus, radius, ulna and femur show a statistically significant difference in the mean compactness between *N. edwardsii* and *S. mirigioliorum* (paired t-test, $t = 2.78$; $P < 0.05$) with the latter exhibiting slightly higher mean compactness values.

The four pachypleurosaurids differ between each other by the grade of the remodelling of the innermost periosteal bone layers of the cortex and the calcified cartilaginous core in the medullary region. They also show variation in the grade of the vascularization of the cortex, the spacing pattern of the growth cycles, the age when sexual maturity is reached, as well as in their longevities.

of the cortex, which is composed of wpc. This inner area is visible as opaque zone in polarized light with round osteocyte lacunae. c.c.: calcified cartilage; wpc: woven-fibered grading into parallel-fibered bone.

Fig. 4. Sections transversales de diaphyse de l'humérus d'un grand *Neusticosaurus edwardsii* (SMNS 807), A, C, E, G sont en lumière transmise normale; B, D, F, H en lumière polarisée; H en lumière polarisée et compensateur lambda. Le cœur cartilagineux calcifié de la zone médullaire (pmz), entièrement remplacé par des trabécules osseuses, est visible dans toutes les parties de l'échantillon, hormis que la limite entre (pb) avec la région médullaire est manquée par endroits sur les images G et H. Les images C et D montrent le nombre de LAGs (matérialisés par les têtes de flèches). Les images E et F montrent le début du cycle de croissance 3 (maturité sexuelle (flèche grise), qui présente des LAGs anormalement (flèches noires), mais pas de diminution d'épaisseur du cycle de croissance. Les images G et H montrent la région la plus interne du périoste du cortex, qui est composée de wpc. La partie interne est visible en tant que zone en lumière polarisée, avec des lacunes d'ostéocyte rondes. c.c.: cartilage calcifié; wpc: os à cellules tissant passant au type 3 fibres parallèles.

3.2. *Serpianosaurus mirigioloensis*

S. mirigioloensis specimens show highly compact limb bones except for the ulna (Table 2), which is the only limb bone exhibiting a relatively thin cortex and a larger medullary region.

The innermost region of the cortex is composed of a bone layer of wp (Fig. 3C–D), which is visible as an opaque zone in polarized light and characterized by a high quantity of round osteocyte lacunae (Fig. 3D).

Throughout ontogeny, the calcified cartilage often remains the main component in the medullary region of the long bones. Large specimens show more osseous deposits in the diaphyseal cartilaginous matrix and less towards the epiphyseal area of the medullary region. In a few large specimens, the calcified cartilaginous core is entirely replaced by secondary bone trabeculae in the diaphysis. The calcified cartilage of the medullary region generally shows a few simple vascular canals which are in some cases secondarily widened and filled with lamellar bone. On average, vascular canals of both the medullary region and cortex comprise 7% of the section area (Table 2).

The long bones reveal large parts of, or even a complete, distinct layer of endosteal lamellar bone (eb) that marks the separation between the medullary and cortical region (Fig. 3C, D) and is preserved along its entire border also at the meta- and epiphyseal regions (Fig. 6).

In *S. mirigioloensis*, the onset of sexual maturity is indicated by several microstructural changes within the corresponding growth cycles: an abrupt decrease in the growth cycle thickness (Fig. 3E–F), a change in the vascularization pattern (Fig. 5A–B), a change in thickness of the growth zones and annuli (Fig. 3E–H; see light and extinction pattern). Based on these changes, the attainment of sexual maturity is indicated between the second to fourth year in *S. mirigioloensis* specimens (Table 1; Fig. 3C–F). The largest specimen (T4510) is also the ontogenetically oldest one with 13 LAGs, therefore being in its 14th year at death. It reached sexual maturity during its second to third year (Fig. 3). T4510 developed an external fundamental system (EFS after Bicknell et al., 2001; or outer circumferential layer, [OCL] after Chinsamy-Turan, 2005) from the age of 10 years onward. The EFS is marked by closely spaced LAGs and is composed of highly organized lamellar bone.

Generally, no or only a few primary osteons and no secondary osteons are found in the cortex of adult specimens. Before sexual maturity is reached, the long bones show several simple radial and several simple longitudinal vascular canals (Fig. 3A–D; Fig. 5A–B). After sexual maturity, scattered primary osteons are displayed as well. On average of all the limb bones, the cortex is 5% less vascularized after the attainment of sexual maturity than before this event (average observed comparison before sexual maturity: 0.02).

In polarized light, the limb bones sometimes (e.g., T4510) reveal a distinct light and extinction pattern based on the different characteristics of the growth zones and the annuli within each growth cycle after the wp layers and before EFS. Although both growth zones and annuli are comprised of lamellar bone tissue, they can be differentiated by their thickness, by the alignment of the organization of the crystallites which is reflected by the birefringence (Chinsamy-Turan, 2005; Ghiorcher and Mink, 1984), as well as by the quantity and shape of osteocyte lacunae (Francillon-Vieillot et al., 1990; Fig. 3E–H). Before the attainment of sexual maturity, the growth zones are thicker, exhibit more and rounder osteocyte lacunae and are less birefringent to polarized light, whereas the annuli are narrower and reveal a decreased number of flattened osteocyte lacunae, as well as higher birefringence (Fig. 3E–F). After sexual maturity, the growth zones become narrower, contain a lower number of flattened osteocyte lacunae and more equally directed crystallites, whereas the annuli are thicker with more rounder osteocyte lacunae and less birefringent. This distinct pattern continues until the EFS is reached. However, the resulting light and extinction pattern in polarized light is often poorly visible due to the strong colonization of the bone due to diagenesis.

3.3. *Neusticosaurus pusillus* and *Neusticosaurus peyeri*

Throughout ontogeny, the calcified cartilaginous core in the medullary region of the long bones of *N. pusillus* and *N. peyeri* is only partly replaced by secondary endosteal osseous infillings (Fig. 2). Only the medullary region in the diaphysis of the humerus in large specimens becomes entirely filled with secondary trabeculae (Sander, 1990).

Sander (1990) stated that *N. pusillus* and *N. peyeri* reached sexual maturity at the age of three to four. Upon reaching sexual maturity, the growth cycles abruptly decrease in thickness. The subsequent LAGs of the third and subsequent growth cycles gradually converge before the EFS, showing an asymptotic growth curve after sexual maturity (Fig. 2; Sander, 1990). The largest specimens of *N. pusillus* studied by Sander (1990) show seven LAGs (Fig. 2) and the age of *N. peyeri* is nine to ten years (Sander, 1990).

3.4. *Neusticosaurus edwardsii*

Some long bones (humerus, tibia and fibula) of the stratigraphically youngest pachypleurosaurid, *N. edwardsii*, entirely replace the calcified cartilaginous core of the diaphyseal, metaphyseal and even parts of the epiphyseal regions with secondary trabeculae and few secondary infillings of the vascular canals. In contrast, the radius, ulna and femur always show remnants of the calcified cartilage core of various sizes in the diaphyseal, metaphyseal and epiphyseal regions (Fig. 8A–B), closely resembling the composition of the long bones of the other pachypleurosaurids. Longitudinally oriented simple vascular canals (alvc) and secondary infillings of the vascular canals dominate the medullary region (often not entirely replaced by secondary trabeculae in large specimens; Fig. 5C–D). The long bones of *N. edwardsii* reveal large parts of, or even a complete distinct layer of endosteal lamellar bone (Figs. 4A–H, 8A–B) between the cortex and the medullary region. All the long bones show one innermost bone layer of wp (Fig. 4E–H).

The preaxial elements of both the forelimbs and hind limbs are slightly more compact than the corresponding postaxial elements, but show no statistically significant dif-

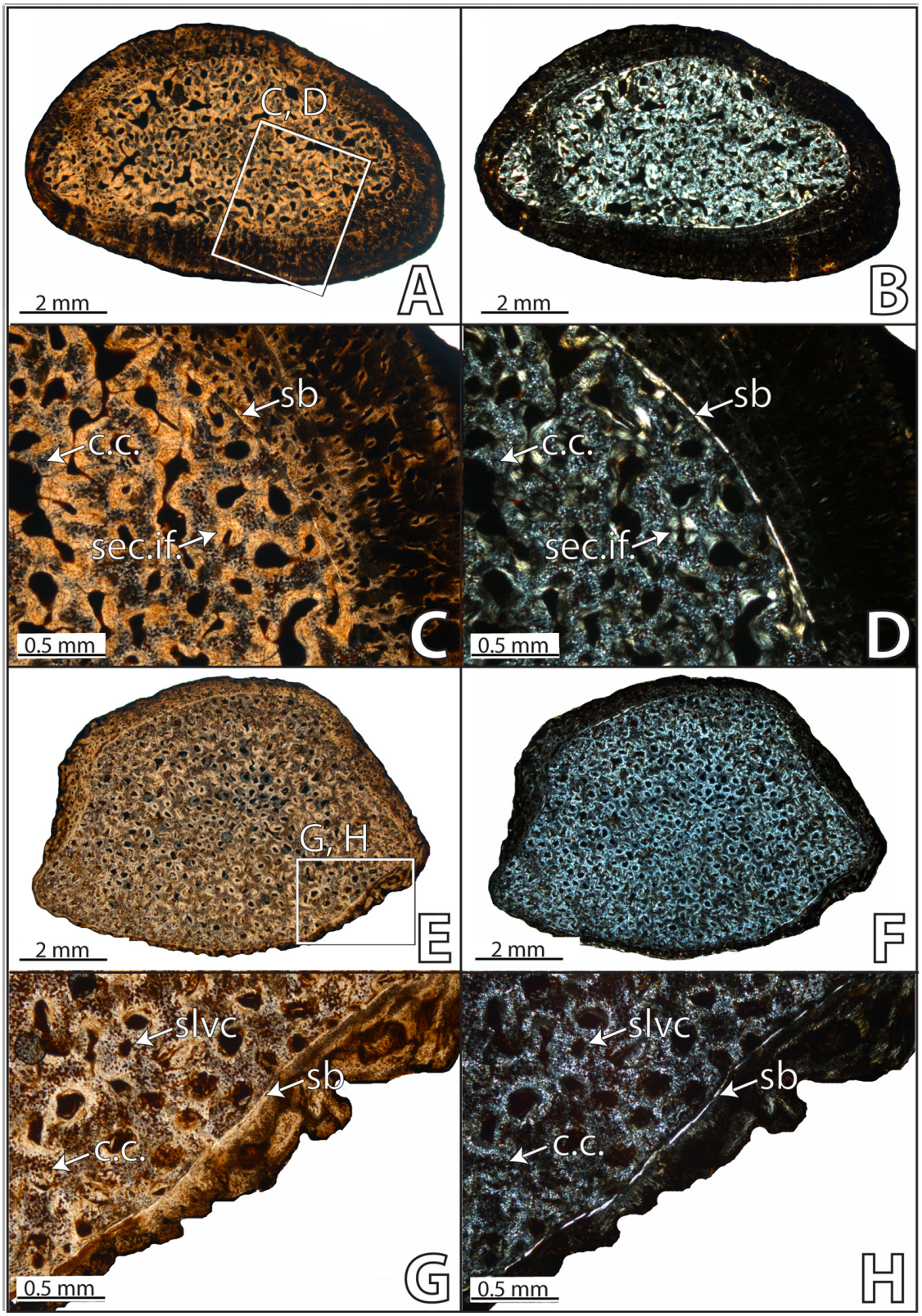

Fig. 8. Transverse sections of the femur of a large *Neusticosaurus edwardsii* (PIMUZ T 2), A, C, E, G in normal transmitted light; B, D, F, H in polarized light. Images A to D display the section through the metaphyseal region, whereas images E to H show the section through the epiphyseal region of the same individual. There is a sharp line (sb) bordering the medullary region and the cortex, which is composed of highly organized endosteal lamellar bone tissue showing high birefringence in polarized light. This sharp border is only perceived in *Serpianosaurus arlettazensis* and *N. edwardsii*. The calcified cartilage on the epiphyseal region (c.c.) differs in the presence of secondary endosteal bony deposits (sec.if.). All the vascular canals of the metaphyseal region of the c.c. are widened and secondarily filled with bone (sec.if.), whereas the c.c. of the epiphyseal region still shows simple vascular canals (slvc).

ference in the mean compactness values and therefore, the null hypothesis cannot be rejected (paired t-test, $t = 4.3$; $P > 0.05$). In the limb bones of large *N. edwardsii*, erosion cavities are more numerous in the medullary region than in the equivalent region of the other pachypleurosaurids studied.

The attainment of sexual maturity is marked by the increased presence of double lines (sensu Castanet et al., 1993) or even more LAGs in the corresponding growth cycle (Fig. 4E–F). Accordingly, a change in the vascularization (Fig. 4C–F; Fig. 5C–D), such as a higher number of arcs (simple reticular to radial vascular canals), a change in the light and extinction pattern (Fig. 4E–F), but no decrease in growth cycle thickness accompanies the onset of sexual maturity (Fig. 4C–F), contrary to what is observed in the vast majority of extant taxa. Before sexual maturity, the cortex houses a few primary osteons, several simple radial and longitudinal vascular canals (except for the humerus, Fig. 5C'). After this event, shorter arcs and a few primary osteons are found in the cortex. Overall, the vascular canals of the cortex are more regularly distributed in *N. edwardsii* than in the other Neusticosaurus taxa and *S. wrighti lenzi* (Figs. 2–5).

N. edwardsii appears to have reached sexual maturity between its fourth and seventh year (Table 1; Fig. 4C–F). The largest studied specimen of *N. edwardsii* (T3457) shows 23 growth cycles, indicating an age of 23 years (Fig. 4C–D). Sexual maturity is attained during its sixth to seventh year (Table 1; Fig. 4). The thickness of all growth cycles remains constant until the fifteenth growth cycle, time at which an EFS developed. Therefore, the EFS is the only event during the life time of *N. edwardsii* causing closely spaced LAGs.

4. Discussion

The pachypleurosaurids from Monte San Giorgio all exhibit parhyostenotherotic limb bones with growth marks throughout the entire cortex. Differences among the four species are shown in the vascularization of the cortex, as well as in the grade of remodelling processes which affect the innermost periosteal layers of the cortex and the calcified cartilaginous core. The pachypleurosaurids also differ in their life history traits, which are reflected in the spacing and light and extinction patterns of the growth cycles, as well as in the longevities and onset of sexual maturity. They all exhibit similar skeletal features when compared to those of Recent secondarily aquatic vertebrates, which live in shallow water and feed either on plants or slow moving/swimming prey (Buffrénil et al., 2010; Caseville and Laurin, 2008; Hugi and Sánchez-Villagra, unpublished; Laurin et al., 2008; Taylor, 2000). An increase in bone compactness is, in the case of the pachypleurosaurids, a result of the retention of the calcified cartilaginous core or its replacement by bony structures, as well as a result of the relatively thickened cortex.

The forelimb and hindlimb elements show similar compactness values in pachypleurosaurids, however, they vary in two aspects regarding: (1) the degree of vascularization; (2) the replacement of the calcified cartilaginous core by bony tissue in the medullary region.

The histological differences between all four pachypleurosaurid taxa might result from size differences or adaptation to different habitats or different swimming modes. However, morphological (indicator of webbing in the forelimb and hind limb morphology, neural spines and transverse processes in the tail, snout–vent lengths and pachyostosis) and new skeletochronological data, such as the spacing pattern of the growth cycles, both clearly separate *S. wrighti lenzi* and *N. edwardsii* from *N. curtilus* and *N. peyeri*. Data from sedimentary analyses support a habitat with more open marine influences for *S. wrighti lenzi*, but more restricted lagoonal habitats for *N. curtilus*, *N. peyeri* and *N. edwardsii*.

All pachypleurosaurids from Monte San Giorgio lived in a subtropical climate with rhythmic monsoons as revealed by sedimentary analyses (Röhl et al., 2001). This strong seasonal climate may have led to the formation of distinct LAGs. Lamellar-zonal bone tissue type is found in generally slow growing ectothermic reptiles as well as in vertebrates showing synchronized endogenous rhythms (Castanet et al., 1993); with the latter often being enhanced when the animals live under strong environmental cycles (i.e. seasonality: effects on food availability and reproduction cycles).

The pachypleurosaurids from Monte San Giorgio give the rare opportunity to study the complete ontogenesis from embryo to adult specimens. All preserved embryos already show an advanced degree of ossification in their entire skeleton (e.g., Hugi and Scheyer, unpublished; Sander, 1988). *S. wrighti lenzi* and *N. edwardsii*, which show no or only very little resorption of the innermost periosteal region of the cortex, always show the complete growth record and therefore, the presence of wp (caused by increased bone deposition rates) represents the ossification in this early stage of ontogenesis. Additionally, *S. wrighti lenzi* and *N. edwardsii* always show a sharp border of lamellar bone between the cortex and the medullary region (Fig. 3C, D). This line is not preserved in *N. curtilus* and *N. peyeri*, because remodelling processes affect more parts of the innermost periosteal region of the cortex in these taxa. The sharp border is not referred to as a hatchling or neonatal line, since this line is continuously preserved within the entire bone and not only in the diaphyseal region (Fig. 8). With this first bone layer of wp being identified as embryonic bone, the first LAG bordering this layer

Fig. 8. Sections transversales dans le fémur d'un grand *Neusticosaurus edwardsii* (T4752). A, C, E, G sont en lumière transmise normale ; B, D, F, H en lumière polarisée. Les images A à D présentent la section 3 (avec la région mésiodiaphysaire, tandis que les images E à H montrent la section 2 (avec la région épiphysaire du même individu). Il y a une ligne nette (sb) à la limite de la région médullaire et du cortex, qui est composée d'un tissu osseux lamellaire de l'endoste, très organisé, montrant une forte biréfringence en lumière polarisée. Cette limite nette n'est conservée que chez *Neusticosaurus wrighti lenzi* et *N. edwardsii*. Le cœur cartilagineux calcifié (c.c.) a été en partie remplacé par du tissu osseux secondaire d'endoste (sec.E). Tous les canaux vasculaires de la région mésiodiaphysaire du c.c. sont simples et accompagnent rarement d'os (sec.A), tandis que le c.c. de la région épiphysaire présente des canaux vasculaires simples (sbvc), c.c. ; cartilage calcifié ; wp : os 3 entourant directement un type 3 fibres parallèles.

represents a possible hatching line. Pairs of the wp are also very often preserved in *N. pumilus* and *N. peyeri* and, based on comparison with the histological characteristics in the other two pachypleurosaurids, are also identified as endosteal bone here.

4.1. Comparison with sauropterygians

The eosauropterygian *Nothosaurus* from Winterswijk, for example, also shows the plesiomorphic lamellar-zonal bone tissue type, but with a varying spacing pattern of growth cycles (Klein, 2010). Basal plesiosauroids often show constant growth cycle thicknesses up to a certain age, but, in contrast to the pachypleurosaurids sampled, also generally exhibit phases of less organized fibrolamellar layers between the parallel-fibered growth cycles (Klein, 2010). The lamellar-zonal bone tissue type generally results from a lower bone deposition rate, which indirectly reflects the metabolism of the animal (Castanet, 2006; Castanet et al., 1993). The frequent increase in the growth rate (i.e., presence of fibrolamellar bone tissue) might be linked to an increased metabolism, but could also be simply size-related (Cubo et al., 2005), which probably enabled at least the (basal) plesiosauroids to spread further through the colder seas as they were the only sauropterygians not restricted to the Tethys (Klein, 2010; Sieppel, 2000).

4.2. Comparison with extant lepidosaurs

Lepidosaurs are the hypothesized living sister group of the Sauropterygia (Hill, 2005; Müller, 2003). The spacing pattern of the growth cycles of the pachypleurosaurids can be compared to that of Recent Lacertilian squamates because they also show the lamellar-zonal bone tissue type (Castanet et al., 1993; Ruimilleo-Viellot et al., 1990). *N. pumilus*, *N. peyeri* and Recent terrestrial squamates show a similar spacing pattern of the growth cycles (Castanet and Baez, 1991; Castanet and Rouiller, 1985) and therefore, a similar life history (including the onset of sexual maturity) is inferred. The growth cycle thicknesses of *N. edwardsii* are the only ones that remain constant throughout the cortex until the EFS is developed; the condition closely resembling the one found in the marine iguanas. *Amblyrhynchus cristatus*, from the Galapagos Islands (Hugi and Sánchez-Villagra, unpublished). These animals are the only living Lacertilian squamates that forage exclusively in the sea (Trillmich and Trillmich, 1986). A comparison to the spacing pattern of terrestrial lizards shows that the distinct spacing pattern of constant growth cycle thicknesses of *A. crassicostatus* most possibly reflects secondary adaptation to a life in water, since it is not found in any of its terrestrial relatives (Hugi and Sánchez-Villagra, unpublished). In *A. crassicostatus*, sexual maturity is histologically indicated by the higher presence of supernumerary LAGs as well as a change in the light and extinction pattern, but neither by an abrupt decrease of growth cycle thickness nor by a change in the bone tissue type (i.e. lamellar-zonal bone tissue type is present throughout the cortex; Hugi and Sánchez-Villagra, unpublished).

Ecological data show that this histological change occurs at the time when sexual maturity is reached (Trillmich and Trillmich, 1984). According to these authors, the onset of sexual maturity in marine iguanas is reflected in a change of the behaviour in both females and males. Males start to show strong territorial behaviour including male competition to monopolise the access to females. Females, on the other hand, aggregate once a year to lay their eggs on beach sites, which are geographically separated from the normal colony sites of all marine iguanas. In both sexes, these behavioural changes start with the onset of sexual maturity (Trillmich and Trillmich, 1984). In accordance with these observations, we conclude, that sexual maturity in *N. edwardsii* was reached well before the EFS developed. According to our interpretations the cortex of all the limb bones of *N. edwardsii* is about 7% less vascularized after the onset of sexual maturity, than before this event (average observed bone compactness before sexual maturity: 0.86).

In *A. crassicostatus* the histological changes, especially the light and extinction pattern, described above might reflect the annual reproduction cycle in this species. This hypothesis is supported by slight differences of this pattern between male and female specimens, as well as by the timing when the pattern changes (Hugi and Sánchez-Villagra, unpublished). The change of the growth zones and the annuli of *A. crassicostatus* may result from the changing availability of food, climate and the associated mating behaviour, which is sex-dependent (Trillmich and Trillmich, 1984). In pachypleurosaurids, this light and extinction pattern is indicated in *S. mirigioliensis* and in *N. edwardsii*. It is either not found in the other pachypleurosaurids or simply obscured due to the strong diagenetic coalescence of the bones. *S. mirigioliensis* additionally shows a mixture of the spacing pattern between *N. pumilus* and *N. peyeri* on the one hand, and the stratigraphically youngest pachypleurosaurid *N. edwardsii* on the other. The prolonged phase of bone deposition after the onset of sexual maturity might be a result of the secondary aquatic adaptation in these rather small reptiles.

Sidne and Chernov (1992) studied the growth rates in Recent squamates and showed that large forms tend to mature well before maximum body size is reached, which appears to be the plesiomorphic reptilian condition (Castanet et al., 1988; Sander, 2000). Phylogenetic analysis confirmed that the evolutionary increase in maximum body size is accompanied by a decrease in the relative size at sexual maturity (Andrews, 1982; Sidne and Chernov, 1992). In summary, large squamates generally display a constant decrease in growth rate after sexual maturity is reached, whereas smaller ones terminate growth at sexual maturity or shortly after this event (Andrews, 1982; Sidne and Chernov, 1992). Changes in growth rate are generally reflected in the bone deposition rate and therefore, in the histology of an individual (Castanet, 1985; Horner et al., 2000; Padian et al., 2001). Small lizard taxa often display an EFS, which is developed earlier during ontogenesis and which occurs soon after sexual maturity (Ortega-Rubio et al., 1985; Zug and Rand, 1987). The early development of the EFS exactly reflects the results of the growth analysis by Andrews (1982) and Sidne and Chernov (1992). Large reptiles, in contrast, frequently increase their growth cycle thickness slightly again after this event for one or

zone growth cycles, the subsequent LAGs then align slowly and continuously closer until an EFS is developed (Castanet et al., 1988; Chinsamy et al., 1995; Chinsamy-Turan, 2005; Erickson, 2005; Hugi and Sánchez-Villagra, unpublished; Sabat, Ghosn et al., 1998). However, in both cases, the first abrupt decrease in growth cycle thickness was verified as the time when sexual maturity is reached. This first abrupt decrease in growth cycle thickness occurs in size class B in *S. mirigioletti* (Table 1) and in size class P in *N. puriliu* and *N. peyeri* (Sander, 1990). This histological change corresponds to the first appearance of sexual dimorphism in these taxa (Hoppel, 1988; Sander, 1988, 1990). The development of the EFS only occurs in larger size classes and therefore, does not coincide with the timing when sexual dimorphism is expressed for the first time (Fig. 2: T4178; size class (). The distinction between the two sexes in *S. mirigioletti*, *N. puriliu* and *N. peyeri* are clearly expressed, for example by the ratio of the maximum distal width of the humerus to the minimum width of the humerus (i.e., mid shaft width) (Sander, 1988). In Hoppel (1988) the same data were given, but the ratios were inverted, i.e., minimum width to maximum distal width of the humerus. This ratio, recorded for all four pachypleurosaurids, shows two morphotypes (summary given in Sander (1988): page 151, table 6), interpreted as sexual dimorphism between sex x and sex y. Measurements of *N. edwardsii* established from Carroll and Gaskill (1985) reveal a first occurrence of the sexual dimorphism at size class B. The histological data for the attainment of sexual maturity coincides with the timing of the first appearance of the sexual size dimorphism (Table 1). In contrast, the development of an EFS only occurs in larger specimens (Table 1) and therefore, does not indicate sexual maturity.

5. Conclusion

The four pachypleurosaurid taxa from Monte San Giorgio differ from one another to an increasing number of morphological and histological features. A comparison with the lacertilian squamates reveals a similar spacing pattern of the growth cycles in completely terrestrial members and suggests similar life history (age at sexual maturation, minimum age at death) for *N. puriliu* and *N. peyeri*. On the other hand, the spacing pattern of *N. edwardsii* resembles that of the marine iguana, *Amblyrhynchus cristatus*. *S. mirigioletti* shows a mixture between the more "terrestrial-like" spacing pattern of *N. puriliu* and *N. peyeri* and the more "aquatic-like" one of *N. edwardsii*.

Skeletochronological data of *N. edwardsii* also support similarities to the marine iguana by revealing comparable elongated phases of low bone deposition rates, prolonged longevities and a delayed sexual maturity. Histology separates the pachypleurosaurids from *A. cristatus* by the vascularization of the cortex and the retention of the calcified cartilaginous core in the medullary region. The stratigraphically youngest pachypleurosaurid, *N. edwardsii*, might be more adapted to a life in the pelagic zone compared to all the other pachypleurosaurids based on higher vascularization of the bone tissue, the more extensive replacement of the calcified cartilaginous core by cancellous deposits and based on the constant growth cycle thickness in the cortex. *S. mirigioletti* was common in marine environments with higher open sea influences, although showing a mixture of the spacing pattern of *N. edwardsii* and the other *Neusticosaurus* spp. The data of *S. mirigioletti* might reflect a less developed adaptation compared to *N. edwardsii* to a similar habitat as a result of its older stratigraphical age.

Therefore, the varying spacing pattern, the grade of the secondary replacement of the cartilaginous core and the vascularization of the cortex are assumed to be linked to different habitat preferences among pachypleurosaurids.

Our interpretations of the sexual maturity and the EFS in *N. edwardsii* appear to be different from the usual reptilian pattern. Indeed, scepticism about the interpretation of the age of sexual maturity has been expressed in the case of *N. edwardsii*, which does not show an abrupt decline in the growth cycle thickness before the EFS. However, the first appearance of sexual dimorphism in *N. edwardsii* coincides with histological change in the characteristics of the growth zones and annuli, the change in vascularization, as well as with the higher number of supernumerary LAGs.

Acknowledgements

We are thankful to Heinz Furrer who kindly gave the permission for invasive sampling and provided information on the specimens. We also would like to thank Marcus Hebelsen for precious advice on preparations and Katja Waskow for taking pictures of the *N. puriliu* and *peyeri* specimens. We are very thankful to Jennifer Botha-Brink and one anonymous reviewer for the helpful comments on the manuscript. We also would like to thank the volume editor Michel Laurin for corrections which certainly improved the manuscript. This project has been funded by the Swiss National Science Foundation grant No. 31003A_127153/1 to TMS and 31003A-113032/1 to MSS-V.

References

Andrews, R.M., 1982. Patterns of growth in reptiles. In: Gans, C., Pough, F.H. (Eds.), Biology of the Reptilia, vol. 13, Physiology B. Academic Press, London, pp. 273–320.

Buffrénil de, V., Castanet, J., 2000. Age estimation by skeletochronology in the site monitor (*Varanus albigularis*), a highly exploited species. J. Herpetol. 34 (3), 414–424.

Buffrénil de, V., Mazin, J.M., 1990. Bone histology of the Ichthyosaurus *Grippia* (Reptilia: Ichthyosauria) and the problem of polyostosis in aquatic tetrapods. Hista, Biol. 3, 311–322.

Buffrénil de, V., Canoville, A., D'Anatasio, R., Dyoning, D.P., 2010. Evolution of the bone pachyostosis, a model-case for the study of bone structure in aquatic tetrapods. J. Morphol. Biol. 17 (2), 101–108.

Canoville, A., Laurin, M., 2009. Microanatomical diversity of the humerus and lifestyle in lissamphibians. Acta Zool.-Stockholm 90, 110–122.

Canoville, A., Laurin, M., 2010. Evolution of humeral microanatomy and lifestyle in amniotes, and some comments on paleobiological interferences. Biol. J. Linn. Soc. 100, 384–406.

Carroll, R., Gaskill, P., 1985. The nothosaur Pachypleurosaurus and the origin of plesiosaurs. Philos. T. Roy. Soc. London, B Biol. Sci. 309 (1139), 343–393.

Castanet, J., 1985. La squelettochronologie chez les reptiles. I. Résultats expérimentaux sur la signification des marques de croissance squelettiques chez les lézards et les tortues. Ann. Sci. Nat. Zool. Paris 7, 23–40.

Castanet, J., 2008. Time-recording in bone microstructures of endothermic animals; functional relationships. C. R. Palevol 5, 929–938.

Castanet, J., Rage, M., 1981, Adaptation and evolution in Cretaceous lizards from the Canary Islands: age, growth, maturity and longevity, Amphibia-Reptilia 12, 81–102.

Castanet, J., Meunier, G., 1985, La squelettochronologie chez les reptiles. II. Identification expérimentale sur la signification des marques de croissance squelettiques chez les serpents, Remarques sur la croissance et la longévité de la vipère aspic, Ann. Sci. Nat. Zool., Paris 7, 41–62.

Castanet, J., Newman, R.G., Sobel-Simon, H., 1988, Skeletochronological data on the growth, age, and population structure of the Tuatara, Sphenodon punctatus, on Stephens and Lady Alice Islands, New Zealand, Herpetologica 44, 25–37.

Castanet, J., Rozenblut-Viellot, B., Meunier, F.J., de Ricqlès, A.J., 1993, Bone and individual aging, In: Hall, B.K. (Ed.), Bone, vol.7, Bone Growth–B, CRC Press, Boca Raton, Florida, pp. 245–283.

Chinsamy, A., Hurum son, S.A., Hein, R.M., Scelzi, M., 1995, Skeletochronological assessment of age in Anguimorph skeletal, a nonlyrid lizard living in an ecotonal environment, J. Herpetol. 29 (3), 457–468.

Chinsamy-Turan, A., 2005, The Microstructure of Dinosaur Bone; Deciphering Biology with Fine-Scale Techniques, The Johns Hopkins University Press, Baltimore and London, 195 p.

Cubo, J., Ponton, F., Laurin, M., Margerie de, R., Castanet, J., 2005, Phylogenetic signal in bone microstructure of sauropsids, Syst. Biol. 54, 562–574.

de Ricqlès, A.J., 1978, On bone histology of fossil and living reptiles, with comments on its functional and evolutionary significance, In: de Buffrénil, A., Dor, C.R. (Eds.), Morphology and Biology of Reptiles, Linnean Society Symposium, Series 3, Academic press, London, pp. 123–150.

de Ricqlès, A.J., Buffrénil, V. de, 2001, Bone histology, heterochronies and the return of tetrapods to life in water; where are we?, In: Mazin, J.M., Buffrénil, V. de (Eds.), Secondary Adaptation of Tetrapods to Life in Water, Proceedings of the International Meeting Poitiers, 2000, Verlag Dr Friedrich Pfeil, München, pp. 289–310.

Erickson, G.M., 2005, Assessing dinosaur growth patterns: a microscopic revelation, Trends Ecol. Evol. 20 (12), 677–684.

Erickson, G.M., Rogers, K.C., Yerkovich, B.J., Norell, M.A., Xu, X., 2007, Growth patterns in brooding dinosaurs reveal the timing of sexual maturity in non-avian dinosaurs and genesis of the avian condition, Biol. Lett. 3, 558–561.

Rieppel, O., 1985, The Kalkschieferzone (Upper Middle Ladinian) near Meride (Canton Ticino, southern Switzerland) and the evolution of a Middle Triassic lagoonal/lagoon fauna, Eclogae Geol. Helv. 78 (3), 837–852.

Francillon-Viellot, H., de Buffrénil, V., Castanet, J., Géraudie, J., Meunier, F.J., Sire, J.Y., Zylberberg, L., de Ricqlès, A.J., 1990, Microstructure and mineralization of vertebrate skeletal tissues, Chapter 20, In: Carter, J.G. (Ed.), Skeletal Biomineralization: Patterns, Processes, Evolutionary Trends, vol.1, Van Nostrand Reinhold, New York, pp. 471–530.

Germain, D., Laurin, M., 2005, Microanatomy of the radius and lifestyle in amniotes (Vertebrata, Tetrapoda), Zool. Scr. 34, 335–350.

Girondot, M., Laurin, M., 2003, Bone profiler: a tool to quantify, model, and statistically compare bone-section compactness profiles, J. Vert. Paleontol. 23 (2), 458–461.

Gilmour, M.J., Meek, H., 1994, Recent studies of the mineral phase in bone and its possible linkage to the organic matrix by protein-bound phosphate bonds [and Discussion], Philos. T. Roy. Soc. London B 304 (1121), 479–508.

Hill, R.V., 2005, Integration of morphological data sets for phylogenetic analysis of Amniota: the importance of integumentary characters and increased taxonomic sampling, Syst. Biol. 54 (4), 530–547.

Houssaye, A.L., de Ricqlès, A.J., Pellas, E., 2010, Long bone histology of the Late Jurassic dinosaur Allosaurus: a preliminary; growth dynamics and physiology based on an ontogenetic series of skeletal elements, J. Vert. Paleontol. 30, 115–128.

Houssaye, A.L., Pellas, E., de Ricqlès, A.J., 2011, Comparative osteohistology of some cartilaginous and archaic actinopterygians: developmental and behavioral implications for dinosaurs, Paleobiology 37 (1), 30–58.

Klein, N., 2010, Long bone histology of Sauropterygia from the Lower Muschelkalk of the Germanic basin provides unexpected implications for phylogeny, PLoS ONE 5 (7), e11613 (doi:10.1371/journal.pone.0011613).

Laurin, M., Canoville, A., Quilhac, A., 2008, Use of paleontological and molecular data in supertrees for comparative studies; the example of lissamphibian femoral microanatomy, J. Anat. 215, 110–123.

Müller, J., 2003, Early loss and multiple return of the lower temporal arcade in diapsid reptiles, Naturwissenschaften 90, 473–476.

Rieppel, O., Hotzeldt, R., 1994, Über eine pachypleurotische Hippe aus der Kreide Libyens, Acta Zool.-Stockholm 75, 451–455.

O'Keefe, F.R., Rieppel, O., Sander, P.M., 2006, Shape disassociation and inferred heterochrony in a clade of pachypleurosaurs (Reptilia, Sauropterygia), Paleobiology 32 (4), 504–517.

Ortega-Bulnes, A., Khabbatbout, M., Sander, P., 2009, Skeletochronology in the Mesozoic lizards Xinjiangsaurus grossidens, P. Chinkaloma Acad. Sci. 73, 31–34.

Pellas, E., de Ricqlès, A.J., Bonner, J.F., 2001, Dinosaurian growth rates and bird origins, Nature 412, 405–408.

Peyer, B., 1932, B. Peyer, die Triasfauna der Tessiner Kalkalpen, V. Pachypleurosaurus edwardsii, Cocc. spec. Schw. Pal. Ab 52, 3–18.

Rieppel, O., 1998, A new pachypleurosaur (Reptilia; Sauropterygia) from the Middle Triassic of Monte San Giorgio, Switzerland, Philos. T. Roy. Soc. London Biol. Sci. 353, 1–73.

Rieppel, O., 2000, Sauropterygia I, In: Wellnhofer P. (Ed.), Encyclopedia of Paleoherpetology, vol.12A, Verlag Dr Friedrich Pfeil, München, pp. 1–134.

Rühl, H.J., Schmidt-Rühl, A., Peyer, B., Rimann, A., Carlsmann, W., Schwab, E., 2001, Mikrofossilien, gracile-natur and paleoecology of the Middle Triassic Gesteinsbitumenzone from Monte San Giorgio (Canton Ticino, Switzerland), Geol. Insubr. 6 (1), 1–13.

Ruthchild, B.M., Storrs, G.W., 2003, Decomposition sequence in plesiosaurs (Sauropterygia; Reptilia), J. Vert. Paleontol. 23 (2), 334–338.

Saint-Girons, H., Castanet, J., Bonnin-Low, S.D., Bonnin, J.P., 1980, Différences composée de deux populations françaises de Lacerta viridis (Laurenti, 1768), Rev. Ecol. (Terre Vie) 44, 381–386.

Sander, P.M., 1988, A fossil reptile embryo from the Middle Triassic of the Alps, Science 239 (4841), 780–783.

Sander, P.M., 1989, The pachypleurosaurids (Reptilia: Nothosauroidea) from the Middle Triassic of Monte San Giorgio (Switzerland) with the description of a new species, Philos. T. Roy. Soc. London B. Biol. Sci. 325 (1228).

Sander, P.M., 1990, Skeletochronology in the small Triassic reptile Neusticosaurus, Ann. Sci. Nat. Zool., Paris 11 (13e Série), 213–217.

Sander, P.M., 2000, Longbone histology of the Triassic sauropods; implications for growth and biology, Paleobiology 26 (3), 466–488.

Scheyer, T.M., Sánchez-Villagra, M.R., 2007, Carapace bone histology in the giant pleurodiran turtle Stupendemys geographicus: phylogeny and function, Acta Palaeontol. Pol. 52, 137–154.

Shine, R., Charnov, E.L., 1992, Patterns of survival, growth, and maturation in snakes and lizards, Am. Nat. 139 (6), 1257–1269.

Taylor, M.A., 2000, Functional significance of bone ballast in the evolution of buoyancy control strategies by aquatic tetrapods, Hist. Biol. 14, 15–31.

Tillerich, R., Tillerich, E.G.E., 1984, The scaling systems of pleurodont and acrodont lizards; convergent evolution of polygyny, Biol. J. Lin. Soc. 21, 209–216.

Tillerich, E.G.E., Tillerich, R., 1989, Ranging strategies of the acrodont lizards, Amblyrhynchus cristatus, Belize, Biol. Sociobiol. 18 (4), 259–269.

Wenzhong, L., Hugi, J., Müller, J., Sánchez-Villagra, M.R., 2008, Endochondral ossification of Sinopterus singlehsieni (Sclerodactylus, Pterosauria, Diapsida) and patterns of basic developmental, Rev. Paleobiol. 338 (11), 2770–2788.

Zangerl, R., 1935, B. Peyer, die Triasfauna der Tessiner Kalkalpen, IX. Pachypleurosaurus edwardsii, Comollia, Schw. Pal. Ab. 58, 1–88.

Zug, G.R., Reed, A.S., 1997, Estimation of age in nesting female Agassiz's iguanas: testing skeletochronology in a tropical lizard, Amphibia-Reptilia 8, 237–250.

Chapter 6:

The long bone histology of *Ceresiosaurus* (Sauropterygia, Reptilia) in comparison to other eosauropterygians from the Middle Triassic of Monte San Giorgio (Switzerland/Italy)

Jasmina Hugi

Submitted to *Swiss Journal of Paleontology*

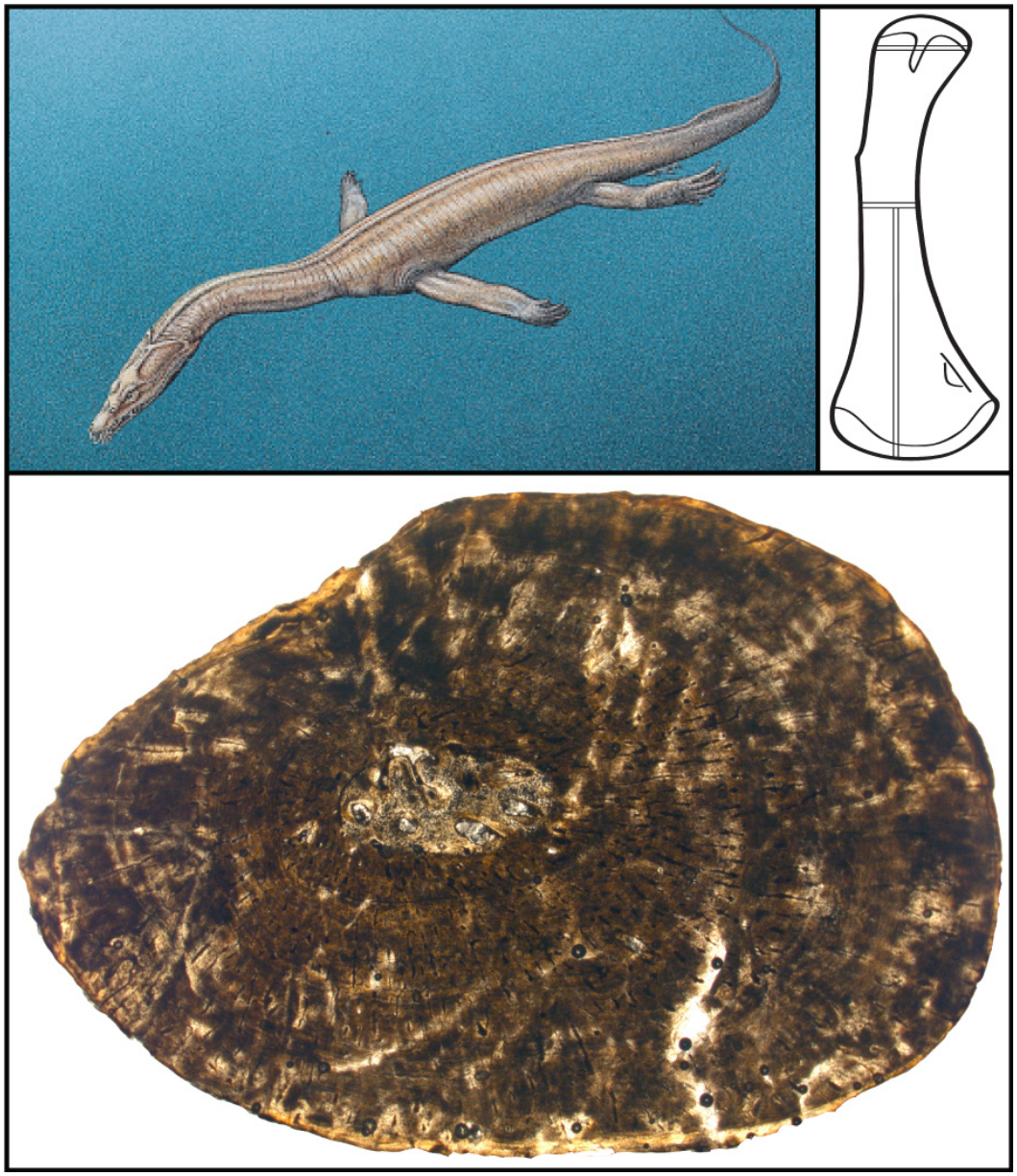

Drawing upper left: B. Scheffold
Drawing upper right and photograph: J. Hugi

The long bone histology of *Ceresiosaurus* (Sauropterygia, Reptilia) in comparison to other eosauropterygians from the Middle Triassic of Monte San Giorgio (Switzerland/Italy)

JASMINA HUGI

Paleontological Institute and Museum, University Zurich, Karl-Schmid Straße 4, 8006 Zurich, Switzerland. jasmina.hugi@pim.uzh.ch, Tel. +41-44 634 23 47, Fax +41-44 634 49 23

Abstract

Ceresiosaurus is a secondarily marine eureptile that lived during the Middle Triassic (Ladinian-Anisian) in a subtropical lagoonal environment with varying open marine influences. The genus comprises two species, *Ceresiosaurus calcagnii* and *C. lanzi*, and represents one of the largest vertebrate known from the UNESCO World Heritage Site Monte San Giorgio, which is settled along the Suisse-Italian border. Earlier morphological studies identified this genus as basal sauropterygian that largely resembles the plesiomorphic terrestrial condition, but also indicated an evolutionary trend between the two species by ascribing two locomotion types for each of them (axial vs. paraxial). Histological results showed that both species retain a calcified cartilaginous core in the medullary region in at least young individuals. *Ceresiosaurus* exhibits cyclical bone growth with undulating incremental growth marks and a lamellar-zonal bone type. The vascularisation of the cortex is dominated by longitudinally and radially orientated simple vascular canals and primary osteons. Data indicate low bone deposition rates which are locally slightly increased with loosely packed parallel-fibered bone tissue and a higher amount of longitudinal vascular canals in young ontogenetic stages. Intraspecific variation comprises differences in the vascularisation and growth pattern. The cortex of the rib of *C. lanzi* is vascularised with larger, longitudinally orientated simple vascular canals and primary osteons in a higher amount of loosely packed parallel-fibered bone matrix, whereas the bone samples of *C. calcagnii* show a higher amount of radially orientated primary osteons and simple vascular canals in a predominantly lamellar bone matrix. The differences in the vascularisation pattern and bone matrix might be linked to a more pelagic mode of life within the restricted lagoonal basin for *C. lanzi*, which has also been indicated by earlier studies on the morphology.

Key words: Eosauropterygia, Switzerland/Italy, Triassic, bone histology, lifestyle

Introduction

Sediments of the Middle Triassic of Monte San Giorgio, a UNESCO World Heritage Site located along the Swiss and Italian border have yielded eight excellently preserved specimens of a rather large secondarily aquatic eureptile with the genus name *Ceresiosaurus*, 'the lizard of Lugano' (Peyer 1931, 1932). The genus *Ceresiosaurus* comprises different ontogenetic stages of two species, *C. calcagnii* PEYER (Peyer 1931) and *C. lanzi* HÄNNI (Hänni 2004), which are both known from the Lower Meride Limestone (Peyer 1931; Bürgin et al. 1989; Furrer 1995; Hänni 2004). *C. calcagnii* has been found in the Cava superiore and Cava inferiore beds, whereas *C. lanzi* has been preserved only in the stratigraphically younger Cassina beds (Peyer 1931; Bürgin et al. 1989; Furrer 1995; Hänni 2004). *Ceresiosaurus* spp. are basal sauropterygians (e.g., Rieppel 2000; Müller et al. 2010) that lived in subtropical marine environments of the Tethys (e.g., Parrish et al. 1982; Röhl et al. 2001). Facies analyses revealed an increasing restriction of the basin during the sedimentation of Cava superiore, Cava inferiore beds and Cassina beds (e.g., Parrish et al. 1982; Röhl et al. 2001). Morphological differences studied by Hänni (2004) accredited a possible evolutionary trend of two locomotion types between each species. The stratigraphically older *C. calcagnii* is described as an axial to paraxial swimmer based on a massiv pectoral girdle, a long tail with high neural arches in the anterior caudal vertebrae, and pachyostosis in the ribs of the trunk. The adult morphology of the stratigraphically younger *C. lanzi* was proposed to be adapted to a more pelagic environment based on the development of a paraxial locomotion, which is indicated by the absence of pachyostotic ribs of the trunk, a shorter tail with vertebrae without high neural arches (Hänni 2004). The investigation of the morphology of the microstructure of the bone might reveal further information on different modes of life in these two species.

Bone histology is a comparative approach to study the life history of extant and extinct vertebrates. It is based on the individual's growth record and can indicate the life history by reflecting function (e.g., locomotion), ecology (e.g., habitat) and/or phylogeny (e.g., Castanet et al. 1993; Wiffen et al. 1995; Sheldon 1997; Klein 2010; Scheyer et al. 2010). Changes in the microstructure of the bones of secondarily aquatic vertebrates, compared to their terrestrial relatives, are either achieved by increasing or decreasing the bone density (e.g., Buffrénil and Schoevaert 1988, Ricqlès 1989; Ricqlès and Buffrénil 2001; Houssaye 2010). Tetrapods which secondarily adapted to shallow marine environments often show very dense long bones (Ricqlès and Buffrénil 2001) in which they are considered to play the functional role of ballast for hydrostatic regulation of the body trim (Taylor 2000). An increased bone density can be achieved by the inhibition of resorption processes and/or a continuous deposition of primary bone material along the outer wall of the cortex that leads to a hyperplasy of the cortex (i.e., pachyostosis). Pachyostosis is also visible from external view as already observed in the ribs of *C. calcagnii*. The internal bone structure can reveal higher bone density by an incomplete endochondral ossification (i.e., retention of a calcified cartilaginous core in the medullary region) and/or by remodelling processes of the medullary cavity (i.e., osteosclerosis; after Ricqlès and Buffrénil 2001; Houssaye 2010). The combination of pachyostosis and osteosclerosis is summarised as

pachyosteosclerosis, which has been noted for "*Ceresiosaurus"* by Ricqlès and Buffrénil (2001) without further specific or histological information. Secondarily aquatic tetrapod taxa that live in a pelagic environment, as exemplified for example by extant cetaceans (e.g., Buffrénil and Schoevaert 1988) and extinct ichthyosaurs (e.g., Buffrénil and Mazin 1990; Kolb et al. 2011), often display an osteoporotic-like condition that corresponds to an inner reduction in bone volume due to a higher primary vascularisation and/or more remodelling processes in the cortex (Ricqlès and Buffrénil 2001). In some cases, osteoporotic-like bones are observed in adult individuals, whereas younger ontogenetic stages show (pachy)osteosclerosis (Wiffen et al., 1995; Krahl et al. 2009; Klein 2010). Another histological feature that might be linked to open marine environments in sauropterygians is the predominant presence of fibrolamellar bone which is a result of fast bone deposition rates and hence, hypothesised to be as indicator for increased metabolic rates (Ray et al. 2004; Ricqlès et al. 2008; Stein and Langer 2009). Among Sauropterygia, fibrolamellar bone has been found in *Nothosaurus,* the pachypleurosaurid *Anarosaurus heterodontus*, as well as in basal and derived pistosauroids (e.g., Wiffen et al. 1995; Krahl et al. 2009; Klein 2010). A recent study on the bone histology in eosauropterygians pushes the origin of fibrolamellar bone in Sauropterygia back to the early Middle Triassic (early Anisian) with abundant fibrolamellar bone throughout the cortex in *A. heterodontus* and *Cymatosaurus* and irregular deposition of fibrolamellar bone in *Nothosaurus* (Klein 2010).

The phylogenetic interrelationships of *Ceresiosaurus* and closely related sister taxa (*Lariosaurus* and *Silvestrosaurus*) changed several times and the synonymy of *Ceresiosaurus* and *Lariosaurus* still is debated (Sues 1987; Storrs 1993; Rieppel 1998; Hänni 2004). *Ceresiosaurus*, *Lariosaurus* and *Silvestrosaurus* form together the monophyletic Lariosauridae (Rieppel 2000). The relationship between the Lariosauridae as the sister group of the Nothosauridae which together represent the group Nothosauria is consistent (Sues 1987; Storrs 1993; Rieppel 1999, 2000; Hänni 2004). Nothosauria further are regarded to be the sister group of the Pachypleurosauria (after Rieppel 1999, 2000), which are preserved in sediments from Monte San Giorgio in high quality and quantity (Carroll and Gaskill 1985; Sander 1989; Rieppel 1989). Histology could be a complementary method for testing the phylogeny or a potential synonymy of *Ceresiosaurus* and *Lariosaurus*. However, *Lariosaurus* long bones are even more rarely preserved than equivalent *Ceresiosaurus* specimens and hence, have not been accessible for invasive thin-sectioning.

In this study, detailed data on the microstructure of the long bones is given for the rare material of the genus *Ceresiosaurus* for putting the findings in a paleoecological and phylogenetic context with comparison to *Nothosaurus* and the pachypleurosaurids from Monte San Giorgio.

Material and Methods

Five isolated long bones of three specimens of *Ceresiosaurus* were used for thin-sectioning (Table 1). One element is assigned to *C. lanzi* and two belong to *C. calcagnii*, whereas the rest is of uncertain species relationship (Table 1). The material which was available for processing into thin sections is all housed in the Paleontological Institute of the University of

specimen	element	Length/diameter
C. lanzi		
T5454	Rib	12.3cm/0.7cm
C. calcagnii		
T5153 (belongs to T5152	Rib	?/0.6cm
T5152	Tibia	?/0.9cm
T5622	Femur	6.5cm/0.7cm
T5622	Rib	9.7cm/0.6cm
S. mirigiolensis		
T105	Femur	2.4cm/0.4cm
N. edwardsii		
T3437	Femur	8.3cm/0.9cm
Nothosaurus		
AIII 0001	Femur	20.7cm/5.2cm

Table 1. Bone compactness parameters of a sample of eosauropterygians from Monte San Giorgio. Question marks indicate that the bone sample is not entirely preserved.

Zurich (PIMUZ). Thin-sections of the mid-shaft region of the long bones were processed and documented at the PIMUZ, following standard petrographic preparation techniques (e.g., Chinsamy and Rath 1992). The diaphyseal region of the long bones is known to yield the strongest ecological signal (Canoville and Laurin, 2010) and generally preserves the most complete growth record of the bones among vertebrates (Francillon-Vieillot et al. 1990). Histological data comprise the description of bone tissues of the long bones based on the amount of vascularisation and orientation of the crystallites of each individual. The bone density was also quantitatively analysed (Table 2) using the PC Version of the program Bone Profiler (Girondot and Laurin 2003). The images were prepared using Adobe Photoshop CS3 and Adobe Illustrator CS3.

Histological abbreviations
cc: calcified cartilaginous core
co: cortex
efs: external fundamental system
flb: fibrolamellar bone
lzb: lamellar-zonal bone
pfb: parallel-fibered bone
po: primary osteon
ed.: endosteal infilling of vascular canals in the medullary region
med: medullary region
lags: lines of arrested growth
lb: lamellar bone
svc: simple primary vascular canals
wb: embryonic woven-fibered bone

Results

Long bone histology of *Ceresiosaurus*

Ceresiosaurus shows the plesiomorphic lamellar-zonal bone type in the cortex of the long bones. The vascularisation of the cortex mainly comprises simple radial and longitudinal vascular canals, as well as primary osteons of the same orientation. The growth cycles are regularly distributed with a constant spacing pattern and consist of undulating bone layers that are bordered by lags which are in some cases subannually deposited (i.e., supernumerary lags; Zug and Rand 1987). One layer of embryonic woven-fibered bone is

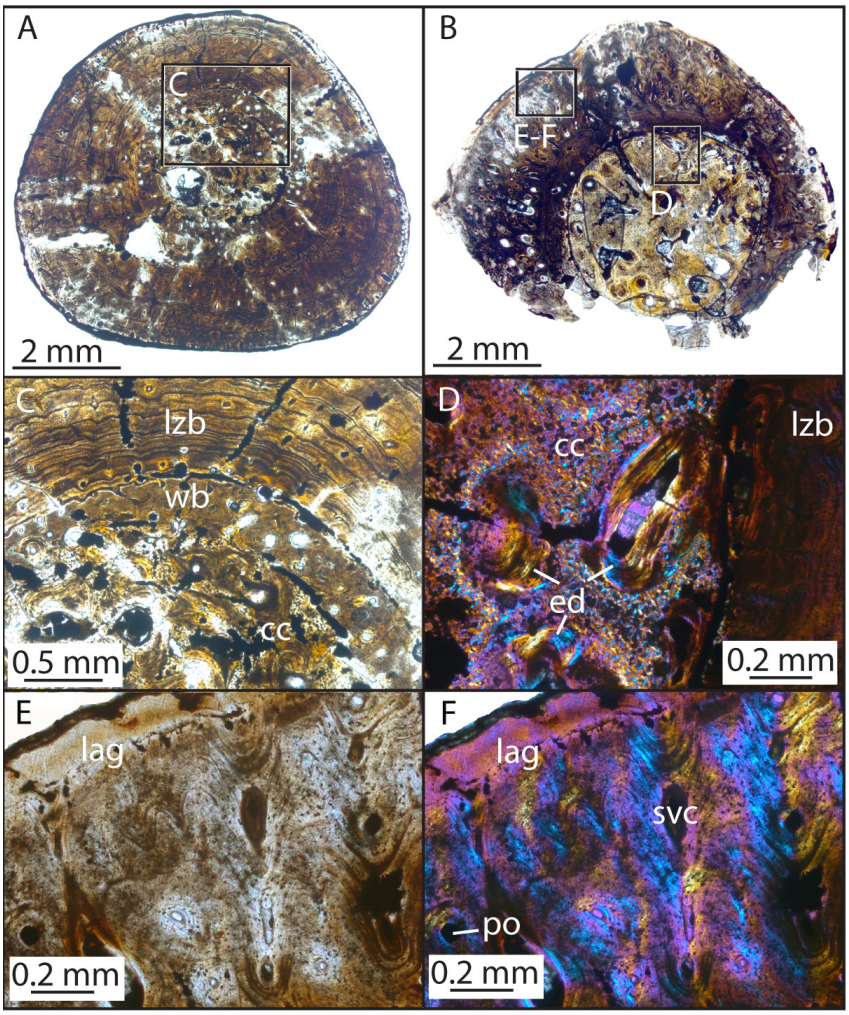

Fig. 1. The microstructure of the long bones of *Ceresiosaurus*. Transverse mid shaft section of A: the pachyosteosclerotic femur of *C. calcagnii* (T5622) and B: the osteosclerotic trunk rib of *C. lanzi* (T5454). C: The inner periosteal cortical region comprises a layer of embryonic bone that is composed of woven-fibered bone (wb). The cortex is of thick lamellar-zonal bone type (lzb) with undulating growth zones, annuli and lags. D: the medullary cavity is filled with a calcified cartilaginous core (cc) that is remodelled by resorption and endosteal bone deposition processes (ed). E and F: magnification of the lzb of *C. lanzi* showing the funnel-shaped arrangement of the cristallites around the vascular canals in normal light (svc: simple vascular canal; po: primary osteon) and polarised light with lambda compensator.

deposited as the innermost cortical region in the limb bone samples adjacent to the calcified cartilaginous core, whereas the rib samples exhibit no comparable inner layer. The layer of woven-fibered bone is opaque in polarised light and characterised by a high quantity of simple longitudinal primary vascular canals and round osteocyte lacunae. The innermost periosteal growth layers are entirely preserved as no or only minor resorption occurs along the border between the cortex and the medullary region (Fig. 1). In all long bones of *Ceresiosaurus*, the medullary region is entirely filled with a matrix of calcified cartilage that persists as the main component in at least juvenile to subadult individuals (Fig. 1). All samples show resorption processes in the calcified cartilage which are either erosion cavities or widened simple vascular canals that are refilled with centripetally deposited endosteal lamellar bone layers (Fig. 1). Compactness values show high and constant compactness profiles based on the persistence of the calcified cartilaginous core and minor remodelling of the inner wall of the cortex (Table 2). None of the bone samples shows an indicator that sexual maturity (i.e., a change in the bone tissue, thickness of the growth cycles after Castanet et al. 1993) was reached or that the growth of an individual was terminated (efs sensu Horner et al. 2001).

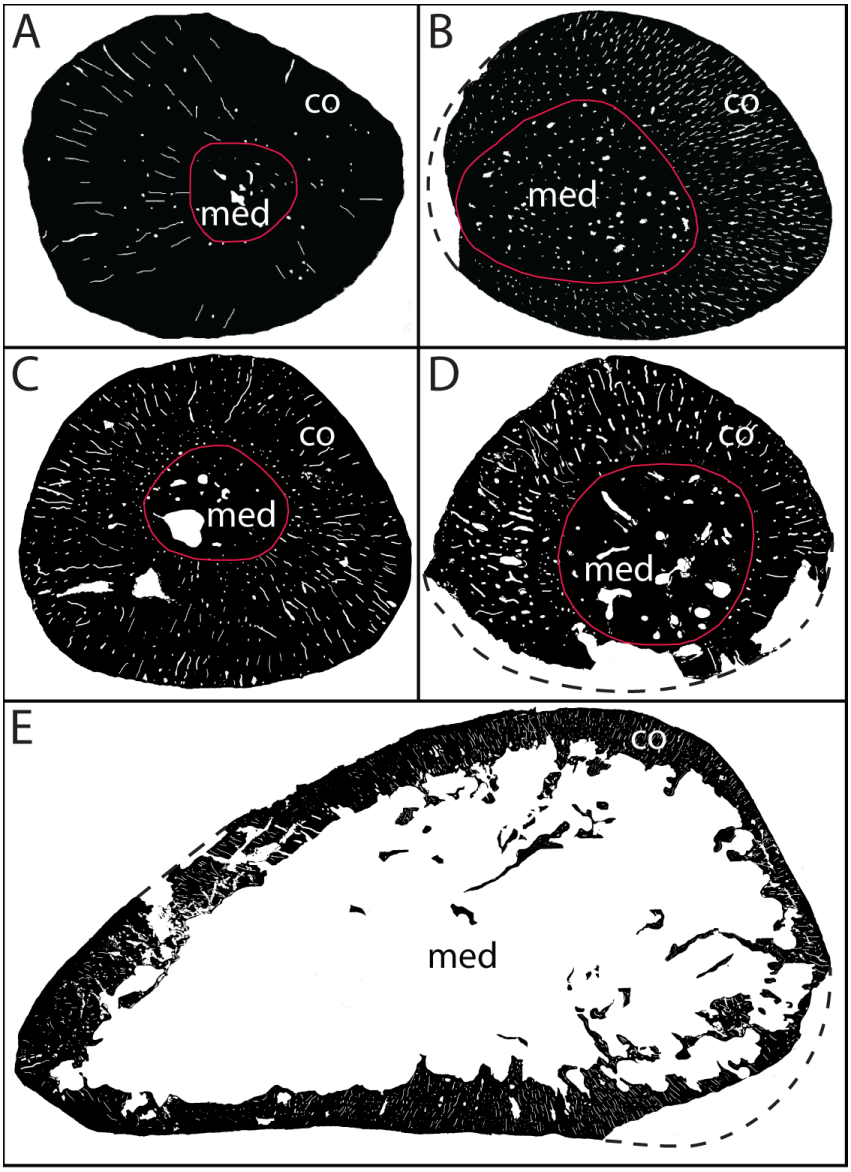

Fig. 2. Black and white sketches of the transverse mid shaft sections of the femur of sauropterygians from Monte San Giorgio. A: *Serpianosaurus mirigiolensis* (T105), B: *Neusticosaurus edwardsii* (T3437), C: *Ceresiosaurus calcagnii* (T5622), D: *Ceresiosaurus lanzi* (T5454), E: *Nothosaurus* (AIII 0001). Compactness values are given in Table 1. Stippled line: reconstructed outline of the outer wall of the cortex (co); red line: outline of the medullary region (med).

Differences in the bone samples that could have been assigned to species level are expressed through: variation in the 1) growth pattern (i.e., bone matrix) and in the 2) vascularisation of the cortex; *C. calcagnii* shows a rather thick cortex of predominantly lamellar bone matrix contrary to the thiner cortex with a relatively large medullary region of *C. lanzi* of approximately equivalent ontogenetic age (Figs. 1, 2). The stratigraphically older *C. calcagnii* predominantly shows long, radial simple vascular canals and primary osteons and less longitudinally orientated ones, whereas *C. lanzi* reveals the reverse condition (Figs. 1, 2). *C. lanzi* further exhibits a higher amount of parallel-fibered bone with a scattered distribution of relatively large longitudinally orientated simple vascular canals, primary osteons and at least one isolated secondary osteon in the cortex (Fig. 1).

Discussion

Comparison to other Nothosauria: *Nothosaurus* of the Upper Muschelkalk

Ontogenetically old *Nothosaurus* specimens show very thin cortices of lamellar-zonal bone

Specimen	element	O.C.	S(SE)	P(SE)
C. lanzi				
T5454	Rib	0.937	1.051086(0.1023045)	-2.490762(0)
C. calcagnii				
T5153 (belongs to T5152	Rib	0.958	0.1111562(n.a.)	-195.1377(n.a.)
T5152	Tibia	0.942	0.5493211(0.0300717)	-0.2533822(0.1463694)
T5622	Femur	0.947	0.0020549(0.0004912)	0.2707274(0.0005591)
T5622	Rib	0.983	0.430127(n.a.)	-1.537819(n.a.)

Specimen	element	Min(SE)	Max(Se)	R^2
C. lanzi				
T5454	Rib	0.7347019(0)	0.9468985(0.0014604)	0.0052763
C. calcagnii				
T5153 (belongs to T5152	Rib	0.999999(n.a.)	0.9576608(n.a.)	7.680426e-11
T5152	Tibia	0.7696803(0.0346246)	0.9768469(0.0020469)	0.3857162
T5622	Femur	0.8148981(0.0011364)	0.9575337(0.0001391)	0.6160583
T5622	Rib	0.999999(n.a.)	0.9829417(n.a.)	1.250220e-12

Table 2. Compactness parameters given by the program Bone Profiler (Girondot and Laurin 2003).
The observed compactness (o.c.) are comparable to other secondarily aquatic reptiles with pachyosteosclerotic bones (e.g., Hugi et al. 2011). The parameters are given as supplementary information, but are not representative because the specimens are of young ontogenetic age and hence, the later possible changes in the bone microstructure are unknown (Wiffen et al. 1995; Klein 2010; Kolb et al. 2011). Abbreviations: n.a.: not available; S: starting point; SE: standard deviation; P: the distance to the centre where the most abrupt change of compactness is observed; Min: minimal value measured; Max: maximal value measured.

type surrounding a large medullary cavity filled with trabeculae as remains of the resorption process of the inner cortical growth record during the ontogeny (Krahl et al. 2009). Lamellar-zonal bone of *Nothosaurus* comprises growth marks within a matrix of lamellar bone and loosely packed parallel-fibered bone that irregularly grades into woven-fibered bone (Fig. 3). The spacing pattern of the lags is variable (Klein 2010). Ontogenetically young individuals in contrast show a calcified cartilaginous core that often infills the entire medullary region (Krahl et al. 2009). Therefore, *Nothosaurus* from the Germanic Basin shows an ontogenetic shift from an osteosclerotic to a lighter, "osteoporotic-like" bone structure that is interpreted as an adaptation to an increasingly pelagic habitat in more open marine environments in adults (e.g. Krahl et al. 2009). The bone sample of the ontogenetically young *Ceresiosaurus lanzi* resembles the histotype of young *Nothosaurus*. *Nothosaurus* bones are only fragmentarily preserved in the sediments of Monte San Giorgio (e.g., Rieppel 2001), which might be linked to the fact that they presumably lived in open marine environments as also indicated by morphological and histological data.

Comparison to Pachypleurosauria from Monte San Giorgio

Four pachypleurosaurid species have been found in sediments of Monte San Giorgio. The stratigraphically oldest taxon *Serpianosaurus mirigiolensis* is exclusively found in sediments of the Besano Formation (former Grenzbitumen beds; e.g., Carroll and Gaskill 1985). The stratigraphically younger genus *Neusticosaurus* is preserved in the same beds as *Ceresiosaurus*

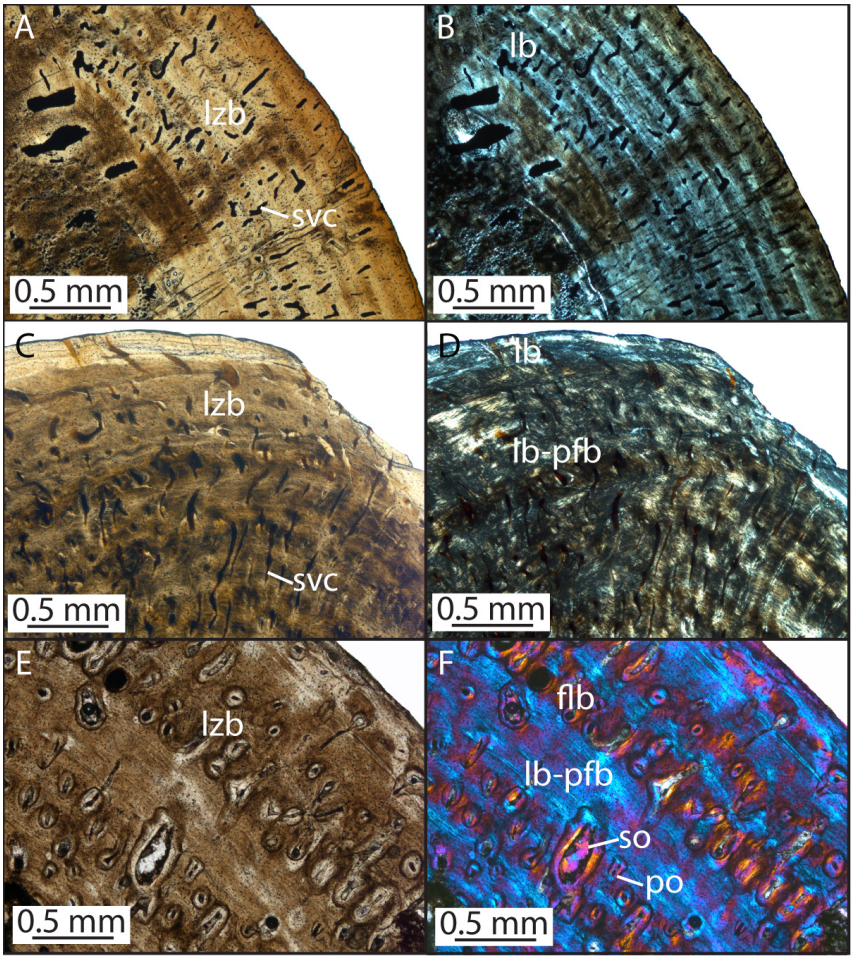

Fig. 3. The cortical growth pattern of *Serpianosaurus mirigiolensis* (A and B), *Neusticosaurus edwardsii* (C and D) from Monte San Giorgio, and *Nothosaurus* (E and F) from the Germanic Basin. All show a lamellar-zonal bone type with a varying vascularisation and growth pattern. The cortex of *S. mirigiolensis* comprises lamellar bone with simple vascular canals (svc), *N. edwardsii* shows parallel-fibered and lamellar bone with the same vascularisation as in *S. mirigiolensis*, whereas *Nothosaurus* reveals lamellar-zonal bone of lamellar (lb) and parallel-fibered bone (pfb), which is irregularly interrupted by bands of fibrolamellar bone (flb). The vascularisation comprises primary (po) and secondary osteons (so).

spp., the Cava inferiore, Cava superiore, as well as the Cassina beds (e.g., Sander 1989). They all show pachyosteosclerosis in the long bones with a thick cortex and a calcified cartilaginous core in the medullary region (Zangerl 1934; Ricqlès 1976; Hugi et al. 2011). The calcified cartilaginous core is partially, or in one species even entirely, replaced at the diaphyseal and/or metaphyseal region by endosteally deposited bone (e.g., Hugi et al. 2011). The stratigraphically well separated pachypleurosaurid species show similarities, but also differences in their long bone histology most possibly reflecting different modes of life (*S. mirigiolensis* and *N. edwardsii*: pelagic, more nectonic?; *N. pusillus* and *N. peyeri*: pelagic and more demersal; Hugi et al. 2011). All pachypleurosaurids show the plesiomorphic lamellar-zonal bone type in the cortex (Fig. 3). The cortex of the bones of *S. mirigiolensis* comprises differently organised lamellar bone, whereas the ones of the *Neusticosaurus* species consist both of parallel-fibered and lamellar bone. The lamellar-zonal bone type of *N. edwardsii* varies in the growth and vascularisation pattern during the ontogeny (Hugi et al. 2011). The growth zones are of parallel-fibered bone tissue that is loosely packed, with increased vascularisation of simple longitudinal vascular canals in young specimens and more simple radial vascular canals in adult ones. The crystallites around the simple vascular canals show a funnel-shaped arrangement and locally overlap with each other, producing the impression of a patchy presence of woven-fibered bone tissue (Fig. 4 in Hugi et al. 2011). This impression is also

present in the *Ceresiosaurus* samples (Fig. 1). Bones of *C. calcagnii* resemble the histotype of *N. edwardsii* from Monte San Giorgio with pachyosteosclerotic lamellar-zonal bone in the cortex and long, radially orientated vascular canals. Contrary to the exclusive simple primary vascularisation in *N. edwardsii*, the long bones of *C. calcagnii* are further vascularised by primary osteons, but with less vascularisation than in the former (Fig. 2). In young *C. lanzi* the simple vascular canals and primary osteons are predominantly longitudinally arranged and of larger size than in *C. calcagnii* and *N. edwardsii*. The young ontogenetic stage of the only *C. lanzi* sample shows no pachyostosis, but osteosclerosis.

Comparison to basal Pistosauroidea

All of the discussed eosauropterygians are Nothosauroidea which predominantly show lamellar-zonal bone type with a varying growth pattern (i.e., irregularly deposited bone bands of lamellar bone, parallel-fibered bone and fibrolamellar bone). In contrast, in basal and derived members of the Pistosauroidea, the loosely packed parallel-fibered bone tissue is frequently and regularly interrupted by woven-fibered bone (e.g., Wiffen et al. 1995; Klein 2010). The presence of lamellar-zonal bone generally reflects a slow bone deposition rate and therefore, might also indicate low metabolic rates, whereas the frequent presence of fibrolamellar bone is a result of quicker growth rates in vertebrates of higher metabolic rates (e.g., Horner et al. 2000; Padian et al. 2001). As indicated by Klein (2010), continuous higher metabolic rates might be responsible for the ability of early pistosauroids to spread over the Tethys by also conquering colder sea regions. Pistosauroids generally show a spacing pattern of continuous thickness throughout the cortex (Klein 2010).

Conclusion

Data on the long bone histology support the evolutionary trend of two different modes of locomotion in *Ceresiosaurus calcagnii* and *C. lanzi* based on morphological studies (Hänni 2004). The bone sample of *C. calcagnii* shows pachyosteosclerotic limbs and ribs similarly to *Neusticosaurus edwardsii*. The rib sample of *C. lanzi* is osteosclerotic and reveals a different growth pattern with larger vascular canals in a more unorganised bone matrix. However, further information on the growth pattern during the subsequent ontogeny remains unknown. The adult histotype could either remain osteosclerotic as in *C. calcagnii* or become osteoporotic as in *Nothosaurus*.

Acknowledgment

I would like to thank all the members of the Sánchez' lab and especially T. Scheyer and M. Sánchez-Villagra for the helpful discussion on earlier versions of the manuscript. This work would have never been possible without the permission of H. Furrer for processing the thin sections of the sampled *Ceresiosaurus* specimens. This project has been funded by the Swiss National Science Foundation grant No. 31003A-133032/1 to MRS-V.

Literature cited

Bürgin, T., Rieppel, O., Sander, M., Tschanz, K. Y. (1989). Trias-Fossilien aus dem Ur-Mittelmeer. Spektrum der Wissenschaft, 8, 110-119.

Buffrénil, V. de, Schoevaert, D. (1988). On how the periosteal bone of the delphinid humerus becomes cancellous: Ontogeny of a histological specialization. Journal of Morphology, 198(2), 149-164.

Buffrénil, V. de, Mazin, J.-M. (1990). Bone histology of the Ichtyosaurs: comparative data and functional interpretation. Paleobiology, 16(4), 435-447.

Carroll, R.L., Gaskill, P. (1985). The nothosaur *pachypleurosaurus* and the origin of plesiosaurs. Philosophical Transactions of the Royal Society of London. Series B, Biological Sciences, 309(1139), 343-393.

Castanet, J., Francillon-Vieillot, H., Meunier, F. J., Ricqlès, A. de. (1993). Bone and individual aging. In B. K. Hall (Ed.), Bone, Vol. 7. Bone Growth-B (pp. 245-283). Boca Raton, Florida: CRC Press.

Chinsamy, A., Raath, M. A. (1992). Preparation of Fossil Bone for Histological Examination. Palaeontologica Africana 29, 39-44.

Francillon-Vieillot, H., Buffrénil, V. de, Géraudie, J., Meunier, F. J., Sire, J. Y., Zylberberg, L., Ricqlès, A. de. (1990). Microstructure and mineralization of vertebrate skeletal tissues. In J. G. Carter (Ed.), Skeletal biomineralization- patterns, process and evolutionary trends (pp. 471-530). New York: Van Nostrand Reinhold.

Furrer, H. (1995). The Kalkschieferzone (Upper Meride Limestone) near Meride (Canton Ticino, Southern Switzerland) and the evolution of a Middle Triassic intraplatform basin. Eclogae Geologae Helvetica, 88(3), 827-852.

Girondot, M., Laurin, M. (2003). Bone profiler: a tool to quantify, model, and statistically compare bone-section compactness profiles. Journal of Vertebrate Paleontology, 23(2), 458-461.

Hänni, K. (2004). Die Gattung *Ceresiosaurus* - *Ceresiosaurus calcagnii* PEYER und *Ceresiosaurus lanzi* n. sp. (Lariosauridae, Sauropterygia). PhD thesis. vdf Hochschulverlag AG an der ETH Zürich.

Horner, J. R., Ricqlès, A. de, Padian, K. (2000). Long bone histology of the hadrosaurid dinosaur *Maiasaura peeblesorum*: growth dynamics and physiology based on an ontogenetic series of skeletal elements. Journal of Vertebrate Paleontology, 20, 115-129.

Horner, J. R., Padian, K., Ricqlès, A. de (2001). Comparative osteohistology of some embryonic and perinatal archosaurs: developmental and behavioral implications for dinosaurs. Paleobiology, 27(1), 39-58.

Houssaye, A. (2010). A new aquatic pythonomorph (Reptilia, Squamata) from the Turonian (Late Cretaceous) of France. C.R. Palevol 9, 39-45.

Hugi, J., Scheyer, T. M., Klein, N., Sander, P. M., Sánchez-Villagra, M. R. (in press). Long bone microstructure gives new insights into the life history data of pachypleurosaurids from the Middle Triassic of Monte San Giorgio, Switzerland/Italy. Comptes Rendues Palevol.

Klein, N. (2010). Long bone histology of Sauropterygia from the Lower Muschelkalk of the germanic basin provides unexpected implications for phylogeny. PlosOne, 5(7), e11613.

Kolb, C., Sanchez-Villagra, M. R., Scheyer, T.

M. (2011). The palaeohistology of the basal ichthyosaur *Mixosaurus* Baur, 1887 (Ichthyopterygia, Mixosauridae) from the Middle Triassic: palaeobiological implications. Comptes Rendues Palevol doi:10.1016/j.crpv.2010.10.008.

Krahl, A., Sander, P. M., Klein, N. (2009). Long bone histology of Middle Triassic eusauropterygians (Nothosauria and Pistosauria) and its implications for paraxial swimming. Journal of Vertebrate Paleontology, 29, 129A.

Müller, J., Scheyer, T. M., Head, J. J., Barrett, P. M., Werneburg, I., Ericson, P. G. P., Pol, D., Sánchez-Villagra, M. R. (2010). The evolution of vertebral numbers in recent and fossil amniotes: The roles of homeotic effects and somitogenesis. PNAS, 107(5), 2118-2123.

Padian, K., Ricqlès, de A. J., Horner, J. R. (2001). Dinosaurian growth rates and bird origins. Nature, 412, 405-408.

Parrish, J., Ziegler, A. M., Scotese, C. R. (1982). Rainfall patterns and the distribution of coals and evaporites in the Mesozoic and Cenozoic. Palaeogeography Palaeoclimatolology Palaeoecology, 40, 67-101.

Peyer, B. (1931). Die Triasfauna der Tessiner Kalkalpen, IV. *Ceresiosaurus calcagnii* nov. gen. nov. spec. Abhandlungen der Schweizerischen Palaeontologischen Gesellschaft, 51, 1-68.

Peyer, B. (1932). Die Triasfauna der Tessiner Kalkalpen, V. *Pachypleurosaurus edwardsii* Corn. spec. Abhandlungen der Schweizerischen Palaeontologischen Gesellschaft, Band LII, 3-18.

Ray, S., Botha, J., Chinsamy, A. (2004). Bone histology and growth patterns of some nonmammalian therapsids. Journal of Vertebrate Paleontology 24: 634–648.

Ricqlès, A. de. (1976). Recherches paleohistologiques sur les os longs des tetrapodes. VII. Sur le classification, la signification fonctionelle et l'histoire des tissus osseux des tetrapodes. Annales de Paléontologie, 62, 71-126.

Ricqlès, A. de, Buffrénil, V. de. (2001). Bone histology, heterochronies and the return of tetrapods to life in water: were are we? In J. M. Mazin & V. de Buffrénil (Eds.), Secondary adaptation of tetrapods to life in water (pp. 289-310). München, Germany: Verlag Dr. Friedrich Pfeil.

Ricqlès, A. de, Padian, K., Knoll, F., Horner, J. R. (2008). On the origin of high growth rates in archosaurs and their ancient relatives: complementary histological studies on Triassic archosauriforms and the problem of a ‘‘phylogenetic signal’’ in bone histology. Annales de Palaeontologie, 94, 57-76.

Rieppel, O. (1989). A new pachypleurosaur (Reptil ia: Sauropterygia) from the Middle Triassic of Monte San Giorgio, Switzerland. Philosophical Transactions of the Royal Society of London B, 323, 1-73.

Rieppel, O. (1998). The status of the sauropterygian reptile genera *Ceresiosaurus*, *Lariosaurus*, and *Silvestrosaurus* from the Middle Triassic of Europe. Fieldiana: Geology, N.S., 38, 46pp.

Rieppel, O. (1999). Phylogeny and paleobiogeography of Triassic Sauropterygia; problems solved

and unresolved. Palaeogeography, Palaeoclimatology, Palaeoecology, 153, 1-15.

Rieppel, O. (2000). Chapter 12: Sauropterygia. In O. Kuhn & P. Wellnhofer (Eds.), Handbuch der Paläoherpetologie/ Handbook of Paleoherpetology (pp. 1-134). München: Verlag Dr. Friedrich Pfeil.

Rieppel, O. (2001). Marine reptiles from the Triassic of the Tre Venezie Area, Northeastern Italy. Geology, 44(New series), 1-22.

Röhl, H. J., Schmid-Röhl, A., Furrer, H., Frimmel, A., Oschmann, W., Schwark, L. (2001). Microfacies, geochemistry and palaeoecology of the Middle Triassic Grenzbitumenzone from Monte San Giorgio (Canton Ticino, Switzerland). Geologica Insubrica, 6(1), 1-13.

Sander, P. M. (1989). The pachypleurosaurids (Reptilia: Nothosauria) from the Middle Triassic of Monte San Giorgio (Switzerland) with the description of a new species. Philosophical Transactions of the Royal Society of London. B, Biological Sciences, 325(1230), 561-666.

Scheyer, T. M., Klein, N., Sander, P. M. (2010) Developmental palaeontology of Reptilia as revealed by histological studies. Seminars in Cell & Developmental Biology, 21(4), 462-470.

Sheldon, A. (1997). Ecological implications of Mosaur bone microstructure. In J. Callaway & E. Nicholls (Eds.), Ancient Marine Reptiles (pp. 333-354). Academic Press.

Stein, K., Langer, M. C. (2009). The long bone histology of the stem sauropodomorph *Saturnalia tupiniquim*, implications for the early evolution of dinosaur bone microstructure. Journal of Vertebrate Paleontology 29: 185A.

Storrs, G. W. (1993). The systematic position of *Silvestrosaurus* and a classification of Triassic sauopterygians. Paläontologische Zeitschrift 67,177-191.

Sues, H.-D. (1987). Postcranial skeleton of *Pistosaurus* and interrelationships of the Sauropterygia (Diapsida). Zoological Journal of the Linnean Society, 90, 109-131.

Taylor, M. A. (2000). Functional significance of bone ballast in the evolution of buoyancy control strategies by aquatic tetrapods. Historical Biology 14, 15-31.

Wiffen, J., Buffrénil, V. de, Ricqlès, A. de, Mazin, J. M. (1995). Ontogenetic evolution of bone structure in Late Cretaceous Plesiosauria from New Zealand. Geobios, 28(5), 625-640.

Zangerl, R. (1935). *Pachypleurosaurus edwardsii*, Cornalia, Osteologie, Variationsbreite, Biologie. In: Peyer B, ed. Trias Fauna der Tessiner Kalkalpen IX, *Pachypleurosaurus*, Abhandlungen der Schweizerischen Paläontologischen Gesellschaft/Mémoires de la Société Paléontologique Suisse 66, 1–80.

Zug, G. R., Rand, A. S. (1987). Estimation of age in nesting female *Iguana iguana*: testing skeletochronology in a tropical lizard. Amphibia-Reptilia, 8, 237-250.

Chapter 7:

Life history and skeletal adaptations in the Galapagos Marine Iguana (*Amblyrhynchus cristatus*) as reconstructed with bone histological data - a comparative study of iguanines

Jasmina Hugi and Marcelo R. Sánchez-Villagra

In Review, *Journal of Herpetology*

Upper photographs: U. Koller
Lower photographs: J. Hugi

Life history and skeletal adaptations in the Galapagos Marine Iguana (*Amblyrhynchus cristatus*) as reconstructed with bone histological data - a comparative study of iguanines

Jasmina Hugi[1*] and Marcelo R. Sánchez-Villagra[1]

[1]Palaeontological Institute and Museum, University of Zurich, Karl Schmid-Straße 4, 8006 Zurich, Switzerland

*corresponding author: jasmina.hugi@pim.uzh.ch, Tel. +41-44 634 23 47, Fax +41-44 634 49 23

Abstract

Marine Iguanas (*Amblyrhynchus cristatus*) are the only living lacertilian squamates which exclusively forage in the sea. Their amphibious life style and anatomy have been subject to scientific studies for several decades, but the information obtained by bone microstructure has never been studied in detail. For the first time, thin sections of the long bones of the Marine Iguana and its terrestrial iguanid relatives are described and compared.

Results indicate differences in the microstructure and the bone compactness values compared to the terrestrial iguanid relatives. Marine Iguana limb bones constitute of thick periosteal cortices with nearly avascular lamellar-zonal bone type. In addition, minor remodelling processes affect the inner wall of the cortex. A characteristic spacing pattern of the LAGs based on the continuity of the growth cycle thicknesses during the ontogeny distinguishes them from corresponding data of terrestrial lizards. The cortex of *A. cristatus* and its sister group, the Galapagos Land Iguana (*Conolophus subcristatus)*, show a specific light and extinction pattern preserved in the cortex, visible in polarised light.

In conclusion, the life history data of *A. cristatus* reconstructed with bone histology and skeletochronology is congruent with observations provided by ecological studies. Histology of a Marine Iguana reveals low but rather regular growth rates until an EFS is developed, prolonged longevities and a delayed sexual maturity. Bone histological data further probably also reflect climate-dependant reproduction seasons which was already documented by field studies. Microstructural changes are regarded as a result of secondary adaptation to the amphibious life.

Introduction

Amblyrhynchus cristatus BELL (Reptilia: Iguanidae) is a middle-sized lizard (200 – 340 mm, adult snout-vent length) distributed on the islands of the Galapagos Archipelago (e.g., Boersma, 1983). They show an unique life style among all lizards by exclusively foraging in the cold sea (e.g., Trillmich and Trillmich, 1986; Laurie and Brown, 1990). Their habitat and specialized diet have led to many studies on their physiology with focus on the thermoregulatory behaviour (e.g., Bartholomew, 1966; Bennett et al., 1975; Bartholomew et al., 1976; Boersma, 1983), as well as on their ecology (e.g., Trillmich and Trillmich, 1984; Laurie and Brown, 1990; Wikelski and Hau, 1995; Wikelski and Trillmich, 1997). The climate of the Galapagos Archipelago is characterized by two seasons, a warm season which lasts from January to June and a dry season from July to December (e.g., Colinvaux, 1972). The seasons are regular except for the returning El Niño rainfalls in every fourth or fifth year (e.g., Colinvaux, 1972). These two distinct seasons favour or decrease the growth of the macrophytic algae, the main food supply of the Marine Iguana (e.g., Laurie and Brown, 1990) and, as a result of this high dependence, the reproduction starts during the cold and dry season (e.g., Trillmich and Trillmich, 1984).

Is the unique lifestyle of the Marine Iguanas coupled with changes in the bone microstructure compared to the completely terrestrial iguanid relatives? Little information exists on the bone histology of the Marine Iguana and only concerning the bone compactness values (Taylor, 2000; Germain and Laurin, 2005; Kriloff et al., 2008; Canoville and Laurin, 2010). The long bones of vertebrates generally are informative structures to study life histories using histological data (e.g., Francillon-Vieillot et al., 1990). These data can provide information on rate and duration of growth by analysis of bone tissue and bone tissue types (histology), whereas counting of growth marks (skeletochronology) allows estimation of the age at sexual maturity and the longevity of an individual (e.g., Castanet et al., 1993). The varying bone tissue type and the grade of remodelling processes result in specific compactness value which can be evaluated with the program Bone Profiler (Girondot and Laurin, 2003). Skeletochronology is a useful tool assessing the age of an individual on the basis of counting the number of growth cycles. A growth unit is composed of a growth zone, annulus and line of arrested growth (LAG after Castanet et al., 1993), which is assumed to be deposited annually. Several studies confirm the successful use of skeletochronological methods in ageing reptiles by using capture/recapture techniques, conducting periodic chemical labelling, or studying growth series of known-age reptiles (e.g., Castanet and Naulleau, 1985; Erickson et al., 2001). Although LAGs are most obvious in individuals living in high latitudes/ altitudes (areas with marked seasonality), their occurrence also has been reported in the bones of individuals living in aseasonal environments (e.g., Patnaik and Behera, 1981; Castanet and Gasc, 1986). Castanet et al. (1993) proposed that LAGs arise as a result of an endogenous biological rhythm that may be synchronised by external factors such as the food availability. Such external and internal factors often are preserved in the histological record by remodelling processes (e.g., for the production of eggs), a change in the bone tissue, as well as a decrease in the spacing between the LAGs (e.g., sexual maturation, termination of growth).

The termination of growth is histologically expressed by the development of an external fundamental system (EFS after Horner et al., 2001; or OCL: outer circumferential layer after Chinsamy-Turan, 2005).

The aim of this study is to primarily assess the life history of the Marine Iguanas, in comparison to its terrestrial iguanid relatives, using data on the microstructure of the bones. We present the first comprehensive histological and skeletochronological study of the long bones of the Marine Iguana in comparison to other iguanines (Fig. 1). The questions we address here are: 1) whether the bone histology of the Marine Iguana is altered as a result of the amphibious lifestyle when compared to terrestrial iguanid relatives; and 2) whether skeletochronological data correspond to ecological data on the plasticity of the reproduction cycle, longevity, as well as the age when sexual maturity is reached (Table 1).

The interpretations of this study are in some cases speculative because the results are based on a relatively small sample size. The obtainment of the museum specimens used in this study was critical because these lizards are in some cases of endangered status. Further development of imaging techniques, which also enable the study of skeletochronological data without being invasive, may be used to further test the hypotheses we present here with additional data.

Material and Methods

The stylo- and zeugopodial bones of the forelimbs (humerus, radius, ulna) and hind limbs (femur, tibia, fibula) of four Marine Iguanas from two different islands (*Amblyrhynchus cristatus venustissimus* EIBL-EIBESFELDT: NKMB-30260, Española; *Amblyrhynchus cristatus cristatus* BELL: ZFMK-uncatalogued Fernandina, Table 1), as well as individuals of seven completely terrestrial iguanines, including the Galapagos Land Iguana (*Conolophus subcristatus*), were investigated (Fig. 1; Table 1). Males were preferred as samples since the long bones of the females usually serve as a calcium storage during reproduction (e.g., Buffrénil et al., 2010). Mid-shaft Diaphyseal thin-sections were prepared and documented following standard petrographic preparation techniques (Scheyer and Sánchez-Villagra, 2007). Bone compactness profiles and values were quantified (Table 2) using the PC version of the program Bone Profiler 3.20 (Girondot and Laurin, 2003). The histology was assessed qualitatively (Table 3). Student's paired t-tests were performed to report the probability (p) of the following null hypotheses: 1) there is no statistically significant difference in the mean compactness values of the limb bones between the female and the male Marine Iguanas, 2) there is no statistically significant difference in the mean compactness values of the limb bones between the Marine Iguanas and the other iguanid taxa, 3) there is no statistically significant difference in the mean compactness vales of the forelimbs and hind limbs in the Marine Iguanas, 4) there is no statistically significant difference in the mean compactness vales of the forelimbs and hind limbs in the completely terrestrial iguanid taxa. A rejection of the second, third and fourth null hypothesis was expected. The black and white sketches were prepared using Adobe Photoshop CS3. Several long bones which are pictured appear blurred, which is a result of the high amount of lipid deposits in the cortex. It could not completely be chemically removed although the long bones have been treated for

almost half a year with Methylenchorid.

Results

Results are summarized in Figure 1.

Bone compactness, histology and skeletochronology of Amblyrhynchus cristatus

All long bones of the forelimb show high compactness values, except for the femur and tibia (Table 2). The mean compactness values of the limb bones of the Marine Iguanas are statistically significantly higher than the equivalent data of the completely terrestrial iguanines (paired t-test: $t = 1.998$, $p < 0.05$). The mean compactness values of the forelimbs of the Marine Iguanas are statistically significantly different from the equivalent data of the hind limbs (paired t-test: $t = 2.1$, $p< 0.05$). The increase in high bone compactness values is mainly reached by a continuous and regular accretion of lamellar-zonal bone along the outer wall of the cortex combined with a few remodelling processes of the inner wall of this region. The humerus, radius, ulna and fibula of *Amblyrhynchus cristatus* show the less resorption of the inner wall of the cortex. In addition, small circular layers of endosteal lamellar bone are deposited along parts or even along the entire inner wall of the cortices (Fig. 2C-D; Fig. 3B, D). The humeri of some of the male specimens (from Fernandina) further show primary trabeculae which are not only preserved in the medullary cavity of the epiphyseal and metaphyseal region, but also in this region at the mid shaft (Fig. 3G-H). The female specimen is the only sampled Marine Iguana in showing resorption processes which are not only restricted to the inner wall of the cortex (e.g., Fig. 3A-B). Various erosion cavities are preserved in the cortex of the tibia (ZFMK-uncatalogued female), whereas the humerus, radius and ulna only show one single erosion cavity in the same region. The mean compactness values of the limb bones of the female specimen does not show a statistically significant difference from equivalent data of the male Marine Iguanas (paired t-test: $t = 2.2$, $p < 0.05$).

The cortices of the long bones display regular growth marks. The long bones with minor remodelling processes (humerus, radius, ulna and fibula) show one innermost periosteal bone layer of embryonic bone which is composed of less organised woven-fibered grading into parallel-fibered bone tissue (wp; Fig. 2C-D, 3D). The wp layer is bordered by a LAG which represents the hatching line (e.g., Fig. 3D). The embryonic bone is characteristically opaque in polarised light and shows a large quantity of round osteocytes (Fig. 2G-H, 3E-F). All subsequent growth cycles are of lamellar-zonal bone type which is characterised by an avascular lamellar bone tissue with neither secondary and primary osteons, nor simple vascular canals (Fig. 2 and 3).

All specimen show regular and rather constant growth cycle thicknesses up to a certain age, which result in a characteristic spacing pattern (Buffrénil and Castanet, 2000) of the LAGs. The growth cycles show no decrease in thickness when sexual maturity is reached (see below) (Fig. 2C-H, Fig. 3D-H). In both females and males, the growth cycle thicknesses abruptly decrease as soon as the EFS is developed (Fig. 2C-D, Fig. 3D-F). The EFS is characterised by the deposition of closely spaced LAGs of highly organised lamellar bone. NKMB 30260 and the ZFMK female are the only sampled specimens with already developed an EFS (Table 3). NKMB

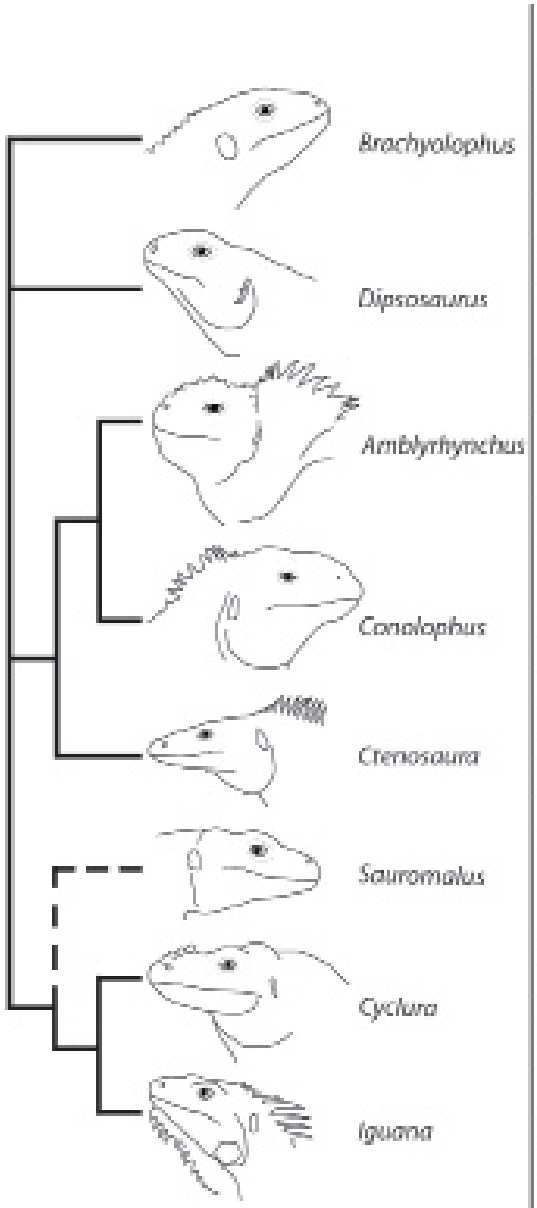

	Completely terrestrial iguanines	Amphibious Marine Iguana
	Balance between bone accretion in the outermost cortex region and bone resorption of the innermost cortex region	Imbalance between bone accretion in the outermost cortex region and bone resorption of the innermost cortex region
	Forelimbs slightly more compact than hind limb	Forelimbs significantly more compact than hind limb
	Constant growth cycle thickness until sexual maturity	Constant growth cycle thickness until sexual maturity
	Steep decrease in growth cycle thickness at onset of sexual maturity	No change in growth cycle thickness at onset of sexual maturity
	Continuous approximation of the LAGs after sexual maturity, "fluent transition" into EFS Only *Conolophus subcristatus*: rather abrupt approximation of the LAGs when EFS is developed	Abrupt approximation of the LAGs when EFS is developed
	EFS marks termination of growth	EFS marks termination of growth
	Only *Conolophus subcristatus*: Specific light and extinction pattern of growth zones and annuli before and after onset of sexual maturity, but not at EFS	Specific light and extinction pattern of growth zones and annuli before and after onset of sexual maturity, but not at EFS
	All other studied iguanines: specific light and extinction pattern **rarely** found in humerus and then only before reaching sexual maturity. Otherwise random light and extinction pattern	

Fig. 1. Phylogeny of the studied iguanines and summary of results. Left column shows the phylogeny of the studied iguanines which is modified from Wiens and Hollingsworth (2000). The results are summarised on the right column of the Figure.

30260 displays the EFS after the age of ten and died at 18 years of age. The adult female from Fernandina was only ten years old when it died and developed an EFS after six years of age, which indicates that female specimens show shorter phases of regular bone deposition than males.

All specimens show an alternating light and extinction pattern in the cortex visible in polarised light with the males exhibiting a stronger or more obvious pattern (e.g., Fig. 2E-H; Fig. 3E-F). The subunits of each growth cycle (i.e., growth zone and annulus) differ in regards of the birefringence based on the level of the equality in orientation of the collagenous fibres (Glimcher and Muir, 1984), as well as

General information

Species	Species Range	Climate	Seasons
Amblyrhynchus cristatus	Galapagos Archipelago	"summer" (warm and rainy), "winter" (cold and dry)	warm season (January-June), dry season (July-December)
Brachyolophus fasciatus	Fiji Islands	summer (hot, humid), winter (warm, dry)	summer: november-february; winter: april-september
Conolophus subcristatus	Galapagos Archipelago	"summer" (warm and rainy), "winter" (cold and dry)	warm season (January-June), dry season (July-December)
Ctenosaura similis	Mexico to Panama	summer (rainy), winter (dry)	summer: may-october, winter: november-april
Cyclura cornuta	Hispaniola (Domenican Republic)	summer (hot and rainy), winter (warm and dry),	summer: may-october, winter: november-april
Dipsosaurus dorsalis	SW U.S./NW Mexico	summer and winter rainfall; arid and hot	arid/ hot, two rainfall seasons (October-march: winter, july-september: summer), winter: hibernation
Iguana iguana	Mexico to South America; West Indies	summer (rainy), winter (dry)	summer: may-october, winter: november-april
Sauromalus obesus	SW U.S./NW Mexico	summer and winter rainfall; arid and hot	arid/hot, two rainfall seasons (October-march: winter, july-september: summer), winter: hibernation

Species	sm-t/longevity*	Diet (h, a)	References
Amblyrhynchus cristatus	female: 3-5, male: 6-8/ca. up to 20-30 years	h and a: primarily herbivorous	Etheridge, 1982; Laurie, 1990; Wikelski et al., 1993
Brachyolophus fasciatus	2.5 years (ca. 16 months)/ca. up to at least 20 years	h and a: primarily herbivorous	Etheridge, 1982; Iverson, 1982; Gibbons, 1984
Conolophus subcristatus	female: 7-10, male: 11-16 /ca. up to 20-30 years	h and a: primarily herbivorous	Etheridge, 1982; Werner, 1982; Christian et al., 1984
Ctenosaura similis	2 years/ca. up to 13 years	h: carnivorous, a: herbivorous	Fitch, 1977; Etheridge, 1982; Iverson, 1982
Cyclura cornuta	female: 12 years, male: ? years, in captivity: female: 6-7 years, male: 4-5 years/ca. at least up to 20-30 years	h and a: primarily herbivorous	Etheridge, 1982; Iverson, 1982; Pérez-Buitrago et al., 2008
Dipsosaurus dorsalis	2 years (up to 30 months)/ca. up to 14 years	h and a: primarily herbivorous	Moberly, 1963; Etheridge, 1982; Iverson, 1982; Mautz

			and Nagy, 1987
Iguana iguana	18-24 months/ca. up to 20-30 years	h and a: primarily herbivorous	Etheridge, 1982; Iverson, 1982; Troyer, 1984; Zug and Rand, 1987
Sauromalus obesus	females: 2 years, males: 2-3 years /ca. up to 14 years	h and a: primarily herbivorous	Nagy, 1973; Etheridge, 1982; Abts, 1987
Sampled animals			
Species	Collection number	Sex	Lived in …
A. c. venustissimus	NKMB-30260	Adult male	Natural habitat, SVL 390mm. Weight 2570 g, male, Española (former Hood island), Capture date 10.01.1973
A. c. cristatus	ZFMK-uncatalogued	Adult male	Natural habitat, Fernandina
A. c. cristatus	ZFMK-uncatalogued	Adult female	Natural habitat, Fernandina
A. c. cristatus	ZFMK-uncatalogued	Subadult male	Natural habitat, Fernandina
B. fasciatus	SMF-72758	Adult male	Natural habitat
C. subcristatus	CAS-10475	Adult male	Natural habitat, SVL 480mm, male, South Seymour Islands. Capture date 21.11.1905 by J.R. Slevin
C. similis	SMF-52071	Adult male	Natural habitat
C. cornuta	ZFMK-5223	Adult male	Natural habitat
D. dorsalis	SMF-71284	Subadult female	Kept in captivity
I. iguana	NMB-5743	Adult male	Kept in captivity
S. obesus	NMB-13801	Adult female	Kept in captivity

Table 1. General information about the studied iguanine lizards regarding their home range, the climate they live in, the age of reaching sexual maturity, the longevity and an ontogenetic shift in diet is shown. * The longevity is often unknown for wild animals. These are only estimates. Abbreviations: age sex. mat.: age at sexual maturity, a: adult, h: hatchling.

on the quantity and shape of the osteocytes. The thickness and the listed characteristics of the growth zones and annuli distinctly change one time during the ontogeny. Before this change, the growth zones are thick, showing less birefrigence and round osteocytes of high quantity, whereas the annuli are thin, highly birefringent with single flattened osteocytes. After this change, the growth zones are thin, highly birefringent and with less osteocytes of flattened shape, whereas the annuli are thick with round and more osteocytes and less birefringent (Fig. 2F, H; Fig. 3F). This distinct change is accompanied by the higher presence of supernumerary LAGs and is regarded as indicator when sexual maturity is reached. This event occurs during the sixth and eighth year in the male specimens (e.g., Fig. 2C-H, Fig.

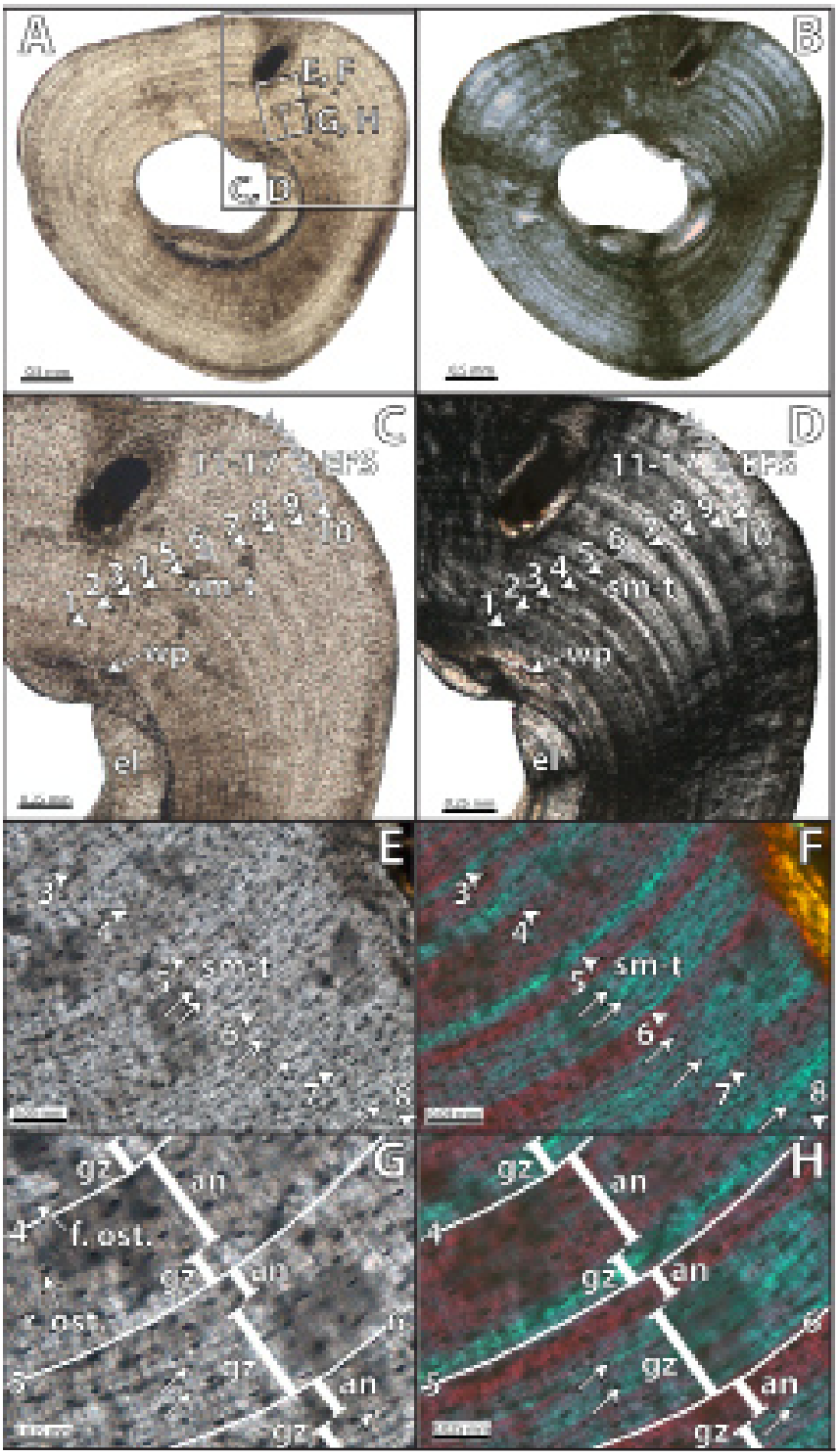

Fig. 2. Microstructure of the long bones of *Amblyrhynchus cristatus* (I).
Diaphyseal transverse sections of the radius of the adult male *Amblyrhynchus cristatus* from Española (NKMB 30260). Images A, C, E, G is normal transmitted light, whereas images B, D, F, H is polarised light. Images C and D show the complete growth record with up to 17 growth cycles (numbered arrow heads). Embryonic bone (wp) is still visible in the innermost periosteal cortex region, although remodelling processes occurred by the deposition of lamellar bone layers along the inner wall of the cortex (el). The growth cycles only decrease in thickness after the age of ten years when the EFS is developed (grey arrow heads in the outermost region of the cortex). Images E and F show the histological features when sexual maturity is reached (sm-t). The thickness of the growth zones (gz) and annuli (an) change, as well as the birefringence in polarised light. Images G and H give a more detailed look at the histological change which occurs at and sexual maturity is reached. Further abbreviations: f. ost.: flattened osteocyte, r. ost.: round osteocyte, el: endosteal lamellar bone, wp: woven-fibered bone grading into parallel-fibered bone.

3G-H; Table 3) and during the third to fourth year in the female individual (Fig. 3D-F; Table 3). The sampled female shows slight variation in the light and extinction pattern compared to the males. The growth zones and annuli are almost of equal thickness after sexual maturity is indicated (Fig. 3F).

The presence of embryonic wp, the change in the light and extinction pattern at sexual maturity, as well as the development of the EFS as a result that the growth is mainly terminated are distinct changes reported in the bone histology which most possibly represent single life stages of a Marine Iguana.

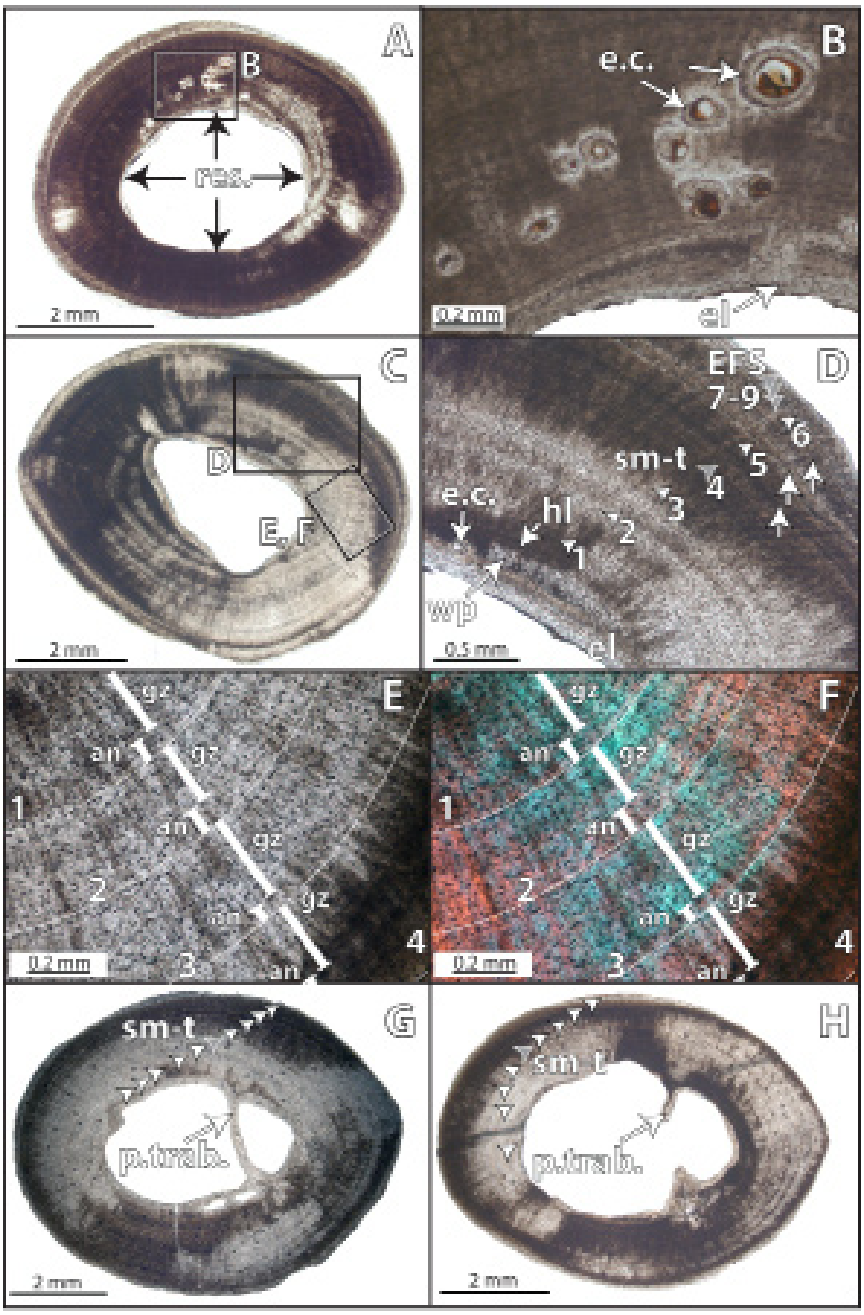

Fig. 3. Microstructure of the long bones of *Amblyrhynchus cristatus* (II).
Images A, B show the diaphyseal transverse sections of the tibia of the adult female *Amblyrhynchus cristatus* from Fernandina (ZFMK-uncatalogued) in normal transmitted light. The tibia is one of the limb bones which is comparable to the equivalent data on the bone compactness values of the completely terrestrial iguanines with showing higher resorption processes of the inner wall of the cortex (res.). Furthermore, the female specimen is the only sampled Marine Iguana which exhibits secondary erosion cavities (e.c.) in its limb bones, especially found in the tibia. Images C, D, E and F show the diaphyseal transverse section of another limb bone of the female Marine Iguana. Images C, D and E display the humerus in normally transmitted light, whereas image F is in polarised light with Lambda compensator. The sampled female was in its tenth year of life with nine preserved LAGs (arrow heads). Parts of the embryonic bone (wp), as well as of the hatching line (hl) still are preserved. The distinct light and extinction pattern is shown in image E and F with a less drastic change in the thickness of the growth zones and the annuli after the sm-t compared to the sampled males. Image G show the exact transverse sections of the mid shaft of the humerus of the adult male *A. cristatus* from Fernandina (ZFMK-uncatalogued), whereas image H shows the subadult male individual from the same island. Both males exhibit some primary trabeculae (prim. trab.) within the medullary cavity. For further abbreviations see Figure 2.

Bone compactness, histology and skeletochronology of the completely terrestrial iguanines

All terrestrial iguanines share several histological features, including avascular lamellar-zonal bone type in their long bones (e.g., Fig. 4, Fig. 5 and Fig. 6). The mean compactness values of the forelimbs are statistically significantly higher than the equivalent means of the hind limbs (paired t-test: $t = 2.02$, $p < 0.05$). Large terrestrial iguanines show major resorption along the inner wall of the medullary cavity in their limb bones (e.g., Fig. 4 and 6), whereas small bodied groups only display minor occurrence of this process in the same area (e.g., Fig. 5). Small iguanines, therefore, often still display parts of the embryonic bone (Fig. 5). In only a few cases, erosion cavities are preserved in the cortex and not only restricted to the inner wall of this region. Additionally, thin

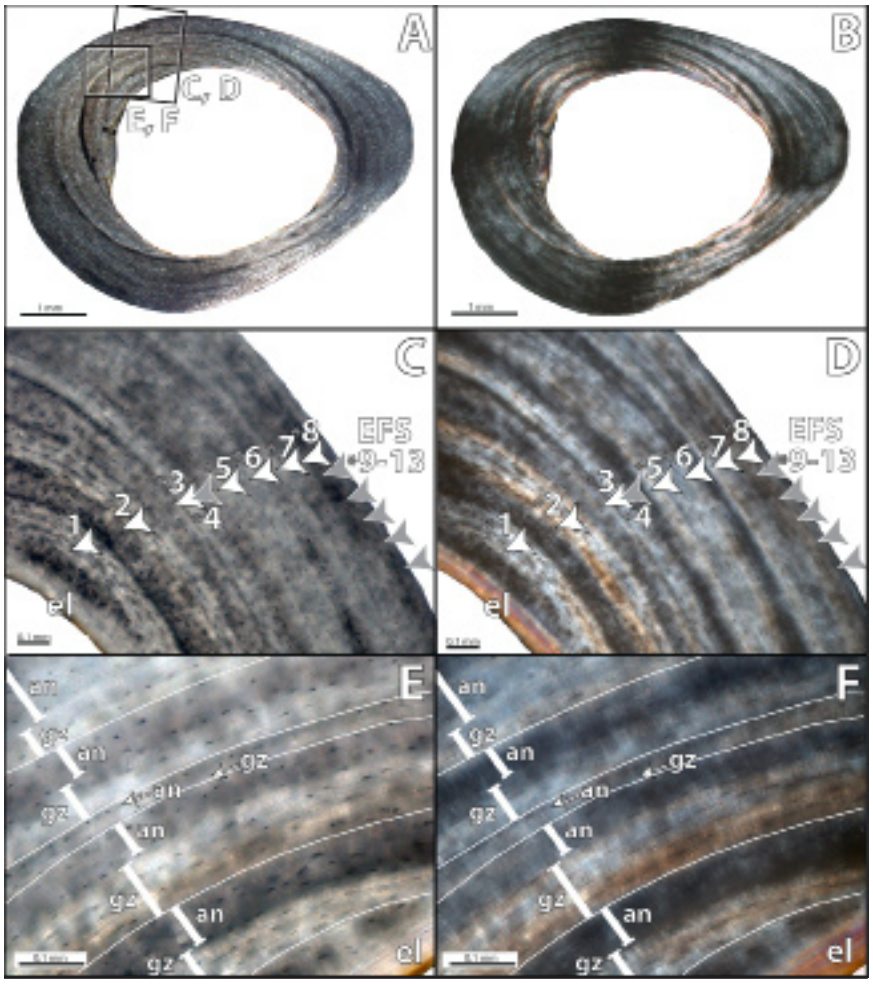

Fig. 4. Microstructure of the long bones of *Conolophus subcristatus*.
Diaphyseal transverse sections of the fibula of an adult male Galapagos Land Iguana (CAS 10475). Images A, C and D in normal transmitted light, image B, D and F in polarised light. Images C and D shows the region with the less destroyed growth record by resorption of the inner wall of the cortex. 13 growth cycles are preserved (arrow heads). Although the growth cycles decrease in thickness at the sm-t, they are of rather equal thickness until the EFS is developed (grey arrow heads in the outermost region of the cortex). Images E and F additionally give a more detailed view on the distinct change in the thicknesses of the growth zone and the annulus within the growth cycles before, at and after this event. For abbreviations see Figure 2.

lamellar bone layers are deposited partly around the medullary cavity (e.g., Fig. 4C-F, Fig. 5 and Fig. 6C-F).

Sexual maturity is indicated by an abrupt decrease in growth cycle thickness. The spacing pattern is of continuous thickness before sexual maturity is reached, whereas growth cycles after this event increase their thickness for one or two growth cycles before continuously decreasing until an EFS is developed (Fig. 5, Fig. 6C-F). Small bodied iguanines show a shorter phase of bone deposition between the timing when sexual maturity is reached and the development of an EFS (e.g., Fig. 5). Therefore, the growth rate of small iguanines is mainly restricted to the time before sexual maturity is reached. The growth rate of larger iguanines, in contrast, decreases more slowly after this event and therefore, sexual maturity occurs well before the final size is reached (e.g., Fig. 6).

The light and extinction pattern, based on the level of the equality in the orientation of the collagenous fibres within the growth cycles, appears to be randomly preserved in all studied terrestrial iguanines (e.g., Fig. 5C; Fig. 6D, F), except for *C. subcristatus* (Fig. 4D, F). In a few cases a similar light and extinction pattern is preserved as in *C. subcristatus* and *A. cristatus*. If this is the case, it is most likely shown in the humerus and only before sexual maturity is reached (e.g., Fig. 5C).

The studied specimen of *C. subcristatus* shows 13 growth cycles in the area with the most

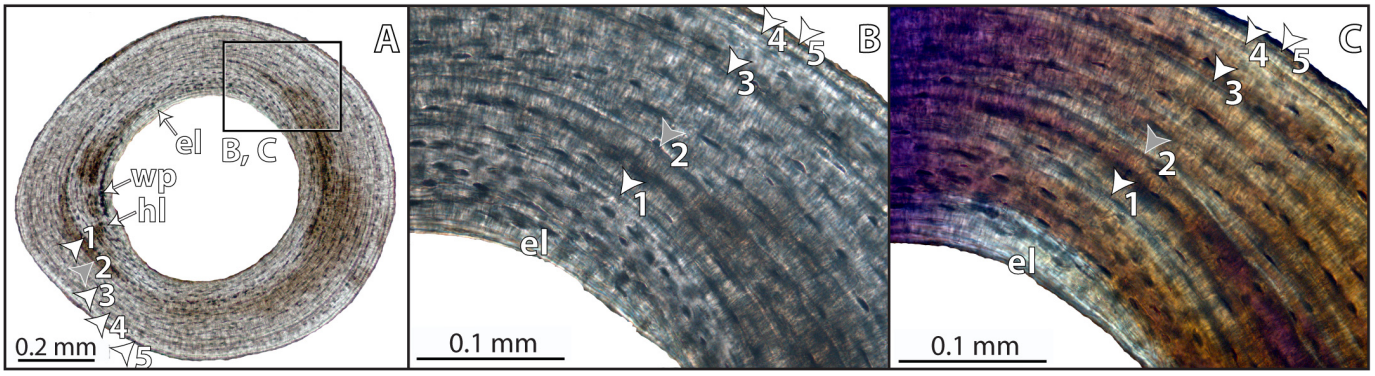

Fig. 5. Microstructure of the long bones of *Dipsosaurus dorsalis.*
Diaphyseal transverse sections of the humerus of an adult Desert Iguana (SMF 71284) as an example for the spacing pattern of small-bodied lizards and random colour pattern within the growth cycles in completely terrestrial iguanines, with *Conolophus subcristatus* as an exception. Image A and B is normal transmitted light. Image C is polarised light with Lambda compensator. In all images A, B and C, the individual shows five LAGs (arrow heads) and therefore, was at its sixth year at death. Image A shows the steep decrease in the thickness at sexual maturity (number 2). The subsequent growth cycles increase in thickness after this event before decreasing again until the EFS is developed. For abbreviations see Figure 2.

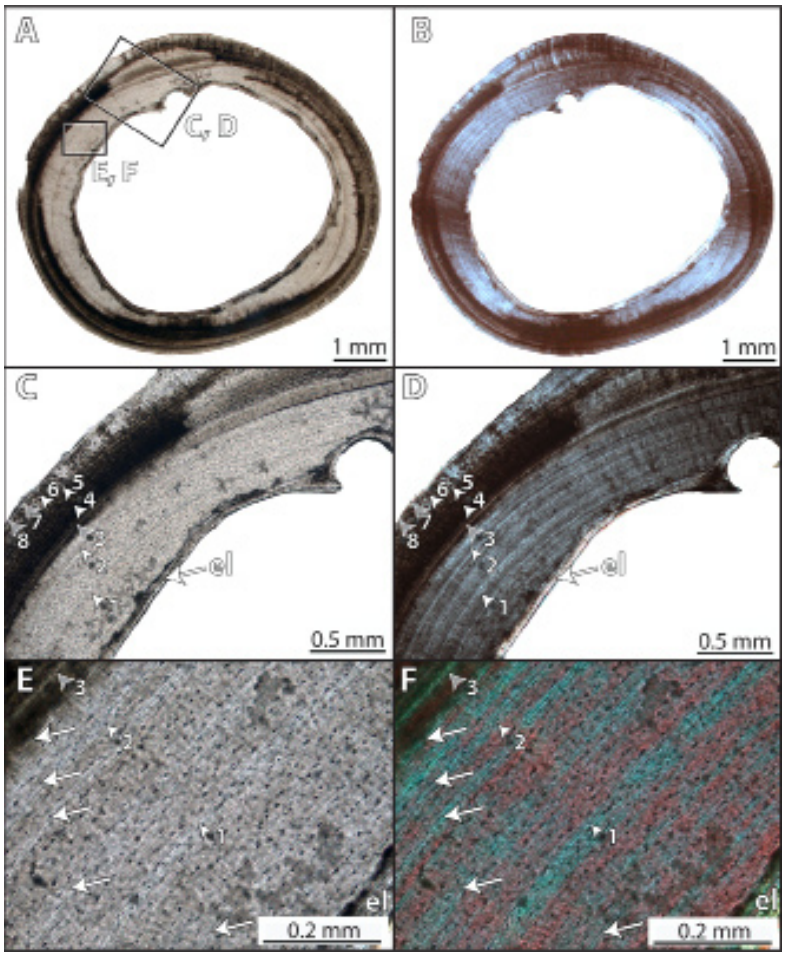

Fig. 6. Microstructure of the long bones of *Cyclura cornuta*
Diaphyseal transverse section of the tibia (image A to F) of an adult male Rhinoceros Iguana (ZFMK 5223) as an example of the spacing pattern in completely terrestrial iguanines, with *Conolophus subcristatus* as an exception. The growth cycles continuously decrease in thickness after the onset of sexual maturity (grey arrow head nr. 3*), which is marked by a steep decrease in the growth cycle thickness. The growth cycle thicknesses continuously decrease until the EFS is developed (grey arrow heads in the outermost region of the cortex, nr. 7 to 8). Images A, C, E is normal transmitted light, whereas image B, D, F is polarised light. Image C and D show a minimum number of eight LAGs. The more detailed view of images E and F do not reveal a distinct light and extinction pattern at least not after sexual maturity is reached. Growth cycles are randomly composed of lighter and darker coloured bone layers in polarised light. For abbreviations see Figure 2.

	Specimen	Elements	O.c.	S(SE)	P(SE)	Min(SE)	Max(SE)	R^2
A. cristatus	NKMB 30260	Humerus	0.884	0.0191065(0.0000701)	0.3367103(0.0001271)	6.824271e-7(1.608939e-6)	0.999999(0.0000188)	0.998925
		Radius	0.901	0.0148327(0.0000537)	0.3119535(0.0000974)	7.972226e-7(7.893261e-7)	0.999999(0)	0.999363 4
		Ulna	0.921	0.0187626(0.0001162)	0.2773236(0.0002108)	6.839338e-7(2.214489e-6)	0.999999(0.0000102)	0.999118 6
		Femur	0.62	0.0061508(0.0000258)	0.6118705(4.118891e-6)	3.439419e-8(0)	0.999999(0)	0.999977 2
		Tibia	0.719	0.0104325(0.0000459)	0.526584(0)	1.881833e-7(0)	0.999999(0)	0.999576 9
		Fibula	0.895	0.0208726(0.000129)	0.3190775(0.000234)	8.042837e-7(1.674344e-6)	0.999999(0)	0.997771 8
	Bonn1	Humerus	0.831	0.0257594(0.0000916)	0.4194168(0.0001545)	0.0684016(0.0005613)	0.999999(8.94168e-6)	0.992874 5
		Radius	0.899	0.0169391(0.0001081)	0.3142945(0.0001959)	6.821047e-7(2.386869e-6)	0.999999(0.986666e-6)	0.999450 6
		Ulna	0.906	0.0182104(0.0000539)	0.3026399(0.0000977)	5.942616e-7(1.070618e-6)	0.999999(0)	0.998780 1
		Femur	0.659	0.0093165(0.000029)	0.5798301(0)	6.104330e-8(3.526714e-7)	0.999999(0)	0.999865 7
		Fibula	0.886	0.014307(0.0001005)	0.3335298(0.0001796)	2.567210e-7(3.386654e-6)	0.999999(0)	0.999300 2
		Tibia	0.712	0.0188555(0.0000607)	0.5318063(0.0001089)	3.276914e-7(6.146109e-7)	0.999999(0)	0.998539 3
	Bonn2	Humerus	0.868	0.0316816(0.0000851)	0.356075(0.0001544)	8.042837e-7(7.274741e-7)	0.999999(5.087346e-6)	0.993510 8
		Radius	0.918	0.0124991(0.0000586)	0.2819566(0.0001)	8.741075e-7(2.720769e-6)	0.9992439(0.0000205)	0.999607 9
		Ulna	0.909	0.0133739(0.0000503)	0.2985137(0.0000909)	3.261969e-7(8.221851e-7)	0.9994955(0.0000149)	0.998905 4
		Femur	0.702	0.0188176(0.0000488)	0.5414738(0.0000887)	3.777583e-7(8.115426e-7)	0.999999(6.127931e-6)	0.999679 2
		Tibia	0.766	0.0118327(0.0000633)	0.4770131(0.0001093)	3.386207e-7(7.202842e-7)	0.9978603(0.0000543)	0.999594 3
		Fibula	0.793	0.0175584(0.0000485)	0.4514094(0.0000945)	3.757724e-7(0)	0.999999(0.0000172)	0.997723 1
	Bonn3	Humerus	0.744	0.0187148(0.0000798)	0.5120425(0.0001227)	0.0424399(0.0003816)	0.999999(0)	0.995577 1
		Radius	0.875	0.0164652(0.0000582)	0.3493796(0.0001053)	2.669599e-7(2.087440e-7)	0.999999(0)	0.997801 4
		Ulna	0.927	0.013047(0.000106)	0.2679372(0.0001922)	6.747306e-7(3.050201e-6)	0.999999(0.0000133)	0.998844 9
		Femur	0.628	0.0139987(0.0000397)	0.6050044(0.0000714)	3.142804e-7(0)	0.999999(0)	0.999093
		Tibia	0.74	0.0102106(0.0000516)	0.505376(3.639125e-6)	1.076526e-7(5.60242e-7)	0.999999(0)	0.999724 3
		Fibula	0.793	0.016029(0.0000498)	0.4511256(0.0000843)	3.264554e-7(5.491415e-7)	0.999999(0)	0.998980 5
B. fasciatus	SMF 72758	Humerus	0.826	0.057026(0.0001621)	0.4011294(0.0002936)	7.434224e-7(1.604642e-6)	0.999999(0)	0.967110 3
		Radius	0.728	0.0469663(0.0000949)	0.511619(0.0001717)	3.854155e-7(9.326261e-7)	0.999999(0)	0.992838 4

		Ulna	0.757	0.0199739(0.0000687)	0.4889012(0.0001301)	3.260678e-7(6.701218e-7)	0.999999(0.0000194)	0.9994634
		Femur	0.665	0.0247121(0.0000746)	0.5729092(0.0001353)	3.863992e-7(7.526933e-7)	0.999999(0)	0.9932853
		Tibia	0.696	0.0329525(0.0001054)	0.5441887(0.0001922)	1.295591e-7(0)	0.999999(0)	0.995877
		Fibula	0.544	0.0287189(0.0000696)	0.6692828(0.0001261)	8.543985e-8(1.672502e-7)	0.999999(4.536369e-6)	0.9985537
C. subcristatus	CAS 10475	Humerus	0.724	0.0298013(0.0000557)	0.5189919(0.0001009)	6.839338e-7(7.122264e-7)	0.999999(4.337513e-7)	0.9944589
		Radius	0.704	0.0294456(0.0000839)	0.5370849(0.000152)	3.845073e-7(7.072207e-7)	0.999999(3.895843e-6)	0.9971938
		Ulna	0.74	0.0345053(0.0000804)	0.5025226(0.0001455)	1.039551e-6(1.365153e-6)	0.9998731(0.0000194)	0.9972728
		Femur	0.605	0.0271383(0.000054)	0.6216238(0.0000978)	3.843847e-7(4.932045e-7)	0.999999(3.524365e-7)	0.9974439
		Tibia	0.652	0.0227959(0.0000537)	0.5846224(0.0000898)	2.011849e-7(6.548085e-7)	0.9997472(0.0000253)	0.997807
		Fibula	0.618	0.0232462(0.0000686)	0.6117166(0.0001244)	4.443171e-7(7.060679e-7)	0.999999(0)	0.999098
C. similis	SMF 52071	Humerus	0.631	0.0213275(0.000062)	0.6019302(0.0001123)	3.869343e-7(6.787899e-7)	0.999999(0)	0.9965733
		Radius	0.731	0.0172988(0.0000563)	0.5148014(0.0001025)	2.666661e-7(3.302054e-7)	0.999999(6.617535e-6)	0.9975815
		Ulna	0.723	0.0124905(0.0000461)	0.5215449(0.0000583)	4.4437303-7(7.641211e-7)	0.999999(0)	0.9988983
		Femur	0.757	0.0199789(0.0000686)	0.488902(0.0001263)	3.272789e-7(7.273960e-7)	0.999999(0.0000112)	0.9994634
		Tibia	0.57	0.0085872(0.0000329)	0.6510199(0)	0.6397420e-8(3.323036e	0.999999(0)	0.9999144
		Fibula	0.644	0.0105307(0.0000618)	0.5924297(0.0002153)	1.469176e-7(5.888314e-7)	0.999999(0.0000123)	0.9996374
C. cornuta	ZFMK 5223	Humerus	0.61	0.0102466(0.000041)	0.6200619(0.0000448)	5.417504e-8(0)	0.999999(0)	0.9998204
		Radius	0.689	0.0188555(0.0001022)	0.5512838(0.0001854)	3.272377e-7(1.327413e-6)	0.999999(0.0000103)	0.9978058
		Ulna	0.679	0.0411143(0.0001329)	0.4430421(0.0002131)	3.899005e-7(1.709339e-6)	0.8536832(0.0003417)	0.9720671
		Femur	0.456	0.0099357(0.0000448)	0.7329796(0.0000842)	4.850888e-8(0)	0.999999(0.0000237)	0.9997343
		Tibia	0.519	0.0198035(0.0000494)	0.6879689(0.0000895)	3.786513e-7(2.859956e-6)	0.999999(7.959745e-6)	0.9989775
		Fibula	0.449	0.0150854(0.0000684)	0.7029174(0.000124)	1.101373e-7(6.663236e-7)	0.999999(0.0000109)	0.9985686
D. dorsalis	SMF 71284	Humerus	0.725	0.0121347(0.0000429)	0.5199708(0)	2.488231e-7(3.679417e-6)	0.999999(2.404878e-6)	0.9994285
		Radius	0.836	0.0145607(0.0000779)	0.4018879(0.0001416)	2.534891e-7(0)	0.999999(7.137321e-6)	0.9987121
		Ulna	0.647	0.0157988(0.0000601)	0.5887567(0.0001056)	3.255542e-7(7.254059e-7)	0.999999(0)	0.9993554
		Femur	0.57	0.0118036(0.000044)	0.6513483(0)	8.618912e-8(1.057029e-7)	0.999999(0)	0.9994823

complete growth record preserved (Fig. 4C-D). Although large parts of the inner periosteal growth record are destroyed by resorption, the transition which marks the sexual maturity still is preserved (Fig. 4C-F). The reported age of sexual maturity is between an age of eight to 15 years for male *C. subcristatus* (e.g., Christian and Tracy, 1982). As a result, the minimum age of the sampled male *C. subcristatus* is estimated to be at least 21 to 28 years old at the time of its death (Fig. 4C-D). In *C. subcristatus*, the growth cycle at sexual maturity becomes abruptly very narrow (Fig. 4C-F) as in other terrestrial iguanid taxa. The growth cycles of *C. subcristatus* also increase a little in thickness after the sm-t, but in contrast to the other terrestrial iguanines, the growth cycle thicknesses remain then rather constant until an EFS is developed (Fig. 4C-D). Therefore, *C. subcristatus* shows a mixture in the spacing pattern between the Marine Iguana and the other completely terrestrial iguanines in displaying an elongated phase of bone deposition rate before the development of the EFS. In addition, the growth zones and annuli can be distinguished by their birefringence in polarised light, as well as by the shape and quantity of the osteocytes until the EFS is developed. The change in the thicknesses of the growth zones and annuli is not that distinct as seen in the male *A. cristatus* with the growth zones and annuli rather being of equal thickness after sexual maturity is reached (Fig. 4E-F). *C. subcristatus* appear to differ from *A. cristatus* by a higher occurrence of resorption processes affecting the inner wall of the cortex, as well as by the change in the growth cycle thickness at sexual maturity. In *C. subcristatus* all limb bones show as much resorption of the inner wall of the cortex as seen in the other completely terrestrial iguanines.

Discussion

Histological data of the Marine Iguanas indicate differences in the bone microstructure and mean bone compactness values compared to terrestrial iguanid relatives. A characteristic spacing pattern of growth cycles distinguishes them from equivalent data of terrestrial lizards, indicating elongated phases of bone deposition rates (Fig. 7B). The Marine Iguana and its sister taxon, the Galapagos Land Iguana (*Conolophus subcristatus)*, share a specific alignment of the collagenous fibres, which results in an alternating light and extinction pattern visible in polarised light (Fig. 7C). The life history pattern of the Marine Iguana reconstructed with bone histology is strikingly congruent with observations provided by ecological studies (Table 1, e.g., Fig. 7D).

Marine Iguanas possess dense and compact long bones with relatively thick cortices. This results from a few remodelling processes of the inner wall of the cortex, as well as from a rather continuous bone deposition rate which cyclically accretes osseous layers in the outermost cortical region. Bone deposition rates are maintained even after sexual maturity is reached, which results in a spacing pattern of the growth cycles with constant thicknesses (Fig. 7B). Therefore, Marine Iguanas show an elongated phase of bone deposition rates which only show an abrupt decrease when the animal reaches its final size, marked by the development of an EFS. The attainment of the sexual maturity of the Marine Iguanas is not indicated by an abrupt decrease in the bone deposition rate as in other lizards, but by a change in the light and extinction pattern, as well as by a higher occurrence of supernumerary LAGs (e.g., Fig. 2C-H; Fig. 3D-F). Bone histology closely reflects data obtained from ecological studies

on longevities, age of sexual maturity, as well as external factors which influence the biological rhythm such as food availability and the closely linked reproduction cycle.

Small bodied lizards generally show short term life histories compared to larger relatives, although inter- and intraspecific variation occurs. All lizards show a quicker growth rate before sexual maturity is reached, when it abruptly decreases. The variation between the size differences of small and large lizards is mainly a result of the differences in the growth rates after this event: large individuals rather show an elongated phase of slowly decreasing growth rates before their growth terminates, whereas small taxa rather reach the final size shortly after sexual maturity is reached (Andrews, 1982; Shine and Charnov, 1992; e.g., *Cyclura cornuta* vs. *Dipsosaurus dorsalis:* in this study). The growth rate often is reflected in the bone deposition rate and therefore, in the characteristics of the bone tissue (e.g., Francillon-Vieillot et al., 1990)

The spacing pattern of the growth cycles of the Marine Iguana is an exception among all lizards. The elongated phases of bone deposition rates of *A. cristatus* are reflected by a characteristic spacing pattern of their growth cycle thicknesses which has, to our knowledge, not been reported in any other lizard in such a regular manner in all of the long bones. The Nile monitor, *Varanus nilotus*, which prefers habitats near water, shows a similar, but less extreme spacing pattern as the Marine Iguana, but with a varying occurrence (Buffrénil and Castanet, 2000).

All lizards show lamellar-zonal bone tissue type which generally results from a low, but wide range of bone deposition rates (Chinsamy-Turan, 2005; de Margerie et al., 2004). The differences between the ranges of this slowly deposited bone tissue type are reflected in the degree of the vascularisation, the amount and shape of osteocytes, as well as in the orientation of the collagenous fibres which is visible in polarised light. Hence, although the growth zones, annuli and LAGs are all composed of lamellar bone tissue, they can slightly differ from each other by these characteristics. The growth zones display a higher presence of round osteocytes with less equally orientated collagenous fibres which result in less birefringence in polarised light than the annuli. In the Marine Iguana, the alternating sequence of the growth zones and the annuli are visible in the entire cortex until the development of the EFS which is only composed of highly organised lamellar bone. In the Marine Iguanas, the very regular alignment of the collagenous fibres within the growth zones and annuli, as well as the elongated phase of the bone deposition rate allow us to study the distinct change in the thickness and the characteristics of the growth zones and annuli when sexual maturity is reached. Another large iguanine, *Cyclura cornuta*, also show a relatively long growth period which is also linked with an elongated phase of bone deposition rates. However, the alignment of the collagenous fibres within the growth cycles result in a random light and extinction pattern, at least after sexual maturity is reached. In addition, the bone which results from the elongated phase of the bone deposition rate after this event appears to be composed of equally high organised lamellar bone and therefore, the growth zones and annuli cannot be distinguished any more.

The distinct change in the light and extinction pattern might reflect the annual reproduction cycles of *A. cristatus* (Fig. 7D). The change in the characteristics of the growth zones and

		Tibia	0.537	0.0192889(0.0000806)	0.6756645(0.0001175)	5.457279e-8(1.106578e-7)	0.998615(0.0000961)	0.9984058
		Fibula	0.694	0.010501(0.0000415)	0.5481516(0)	5.349301e-8(0)	0.999999(0)	0.9995996
S. obesus	NMB 5743	Humerus	0.784	0.0121872(0.0000699)	0.4616258(0.0000322)	1.954733e-7(0)	0.999999(0)	0.9997176
		Radius	0.885	0.0146428(0.000082)	0.3359905(0.0001488)	2.659951e-7(4.356358e-7)	0.999999(0.0000113)	0.9986119
		Ulna	0.816	0.0070622(0.0000452)	0.4253315(0)	2.155909e-8(0)	0.4253315(0)	0.9999808
		Femur	0.636	0.0064403(0.0000346)	0.5992076(0.000034)	4.558876e-8(3.972884e-7)	0.999999(0.0000205)	0.9998462
		Tibia	0.737	0.0182294(0.0000873)	0.506548(0.0001589)	3.854766e-7(1.128553e-6)	0.999999(7.991653e-6)	0.9985869
		Fibula	0.839	0.0107499(0.0000599)	0.3986942(0.0000965)	2.528111e-7(1.419189e-6)	0.999999(0)	0.9994375
I. iguana	NMB 13801	Humerus	0.603	0.0128688(0.0000402)	0.6255007(0.0000856)	9.266757e-6(3.857471e-6)	0.999999(0.000019)	0.9995154
		Radius	0.693	0.0128887(0.0000424)	0.5500359(0.0003947)	1.445104e-7(3.382483e-7)	0.999999(0.0000306)	0.9990535
		Ulna	0.562	0.0095408(0.0000334)	0.6578073(0.0001448)	1.039983e-7(3.746039e-7)	0.999999(0.0000126)	0.9999813
		Femur	0.563	0.0087209(0.0000316)	0.6562026(0)	3.711061e-8(0)	0.999999(0)	0.99977
		Tibia	0.551	0.0142597(0.0000394)	0.6648817(0.0000715)	1.886579e-7(0)	0.999999(4.211771e-6)	0.9988421
		Fibula	0.583	0.0116368(0.0000595)	0.6420367(0.0001134)	2.466030e-7(2.047006e-6)	0.999999(0.0000132)	0.999253

Table 2. Observed individual variation of compactness profile parameter values in the limb elements for all sampled iguanines, as retrieved from Bone Profiler (Girondot and Laurin, 2003). Abbreviations: Max: reflects the compactness in the outermost cortex; Min: reflects the compactness in the centre of the medulla; O.c.: observed compactness; P: is the relative distance to the centre where the most abrupt change in compactness is observed; S: usually reflects the width of the transition zone between the cortical compacta and the medullary cavity; SE: standard error; R2: probability (after Girondot and Laurin, 2003).

the annuli could be a result of the changing availability of food, climate and the associated mating behaviour which is sex dependant (e.g., Trillmich and Trillmich, 1984). The mating cycles of *A. cristatus* are annual and dependant on two distinct seasons (e.g., Werner, 1982; Christian and Tracy, 1982; Fig. 7D). *C. subcristatus*, which shows a similar light and extinction pattern, exhibits the same conserved reproduction cycle as the other terrestrial iguanines (e.g., Wiewandt, 1982; Table 1), starting the mating season at the beginning of the warm season (Fig. 7D). The reproduction season of *A. cristatus*, in contrast, starts in the cold dry season (Fig. 7D) which is introduced by the occurrence of the cold and nutrient-rich Humboldt currents which in turn, strongly influence the reproduction and growth of the algae. *A. cristatus*, therefore, serves as example for the plasticity in the reproduction cycle of lizards, being mainly dependant on the food availability. Ecological data support this assumption. First, the histological change in the light and extinction pattern occurs exactly during the time span when females and males start to reproduce. In *A. cristatus*, this hypothesis is supported by slight differences of this pattern between male and female specimens as well as by the timing when the pattern changes.

Specimen	Sex	Preserved growth cycle number	Age of sex. maturity	Spacing pattern changes	Colour pattern thickness of gz and an
NKMB 30260	Adult male	17	6th year	No change in thickness at sm-t, but abrupt during EFS (13. to 20. growth cycle)	bsm: gz > an; asm: gz < an
ZFMK (uncatalogued)	Adult male*	10	6th year	No change in thickness at sm-t (not yet an EFS)	bsm: gz > an; asm: gz < an
ZFMK (uncatalogued)	Adult female*	13	3rd year	No change in thickness at sm-t, abrupt during EFS (7. to 9. growth cycle)	bsm: gz > an; asm: gz ≤ an
ZFMK (uncatalogued)	Subadult male**	9	7th year	No change in thickness at sm-t (not yet an EFS)	bsm: gz > an; asm: gz < an

Table 3. Specific skeletochronological and histological information for the studied Marine Iguanas. The number of the LAGs varies only in the femur and the tibia, which show higher resorption of the inner wall of the cortex. Abbreviations: an: annulus, asm: after sexual maturity, bsm: before sexual maturity, EFS: external fundamental system, gz: growth zone, sm-t: growth cycle when sexual maturation is reached. *: Fernandina specimens are generally larger than Española specimens (Eibl-Eibesfeldt, 2001: Galapagos - Die Arche Noah im Pazifik, Piper München Zürich). **: this individual is morphologically regarded as a subadult to due smaller size compared to the adults from Fernandina. However, histological data clearly shows that this animal already was sexually mature.

Ecological studies of *A. cristatus* report sexual maturity at an age of three to five years in females and an age six to eight years for males (Laurie, 1990). Second, there is a slight histological variation between males and females (Fig. 2, Fig. 3C-F). In females, the thicknesses of the growth zones and the annuli are more or less equal after sexual maturity is reached, whereas the males show an inverse distribution after this event. This could be explained as follows: *A. cristatus* which are not yet sexually mature spend all their time basking and feeding on algae during the whole year. After they reach sexual maturity, premating and mating period takes most time of the dry season (Trillmich and Trillmich, 1984; Fig. 7D). Males do not feed or feed little during the period of pre- and mating, because they start to be highly territorial showing male competition to monopolize the access to females as soon as they arrive at the mating sites (Trillmich and Trillmich, 1984; Fig.7D). In contrast, females still forage during the pre- and mating period and only cannot stop to feed when aggregating to the nesting ground and while defending their nests for several weeks or a month (Fig. 7D). The relatively long period of fasting of the males compared to the relatively shorter of the females, however, could be reflected by the more drastic change in the characteristics of the growth zone and annulus at and after sexual maturity is reached. Male *C. subcristatus*, in contrast, are not territorial and therefore, still feed, although less, during the

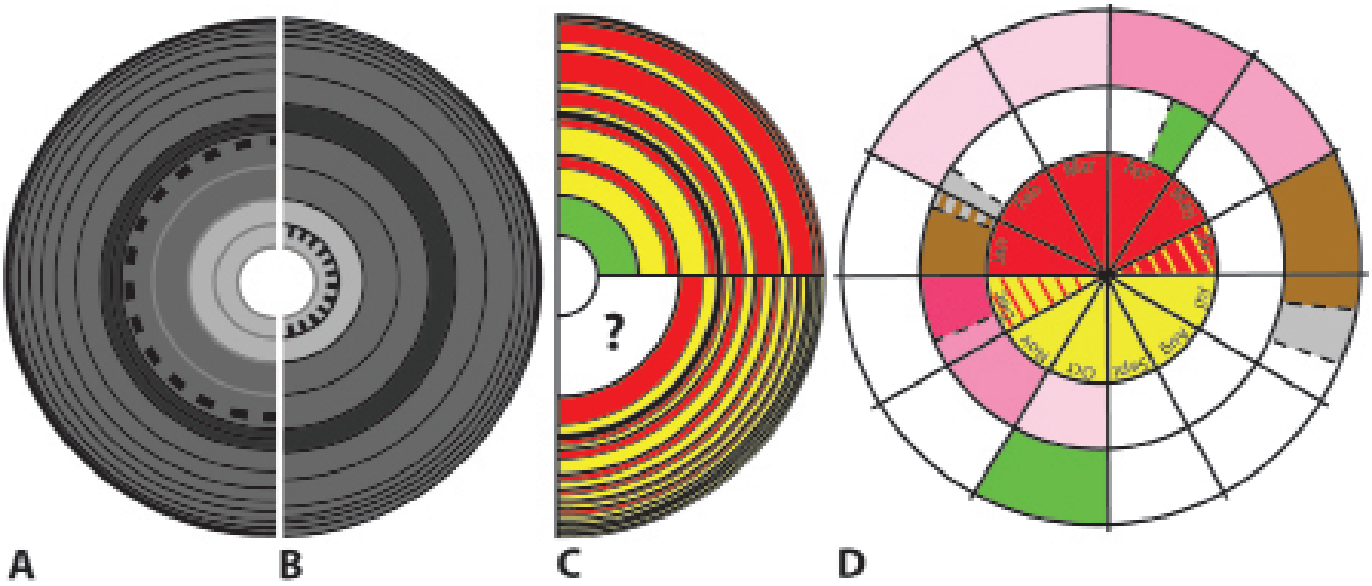

Fig. 7. Spacing pattern of the growth cycles and light extinction pattern in the completely terrestrial iguanines in comparison to the Marine Iguana with its possible link to the reproduction cycle.
A: the general spacing pattern of completely terrestrial iguanines (LAGs). (1) The centripetal deposition of bone in the cortex ( ) and the resorption processes of the inner wall of the cortex ( ) are more or less "balanced", (2) one innermost periosteal bone layer of woven-fibered to parallel-fibered bone (; wp) is deposited during the early ontogeny, (3) continuous decrease of growth cycle thicknesses before the EFS and an abrupt decrease in growth cycle thickness when sexual maturity is reached ( ).
B: general growth pattern of the Marine Iguana. (1) The centripetal deposition of bone in the cortex ( ) and the resorption processes of the inner wall of the cortex ( ) show an "imbalance", (2) one innermost periosteal bone layer of woven-fibered to parallel-fibered bone (; wp) is deposited during the early ontogeny, (3) growth cycle thicknesses remain constant until the EFS is developed and no or only a slight decrease in thickness occurs when sexual maturity is reached ( ).
C: the light and extinction pattern of the *Amblyrhynchus cristatus* and *Conolophus subcristatus*. A: Upper part: preserved light and extinction pattern of the growth zones and annuli in the Marine Iguana; lower coloured part: preserved light and extinction pattern of the growth zones and annuli in *C. subcristatus*, lower uncoloured part: unknown light and extinction pattern due to resorption processes of the inner wall of the cortex.
D: life histories of *A. cristatus* (middle circle) and *C. subcristatus* (outer circle; e.g. Fernandina). Inner circle: : warm season, : dry season; middle and outer circle: : beginning premating season, : peak premating season, : mating season, : nest defense, : nest-sites and egg-laying, : hatching season (see text for references).

reproduction season (e.g., Werner, 1982), which could be the explanation for the less drastic change in the characteristics of the growth zones and annuli at sexual maturity compared to male *A. cristatus*. Another explanation could be the relatively shorter reproduction cycle compared to *A. cristatus* (Fig. 7D).

As in other middle sized or large iguanines, *A. cristatus* reaches sexual maturation well before the attainment of full adult size — the primitive reptilian condition (e.g., Erickson et al., 2007). After sexual maturity, females tend to reabsorb calcium of their hind limb bones for reproduction (e.g. *Varanus niloticus* in Buffrénil and Francillon-Vieillot, 2001). As a result, their bone compactness can decrease with age in female lizards. Although the bone compactness values of the hind limbs of the sampled Marine Iguana female do not differ significantly from the values of the males, it shows secondary erosion cavities in the cortex of the tibia, which are not present in any male individual studied.

The mean bone compactness values are statistically significantly higher than the equivalent data of their terrestrial iguanid

relatives. The compact bones of the Marine Iguanas are most probably used for buoyancy control while exclusively feeding on intertidal and subtidal macrophytic algae (e.g., Trillmich and Trillmich, 1986). Heavy bones act as ballast allowing a hydrostatic control of body trim in water (Hoffstetter, 1955; Taylor, 2000). Increase in bone compactness, especially in the forelimbs, counteracts lung buoyancy and therefore facilitates diving and long-lasting underwater stays (e.g., Kaiser, 1966; Ricqlès and Buffrénil, 1996). Moreover, the increase in body density would counteract the action of waves and improve stability in rough water (Ricqlès and Buffrénil, 1996). This strategy can be seen for example in fossil and recent sirenians (Buffrénil et al., 2010) and Triassic marine eureptiles (Hugi et al., in press). Female Marine Iguanas are generally smaller than males and exclusively feed in the intertidal zones (e.g., Bartholomew, 1966) where diving is not necessary. They show shorter phases of bone deposition rates than males, which might be linked to their foraging strategies as interzonal feeders. In addition, there is a constant deviation in the compactness values between the forelimb and the hind limb elements in the terrestrial iguanas, but it is more obvious in the Marine Iguanas with the stylopodial and zeugopodial region of the forelimbs showing higher values (Table 2).

Compact bone could also be useful for counterbalancing muscular forces (predatory: hawk, *Buteo galapagoensis*, body size and substrate selection pressure). Possible differences in predatory, water temperature or substrate selection pressure might also be responsible for the size and histological differences between the Fernandina and Española males. All the studied bones of *A. cristatus* from Fernandina are larger, but revealed a minor count of the LAGs compared to the male from Española. The males from Fernandina additionally show primary trabeculae in the mid shaft region of the medullary cavity of the humerus.

Wikelski and Thom (2000) examined the growth of Marine Iguanas during El Niño rainfalls and reported that Marine Iguanas “shrink” during these re-occurring rainfalls, most probably due to energetic stress and the low food availability. No histological signs of this phenomenon were found in our sample. However, the exact collection date is only known in a few specimens (Table 1). Size differences between the islands are unlikely to be a result of the El Niño effects because rainfalls are similarly severe among all islands of the Galapagos Archipelago. Additionally, an abrupt decrease in the growth cycle thickness is only preserved when the EFS is developed. If exact information is available, no El Niño rainfall has occurred during these specific years.

In conclusion, the Marine Iguanas exhibit dense and compact long bones. The light and extinction pattern based on the regular alignment of the collagenous fibres within the growth zones and annuli of *Amblyrhynchus cristatus* and *Conolophus subcristatus* are most possibly related to changes in the seasonal climate which affects the availability of food and also the reproduction cycle. Higher compactness values in the long bones of *A. cristatus* are reached by elongated phases of bone deposition. The resulting spacing pattern of constantly thick growth cycles even after sexual maturity is reached, reveals an extended adult development until the growth finally ceases. In conclusion, the bone histology of the Marine Iguana is altered as a result of the amphibious

lifestyle compared to terrestrial iguanid relatives. In addition, skeletochronological data covers ecological data on the plasticity of the reproduction cycle, the longevities, as well as the age when sexual maturity is reached. In contrast, the information of the life history data based on bone histology of the other iguanines is often more or less obscured as a result of higher remodelling processes which very often destroy the innermost growth record of the cortex (e.g., Fig. 6). Only the long bones of the very small sized iguanines, *Ctenosaura similis*, *Dipsosaurus dorsalis* (e.g., Fig. 5), and *Sauromalus obesus* more often reveal the complete growth record in the cortices by showing minor remodelling processes which only affect parts of the inner wall of this region. These data on the skeletochronology also cover previously published demographic and ecological data (Table 1).

Acknowledgment

We would like to thank Torsten Scheyer and two anonymous reviewers for helpful comments on earlier versions of the manuscript. Furthermore, we thank Ursina Koller and Beat Häusler for their help. Samples were kindly made available for the study by Alan E. Leviton (San Francisco), Gunther Köhler (Frankfurt), Raffael Winkler (Basel), Wolfgang Böhme (Bonn), Frank Zachos and Ann-Christin Honnen (formerly Kiel). We are thankful to Nicole Klein and several anonymous reviewers for providing very useful suggestions on earlier versions of the manuscript. The Swiss National Science Foundation supported this project (grant No. 31003A-133032/1 to MRS-V).

Literature Cited

Abts, M. L. 1987. Environment and variation in life history traits of the Chuckwalla, *Sauromalus obesus*. Ecological Monograph 57(3):215-232.

Andrews, R. M. 1982. Patterns of growth in reptiles: In c. Gans and F. H. Pough (eds.), Biology of the Reptilia, pp. 273-320. Volume 13, Physiology D, Academic Press London.

Bartholomew, A. B. 1966. A field study of temperature relations in the Galapagos marine iguana. Copeia 2: 241-250.

Bartholomew, G. A., Bennett, A. F., and W. R. Dawson. 1976. Swimming, diving and lactate production of the marine iguana, *Amblyrhynchus cristatus*. Copeia 4:709-720.

Bennett, A. F., Dawson, W. B., and G. A. Bartholomew. 1975. Effects of activity and temperature on aerobic and anaerobic metabolism in the Galapagos marine iguana. Journal of Comparative Physiology 100:317-329.

Boersma, Dee B. 1983. An ecological study on the Galapagos marine iguana. In R. I. Bowman, M. Berson and A. E. Leviton (eds.), Patterns of Evolution in Galapagos Organisms, pp. 157-176. AAAS, Pacific Division.

Buffrénil, de V., and J. Castanet. 2000. Age estimation by skeletochronolgy in the nile monitor (*Varanus niloticus*), a highly exploited species. Journal of Herpetology 34(3):414-424.

Buffrénil, de V., and H. Francillon-Vieillot. 2001. Ontogenetic changes in bone compactness in male and female nile monitors (*Varanus niloticus*). Journal of

Zoology 254:539-546.

Buffrénil, de V., Canoville, A., D'Anastasio, R., and D. P. Domning. 2010. Evolution of sirenian pachyosteosclerosis, a model-case for the study of bone structure in aquatic tetrapods. Journal of Mammalian Evolution 17(2):101-120.

Canoville, A., and M. Laurin. 2010. Evolution of humeral microanatomy and lifestyle in amniotes, and some comments on palaeobiological inferences. Biological Journal of the Linnean Society 100:384-406.

Castanet, J., and J. P. Gasc. 1986. Age individuel, longevité et cycle d'activite chez *Leposoma guianense*, microteiidé de litière de l'écosysteme forestier guyanais. Memoires de la Musée Historique et Naturelles. (Paris) 132:281-288.

Castanet, J., and G. Naulleau. 1985. La squelettochronologie chez les reptiles. II. Résultats expérimentaux sur la signification des marques de croissance squelettiques chez les serpents. Remarques sur la croissance et la longévité de la Vipère Aspic. Annales des Sciences Naturelles 13^{e} Série (7) : 41-62, Zoologie, Paris.

Castanet, J., Francillon-Vieillot, H., Meunier, F. J., and A. de Ricqlès. 1993. Bone and individual aging. In B. K. Hall (ed.), Bone, Vol. 7. Bone Growth-B, pp. 245-283. CRC Press, Boca Raton, Florida.

Chinsamy-Turan, A. 2005. The Microstructure of Dinosaur Bone, deciphering Biology with Fine-Scale Techniques. The Johns Hopkins University Press, Baltimore and London.

Christian, K. A., and C. R. Tracy. 1982. Reproductive behavior of Galapagos land iguanas, *Conolophus pallidus*, on Isla Santa Fe, Galapagos. In G. M. Burghardt and A. S. Rand (eds.), Iguanas of the World, their Behavior, Ecology, and Conservation, pp. 366-379. New Series in Animal Behavior, Ecology, Conservation and Management.

Christian, K. A., Tracy, C. R., and W. P. Porter. 1984. Diet, Digestion, and Food Preferences of Galapagos Land Iguanas. Herpetologica 40(2):205-212.

Colinvaux, P. A. 1972. Climate and the Galapagos Islands. *Nature* 240:17-20.

Erickson, G. M., Curry Rogers, K., and S. A. Yerby. 2001. Dinosaur growth patterns and rapid avian growth rates. Nature 412:429-433.

Erickson, G. M., Rogers, K. C., Varricchio, D. J., Norell, M. A., and X. Xu. 2007. Growth patterns in brooding dinosaurs reveals the timing of sexual maturity in non-avian dinosaurs and genesis of the avian condition. Biological Letters 3:558-561.

Etheridge, R. E.: Checklist on the iguanine and Malagasy iguanid lizards. In G. M. Burghardt and A. S. Rand (eds.), Iguanas of the World, their Behavior, Ecology, and Conservation, pp. 7-37. New Series in Animal Behavior, Ecology, Conservation and Management.

Fitch, H. S., and R. W. Henderson. 1977. Age and sex differences in the ctenosaur (*Ctenosaura similis*). Milwaukee Publication of the Museum Contribution in Biology and Geology 11:1-11.

Francillon-Vieillot, H., Buffrénil, de V., Castanet, J., Géraudie, J., Meunier, F. J., Sire, J. Y., Zylberberg, L., and A. de Ricqlès. 1990. Microstructure and mineralisation of vertebrate tissue. In J. G. Carter (ed.),

Skeletal Biomineralisation: Patterns, Processes and Evolutionary Trends. Volume I, pp. 471-530. Van Nostrand Reinhold, New York.

Germain, D., and M. Laurin. 2005. Microanatomy of the radius and lifestyle in amniotes (Vertebrata, Tetrapoda). Zoologica Scripta 34, 335-350.

Gibbons, J. 1984. Iguanas of the South Pacific. Oryx 18(2):82-91.

Girondot, M., and M. Laurin. 2003. Bone profiler: a tool to quantify, model, and statistically compare bone-section compactness profiles. Journal of Vertebrate Paleontology 23(2):458-461.

Glimcher, M. J., and H. Muir. 1984. Recent studies of the mineral phase in bone and its possible linkage to the organic matrix by protein-bound phosphate bonds [and Discussion]. Philosophical Transactions of the Royal Society of London. Series B, Biological Sciences

304(1121), 479-508.

Hoffstetter, R. 1955. Squamates de type moderne. In J. Piveteau (ed.), Traité de Paléontologie 5, pp. 605-662. Masson, Paris.

Horner, J. R., Padian, K., and A. de Ricqlès. 2001. Comparative osteohistology of some embryonic and perinatal archosaurs: developmental and behavioral implications for dinosaurs. Paleobiology 27(1):39-58.

Hugi, J., Scheyer, T. M., Klein, N., Sander, P. M., and M. R. Sánchez-Villagra. in press. Long bone microstructure gives new insights into the life history data of pachypleurosaurids from the Middle Triassic of Monte San Giorgio, Switzerland/Italy. Comptes Rendues de Palevol.

Iverson, J. B. 1982. Adaptations to herbivory in iguanine lizards. In G. M. Burghardt and A. S. Rand (eds.), Iguanas of the World, their Behavior, Ecology, and Conservation, pp. 60-76.. New Series in Animal Behavior, Ecology, Conservation and Management.

Kaiser, H. E. 1966. Functional anatomy of breathing and balance in seacows (Sirenia). Anatomical Record 55:246.

Kriloff, A., Germain, D., Canoville, A., Vincent, P., Sache, M., and M. Laurin. 2008. Evolution of bone microanatomy of the tetrapod tibia and its use in paleobiological inference. Journal of Evolutionary Biology 21: 807-826.

Laurie, W. A. 1990. Population biology of marine iguanas (*Amblyrhynchus cristatus*). I. Changes in fecundity related to a population crash. Journal of Animal Ecology 59(2):515-528.

Laurie, W. A., and D. Brown. 1990. Population biology of marine iguanas (*Amblyrhynchus cristatus*). II. Changes in annual survival rates and the effects of size, sex, age and fecundity in a population crash. Journal of Animal Ecology 59(2):529-544.

Margerie, de E., Robin, J. P., Verrier, D., Cubo, J., Groscolas, R., and J. Castanet. 2004. Assessing a relationship between bone microstructure and growth rate: a fluorescent labelling study in the king penguin chick (*Aptenodytes patagonicus*). Journal of Experimental Biology 207:869-879.

Mautz, W. J., and K. A. Nagy. 1987. Ontogenetic changes in diet, field metabolic rate, and water flux in the herbivorous lizard

Dipsosaurus dorsalis. Physiological Zoology 60(6):640-658.

Moberly, W. R. 1963. Hibernation in the desert iguana, *Dipsosaurus dorsalis*. Physiological Zoology 36(2):152-160.

Nagy, K. A. 1973. Behavior, diet and reproduction in a desert lizards, *Sauromalus obesus*. Copeia 1:93-102.

Patnaik, B. K., and H. N. Behera. 1981. Age determination in the tropical agamid garden lizard, *Calotes versicolor* (DAUDIN), based on bone histology. Experimental Gerontology 16:295-307.

Pérez-Buitrago, N., García, M. A., Sabat, A., Delgado, J., Álvarez, A., McMillan, O., and S. M. Funk. 2008. Do headstart programs work? Survival and body condition in headstarted Mona Island iguanas *Cyclura cornuta stejnegeri*. Endangered Species Research 6:55-65.

Ricqlès, de A., and V. de Buffrénil. 1996. Bone histology, heterochronies and the return of tetrapods to life in water: where are we? In J. M. Mazin and V. de Buffrénil, Secondary Adaptation of Tetrapods to Life in Water, pp. 289-310. Proceeding of the international meeting Poitiers, Verlag Dr. Friedrich Pfeil, München.

Sander, P. M. 1989. The pachypleurosaurids (Reptilia: Nothosauria) from the Middle Triassic of Monte San Giorgio (Switzerland) with the description of a new species. Philosophical Transaction of the Royal Society B 325(1230):561-666.

Scheyer, T. M., and M. R. Sánchez-Villagra. 2007. Carapace bone histology in the giant pleurodiran turtle *Stupendemys geographicus*: phylogeny and function. Acta Palaeontologica Polonica 52:137-154.

Shine, R., and E. L. Charnov. 1992. Patterns of survival, growth, and maturation in snakes and lizards. American Naturalist 139(6):1257-1269.

Taylor, M. A. 2000. Functional significance of bone ballast in the evolution of buoyancy control strategies by aquatic tetrapods. Historical Biology 14:15-31.

Trillmich, F., and K. G. K. Trillmich. 1984. The mating system of the marine iguana (*Amblyrhynchus cristatus*). Zeitschrift für Tierpsychologie 63:141-172.

Trillmich, K. G. K., and F. Trillmich. 1986. Foraging strategies of the marine iguana, *Amblyrhynchus cristatus*. Behavior, Ecology and Sociobiology 18(4):259-266.

Troyer, K. 1984. Small differences in daytime body temperature affect digestion of natural food in an herbivorous lizard (*Iguana iguana*). *Comparative Biochemistry and Physiology* (A) 87:623-626.

Werner, D. I. 1982. Social organization and ecology of land iguanas, *Conolophus subcristatus*, on Isla Fernandina, Galapagos. In G. M. Burghardt and A. S. Rand (eds.), Iguanas of the World, their Behavior, Ecology, and Conservation, pp. 342-365. New Series in Animal Behavior, Ecology, Conservation and Management.

Werner, D. I. 1983. Reproduction in the iguana *Conolophus subcristatus* on Fernandina Island, Galapagos: clutch size and migration costs. American Naturalist 121(6):757-775.

Wiens, J. J., and B. D. Hollingsworth. 2000. War of the iguanas: conflicting molecular and morphological phylogenies and

long-branch attraction in iguanid lizards. Systematic Biology 49(1):143-159.

Wiewandt, T. A. 1982. Evolution of nesting patterns in iguanine lizards. In G. M. Burghardt and A. S. Rand (eds.), Iguanas of the World, their Behavior, Ecology, and Conservation, pp. 119-141. New Series in Animal Behavior, Ecology, Conservation and Management.

Wikelski, M., and M. Hau. 1995. Is there an endogenous tidal foraging rhythm in marine iguanas? Journal of Biological Rhythms 10(4):335-350.

Wikelski, M., and C. Thom. 2000. Marine iguanas shrink to survive El Niño - Changes in bone metabolism enable these adult lizards to reversibly alter their length. Nature 403:37-38.

Wikelski, M., and F. Trillmich. 1997. Body size and sexual size dimorphism in marine iguanas fluctuate as a result of opposing natural and sexual selection: an island comparison. Evolution 51(3): 922-936.

Wikelski, M., Carrillo, V., and F. Trillmich. 1997. Energy limits to body size in a grazing reptile, the Galapagos marine iguana. Ecology 78(7):2204-2217.

Wikelski, M., Gall, B., and F. Trillmich. 1993. Ontogenetic changes in food intake and digestion rate of the herbivorous marine iguana (*Amblyrhynchus cristatus*, Bell). Oecologia 94:373-379.

Zug, G. R., and A. S. Rand. 1987. Estimation of age in nesting female *iguana iguana*: testing skeletochronology in a tropical lizard. Amphibia-Reptilia 8:237-250.

Chapter 8:

Conclusion

Drawing: B. Scheffold
Middle photograph: U. Koller
Lower left photograph: I. Williams
Lower right photograph: Nadav Pezaro

The chapters of this thesis present the first exploration of limb formation on the basis of osteogenesis for explaining the morphological diversity in two parallel radiations of eureptiles. It is showed that osteogenesis, including the order in the ossification sequences and the bone microstructure, reflects not only phylogeny but is also highly influenced by similar modes of life in both fossil and Recent eureptilian taxa.

The timing of when bones are formed reflects their relative importance for developmental processes and/or selection pressures in tetrapods with different modes of life (Chapter 3; Greer et al., 1998; Shapiro et al., 2007; Fröbisch, 2008). In Recent reptiles, ossification studies are mainly based on cleared and double-stained embryos and neonates (e.g., Chapter 2 and 3, Appendix 1; e.g., Rieppel, 1992; Sheil and Greenbaum, 2005; Werneburg et al., 2009), thus, reflecting primary perichondral and primary endochondral ossification processes (Castanet et al., 1993). Immature fossil pachypleurosaurids reveal additional ossification (i.e., compaction) processes that lead to pachyosteosclerotic bones (Chapter 4 to 5). Conspicuous taphonomic compression patterns, which are visible from external view, reflect the grade in periosteal accretion of primary bone material along the outer wall of the cortex, as well as the endosteal remodelling processes in the medullary region (Chapter 4). These bone deposition activities, which are summarised as additional compaction processes, start in the same conserved order as the onset of the ossification in Recent surface dwelling terrestrial lacertilian squamates (plesiomorphic ancestral condition for terrestrial surface dwelling eureptiles; Chapter 2 and 4). In contrast, the data of the order of the final phase of these additional compaction processes reveals similar trends, although with interspecific variation, to the ossification pattern of Recent semi-aquatic or aquatic (eu)reptiles (Chapter 4; Rieppel, 1993; Fröbisch, 2008; Werneburg et al., 2009). Results show that the phases of the compaction processes of the stratigraphically oldest pachypleurosaurid taxon, *Serpianosaurus mirigiolensis,* is more similar to ossification sequences of Recent terrestrial surface dwelling lizards than all other pachypleurosaurids. This is contrary to the findings of the osteogenetic pattern in the stratigraphically youngest pachypleurosaurid taxon, *N. edwardsii,* which shows the most differences to the hypothesised plesiomorphic ancestral condition for terrestrial surface dwelling eureptiles. The ossification sequence in lizards with body elongation and/or limb reduction shows heterochronic shifts in relation to the order of ossification in Recent terrestrial surface dwelling lizards. The number of heterochronic shifts increases with a mode of life that develops towards fossoriality (Chapter 3). The osteogenetic sequences of burrowing lizards, that show a similar locomotor mode to the aquatic pachypleurosaurids when moving through leaf-litter or sand, share abundant features with both surface dwelling relatives and aquatic reptiles (Chapters 3 and 4). Similar morphological changes in body form that are observed in the stratigraphical series of the pachypleurosaurids (Chapter 4), as well as in the transformation series of Recent burrowing lizards (Chapter 3) are presumably the result of similar selection pressures and developmental processes. However, the relative importance of these factors remains unknown at this point, as are the functional consequences of limb reduction (Chapter 3 and 4; e.g., Gans 1975; Gans and Gasc 1990; Gasc and Gans 1990; Brandley et al., 2008). A few studies investigate

the developmental basis for these morphological trends (Chapter 3 and 4; Cohn and Tickle 1999; Shapiro 2002; Shapiro et al. 2003; Carroll et al. 2005), but further studies are needed to understand these processes.

Studies on bone histology often focus on the description of bone tissue matrices and its vascularisation without further consideration of changes in the spacing pattern of lines of arrested growth in combination with the bone compactness data (Girondot and Laurin, 2003). As these bone histological parameters support ecological data of Recent reptiles (Chapter 7; e.g., Castanet, 1985; Castanet and Baez, 1991), they can reveal further information on the life history of fossil clades (see Chapter 5; Canoville and Laurin, 2010) and even allow a more resolved classification than only the classic bone histological differentiation of lamellar-zonal and fibrolamellar bone types (Francillon-Viellot et al., 1990). Chapter 7 shows that in the case of the marine iguana (*Amblyrhynchus cristatus*), bone histological data also reflects seasonal shifts in the temperature and therefore, its implications can be used to observe growth pattern before and after sexual maturity is reached. The reproduction cycle that influences bone growth of the marine iguana can be observed especially well in this case based on the elongated phases of slow bone deposition, which leads to avascular lamellar-zonal bone. Therefore, avascular lamellar-zonal bone type that shows neither a change in vascularisation pattern nor a change in bone tissue during ontogeny, still possesses the potential to reveal detailed information on life history traits in the marine iguana, such as the age of sexual maturity, as well as the rate of growth.

Recent lizards show the same type of lamellar-zonal bone as the pachypleurosaurids from Monte San Giorgio, although the latter displays more variation in growth rates that result in bone matrices with different grade of organisation of the collagenous fibres, the vascularisation pattern, as well as in the alignment of the LAGs (i.e., spacing pattern). Therefore, lamellar-zonal bone type can display a wide range of different vascularisation pattern differently packed bone tissue that are used as indicators for two different lifestyles within the four pachypleurosaurids (Chapter 5). Bone histology data further reveal an evolutionary trend for an increased adaptation to the same mode of life for *N. edwardsii* in comparison with *S. mirigiolensis* (Chapter 5).

The conducted studies on bone histology further show that none of the sauropterygians from Monte San Giorgio reveal fibrolamellar bone in the long bones, except for *Nothosaurus* which has been only fragmentarily recorded in the lagoonal sediments of Monte San Giorgio. *Nothosaurus* is regarded as a pelagic swimmer in open marine environments as revealed by osteoporotic-like long bones in adults with an abundant, but irregular amount of fibrolamellar bone distributed between lamellar-zonal bone type (Krahl et al., 2009; Klein, 2010). However, the Nothosauria, which include both *Nothosaurus* and *Ceresiosaurus*, and the Pachypleurosauria (except for *Anarosaurus heterodontus*) both predominantly show the slow growing plesiomorphic lamellar-zonal bone type as seen in Recent lacertilian squamates (Chapter 5 to 7; Krahl et al., 2009; Klein, 2010). Although a wide range of bone deposition rates can produce similar bone tissues (Margerie et al., 2004), lamellar-zonal bone type is generally hypothesised to result from low bone deposition

rates and thus, reflect lower metabolic rates. In contrast, fibrolamellar bone type results from high metabolic rates (Horner et al., 2001; Padian et al., 2001) and is the predominant bone matrix of pistosauroids, which were globally distributed (e.g., Rieppel, 2000). Their high metabolism possibly allowed them to spread through the colder seas. Therefore, bone histological data reveals an increased dependence of the Nothosauria and the Pachypleurosauria on external conditions most possibly restricted them to the warm epicontinental seas that vanished at the end of the Triassic (Klein, 2010). In summary, bone histology indicates growth and metabolic rates, age at sexual maturity, longevities and habitat preferences in the sauropterygians. The occurrence of lamellar-zonal bone type is typical for sauropterygians in lagoonal environments (pachypleurosaurids and *Ceresiosaurus* spp. from Monte San Giorgio;), whereas fibrolamellar bone type is preserved in species with a more open marine lifestyle (i.e., *Nothosaurus* spp., pistosauroids; Chapter 6).

Whilst chapter 5 to 7 indicate that bone tissue types in combination with the spacing pattern of the LAGs can provide information on life history traits of sauropterygians and lizards the lack of such histological information for any other Recent reptile currently precludes further evaluation of these findings in the context of different modes of life. However, with the advancement of imaging techniques that permit the recognition of these features without invasive methods, the outlook is likely to change in the near future. Possible changes in the microstructure of bones in lizards with different modes of life, such as surface dwelling versus burrowing forms which show body elongation and/or reduced limbs (decreased number of phalanges and/or shortening of the distoproximal length of the stylopodial and zeugopodial regions), would be worth investigating. Future projects could address questions such as: 1) How is the bone microstructure of limbs in a transformation series of lizard species towards fossoriality modified during their ontogeny or phylogeny? 2) Is an imminent reduction of a skeletal element linked to an incomplete resorption of the calcified precursor during the ontogeny of different lizard morphotypes? 3) How is the musculature altered in different lizard morphotypes? 4) How are possible changes in the musculature linked to heterochronic shifts in the osteogenetic sequences?

Literature cited

Brandley, M. C., Huelsenbeck, J. P., Wiens, J. J. 2008. Rates and patterns in the evolution of snake-like body form in squamate reptiles: evidence for repeated re-evolution of lost digits and long-term persistence of intermediate body forms. *Evolution* 1-23 [doi:10.1111/j.1558-5646.2008.00430.x].

Canoville, A., Laurin, M. 2010. Evolution of humerual microanatomy and lifestyle in amniotes, and some comments on paleobiological inferences. *Biological Journal of the Linnean Society* 100: 384-406.

Caldwell, M. W. 1997. Limb osteology and ossification patterns in *Cryptoclidus* (Reptilia: Plesiosauria) with a review of sauropterygian limbs. *Journal of Vertebrate Paleontology* 17: 295-307.

Castanet, J. 1985. La squelettochronologie chez les Reptiles, I. Résultats expérimentaux sur la signification des marques de

croissance squelettiques chez les Lézards et les Tortues (1). *Annales des Sciences Naturelles*, *Zoologie, Paris* 13e Série Volume 7: 23-40.

Castanet, J., Baez, M. 1991. Adaptation and evolution in Gallotia lizards from the Canary Islands: age, growth, maturity and longevity. *Amphibia-Reptilia* 12: 81-102.

Castanet, J., Francillon-Vieillot, H., Meunier, F. J., Ricqlès, A. de. 1993. Bone and Individual Aging: In: Bone, Vol. 7. Bone Growth-B, B. K. Hall (Ed.), CRC Press, Boca Raton, Florida, pp. 245-283.

Carroll, S. B., Grenier, J. K., Weatherbee, S. D. 2005. From DNA to Diversity: Molecular Genetics and the Evolution of Animal Design. 2nd edition, Blackwell Publishing, Malden, MA.

Cohn, M. J., Tickle, C. 1999. Developmental basis of limblessness and axial regionalization in snakes. *Nature* 399: 474-479.

Gans, C. 1975. Tetrapod limblessness: evolution and functional corollaries. *American Zoologist* 15: 455-467.

Gans, C., Gasc, J.-P. 1990. Tests on the locomotion of the elongate and limbless reptile *Ophisaurus apodus* (Sauria: Anguidae). *Journal of Zoology London* 222: 517-536.

Gasc, J.-P., Gans, C. 1990. Test on locomotion of the elongate and limbless lizard *Anguis fragilis* (Squamata: Anguidae). *Copeia* 1990: 1055-1067.

Girondot, M., Laurin, M. 2003. Bone profiler: a tool to quantify, model, and statistically compare bone-section compactness profiles. *Journal of Vertebrate Paleontology* 23(2): 458-461.

Greer, A., Caputo, V., Lanza, B., Palmieri, R. 1998. Observations on limb reduction in the scincid lizard genus *Chalcides*. *Journal of Herpetology* 32: 244-252.

Francillon-Vieillot, H., Buffrénil, V. de, Castanet, J., Géraudie, J., Meunier, F. J., Sire, J. Y., Zylberberg, L., Ricqlès, A. de. Microstructure and mineralization of vertebrate skeletal tissues. 1990. Chapter 20. In: Skeletal Biomineralization: Patterns, Processes and Evolutionary Trends, J.G. Carter (Ed.), Volume I., Van Nostrand Reinhold, New York, pp. 471-530.

Fröbisch, N. B. 2008. Ossification patterns in the tetrapod limb – conservation and divergence from morphogenetic events. *Biological Reviews* 83: 571-600.

Horner, J. R., Ricqlès, A. de, Padian, K. 2000. Long bone histology of the hadrosaurid dinosaur *Maiasaura peeblesorum*: growth dynamics and physiology based on an ontogenetic series of skeletal elements. *Journal of Vertebrate Paleontology* 20: 115-129.

Klein, N. 2010. Long bone histology of Sauropterygia from the Lower Muschelkalk of the Germanic Basin provides unexpected implications for phylogeny. *PLoS ONE* 5(7): e11613. doi:10.1371/journal.pone.0011613.

Krahl, A., Sander, P. M., Klein, N. 2009. Long bone histology of Middle Triassic eusauropterygians (Nothosauria and Pistosauria) and its implications for paraxial swimming. *Journal of Vertebrate Paleontology* 29: 129A.

Margerie, E. de, Robin, J.-P., Verrier, D., Cubo, J., Groscolas, R., Castanet, J. Assessing a relationship between bone microstructure

and growth rate: a fluorescent labelling study in the king penguin chick (*Aptenodytes patagonicus*). *The Journal of Experimental Biology* 207: 869-879.

Padian, K., Ricqlès, A. de, Horner, J. R. 2001. Dinosaurian growth rates and bird origins. *Nature* 412: 405-408.

Rieppel, O. 1992. Studies on skeleton formations in reptiles. III. Patterns of ossification in the skeleton of *Lacerta vivipara* Jacquin (Reptilia: Squamata) *Fieldiana*, *Zoology*, N.S. 68: 1-25.

Rieppel, O. 1993. Studies on skeleton formation in reptiles. V. Patterns of ossification in the skeleton of *Alligator mississipiensis* Daudin (Reptilia, Crocodylia). *Zoological Journal of the Linnean Society* 109: 301-325.

Rieppel, O. 2000. Sauropterygia I: Placodontia, Pachypleurosauria, Nothosauroidea, Pistosauroidea. In: Encyclopedia of Paleoherpetology, P. Wellnhofer (Ed.), Verlag Dr. Friedrich Pfeil, München, p. 334.

Sander, P. M. 1990. Skeletochronology in the small Triassic reptile *Neusticosaurus*. *Annales des Sciences Naturelles, Zoologie*, Paris 13ème Série 11: 213-217.

Shapiro, M. D. 2002. Developmental morphology of limb reduction in *Hemiergis* (Squamata: Scincidae): chondrogenesis, osteogenesis, and heterochrony. *Journal of Morphology* 254: 211-231.

Shapiro, M. D., Hanken, J., Rosenthal, N. 2003. Developmental basis of evolutionary digit loss in the Australian lizard *Hemiergis*. *Journal of Experimental Zoology B (Molecular and Developmental Evolution)* 297B: 48-56.

Shapiro, M. D., Shubin, N. H., Downs, J. P. 2007. Limb diversity and digit reduction in reptilian evolution. In: Fins into Limbs, B. K. Hall (Ed.), The University of Chicago Press. pp. 225-244.

Sheil, C. A., Greenbaum, E. 2005. Reconsideration of skeletal development of *Chelydra serpentina* (Reptilia: Testudinata: Chelydridae): evidence for intraspecific variation. *Journal of Zoology*, London 265: 235-267.

Sheldon, M. A. 1997. Ecological implications of mosasaur bone microstructure. In: Ancient Marine Reptiles, J. M. Callaway and E. L. Nicholls (Eds.), Academic Press: pp. 333-354.

Werneburg, I., Hugi, J., Müller, J., Sánchez-Villagra, M. R. 2009. Embryogenesis and ossification of *Emydura subglobosa* (Testudines, Pleurodira, Chelidae) and patterns of turtle development. *Developmental Dynamics* 238: 2770-2786.

Wiffen, J., Buffrénil, V. de, Ricqlès, A. de, Mazin, J. M. 1995. Ontogenetic evolution of bone structure in Late Cretaceous Plesiosauria from New Zealand. *Geobios* 28(5): 625-640.

Zangerl, R. 1935. *Pachypleurosaurus edwardsi* Cornalia. Osteologie, Variationsbreite, Biologie. In: Triasfauna der Tessiner Kalkalpen IX *Pachypleurosaurus* Schweizer, B. Peyer (Ed.), *Abhandlungen der Schweizerischen Palaeontologischen Gesellschaft* 66, 80 p.

Appendix 1:

Embryogenesis and Ossification of *Emydura subglobosa* (Testudines, Pleurodira, Chelidae) and Patterns of Turtle Development

Ingmar Werneburg, Jasmina Hugi, Johannes Müller, and Marcelo R. Sánchez-Villagra

Published in *Developmental Dynamics* 238, 2770-2786, 2009 / DOI 10.1002/dvdy.22104

Photographis of embryos: J. Hugi
Photograph upper right: Petra Karstedt/ Tiermotive.de

Embryogenesis and Ossification of Emydura *subglobosa* (Testudines, Pleurodira, Chelidae) and Patterns of Turtle Development

Ingmar Werneburg,[1]* Jasmina Hugi,[1] Johannes Müller,[2] and Marcelo R. Sánchez-Villagra[1]

Using the Standard Event System (SES) to study patterns of vertebrate development, we describe a series of 17 embryos of the pleurodire turtle *Emydura subglobosa*. Based on a sequence heterochrony analysis including 23 tetrapod taxa, we identified autapomorphic developmental shifts that characterise Testudines, Cryptodira, and Pleurodira. The main results are that Testudines are characterised by an autapomorphic late neck development, whereas pleurodires and cryptodires show a different developmental timing of the mandibular process. Additionally, we described the ossification pattern of *E. subglobosa* and compared the data to those of five other turtles. Pleurodires show the epiplastron to ossify before or simultaneously with maxilla and dentary. In contrast, cryptodires show a later ossification of this bone. Because evolutionary developmental studies on turtles have previously focused only on "model organisms" that all belong to Cryptodira, we underline the necessity to include a pleurodire taxon for a more comprehensive, phylogenetically more informative approach. *Developmental Dynamics 238:2770–2786, 2009.* © 2009 Wiley-Liss, Inc.

Key words: staging system (SES); heterochrony; embryogenesis; Parsimov; skeletogenesis; Pleurodira; Cryptodira; skull, skeleton

Accepted 22 August 2009

INTRODUCTION

Several methods have been developed to analyse developmental patterns within a phylogenetic framework (Smith, 1997; Richardson et al., 2001; Jeffery et al., 2005; Colbert and Rowe, 2008; Harrison and Larsson, 2008). As a basis for comparison in both molecular and morphological studies, a reference system is necessary to describe the developmental features of an embryo, which is usually done by focusing on only a few selected species, or "model organisms." However, there are changes in the timing of developmental characters (Haeckel, 1896), so-called sequence heterochronies (Smith, 1997; Velhagen, 1997), that become obvious when embryos of different species are compared to each other. This makes it difficult to use a staging system developed for a species A to analyse the development of a species B. As a result, the use of "model organisms" has recently been questioned (Mitgutsch, 2003; Sellier et al., 2006; Jenner and Wills, 2007) and new "staging tables" were developed for many additional species (Cretekos et al., 2005; Boughner et al., 2007; Sanger et al., 2008; Nolte et al., 2009; de Jong et al., 2009). Because all these are based on a different breadth of sampled specimens, a certain degree of simplification, and a somewhat typologically confined morphological scope (Hopwood, 2005, 2007), Werneburg (2009) developed a standard system that explicitly considers variation to describe developmental characters in a comparable and traceable way that may serve as reference in Evo-Devo research. This new system avoids typologisation and simplification as seen in many "staging tables," and includes an expandable standard reference list of vertebrate

Additional Supporting Information may be found in the online version of this article.

[1]Paläontologisches Institut und Museum der Universität Zürich, Zürich, Switzerland
[2]Museum für Naturkunde, Leibniz-Institut für Evolutions- und Biodiversitätsforschung an der Humboldt-Universität zu Berlin, Berlin, Germany

Grant sponsor: Swiss National Fond; Grant number: 3100A0-116013; Grant sponsor: Forschungskredit der Universität Zürich; Grant number: 3772; Grant sponsor: Deutsche Forschungsgemeinschaft; Grant number: Mu 1760/2-3.

***Correspondence to: Ingmar Werneburg, Paläontologisches Institut und Museum, Karl Schmid-Strasse 4, 8006 Zürich, Switzerland. E-mail: ingmar_werneburg@yahoo.de**

DOI 10.1002/dvdy.22104
Published online 16 October 2009 in Wiley InterScience (www.interscience.wiley.com).

developmental characters to document both inter- and intraspecific variability.

The growing research on turtle embryology has been triggered by an interest in the evolutionary and developmental origin of the unique turtle shell (Nagashima et al., 2005, 2007, 2009; Gilbert et al., 2001, 2008; Scheyer et al., 2008; Li et al., 2008), and the singular skull anatomy among living reptiles lacking any fenestrations (Rieppel, 1990; Müller, 2003). Although the phylogenetic position of turtles within Amniota (see Rieppel, 2004, 2008) and the phylogenetic relationships within turtles (Gaffney and Meylan, 1988; Joyce, 2007; Scheyer, 2007) remain unresolved, insights from embryology have been successfully employed to address questions on turtle evolution (Goodrich, 1930; Burke, 1991; Eßwein, 1992; Nagashima et al., 2005, 2007; Sánchez-Villagra et al., 2007; Werneburg and Sánchez-Villagra, 2009).

For Testudines, two standard "staging tables" have been traditionally used. Miller (1985) described a "31 staged embryology" for marine turtles (Chelonioidea), which was of interest mostly for biological conservation research (Bell et al., 2003), whereas in many other laboratories the common snapping turtle *Chelydra serpentina* (Cryptodira) became a popular "model organism" based on Yntema's (1968) "27 staged embryology: (Galbraith et al., 1989; Rieppel, 1990, 1993; O'Steen, 1998; Packard et al., 2000; Sheil and Greenbaum, 2005; Franz-Odendaal, 2006). In recent years, the prehatching development of additional turtle species was analysed (Guyot et al., 1994; Beggs et al., 2000; Tokita and Kuratani, 2001; Greenbaum and Carr, 2002). Nevertheless, all these observations used either Miller's (1985) or Yntema's (1968) "staging tables" as a reference, and were of a categorical kind obviating information on intraspecific variability (Werneburg, 2009).

Extant turtles can be subdivided into two monophyletic clades, Pleurodira and Cryptodira (Gaffney and Meylan, 1988). Depending on the phylogenetic hypothesis, the clades either diverged from each other as early as 220 Million years ago, in the Late Triassic, or at the latest in the Middle Jurassic, around 165 Million years ago (Danilov and Parham, 2008; Scheyer and Anquetin, 2008). Pleurodires and cryptodires can be mainly distinguished from each other by the mechanism of head retraction. While the former group, the side-necked turtles, put their neck/head sideward under the anterior edge of the shell, the latter group, hidden-necked turtles, retract their neck/head in an S-shape inside their shell. In addition, there are several further cranial and postcranial characters that characterise the two groups, such as the position of the trochlear process in the jaw adductor chamber (Schumacher, 1973; Gaffney and Meylan, 1988) or the connection mode between the pelvis and the shell (summarised, e.g., by Mickoleit, 2004).

In the present contribution, we provide for the first time a case study of the Standard Event System (SES) (Werneburg, 2009) to describe an embryonic series. While traditional turtle "model organisms" all belong to Cryptodira, species of which possess highly derived characters (Joyce, 2007; Scheyer, 2007), only few studies in comparative embryology have so far considered pleurodires (Eßwein, 1992; Sánchez-Villagra et al., 2007; Vieira et al., 2007, 2009; Scheyer et al., 2008; Fabrezi et al., 2009; Bona and Alcalde, 2009). Here we describe and analyse the early development of the red-bellied short-necked turtle *Emydura subglobosa* (Krefft, 1876), which is a common carnivore species living in freshwater environments of Northern Australia and Papua New Guinea (Legler and Georges, 1993). Tzika and Milinkovitch (2008) have already proposed *E. subglobosa* to be a suitable pleurodiran species for evolutionary developmental studies due to its easy keeping and breeding requirements (Nicol, 1993; Highfield, 1996; Hennig, 2001; Pawlowski, 2001; Schwarz, 2006).

The sequence of developmental events in *Emydura subglobosa*, here described in detail, was previously included in the developmental data set of Werneburg and Sánchez-Villagra (2009), in which the development of 15 turtle species and 8 tetrapod taxa were comparatively analysed using the Parsimov-approach (Jeffery et al., 2005). The authors tested alternative hypotheses for the position of turtles within Amniota as well as hypotheses for turtle ingroup relationships (Fig. 1). A total of 56 heterochronic shifts of developmental events supported a sister group relationship of Testudines to all remaining extant reptiles (crocodiles + birds and lizards/snakes + tuatara) when Chelonioidea (marine turtles) were assumed to be basal within cryptodires (Fig. 1B). By contrast, in the present study we use the heterochrony data from Werneburg and Sánchez-Villagra (2009) to focus on the temporal shifts of external morphology development characterising Testudines, Pleurodira, and Cryptodira. Furthermore, we describe the pattern of ossification of *E. subglobosa* and compare it to the timing of ossification of five other turtle species (Supp. Table S1, which is available online).

RESULTS

Staging System of *Emydura subglobosa* (Figs. 2 and 3, Supp. Figs. S1–S18)

For illustrations, see Figures 2 and 3; additional figures and depictions can be found in Supp. Figures S1–S18, which are available online. Abbreviations: AER = apical epidermal ridge, Cat. No. = Catalogue number, CB = carapace width, CL = carapace length, CRL = crown-rump length, CPH = carapace-plastron height (total height of shell), d = days of incubation, PL = plastron length, PB = plastron width, SES = Standard Event System (Werneburg, 2009).

E. subglobosa 1.

Twenty-three somite pairs are visible. The external nares and the otic vesicle are developed. The eye is characterised by the presence of an optic fissure and a clear contour of the lens/iris. The forelimb ridge has formed. The maxillary process has reached the midline level of the eye and the mandibular process has reached the posterior level. The 2nd to 5th pharyngeal arches as well as the 1st to 4th pharyngeal slits are visible. *Age: 6d, CRL: 5.42 mm, Cat. No.: PIMUZ lab No. 2009.01.*

E. subglobosa 2.

Thirty-two somite pairs are visible. The forelimb bud consists of a

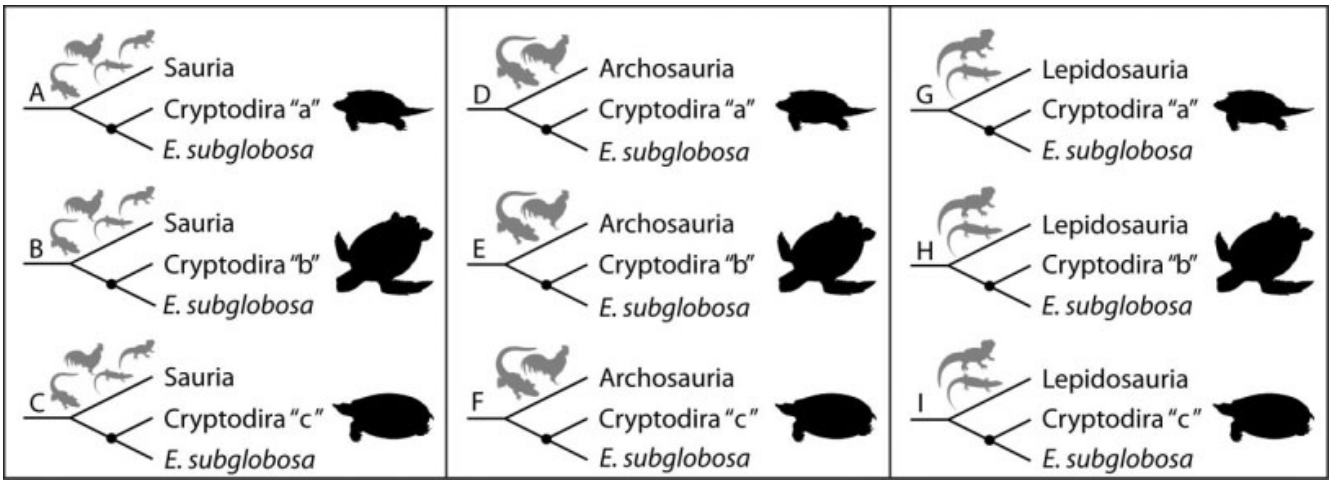

Fig. 1. Tested topologies for the position of Testudines relative to extant reptiles (Sauria, Archosauria, or Lepidosauria) and alternative hypotheses for turtle ingroup relationships. *Emydura subglobosa* represents the only pleurodire species opposing Cryptodira either with (**a**) snapping turtles (Chelydridae), (**b**) marine turtles (Chelonioidea), or (**c**) soft shell turtles (Trionychia) as basal taxa. For details and references, see text. Figure modified from Werneburg and Sánchez-Villagra (2009).

terminal paddle. The maxillary process has reached the anterior level of the lens while the mandibular process has reached its posterior level. The urogenital papilla bud is developed. *Age: 7d, CRL: 13.5 mm, Cat. No.: PIMUZ labNo. 2009.02*.

E. subglobosa 3.

Thirty-nine somite pairs are visible and the pupil has started to form. The forelimb is elongated, forming an elbow, and an apical epidermal ridge has formed. The hind limb is paddle-shaped and also shows an AER. The maxillary process has reached the anterior level of the eye while the mandibular process has reached the midline level. *Age: 9d, CRL: 15.8 mm, Cat. No.: PIMUZ labNo. 2009.03*.

E. subglobosa 4.

The exact somite number is now difficult to discern. The otic capsule has become inconspicuous. The forelimb and the hind limb have developed digital plates. The maxillary and the frontonasal process are fused. The mandibular process has reached the anterior level of the lens. The 2nd pharyngeal arch (the hyoid arch) has formed an opercular flap. The carapacial ridge is now visible. *Age: 12d, CL: ca. 3.5 mm, Cat. No.: PIMUZ labNo. 2008.19*.

E. subglobosa 5.

The thoracal bulbus comprising heart and liver has disappeared. The mandibular process has reached the level of the frontonasal process and simultaneously the point of occlusion with the upper jaw. All pharyngeal slits are closed. A cervical flexure of 90° can be recognised. The lower eyelid has formed and already started overgrowing the eye, reaching the ventral level of the lens. The caruncle is visible. The carapace is clearly delimited around its periphery and projects beyond the root of the tail. *Pigment cells are visible on the carapace, the tail, and the limbs, but not yet on the plastron and the throat. A few cells have already reached the digital plate. The neck and the dorsum of the head also show several scattered pigment cells. Lateral to the neck and on the buccal/ear region, a distinct dark horizontal streak-like cluster of pigment cells has formed. On the dorsolateral face of the snout, anteroventral to the eye, a small concentration of pigment cells is visible. Age: 13d, CL: ca. 9 mm, CB: ca. 7 mm, Cat. No.: PIMUZ labNo. 2008.23*.

E. subglobosa 6.

The fingers are longer than wide. Scales are visible on the neck, and scutes have developed on the carapace. *Pigment cells on the carapace are widespread and the translucent costal and neural sutures leave the impression of a rough orientation of the cells along the sutures of the scutes. The pigment streak lateral to the neck has spread towards the dorsum of the neck. The pigment streak lateral to the buccal/ear region has a horizontal expansion but its posteriormost part is bent dorsally. Together with the dorsal head pigment cells, the buccal/ear streak circumvents a white non-pigmented region posterior to the eye. Age: 21d, CL: ca. 12 mm, CPH: ca. 7.5 mm, PL: ca. 9 mm, Cat. No.: PIMUZ labNo. 2008.24*.

E. subglobosa 7.

All 13 scleral papillae are visible in the eye and the first claws occur as horny, clearly distinct structures. *Pigmentation has increased considerably, particularly in the digital region, the carapace, and the dorsum of the head. In part, the cells are no longer delineable. The pigment cell streak lateral to the neck has completely spread into the dorsal neck pigmentation and is no longer distinguishable either. The claws are not pigmented yet. Pigmentation along the sulci (the sutures) of the carapacial scutes has increased. The buccal/ear streak and the pigment spot dorsolateral to the snout have fused ventral to the eye to form a frontomaxillary streak, the pigmentation of which has expanded onto the ventral part of the lower eyelid. Age: 24d, CL: 13.5 mm, CPH: ca. 7 mm, PL: ca. 9 mm, Cat. No.: PIMUZ labNo. 2008.25*.

E. subglobosa 8.

The occipital head projection has disappeared and a clearly delineated

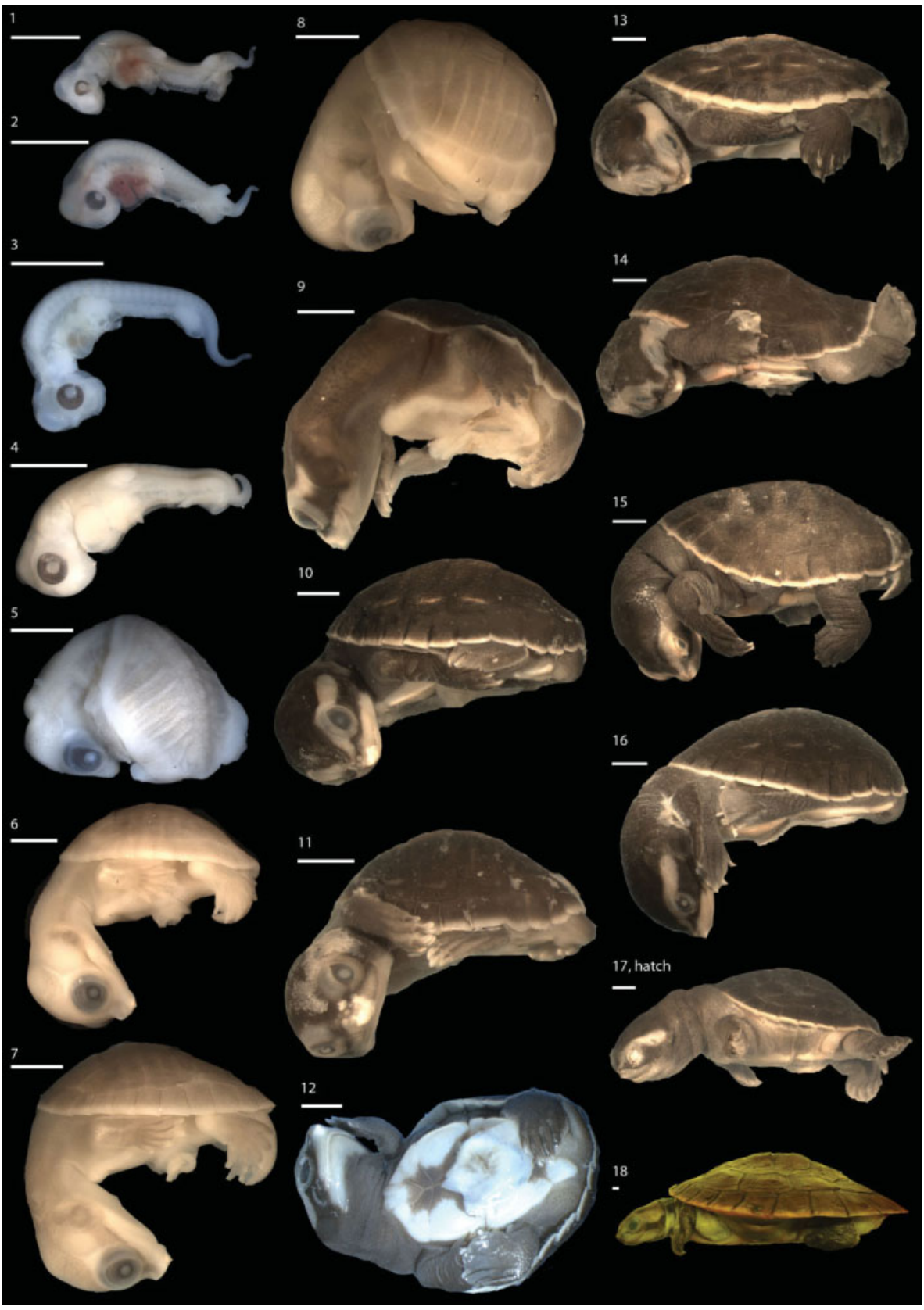

Fig. 2. Developmental series of *Emydura subglobosa* showing the whole body in lateral view. Numbers 1–18 refer to the specimens as described in the text. For detailed illustrations and depictions, see Supp. Figs. S1–18 and Table S1. Scale bars = 3 mm.

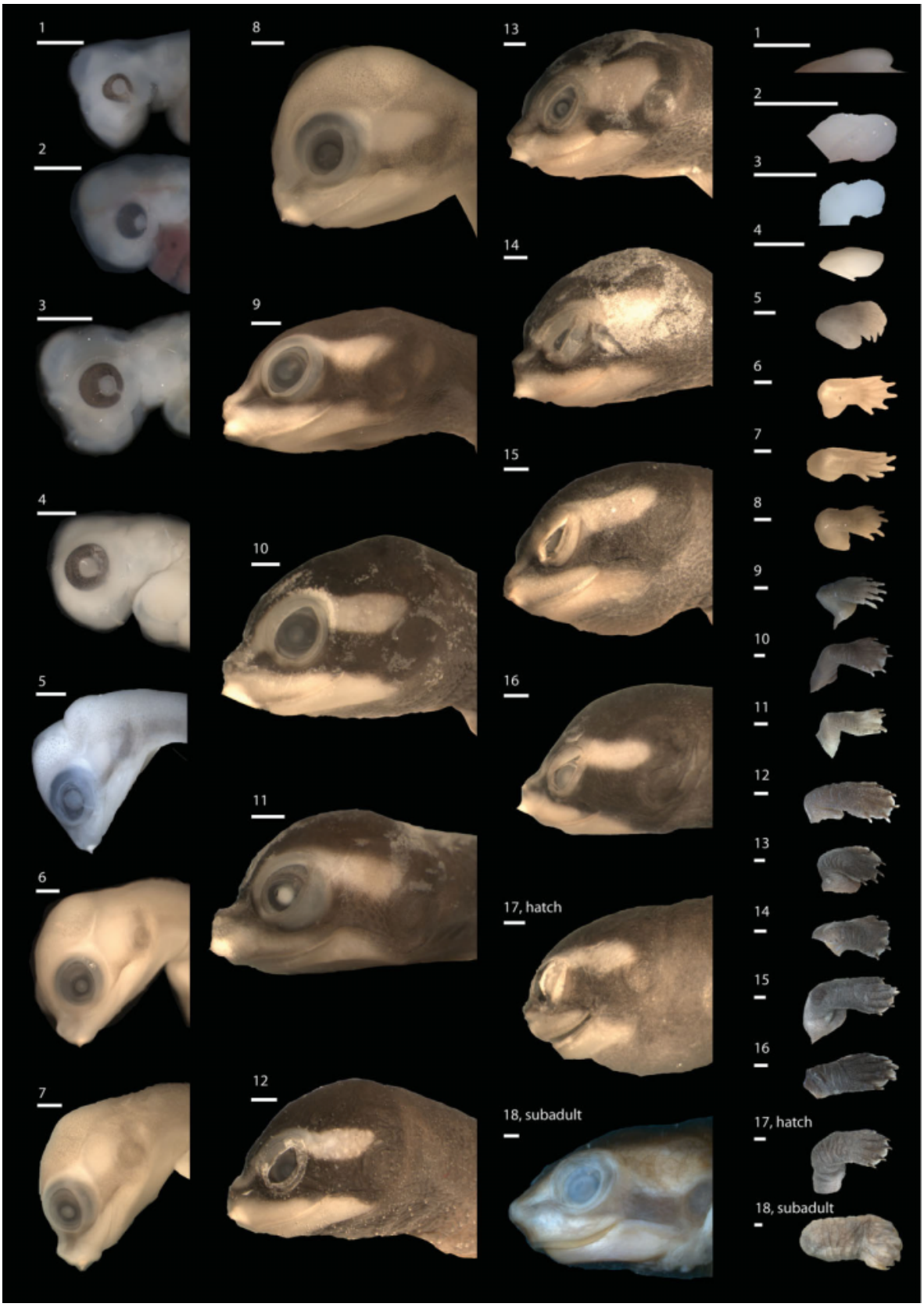

Fig. 3. Developmental series of *Emydura subglobosa* showing the heads (in lateral view) and the left forelimbs (lower arm in dorsal view). Numbers 1–18 refer to the specimens as described in the text. For detailed illustrations and depictions, see Supp. Figs. S1–18 and Table S1. Scale bars = 3 mm.

rhamphotheca has formed. *The white area dorsal to the buccal/ear streak has extended caudad and forms a white temporal streak that from now on is more distinct than the buccal/ear streak. Verrucas occur on the dorsum of the neck. A few pigment cells are detectable on the throat. Age: 26d, CL: 11.08 mm, CB: 8.5 mm, CPH: 8.15 mm, PL: 6.95 mm, PB: 6.75 mm, Cat. No.: PIMUZ labNo. 2009.04.*

E. subglobosa 9.

Scales are now visible on the dorsum of the head and on the throat. Limb scales occur up to the digital region. Scales are also visible on the tail. The urogenital papilla has become inconspicuous and the periphery of the carapace is irregular. *The pigmentation of the carapace has increased and a white non-pigmented border remains around its periphery. Pigment cells are visible on the plastron. The pigmentation of the whole body has extremely increased and pigment cells are only visible on the plastron. The rhamphotecae of both jaws have been entered by pigment cells where they attach the frontomaxillary pigment streak. The rhamphoteca of the upper jaw is also pigmented along its ventral border. The frontomaxillary streak only includes parts of the lower eyelid and the white temporal streak shows a rostrad extension over the upper lid, over parts of the lower eyelid, and over the dorsum of the snout towards the nose. It forms a white frontotemporal streak. Neck and head are peculiarly flexed left laterally and remain in this position until shortly before hatching. Age: 28d, CL: 13.74 mm, CB: 11.26 mm, CPH: 7.19 mm, PL: 10.15 mm, PB: 5.38 mm, Cat. No.: PIMUZ labNo. 2008.28.*

E. subglobosa 10.

The scleral papillae have become inconspicuous. *With an enlarged number of scales, the pigmentation of the whole body has increased. The white frontotemporal streak is sharply contoured and pigment cells are not scattered any longer; its temporal part has moved more dorsal to surround the posterodorsal edge of the eye formed by the eyelids. The digital plates clearly show a web-like shape. Age: 33d, CL: min. 19.1 mm, CB: 16.47 mm, CPH: 9.02 mm, PL: 14.32 mm, PB: 8.6 mm, Cat. No.: PIMUZ labNo. 2009.05.*

E. subglobosa 11.

The pigmentation of the claws has increased. Age: 35d, CL: 13.62, CB: min. 10.75 mm, CPH: 7.21 mm, PL: 10.59 mm, PB: 7.61 mm, Cat. No.: PIMUZ labNo. 2008.29.

E. subglobosa 12.

The upper eyelid has enlarged and covers the eye dorsally up to the level of the upper pupil border. *Age: 36d, CL: 20.26 mm, CB: min. 14.61 mm, CPH: 11.64 mm, PL: 15.7 mm, PB: 8.45 mm, Cat. No.: PIMUZ labNo. 2008.73.*

E. subglobosa 13.

No distinct changes can be noted. *Age: 38d, CL: 22.93 mm, CB: 17.56 mm, CPH: 10.89 mm, PL: 19.29 mm, PB: 9.75 mm, Cat. No.: PIMUZ labNo. 2009.06.*

E. subglobosa 14.

The lower eyelid covers more than half of the eye. *Age: 43d, CL: 21.8 mm, CB: min. 15.44 mm, CPH: 11.17 mm, PL: 15.71 mm, PB: 9.17 mm, Cat. No.: PIMUZ labNo. 2008.74.*

E. subglobosa 15.

The pigmentation of the inframarginal shields (between carapace and plastron) has increased. Age: 50d, CL: 23.03 mm, CB: 18.15 mm, CPH: 11.56 mm, PL: 18.54 mm, PB: 11.73 mm, Cat. No.: PIMUZ labNo. 2009.07.

E. subglobosa 16.

No distinct changes. *Age: 55d, CL: 20.32 mm, CB: 14.28 mm, CPH: 10.02 mm, PL: 16.85 mm, PB: 8.09 mm, Cat. No.: PIMUZ labNo. 2008.75.*

E. subglobosa 17.

The animal has hatched and the cervical flexure of 90° has disappeared. *No specific coloration except for the brownish primary colour. Age: 65d, CL: 24.08 mm, CB: 19.66 mm, CPH: 12.61 mm, PL: 20.47 mm, PB: 11.43 mm, Cat. No.: PIMUZ labNo. 2009.08.*

E. subglobosa 18.

Specific coloration is visible: a reddish periphery of the carapace and a reddish plastron. The frontomaxillary streak remains but is constricted by the light upper rhamphotheca. The white frontotemporal streak has become much darker. Age: subadult, CL: 79.2 mm, CB: 70.95 mm, CPH: 30.36 mm, PL: 60.96 mm, PB: 49.95 mm, Cat. No.: PIMUZ lab No. 2009.09.

Heterochronic Shifts (Tables 1, 2)

Independent of cryptodire ingroup relationships, the shifted events characterising Testudines include the character complexes (as defined by Werneburg, 2009) of general head, eye, and scale development (Table 1a–c), whereas only three neck-related developmental features are common to all tested topologies (Table 1d). When assuming Sauria to be the sister group of turtles (Fig. 1B, Werneburg and Sánchez-Villagra, 2009), Testudines are supported by eight characters (Table 1a), whereas two other sister-group arrangements include fewer shifts for Testudines (Table 1b,c; Archosauria hypothesis: 5; Lepidosauria hypothesis: 6).

For *Emydura subglobosa*, we found 16 terminal shifts common to all tested topologies, which all are in the head and refer to the character complexes of nose, eye, maxillary and mandibular process (Table 2a). For Cryptodira, only one temporal shift is common to all topologies, which is associated with the development of the mandibular process (Table 2b).

Adult Limb Anatomy (Figs. 4 and 5: box)

The adult limb anatomy of *Emydura subglobosa* has not been described so far. Based on the architecture of chondral precursors, we anticipate that the carpus in the adult consists of three carpal rows plus one postaxial element, the pisiform. The proximal carpal row consists of the ulnare and intermedium, the central carpal row of centrale 1 and 2, and the distal row of five carpals named distal carpal 1 to 5. The phalangeal formula for the

TABLE 1. Number of Heterochronic Shifts That Characterise Testudines[a]

Event	Moved	Relative to event(s)
a. Testudines (consensus of all Sauria hypotheses, Fig. 1A–C)		
Head projection disappeared	Early	Throat scales, whole forelimb scales*
Pupil forms	Early	Hind limb paddle
Cervical flexure 90°	Late	Forelimb AER
Cervical flexure disappeared	Late	First claw, whole forelimb scales*, eyelid begun overgrow*, lower half eye
b. Testudines (consensus of all Archosauria hypotheses, Fig. 1D–F)		
Head projection disappeared	Early	Whole forelimb scales
Pupil forms	Early	Mand midline eye
Cervical flexure 90°	Late	Forelimb AER
Cervical flexure disappeared	Late	First claw, whole forelimb scales
c. Testudines (consensus of all Lepidosauria hypotheses, Fig. 1G–I)		
Tail scales	Late	Finger
Cervical flexure 90°	Late	Forelimb AER*
Cervical flexure disappeared	Late	Scleral papillae inconspicuous, first claw, whole forelimb scales*, lower half eye*
d. Testudines (consensus of all hypotheses, Fig. 1A–I)		
Cervical flexure 90°	Late	Forelimb AER
Cervical flexure disappeared	Late	First claw, whole forelimb scales

[a]The heterochronic shifts for all nine tested hypotheses were compared against each other. First only the three saurian-related topologies (a), then only the three archosaur-related topologies (b), the lepidosaur-related topologies (c), and finally a consensus of all hypotheses (d) were compared and the consensus of each was calculated. Results of the tie-included analysis are shown. Results of the tie-excluded analysis overlapping with the tie-included analysis are marked with asterisks. For details see text. The nomenclature of events and their abbreviations follow Werneburg (2009).

TABLE 2. Number of Heterochronic Shifts That Characterise *Emydura subglobosa* and Cryptodira[a]

Event	Moved	Relative to event(s)
a. *Emydura subglobosa* (consensus of all hypotheses, Fig. 1A–I)		
External nares	Early	Optic fissure, 4th arch, 5th arch, 3th slit, 4th slit
Scleral papillae	Late	Finger*, first claw
Max midline eye	Early	Optic fissure, 5th arch, 3th slit
Mand posterior eye	Early	Relative to optic fissure, contour lens/iris
Mand posterior lens	Early	Forelimb paddle, urogenital papilla bud
Mand level frontonasal	Early	Caruncle, carapace beyond tail
b. Cryptodira (consensus of all hypotheses, Fig. 1A–I)		
Mand posterior lens	Late	Hind limb digital plate

[a]Number of heterochronic shifts that characterize *Emydura subglobosa* and Cryptodira when calculating a consensus of all nine test hypotheses (Fig. 1A–I). Tie-including shifts are listed. Results of the tie-excluded analysis overlapping with the tie-included analysis are marked with asterisks. For details see text.

manus is 2-3-3-3-3, the plesiomorphic formula for pleurodirans (Boulenger, 1889; Sánchez-Villagra et al., 2007, Fig. 5). The pes shows a reduced phalangeal formula of 2-3-3-3-2. The tarsus is formed by two tarsal rows. The proximal row consists of the intermedium and fibulare. The distal row is made of five distal tarsals, named distal tarsal 1 to 5. All epiphyses and all tarsals are ossified in the subadult specimen of *E. subglobosa* (specimen 18). In the subadult carpus, the pisiform and the ulnare are still cartilaginous (Fig. 5E).

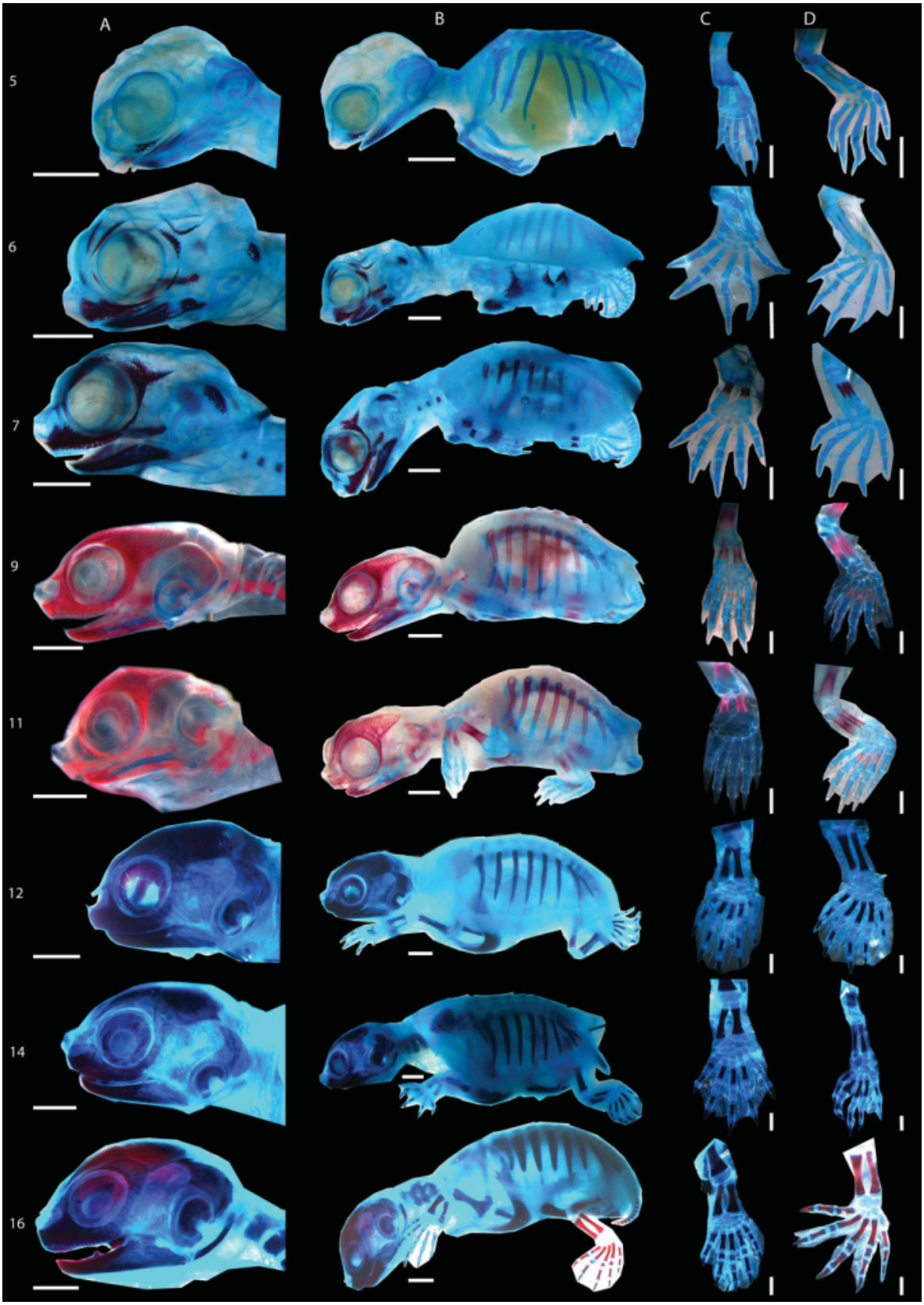

Fig. 4. Cleared and stained specimens of *Emydura subglobosa*. Red, calcified structures (alizarin red); dark blue, cartilage (alcian blue); light blue, connective tissue. Skull (**A**) and whole skeleton (**B**) in lateral view. The left manus (**C**) and pes (**D**) are shown in dorsal view. Row-numbers refer to the specimen numbers as described in the text. Scale bar = (A, B) 2 mm, (C, D) 1 mm.

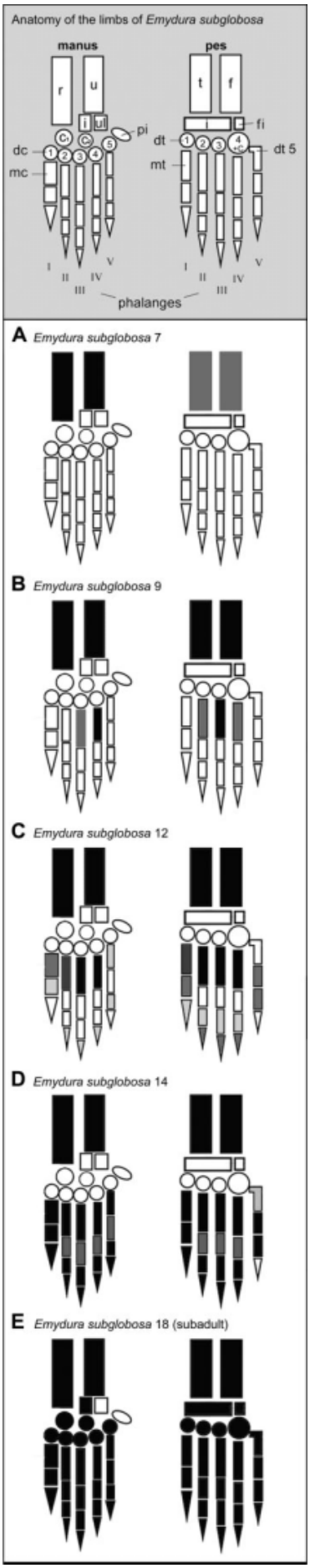

Fig. 5.

Ossification Pattern of *Emydura subglobosa* (Figs. 4, 5, Table 3)

The recorded ossification sequence of *Emydura subglobosa* is summarised in Table 3 and illustrated in Figure 4, the ossification of the forelimb and hind limbs is shown in Figure 5. Note that the younger *E. subglobosa* specimen No. 9 was found to be more advanced in ossification than the older specimen No. 11. These two specimens were not distinguishable by SES-characters when considering the external development. Hence, the order in Table 3 is based on the progress of ossification and not on the age of the specimens (as for the description of external development).

The very first onset of ossification was recorded in two cranial and two postcranial elements of specimen 5, showing the fine-grained sequence epiplastron > maxilla > dentary > humerus. As soon as all plates of the plastron, most parts of the dermatocranium, and all cervical centra start ossification (specimen 6), skeletogenesis starts perichondrally at mid shaft of the cornu branchiale I (specimen 7). The cornu branchiale I is the first element of the splanchnocranium starting ossification. In the same specimen, ossification occurs at the mid shafts of the hind limb stylopods and sequentially at the same region of both the forelimb and hind limb zeugopods. The fine-grained sequence (see Experimental Procedures section) is as follows: radius, ulna > femur > fibula > tibia. In *E. subglobosa*, the timing of the onset of ossification of the forelimb precedes the hind limb in stylopodial and zeugopodial regions. The humerus, radius, and ulna start ossification before corresponding elements of the hind limb. However, first retention of Alizarin Red is visible simultaneously in the metapodials of the forelimbs and hind limbs (specimen 9).

Conversely, the first sign of ossification in the phalanges is visible earlier in the hind limbs than in the forelimbs. In general, ossification starts perichondrally at mid shaft of the diaphyses in every long bone of the limbs and proceeds from proximal to distal with a postaxial dominance.

Anterior dorsal centra as well as anterior dorsal ribs show onset of ossification at the same time as the ulna and radius (specimen 7), closely preceding timing of beginning ossification of the femur. Then, tibia and fibula are next to show perichondral ossification at mid shaft.

All structural elements of the cervical, dorsal, sacral, and caudal vertebrae (i.e., centra, neural arches, and ribs) start ossification independently from each other. Onset of ossification of centra starts cranially (specimen 7) and proceeds in an intervallic anteroposterior direction along the axial skeleton (specimen 11, 9). The centra are the first vertebral structures to show onset of ossification. Onset of ossification of the centra starts first in anterior cervical vertebrae. Later, onset of ossification of the centra is sequentially visible in anterior dorsal vertebrae, middle cervical vertebrae, middle dorsal vertebrae, anterior sacral vertebrae, anterior caudal vertebrae, posterior cervical vertebrae, posterior dorsal vertebrae, and so on.

Neural arches also show an anterior to posterior ossification sequence (specimens 11, 12) with the exception of the sacral neural arches, which are the last in this order (specimen 12). The dorsal spines of the neural arches are mostly reduced in the cervical region. However, they can be seen in the dorsal, sacral, and caudal vertebrae.

Ribs generally ossify first at their mid-shaft (specimen 7), before expanding in proximal and distal directions. Ribs sequentially display ossification in the dorsal, caudal (transverse process sensu Rieppel, 1993), and last at the sacral region.

After the onset of ossification of the tibia and fibula, the dorsal process of

Fig. 5. General anatomy of the limb (grey box) and a diagram of the sequential ossification of the zygopodial and autopodial bones in *Emydura subglobosa* (**A–E**). Elements shown in white are still cartilaginous, processed ossification is marked by different degrees of grey scale (light grey corresponds to early ossification, dark grey corresponds to advanced ossification), and well-ossified elements are marked in black. c, centrale; dcI-IV, distal carpal 1 to 4; i, intermedium; mc, metacarpal; dt, distal tarsal; dt 5, distal tarsal 5 (hooked fifth element); mt, metatarsal; pi, pisiform; r, radius; u, ulna; ul, ulnare; IV + c, distal tarsal 4 fused with centrale. Numbers of specimens refer to the numbers used in the text. Scale bars = 3 mm.

TABLE 3. Ossification Sequence of *Emydura subglobosa*[a]

Specimen no.	Skeletal region	Skeletal elements that start ossification
5	Dermatocranium	Dentary, maxilla
	Pectoral girdle	Humerus (−)
	Plastron	Epiplastron (+)
6	Dermatocranium	Angular, frontal, jugal, palatine, parietal, postorbital, premaxilla, prefrontal, pterygoid, surangular, squamosal
	Plastron	Entoplastron, hyoplastron, hypoplastron, xiphiplastron
7	Dermatocranium	Nasale
	Splanchnocranium	Cornu branchiale I
	Shoulder girdle	Radius, ulna
	Pelvic girdle	Femur (−), tibia (−), fibula (−)
	Cervical vertebrae	Centra (+)
	Dorsal vertebrae	Centra, ribs
11	Dermatocranium	Coronoid
	Neurocranium	Basioccipital, basisphenoid, exoccipital, opisthotic, supraoccipital
	Splanchnocranium	Columnella, quadrate
	Shoulder girdle	Dorsal process of the scapula (+)
	Dorsal vertebrae	Neural arches (−)
9	Dermatocranium	Prearticular, vomer
	Shoulder girdle	Metacarpals III, IV (+)
	Pelvic girdle	Metatarsals II (−), III (+), IV
	Cervical vertebrae	Neural arches (+)
	Sacral vertebrae	Centra
	Caudal vertebrae	Centra (−)
12	Splanchocranium	Articular
	Shoulder girdle	"Acromion" process of the scapula (+), coracoid (+), metacarpal I (−), metacarpal II, metacarpal V (−), phalange 1 digit I (−), phalange 2 digit I (−), phalange 2 digit II (−), phalange 3 digit II (−), phalange 2 digit III (−), phalange 3 digit III (−), phalange 2 digit IV (−), phalange 3 digit IV (−), phalange 2 digit V (−), phalange 3 digit V (−)
	Pelvic girdle	Ilium (+), ischium (+), pubis (+), metatarsal I, metatarsal V (−), phalange 1 digit I (−), phalange 2 digit I (−), phalange 2 digit II (−), phalange 3 digit II (−), phalange 2 digit III (−), phalange 3 digit III (−), phalange 2 digit IV (−), phalange 3 digit IV (−), phalange 1 digit V (−)
	Sacral vertebrae	Neural arches (−)
	Caudal vertebrae	Neural arches
14	Shoulder girdle	Phalange 1 digit II, phalange 1 digit III, phalange 1 digit IV, phalange 1 digit V
	Pelvic girdle	Distal tarsal 5 (−), phalange 1 digit II, phalange 1 digit III, phalange 1 digit IV
	Sacral vertebrae	Ribs
	Caudal vertebrae	Ribs (+)
	Carapace	Nuchal plate (+)
16 [subadult]	Carapace	Costal plates
	Splanchnocranium	Corpus hyoidis, cornu branchiale II
	Shoulder girdle	Intermedium, centrale 1, centrale 2, distal carpal 1, 2, 3, 4, 5
	Pelvic girdle	Intermedium, fibulare, distal tarsal 1, 2, 3, 4, phalange 2 digit V
	Carapace	Peripheral plates, neural plates, suprapygal plate

[a]The sequence is based on the very first onset of ossification in every skeletal element. The signs (−) and (+) indicate the degree of ossification compared in all new occurring elements in the respective specimen. Hence, elements marked with (−) are less advanced in ossification. Elements marked with (+) are more advanced in ossification than other elements that occur in the same specimen. When no (+) or (−) is presented, the elements do not differ conspicuously in their degree of ossification. Note that the progress of ossification was found to be far more developed in specimen 9 than in the older specimen 11.

the scapula starts ossification (specimen 11), closely followed by anterior dorsal neural arches. The dorsal process of the scapula is the first to show beginning ossification among all other pectoral and pelvic girdle elements. The ilium, ischium, pubis, "acromion" process of the scapula and coracoid start ossification at the same time as

the articular (specimen 12) only slightly preceding the first sign of ossification in the sacral and caudal neural arches.

Some regions of the neurocranium (basisphenoid, basioccipital, exoccipital, opisthotic, supraoccipital) and one part of the splanchnocranium (quadrate) exhibit red staining (specimen 11), all preceding the sacral and caudal centra as well as the metapodials of the manus (metacarpals III, IV) and pes (metatarsals II, III, IV).

Sacral and caudal neural arches and all remaining elements of the pectoral girdle ("acromion" process of the scapula, coracoid) and pelvic girdle (ilium, ischium, pubis) show ossification after onset of ossification in metacarpals III, IV, and metatarsals II to IV (specimen 12). The manus reveals the following sequence of ossification: metacarpal IV > metacarpal III > metacarpal II > metacarpal I > metacarpal V. The sequence ossification in the pes is: metatarsal III > metatarsal IV > metatarsal II > metatarsal I > metatarsal V. The fifth metapodial of both the manus and pes start perichondral ossification soon after onset of metapodial I.

The ossification patterns of the phalanges (specimens 12, 14) vary in their direction: digit I of both the manus and pes start ossification in the first and second phalanges in a proximodistal sequence, whereas digits II, III, and IV show a distoproximally directed sequence. Additionally, the fifth digit of the manus shows another, alternative sequence: intermediate phalange > terminal phalange > proximal phalange. The terminal phalange of digit V of the pes starts ossification only after hatching.

The nuchal plate begins ossification simultaneously with the caudal ribs (specimen 14) and shortly before the proximal phalanges of digits II to IV and the terminal phalange of digit V, i.e., shortly before hatching. The costal plates are the next and last carapace elements, which start ossification before hatching (specimen 16), and distal tarsal 5 is the last element of the whole limb to start ossification in prehatching stages (specimen 14). By the oldest prehatching specimen, distal tarsal 5 shows a small, medial center of endochrondral ossification.

DISCUSSION

Grundmuster of Turtle External Development

Our analysis of external developmental characters suggests that Testudines are characterised by two features related to neck development, namely a delayed cervical flexure of 90° and a delayed disappearance of this flexure (Table 1d). Next to the ossification mode of cervical vertebrae (Werneburg and Sánchez-Villagra, 2009), this phenomenon may be correlated with an elongated neck in turtles in comparison to the outgroup species.

In the present study, we did not find temporal shifts in the neck development distinguishing Cryptodira and Pleurodira. However, Werneburg and Sánchez-Villagra (2009) used a different consensus approach than we did (see below). They found the delay of the cervical flexure as one autapomorphic shift in the solely used pleurodire species *E. subglobosa*, as discussed in the following. Because both longer and shorter necks can be observed in cryptodires and pleurodires, the adult neck length may not be correlated with the embryonic shifts, but rather related to head retraction. Whereas cryptodires pull their head into the shell by S-shaping their neck, pleurodires lay their neck/head sideward under the anterior edge of the shell. Different head muscles underlie these movements (Shah, 1963; Herrel et al., 2008) and the duration of their ontogeny, which has not been studied yet, may influence temporal shifts in external development. Werneburg and Sánchez-Villagra (2009) focused only on one single phylogeny (Fig. 1C) to record the neck-related shift in *E. subglobosa*. Here we eliminated topological constraints and found no neck-related shift, which indicates the strong influence of the underlying phylogenetic hypothesis on the occurrence and distribution of heterochronic temporal shifts.

When assuming a Sauria- or Archosauria-relationship of Testudines (Table 1a,b), the early disappearance of the posterodorsal head projection is an autapomorphic character for turtles, independent of cryptodire relationships. This feature may be correlated with the early ossification of the occipital/parietal region of the skull of turtles. This ossification pattern is also present in other amniote groups (Sánchez-Villagra et al., 2008; Hugi et al., 2009).

One character complex, the onset of mandibular process characters, seems to be of phylogenetic relevance and distinguishes the two major turtle clades. Whereas in pleurodires an accelerated development of the lower jaw can be observed (Table 2a), in cryptodires there is only a single delayed mandibular process character (Table 2b). In the context of jaw muscle development, this finding is potentially important because the development of the jaw musculature is directly related to the development of the mandibular process (Edgeworth, 1935; Ziermann, 2008). However, the different patterns could also be related to different feeding modes. While both adult and juvenile pleurodires show the same type of fast prey capture behaviour (Lemell et al., 2002; Schwarz, 2006), some cryptodires change their feeding behaviour during life (Bonin et al., 2006). The accelerated development of the mandibular process in pleurodires may be necessary to enable this fast prey capture.

Werneburg and Sánchez-Villagra (2009) reconstructed a late occurrence of the lower eyelid when compared to the development of the mandibular process. The development of the trigeminal nerve-innervated m. levator bulbi, which connects the upper with the lower eyelid (Ogushi, 1913; Lakjer, 1926), may be associated with the development of the m. adductor mandibulae, which is also innervated by the trigeminal nerve and associated with the mandibular process (Rieppel, 1990). A late differentiation of the m. levator bulbi from the m. adductor mandibulae anlage and/or the small extent of the former muscle in turtles (Lakjer, 1926) may explain the delayed development of the lower eyelid.

Variability Versus "Stage"

To describe the external development, we ordered the investigated *E. subglobosa* specimens chronologically using an average age interval of 3.5 days, which was determined by the availability of specimens. By comparing the length of the embryos, we observed a decrease in carapace length in specimens 14 to 16, which may be interpreted as a case of intraspecific variability but could also be

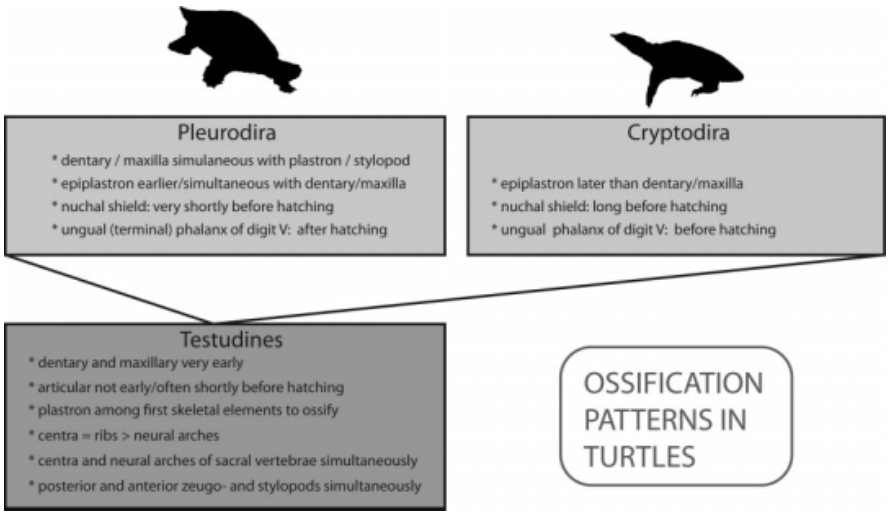

Fig. 6. Trends of ossification within turtles based on the comparison of two pleurodiran and four cryptodiran species. Each character refers to the onset of ossification in the respective element. Note that all characters represent only the distribution of characters, no autapomorphies, because no outgroup comparison or sequence analysis was performed. Some of the trends noted in turtle ossification have previously been identified in other reptiles (e.g., Sánchez-Villagra et al., 2008; Hugi et al., 2009). Thus, some of the characters listed may actually represent reptilian plesiomorphies. For details see text.

correlated to the flexible shell of turtle embryos (Cherepanov, 1995; Alibardi and Thomson, 1999; Gilbert et al., 2008) that deforms by embryonic movements, cervical flexure, and internal organ development.

The older the specimens are, the more intraspecific variation is detectable. In early development, slight differences seem to occur only in somite count, whereas other parts of the embryo are rarely affected. Comprehensive studies on intraspecific variation during external organogenesis are still lacking. Several "staging tables" refer to scale and pigmentation development to describe reptile embryo stages. However, these descriptions are all of a synoptic, typological style (Werneburg, 2009) and neglect both intraspecific variability and the comparability of the examined characters. For instance, many authors describe pigmentation patterns (Beggs et al., 2000) but do not describe their shape or explain whether they are visible as pigment cells ("tail has pale pigmentation"). Another example is limb scale development, which was used to describe very advanced stages of *Chelydra serpentina* (Yntema 1968); the poor applicability of these characters to stage other species was often criticised (Beggs, 2000; Tokita and Kuratani, 2001; Werneburg, 2009). Detailed descriptions and depictions of pigmentation development and its intraspecific variation may help to evaluate more comprehensive studies of neural crest cell distribution and pattern formation (Olsson, 1993).

Patterns of Turtle Ossification (Figs. 4–6, Table S1)

Based on double-stained whole-mounted specimens, the ossification patterns of six turtle species were compared against each other, representing two Pleurodira, *E. subglobosa* (this study), *Phrynops hilarii* (Fabrezi et al., 2009; Bona and Alcalde, 2009), and four Cryptodira, the trionychids *Apalone spinifera* (Sheil, 2003) and *Pelodiscus sinensis* (Sánchez-Villagra et al., 2009) as well as the chelydrids *Chelydra serpentina* (Sheil and Greenbaum, 2005) and *Macrochelys temminckii* (Sheil, 2005). All studied turtles show more or less the same adaptations to feeding mechanisms (snapping), locomotion (paddling), and habitat (fresh water). Tables 3 and S1 summarise the information on the ossification pattern of *E. subglobosa*. In Figure 6, major trends of ossification for Testudines, Pleurodira, and Cryptodira are listed (note that not all listed characters necessarily indicate autapomorphic features because no outgroup comparison was performed in this study).

Cranium.

In *E. subglobosa*, the rough sequence of ossification in the cranium is dermatocranium > splanchnocranium > neurocranium. Dentary and maxilla are first to start ossification in the dermatocranium. The cornu branchiale I is the first splanchnocranial element that begins to ossify. The articular ossifies later, showing onset of ossification simultaneously with the relatively late onset in the pelvic girdle in specimen 12. All neurocranial elements start ossification in the same specimen (specimen 11). The rough sequence of ossification in the cranium of *E. subglobosa* is the same in *Pelodiscus sinensis*. Both turtles differ from the reported sequences of the other studied turtles. *Apalone spinifera* shows the dermatocranial parts to ossify first, sequentially followed by neurocranial and splanchnocranial elements. In *Chelydra serpentina, Phrynops hilarii*, and *Macrochelys temminckii* also parts of the dermatocranium start ossification first, followed by a simultaneous onset of ossification in both the neuro- and splanchnocranium. In the pleurodires and partly in the cryptodires (*C. serpentina, M. temminckii, P. sinensis*), the articular shows ossification shortly before or even after hatching. For example, in *P. hilarii* the articular begins ossification shortly after the onset in the nuchal plate, whereas in *E. subglobosa*, the articular starts ossification shortly before. As an exception, *A. spinifera* shows the articular relatively early to retain Alizarin Red, which is approximately in the middle of its ossification sequence. However, *A. spinifera* still displays a later timing in the onset of ossification of the articular than in the quadrate, like almost all of the studied turtles. As an exception, *C. serpentina* displays a simultaneous onset of ossification in the articular and quadrate only in hatched specimens. All studied turtles show the dentary and the maxilla to be among the first cranial elements to ossify. The Pleurodira show at least the epiplastron to start ossification even earlier or simultaneously with the dentary and the maxilla. Conversely, the Cryptodira display onset of ossification of at least the epiplastron later than the onset of ossification in the dentary and maxilla. The maxilla and the

dentary start ossification simultaneously with the first retention of Alizarin Red in the axial skeleton (cervical and dorsal centra) and the plastron (hyo-, hypo-, and xiphiplastron) of *P. sinensis*. Then, other parts of the dermatocranium and the remaining plastron elements begin ossification simultaneously with the first onset in the anterior and posterior stylopods. In *A. spinifera*, stylopodial regions start to ossify as soon as most dermatocranial elements show calcification. In *M. temminckii*, the ossification sequence proceeds to the stylopodial region after the onset in the maxilla. There are no heterochronic shifts of external morphology, as referred to in Table 1 and 2, that seem to correlate with the ossification pattern of the studied turtle species. One may expect a different timing of maxilla and dentary ossification in pleurodires and cryptodires, because both groups are distinguished from each other by the timing of ossification of the maxillary and mandibulary process. In this regard, it may be worthwhile for future studies to also investigate the relative influence of the developing jaw musculature.

Vertebrae.

In *E. subglobosa* and *Pelodiscus sinensis*, the vertebral sequence of ossification is centra > ribs > neural arches. The overall ossification gradient of these single vertebral elements is not strictly anteroposteriorly directed. Only the dorsal, sacral, and caudal centra show a strict overall and region-referred anteroposterior sequence in both species. The neural arches subsequently display ossification in the cervical, dorsal, and caudal regions. The ossification sequence of the ribs is first seen in the dorsal portion, then subsequently in the cervical, caudal, and sacral region. *Chelydra serpentina, Macrochelys temminckii*, and *Phrynops hilarii* show the following vertebral ossification sequence: centra, ribs > neural arches, whereas *Apalone spinifera* displays centra to begin ossification before the simultaneous onset of the ribs and the neural arches. In *P. sinensis* and *M. temminckii*, ossification proceeds in an anteroposterior gradient in all centra as seen in *E. subglobosa*. All other studied cryptodire turtles show partial anteroposterior gradients in single vertebral regions with an overall anteroposterior ossification gradient. *P. hilarii* shows a simultaneous onset of ossification in the anterior half of the vertebral column (cervical and dorsal vertebrae), which later continues to the posterior half (sacral and caudal vertebrae). Neural arches start ossification at the same time in the cervical, sacral, and caudal vertebrae, whereas dorsal neural arches are slightly delayed. In *P. hilarii*, only the dorsal ribs start ossification before hatching; all other ribs tend to ossify only thereafter. In *A. spinifera* and the Chelydridae, every single rib starts ossification before hatching. All compared Testudines studied show a relative early onset of ossification in their vertebral centra, which provide a strong vertebral column, and their overall anterior-posterior gradient of ossification may be correlated with the delayed development of the cervical flexure (Table 1). Werneburg and Sánchez-Villagra (2009) already pointed out the correlation of neck flexure and ossification patterns. Based on its strong vertebral column, the neck may not flex until the spatial limitations in the egg force it to move. Finally, the general architecture of the vertebral column and adjacent soft tissues may also render the axis inflexible.

Pectoral and pelvic girdle.

The dorsal process of the scapula is the first element of the pectoral girdle that shows ossification in *E. subglobosa*. It starts to ossify slightly before the quadrate. All other pectoral and pelvic girdle elements show the beginning of ossification at the same time with the onset of the articular. In *Phrynops hilarii*, the dorsal process of the scapula is also the first element of the pectoral girdle to ossify. In *Pelodiscus sinensis*, the dorsal process and the "acromion" process of the scapula begin to ossify at the same time, preceding the coracoid. In *Apalone spinifera* and *Chelydra serpentina*, the dorsal process of the scapula starts to ossify simultaneously with its "acromion" process and the coracoid. In *Macrochelys temminckii*, the dorsal process of the scapula starts ossification clearly before its "acromion" process, both preceding the coracoid.

Forelimb and hind limb.

In *E. subglobosa* (Figs. 4, 5), stylopodial and zeugopodial elements of the forelimb start ossification before their counterparts of the hind limb (forelimb acceleration, Richardson et al., 2009). In contrast, the tarsal region shows either a simultaneous or earlier onset of ossification than the carpal region. The sequence of onset of limb ossification proceeds proximodistally with a postaxial predominance in the zeugopodial and autopodial region. Postaxial predominance in the ossification sequence is considered a characteristic feature of amniotes (Fröbisch, 2008). The phalanges of *E. subglobosa* show ossification sequences either in a proximodistal or distaloproximal direction depending on their digit position. Any acceleration of the forelimb compared to the hind limb is rather ambiguous in trionychids and chelydrids. However, two unambiguous ossification sequences can be determined for *Phrynops hilarii* and *Macrochelys temminckii*. In the former, metatarsals I and IV begin to ossify before metacarpals II to IV. In the latter, metatarsals II, III, and IV start ossification before any metacarpal. The timing of onset of ossification of the ungual phalange of digit V clearly differentiates pleurodires from cryptodires. The ungual phalange of digit V starts ossification after hatching in the studied pleurodires, whereas in all studied cryptodires this element ossifies before hatching. The hooked element in the pes of *Apalone spinifera, P. hilarii*, and *Pelodiscus sinensis* has been described as metatarsal V. However, its ossification is delayed relative to other metatarsals and it ossifies after or shortly prior to hatching. Fabrezi et al. (2009) studied the identity of this hooked tarsal element in *P. hilarii* and other pleurodire turtles. They stated that this element is a distal tarsal rather than a metatarsal bone due to its tarsal morphology. This bone shows a late onset of ossification in an endochondral ossification center. In contrast, other limb bones ossify earlier and show perichondral ossification first. These arguments are also supported by the hooked element of *E. subglobosa*, which determine it as distal tarsal 5 and not as metatarsal V.

Plastron and carapace.

The epiplastron is the first element of the whole skeleton that starts ossification in *E. subglobosa*. The nuchal plate is the first element of the carapace to ossify, but at the same time also among the latest skeletal elements to start ossification in prehatchings. Only in the largest prehatching specimen, the costal plates begin to ossify, whereas the peripheral, neural, and suprapygal ossify only in posthatchings. Pleurodires show at least one plastron element, the epiplastron, to begin ossification before or simultaneously with the very first onset in the dermatocranium. In cryptodires, the epiplastron starts to ossify relatively later than dentary and maxilla do. In addition, the nuchal plate starts to ossify relatively early in the cryptodires and very late (i.e., shortly before hatching) in the pleurodires. Thus, the timing of onset of ossification of the nuchal plate differentiates Pleurodira from Cryptodira. Vallois (1922), Shah (1963), and Herrel et al. (2008) already pointed out major differences in the neck musculature in Pleurodira and Cryptodira due to the diverging behaviour of neck/head retraction in both groups. Especially the mm. corticocervicalum (Herrel et al., 2008), which originate at the nuchal plate and are inserted into the posteriormost cervical vertebrae, seem to develop large stresses onto the nuchal plate. The m. testooccipitis (Scanlon, 1982) and testocapitis (Hoffmann, 1890), which originate from the anterior lower surface of the carapace, do not appear in trionychids (Rathke, 1848; Ogushi, 1913), whereas in other cryptodiran species such as the leatherback turtle *Dermochelys coriacea* (Schumacher, 1972), these muscles may have an additional influence on the early onset of nuchal plate ossification. Cryptodires show a retraction of the neck/head into the shell in late embryology (e.g., Tokita and Kuratani, 2001). Neck retraction may rather be the result of limited space of the egg than of an active retraction mechanism of the musculature. However, early existing neck musculature and also the nuchal plate may underlie indirect stresses that lead to an early onset of ossification. At least the epiplastron ossifies earlier in pleurodires than in cryptodires. Also here the configuration and development of neck/head musculature should be taken into account: The m. plastrosquamosus originates directly from the plastron, and the m. coracohyoideus (Scanlon, 1982) is attaching to the shoulder girdle, which in turn is also connected to the plastron (Fürbringer, 1874; Ogushi, 1913). Detailed anatomical observations are necessary to clarify which elements of the plastron provide the origin site for those muscles and tendons, and hence to understand the ossification pattern of the epiplastron in both turtle groups.

EXPERIMENTAL PROCEDURES

Specimens

Fertilised eggs of *E. subglobosa* were obtained from a private breeder. The embryos came from different clutches and were incubated at a temperature of 29–30° C from February 11th until May 11th 2007. At an average interval of about 3.5 days (beginning at day 6 of incubation and ending at hatching day 65), 17 specimens were intoxicated and mortified in chlorobutanol and fixed in a 4% formalin solution. The subadult specimen was obtained from the pet trade. The crown-rump length (CRL) was measured only for the first three specimens. Thereafter, the anteroposterior expansion of the carapace and other shell dimensions were measured, since the actual CRL became obscured by retraction of the neck under the carapace or by neck torsion (Fig. 1). Specimens are currently deposited at the Paläontologisches Museum und Museum der Universität Zürich (PIMUZ), and are intended to be integrated into the embryological collection of the Museum für Naturkunde Berlin.

Description of External Development (Figs. 2, 3, S1–S18)

Following Werneburg (2009), we refrained from categorising our specimens into "stages" and ordered them by days of incubation. For each of the 18 specimens, we assigned a progressional number. In the following, we protocol the developmental events occurring in each specimen referring to the SES-characters of Werneburg (2009). In Werneburg (2009), several staging systems were compared and an overall comparable set of 104 characters was developed, which are easy to recognise in each vertebrate embryo. The characters are clearly defined and prevent any ambiguous interpretation. The SES provides a guideline of documenting and presenting embryological data. Herein only new occurring characters (events) in particular specimens/stages are documented. If those characters are retained in older specimens, they will not be re-described. Because of the coding of individual specimens with a standard system of development characters and an explicit and reproducible consideration of species variation, the SES system of Werneburg (2009) avoids typological features of standard staging systems.

In our descriptions, we also list characters that do not fit to the SES-characters but are assumed to be of a species-characteristic value (Giannini et al., 2006), such as coloration and proportions (italicised letters in Results/Staging system section). Two overview plates are presented picturing lateral views of the whole bodies (Fig. 2), as well as the head and the left forelimb (Fig. 3). In the supplementary information, more detailed illustrations (Figs. S1–S18) are presented following the SES-guide.

Photographs of all specimens were made with a digital camera (Leica DFC420 C) mounted on a stereomicroscope at a resolution of 2592 × 1944 pixels.

Analysis of Temporal Shifts in External Development (Tables 1, 2)

We used the developmental data and the protocol of Werneburg and Sánchez-Villagra (2009) to detect heterochronic shifts for the nine most-discussed topologies of turtle phylogeny (see Introduction section, Fig. 1A–I). We ran Parsimov (Jeffery et al., 2005) to calculate Acctran and Deltran optimisations (Maddison and Maddison, 2001) for each shifting element and, focusing on the branch leading to Testudines, we first calculated the consensus of both optimisation models for each tree separately. Our

approach was to summarise all temporal shifts that autapomorphically characterise Testudines, both independent of any cryptodiran subgroup arrangements (Fig. 1a–c) and of the position of turtles within reptiles (Fig. 1A–I). We created a temporal shift consensus of all Sauria-topologies (Fig. 1A–C), all Archosauria-topologies (Fig. 1D–F), and all Lepidosauria-topologies (Fig. G–I; Table 1a–c). Finally, by creating a consensus of tree topologies, we calculated a conservative list of temporal shifts for Testudines (Table 1d).

Werneburg and Sánchez-Villagra (2009: Supplement) presented 94 temporal consensus shifts for *E. subglobosa* under their favoured topology (Fig. 1B). For Cryptodira the authors found eleven developmental consensus shifts. Here we present the consensus shifts for *E. subglobosa* and Cryptodira common to all tested topologies (Table 2).

For each analysis, we calculated temporal shifts using the data (event pair) matrix including all ties (simultaneously occurring events). The results of the tie-included analysis are shown in Tables 1 and 2. As proposed by different authors (Weisbecker et al., 2008; Ziermann 2008) we also calculated temporal shifts using the same data matrix excluding all ties (not shown). We calculated a consensus of both approaches and marked the overlapping shifts with asterisks (Tables 1 and 2).

Interpretation of Temporal Shifts and Evolutionary Scenarios

Studies on sequence heterochrony developed within the last 20 years (summarised by Ziermann, 2008; Werneburg, 2009) and recent approaches use a parsimony algorithm to estimate developmental shifts for particular nodes in a given phylogeny (Jeffery et al., 2005).

Werneburg and Sánchez-Villagra (2009) adverted to problems of interpreting heterochronic developmental shifts and evolutionary scenarios. For example, accelerated forelimb development has been compared to eye and somite development (Werneburg and Sánchez-Villagra, 2009: Supplement, Shift No. 438), whereas there is no obvious biological reason, at the utmost a shared up-regulation of similar transcription factors, why fast forelimb development, which could be interpreted as necessary to create a good basis for long arms in the adult, should be related to the eye and somite development. Thus temporal shifts are interpreted as simply existing character states and, without overinterpreting their biological significance, they can be taken to support dichotomies when comparing different topologies. Further Evo-Devo studies on molecular features or the onset of hormone control may be able to interpret findings like limb bud/tail bud interferences.

Another problem when analysing sequence heterochrony is that of pseudo shifts. These are shifts Parsimov (Jeffery et al., 2005) reports when the resolution of embryonic stages in one species is higher than in another, making it likely that the characters displayed by the youngest specimen of the less-resolved species have developed earlier. In the Parsimov results of Werneburg and Sánchez-Villagra (2009), there are several delayed (pseudo) shifts in early development that can be interpreted as derived because of the low resolution of the underlying embryonic series. In turtles, for example, several developmental "staging tables" begin when most cranial structures have already started to form, a character set that is mostly comparable to that of Yntema's (1968) stage 12 (Beggs et al., 2000; Greenbaum, 2002; Greenbaum and Carr, 2002; Tokita and Kuratani, 2001; this study). Such pseudo shifts should be excluded when discussing developmental shifts.

Clearing and Staining

In order to study the ossification sequence, we cleared and double-stained eight prehatchlings and the subadult specimen following standard protocols (Taylor and Van Dyke, 1985). Red = calcified structures (alizarin red), dark blue = cartilage (alcian blue), light blue = connective tissue (Fig. 4). The sequence of ossification, as documented in Table 3, is based on the first marking with Alizarin red.

Furthermore, the sequence of ossification is based on the very first visible retention of Alizarin Red in each skeletal element of the embryo. If possible, a fine-grained sequence (Hugi et al., 2009) of ossification is provided, when more than one skeletal element displays the first uptake of Alizarin Red in an embryo. The relative retention of Alizarin Red (i.e., area of the element showing retention of Alizarin Red compared to its adult absolute ossified size) is the basis for this fine-grained sequence. We interpreted an element with a higher degree of ossification to occur earlier than an element with a lower degree. However, the value of the fined-grained sequence to define the onset of ossification of elements should be interpreted with caution. Apparently, an element showing a larger degree of ossification could have been ossified earlier, but it also could have been ossified later and have shown a faster overall ossification.

Nomenclature follows Gaffney (1977, 1979) for the skull bones, and Schumacher (1973) for the hyoid apparatus. Terminology of shell elements corresponds to Zangerl (1969), and that of the remaining postcranial elements to Sheil and Greenbaum (2005).

ACKNOWLEDGMENTS

We thank Christian Mitgutsch, Torsten Scheyer, and Laura A.B. Wilson for discussion, technical support, and useful comments on the manuscript. Two anonymous reviewers provided useful suggestions. Bernd Wolff kindly made the embryos of *Emydura subglobosa* available. This work was supported by Swiss National Fond grant 3100A0-116013 (to M.R.S.-V.), Forschungskredit der Universität Zürich grant 3772 (to I.W.), and Deutsche Forschungsgemeinschaft grant Mu 1760/2-3 (to J.M.)

REFERENCES

Alibardi L, Thompson MB. 1999. Morphogenesis of shell and scutes in the turtle *Emydura macquarii*. Austral J Zool 47: 245–260.

Beggs K, Young J, Georges A, West P. 2000. Ageing the eggs and embryos of the pig-nosed turtle, *Carettochelys insculpta* (Chelonia: Carettochelydidae), from northern Australia. Can J Zool 78: 373–392.

Bell BA, Spotila JR, Paladino FV, Reina RD. 2003. Low reproductive success of leatherback turtles, *Dermochelys coriacea*, is due to high embryonic mortality. Biol Conserv 115:131–138.

Bona P, Alcalde L. 2009. Chondrocranium and skeletal development of *Phrynops hilarii* (Pleurodira: Chelidae). Acta Zool 89:301–325.

Bonin F, Devaux B, Dupré A. 2006. Turtles of the world. Baltimore: John Hopkins University Press.

Boughner JC, Buchtová M, Fu K, Diewert V, Hallgrímsson B, Richman JM. 2007. Embryonic development of *Python sebae*. I: Staging criteria and macroscopic skeletal morphogenesis of the heads and limbs. Zoology 110:212–230.

Boulenger G. 1889. On the characters of the chelonian families Pelomedusidae and Chelydridae. Annu Mag Nat Hist 61:346–347.

Burke AC. 1991. The development and evolution of the turtle body plan: inferring intrinsic aspects of the evolutionary process from experimental embryology. Am Zool 31:616–627.

Cherepanov GO. 1995. Ontogenetic development of the shell in *Trionyx sinensis* (Trionychidae, Testudinata) and some questions on the nomenclature of bony plates. Russ J Herpetol 2:129–133.

Colbert MW, Rowe T. 2008. Ontogenetic sequence analysis: Using parsimony to characterize developmental sequences and sequence polymorphism. J Exp Zool (Mol Dev Evol) 310B.

Cretekos CJ, Weatherbee SD, Chen C-H, Badwaik NK, Niswander L, Behringer RR, Rasweiler JJI. 2005. Embryonic staging system for the short-tailed fruit bat, *Carollia perspicillata*, a model organism for the mammalian order Chiroptera, based upon timed pregnancies in captive-bred animals. Dev Dyn 233:721–738.

Danilov IG, Parham JF. 2008. A reassessment of some poorly known turtles from the middle Jurassic of China, with comments on the antiquity of extant turtles. J Vertebr Paleontol 28: 306–318.

de Jong IML, Witte F, Richardson MK. 2009. Developmental stages until hatching of the Lake Victoria cichlid *Haplochromis piceatus* (Teleostei: Cichlidae). J Morphol 270:519–535.

Edgeworth FH. 1935. The cranial muscles of vertebrates. London: Cambridge University Press.

Eßwein S. 1992. Zur phylogenetischen und ontogenetischen Entwicklung des akinetischen Craniums der Schildkröten. Natürliche Konstruktionen - Mitteilungen des SFB 230 751–55.

Fabrezi M, Manzano A, Abdala V, Zaher H. 2009. Developmental basis of limb homology in pleurodiran turtles, and the identity of the hooked element in the chelonian tarsus. Zool J Linnean Soc 155: 845–866.

Franz-Odendaal T. 2006. Intramembranous ossification of scleral ossicles in *Chelydra serpentina*. Zoology 109:75–81.

Fröbisch NB. 2008. Ossification patterns in the tetrapod limb-conservation and divergence from morphogenetic events. Biological Reviews 83.

Fürbringer M. 1874. Zur vergleichenden Anatomie der Schultermuskeln. II. Theil. Jenaische Z Naturwissenschaften 8:175–280.

Gaffney ES. 1977. The side-necked turtle family Chelidae: a theory of relationships using shared derived characters. Am Mus Novitates 2620:1–28.

Gaffney ES. 1979. Comparative cranial morphology of recent and fossil turtles. Bull Am Mus Nat Hist 164:67–376.

Gaffney ES, Meylan PA. 1988. A phylogeny of turtles. In: Benton MJ, editor. The phylogeny and classification of the tetrapods. Volume 1: Amphibians, reptiles, birds. Oxford: Clarendon Press. p 157–219.

Galbraith DA, Brooks DR, Obbard ME. 1989. The influence of growth rate on age and body size at maturity in female snapping turtles (*Chelydra serpentina*). Copeia: 896–904.

Giannini N, Goswami A, Sánchez-Villagra MR. 2006. Development of integumentary structures in *Rousettus amplexicaudatus* (Mammalia: Chiroptera: Pteropodidae) during late-embryonic and fetal stages. J Mammal 87:993–1001.

Gilbert SF, Loredo GA, Brukman A, Burke AC. 2001. Morphogenesis of the turtle shell: the development of a novel structure in tetrapod evolution. Evol Dev 3:47–58.

Gilbert SF, Cebra-Thomas JA, Burke AC. 2008. How the turtle gets its shell. In: Wyneken J, Godfrey MH, Bels V, editors. Biology of turtles. New York:CRC Press. p 1–16.

Goodrich ES. 1930. Studies on the structure and development of vertebrates. London: Macmillan and Co.

Greenbaum E. 2002. A standardized series of embryonic stages for the emydid turtle *Trachemys scripta*. Can J Zool 80:1350–1370.

Greenbaum E, Carr JL. 2002. Staging criteria for embryos of the spiny softshell turtle, *Apalone spinifera* (Testudines: Trionychidae). J Morphol 254:272–291.

Guyot G, Pieau C, Renous S. 1994. Déávelopement embryonnaire d'une tortue terrestre, la tortue d'Hermann, *Testudo hermanni* Gmelin, 1789. Ann Sci Nat Zool Paris 15:115–137.

Haeckel, E. 1896. Systematische Phylogenie. Zweiter Theil, Systematische Phylogenie der wirbellosen Thiere (Invertebrata). Berlin: Georg Reimer.

Harrison L, Larsson H. 2008. Estimating evolution of temporal sequence changes: a practical approach to inferring ancestral developmental sequences and sequence heterochrony. Systemat Biol 57:378–387.

Hennig AS. 2001. Haltung und Nachzucht der Rotbauch-Spitzkopfschildkröte (*Emydura subglobosa*). Reptilia 9:70–73.

Herrel A, O'Reilly JC, Richmond AM. 2002. Evolution of bite performance in turtles. J Evol Biol 15:1083–1094.

Herrel A, Van Damme J, Aerts P. 2008. Cervical anatomy and function in turtles. In: Wyneken J, Godfrey MH, Bels V, editors. Biology of turtles. New York: CRC Press. p 163–185.

Highfield AC. 1996. Practical encyclopedia of keeping and breeding tortoises and freshwater turtles. London: Carapace Press.

Hoffmann CK. 1890. Schildkröten. Leipzig: C.F. Winter'sche Verlagshandlung. 442 p.

Hopwood N. 2005. Visual standards and disciplinary change: Normal plates, tables and stages in embryology. Hist Sci 43:239–303.

Hopwood N. 2007. A history of normal plates, tables and stages in vertebrate embryology. Int J Dev Biol 51:1–26.

Hugi J, Mitgutsch C, Sánchez-Villagra MR. 2009. Chondrogenic and ossification patterns and sequences in White's skink *Liopholis whitii* (Scincidae, Reptilia). Zoosystemat Evol (in press).

Jeffery JE, Bininda-Emonds ORP, Coates MI, Richardson MK. 2005. A new technique for identifying sequence heterochrony. Systemat Biol 54:230–240.

Jenner RA, Wills MA. 2007. The choice of model organisms in evo-devo. Nature Rev Genet 8:311–319.

Joyce WG. 2007. Phylogenetic relationships of Mesozoic turtles. Bull Peabody Mus Nat Hist 48:3–102.

Krefft G. 1876. Notes on Australian animals in New Guinea with description of a new freshwater tortoise belonging to the genus Euchelymys (Gray). Ann Museo Civico Storia Nat Genova 1:390–394.

Lakjer T. 1926. Studien über die Trigeminus-versorgte Kaumuskulatur der Sauropsiden. Copenhagen: C.A. Reitsel Buchhandlung.

Legler JM, Georges A. 1993. Chapter 21. Family Chelidae. In: Glasby RB, editor. Fauna of Australia 2A: Amphibia and reptilia. Australian Government Publishing Service. http://www.ea.gov.au/biodiversity/abrs/onlineresources/abif/fauna/foa/2a-contents.html.

Lemell P, Lemell C, Snelderwaard P, Gumpenberger M, Wochesländer R, Weisgram J. 2002. Feeding patterns of *Chelus fimbriatus* (Pleurodira: Chelidae). J Exp Biol 205:1495–1506.

Li C, Wu X-C, Rieppel O, Wang L-T, Zhao L-J. 2008. An ancestral turtle from the Late Triassic of southwestern China. Nature 456:497–501.

Maddison DR, Maddison WP. 2001. MacClade 4. In. Sunderland, MA: Sinauer Associates, Inc. Publishers.

Mickoleit G. 2004. Phylogenetische Systematik der Wirbeltiere. München: Verlag Dr. Friedrich Pfeil.

Miller JD. 1985. Embryology of marine turtles. In: Gans C, Billet F, Maderson PFA, editors. Biology of the reptilian, Vol. 14: Development A. New York: John Wiley & Sons. p 269–328.

Mitgutsch C. 2003. On Carl Gegenbaur's theory on head metamerism and the selection of taxa for comparisons. Theory Biosci. 122:204–229.

Müller J. 2003. Early loss and multiple return of the lower temporal arcade in diapsid reptiles. Naturwissenschaften 90:473–476.

Nagashima H, Uchida K, Yamamoto K, Kuraku S, Usuda R, Kuratani S. 2005. Turtle–chicken chimera: an experimental approach to understanding evolutionary innovation in the turtle. Dev Dyn 232:149–161.

Nagashima H, Kuraku S, Uchida K, Ohya Y, Narita Y, Kuratani S. 2007. On the

carapacial ridge in turtle embryos: its developmental origin, function and the chelonian body plan. Development 134: 2219–2226.

Nagashima H, Sugahara F, Takeshi M, Ericsson R, Kawashima-Ohya Y, Narita Y, Kuratani S. 2009. Evolution of the turtle body plan by the folding and creation of New muscle connections. Science 325:193–196.

Nicol E. 1993. Red-bellied short-necked turtle, *Emydura subglobosa*. Tortuga Gazette 29:1–3.

Nolte MJ, Hockman D, Cretekos CJ, Behringer RR, Rasweiler JJI. 2009. Embryonic staging system for the black mastiff bat, *Molossus rufus* (Molossidae), correlated with structure-function relationships in the adult. Anat Rec 292:155–168.

Ogushi K. 1913. Anatomische Studien an der japanischen dreikralligen Lippenschildkröte (*Trionyx japanicus*). II. Mitteilung: Muskel- und peripheres Nervensystem. Morphol Jahrbuch 46: 299–562.

Olsson L. 1993. Pigment pattern formation in the larval salamander *Ambystoma maculatum*. J Morphol 215:151–163.

O'Steen S. 1998. Embryonic temperature influences juvenile temperature choice and growth rate in snapping turtles *Chelydra serpentina*. J Exp Biol 201: 439–449.

Packard GC, Packard MJ, Birchard GF. 2000. Availability of water affects organ growth in prenatal and neonatal snapping turtles (*Chelydra serpentina*). J Comp Physiol B 170:69–74.

Pawlowski S. 2001. Weitere Erkenntnisse zu Reproduktionsvermöögen und Schlupferfolg zweier Weibchen der Rotbauch-Spitzkopfschildkröte, *Emydura subglobosa* (KREFFT 1876). Elaphe 12:35–45.

Rathke H. 1848. Ueber die Entwickelung der Schildkröten. Braunschweig: Druck und Verlag von Friedrich Vieweg und Sohn.

Richardson MK, Jeffery JE, Coates MI, Bininda-Emonds ORP. 2001. Comparative methods in developmental biology. Zoology 104:278–283.

Richardson MK, Gobes S, van Leeuwen A, Poelman A, Pieau C, Sánchez-Villagra MR. 2009. Heterochrony in limb evolution: developmental mechanisms and natural selection. J Exp Zool (Mol Dev Evol) 310B:639–664.

Rieppel O. 1990. The structure and development of the jaw adductor musculature in the turtle *Chelydra serpentina*. Zool J Linnean Soc 98:27–62.

Rieppel O. 1993. Studies on skeleton formation in reptiles: Patterns of ossification in the skeleton of *Chelydra serpentina* (Reptilia, Testudines). J Zool 231:487–509.

Rieppel O. 2004. Kontroversen innerhalb der Tetrapoda: die Stellung der Schildkröten (Testudines). Sitzungsberichte der Gesellschaft Naturforschender Freunde zu Berlin 43:201–221.

Rieppel O. 2008. The relationships of turtles within amniotes. In: Wyneken J, Godfrey MH, Bels V, editors. Biology of turtles. New York: CRC Press. p 345–353.

Sánchez-Villagra MR, Winkler JD, Wurst L. 2007. Autopodial skeleton evolution in side-necked turtles (Pleurodira). Acta Zool (Stockholm) 88:199–209.

Sánchez-Villagra MR, Goswami A, Weisbecker V, Mock O, Kuratani S. 2008. Conserved relative timing of cranial ossification patterns in early mammalian evolution. Evol Dev 10:519–530.

Sánchez-Villagra MR, Müller H, Sheil CA, Scheyer TM, Nagashima H, Kuratani S. 2009. Skeletal development in the Chinese soft-shelled turtle *Pelodiscus sinensis* (Testudines: Trionychidae). J Morphol [DOI: 10.1002/jmor.10766] (in press).

Sanger TJ, Losos JB, Gibson-Brown JJ. 2008. A developmental staging series for the lizard genus *Anolis:* A new system for the integration of evolution, development, and ecology. J Morphol 269: 129–137.

Scanlon TC. 1982. Anatomy of the neck of the western painted turtle (*Chrysemys picta belli* Gray; Reptilia, Testudinata) from the perspective of possible movements in the region. Ann Arbor, MI: The University of Michigan. p 283.

Scheyer TM. 2007. Comparative bone histology of the turtle shell (carapace and plastron): implications for turtle systematics, functional morphology and turtle origins. In: Mathematisch-Naturwissenschaftlichen Fakultät, Institut für Paläontologie. Bonn: Rheinischen Friedrich-Wilhelms-Universität Bonn. p 343 [URN: http://nbn-resolving.de/urn:nbn:de:hbz:5N-12299; URL: http://hss.ulb.uni-bonn.de/diss_online/math_nat_fak/2007/scheyer_torsten].

Scheyer TM, Anquetin J. 2008. Bone histology of the Middle Jurassic turtle shell remains from Kirtlington, Oxfordshire, England. Lethaia 41:85–96.

Scheyer TM, Brüüllmann B, Sánchez-Villagra MR. 2008. The ontogeny of the shell in side-necked turtles, with emphasis on the homologies of costal and neural bones. J Morphol 269:1008–1021.

Schumacher GH. 1972. Die Kopf- und Halsregion der Lederschildkröte *Dermochelys coriacea* (LINNEAUS 1766)– Anatomische Untersuchungen im Vergleich zu anderen rezenten Schildkröten-Mit 7 Figuren im Text und 31 Tafeln. Berlin: Akademie-Verlag.

Schumacher GH. 1973. The head muscles and hyolaryngeal skeleton of turtles and crocodilians. In: Gans C, editor. Biology of the reptilia. New York:Academic Press. p 101–199.

Schwarz AH. 2006. Keeping and breeding the redbelly shortneck turtle, *Emydura subglobosa*. Reptilia (GB) 45:62–65.

Sellier N, Brillard J-P, Dupuy V, Bakst MR. 2006. Comparative staging of embryo development in chicken, turkey, duck, goose, Guinea fowl, and Japanese quail assessed from five hours after fertilization through seventy-two hours of incubation. J Appl Poultry Res 15: 219–228.

Shah RV. 1963. The neck musculature of a cryptodire (*Deirochelys*) and a pleurodire (*Chelonida*) compared. Bull Mus Comp Zool 129:343–368.

Sheil CA. 2003. Osteology and skeletal development of *Apalone spinifera* (Reptilia:Testudines:Trionychidae). J Morphol 256:42–78.

Sheil CA. 2005. Skeletal development of *Macrochelys temminckii* (Reptilia: Testudines: Chelydridae). J Morphol 263: 71–106.

Sheil CA, Greenbaum E. 2005. Reconsideration of skeletal development of *Chelydra serpentina* (Reptilia: Testudinata: Chelydridae): evidence for intraspecific variation. J Zool Lond 265:235–267.

Smith KK. 1997. Comparative patterns of craniofacial development in eutherian and metatherian mammals. Evolution 51:1663–1678.

Tokita M, Kuratani S. 2001. Normal embryonic stages of the Chinese softshelled turtle *Pelodiscus sinensis* (Trionychidae). Zool Sci 18:705–715.

Tzika A, Milinkovitch MC. 2008. A pragmatic approach for selecting evo-devo model species in amniotes. In: Minelli A, Fusco G, editors. Evolving pathways. Key themes in evolutionary developmental biology. Cambridge: Cambridge University Press.

Vallois HV. 1922. Les transformationes de la musculature de l'episome chez les vertébrés. Arch Morphol Gen Exp.

Velhagen WA Jr. 1997. Analyzing developmental sequences using sequence units. Systemat Biol 46:204–210.

Vieira LG, Santos ALQ, Lima FC. 2007. Ontogeny of scleral ossicles of giant amazon river turtles Podocnemis expansa Schweigger, 1812 (Testudines, Podocnemididae). Braz J Morphol Sci 24:220–223.

Vieira LG, Santos ALQ, Lima FC, Pinto JGS. 2009. Ontogeny of the plastron of the giant amazon river turtle, *Podocnemis expansa* (Schweigger, 1812) (Testudines, Podocnemididae). Zool Sci 26:491–495.

Weisbecker V, Goswami A, Wroe S, Sánchez-Villagra MR. 2008. Ossification heterochrony in the mammalian postcranial skeleton and the marsupial-placental dichotomy. Evolution 62:2027–2041.

Werneburg I. 2009. A standard system to study vertebrate embryos. PLoS One 4:e5887 [DOI: 10.1371/journal.pone.0005887].

Werneburg I, Sánchez-Villagra MR. 2009. Timing of organogenesis support basal position of turtles in the amniote tree of life. BMC Evol Biol 9:82 [DOI: 10.1186/1471-2148-9-82].

Yntema CL. 1968. A series of stages in the embryonic development of *Chelydra serpentina*. J Morphol 125:219–251.

Zangerl R. 1969. The Turtle Shell. In: Bellairs Ad'A, Parson TS, editors. Biology of the Reptilia. Morphology A. London and New York: Academic Press. pp 311–339.

Ziermann JM. 2008. Evolutionäre Entwicklung larvaler Cranialmuskulatur der Anura und der Einfluss von Sequenzheterochronien. In: Biologisch-Pharmazeutische Fakultät. Jena: Friedrich-Schiller-Universität. p 347.

Appendix 2:

Co-authored publications linked to this dissertation

Werneburg, I, Hugi, J, Müller, J, Sánchez-Villagra, M. R. 2009. Embryogenesis and Ossification of *Emydura subglobosa* (Testudines, Pleurodira, Chelidae) and Patterns of Turtle Development. *Developmental Dynamics* 238: 2770-2786.

Appendix 3:

Co-authored and own abstracts linked to this dissertation

Position of Turtles within Amniota: Approaches in Comparative Embryology
Ingmar Werneburg, Jasmina Hugi, Christian Mitgutsch, Johannes Müller, Marcelo R. Sánchez-Villagra

Neontological, paleontological, and molecular studies of tetrapod phylogeny result in contradicting results for the position of turtles. We conducted analyses of new and published embryological data to detect shifts in developmental timing during embryogenesis of 15 turtle species and eight tetrapod outgroups. We used the event-pairing and the Parsimov methods for detecting temporal shifts in a phylogenetic framework and tested eight disputed hypotheses for the position of turtles within amniotes, combined to three alternative hypotheses on cryptodire turtle relationships. We developed a new standardised approach to study vertebrate embryos and used it as a basis to describe 104 developmental events that can be easily identified in amniotes, including events occurring during limb, eye, mandibular process, pharyngeal arch, or somite development. The Parsimov analyses of the resulting data, under several different assumptions of character definition and ordering, conclusively support the Testudines + Sauria hypothesis out of the alternative amniote phylogenies.

1st European BioSyst Meeting and 11th Tagung der Deutschen Gesellschaft für Biologische Systematik (GfBS), 10.-14.8.2009 in Leiden / Netherlands, Conference Abstract Booklet, page 137.

Embryological Evidence for a Basal Position of Turtles within Amniota
Ingmar Werneburg, Jasmina Hugi, Christian Mitgutsch, Johannes Müller, Marcelo R. Sánchez-Villagra

Comparative data on cranial anatomy and several paleontological studies suggest a phylogenetic position of turtles within ”anapsids”. In contrast, several recent neontological, paleontological,

osteological and molecular studies support a grouping of turtles within Diapsida. We conducted analyses of new and published embryological data to detect shifts in developmental timing during embryogenesis of 15 turtle species and eight tetrapod outgroups. We used the event-pairing and the Parsimov methods for detecting temporal shifts in a phylogenetic framework and tested eight disputed hypotheses for the position of turtles within amniotes, combined to three alternative hypotheses on cryptodire turtle relationships. We developed a new standardized approach to study vertebrate embryos and used it as a basis to describe 104 developmental events that can be easily identified in amniotes, including events occurring during limb, eye, eyelid, carapace, maxillary and mandibular process, pharyngeal arch, and somite development. The Parsimov analyses of the resulting data, under several different assumptions of character definition and ordering, conclusively support the Testudines + Sauria hypothesis out of the alternative amniote phylogenies. Marine turtles are assumed to be basal within cryptodires. Amongst others, the here obtained arrangement is characterized by an early onset of sense-related characters as compared to mammals. However, based on our developmental data we cannot test if turtles evolved within one of the fossil “Anapsida”-clades or on the branch leading to Sauria within diapsids. Ongoing histological studies of head development, as well as the first detailed investigations on the ontogeny of pleurodire turtles such as *Emydura subglobosa* are likely to produce further insights into this issue.

69th Annual meeting of the Society of Vertebrate Paleontology (SVP) and 57th Symposium of Vertebrate Palaeontology and Comparative Anatomy (SVPCA), 23.-26.9.2009 in Bristol / United Kingdom. Journal of Vertebrate Paleontology 29(3): Supplement, 199A.

Fossilized Ontogenies: Osteological and Bone Mictrostructural Case Studies of Fossil Marine Reptiles from the UNESCO World Heritage Site of Monte San Giorgio, Ticino, Switzerland

Torsten M. Scheyer, Jasmina Hugi, Massimo Delfino, Marcelo R. Sánchez-Villagra

A fossil specimen represents only a snapshot of the ontogenesis spanning the time between fertilization to death of an individual, but it is important to gather as much ontogenetic data as possible for a fossil species if we wish to understand the evolution of extinct life histories. This is generally accomplished by studying growth series, and lately there is an increasing trend to incorporate ontogenetic aspects in palaeobiological studies, and for evolutionary developmental biologists to consider fossils. These studies have been largely restricted to basal groups among Vertebrata (e.g., tetrapodomorphs, temnospondyl amphibians), basically because of exceptionally preserved fossils in these groups. Concurrently, major advances in the study and phylogenetic analyses of skeletal developmental events were achieved over the past two decades. Triassic marine reptiles are well suited to increase the scope of these studies within Amniota. However, even in the UNESCO site of Monte San Giorgio, the most important fossil lagerstätte of marine reptiles

from the Middle Triassic, the discovery of fossils of different age stages (embryos, juveniles, and adults) is still a rare circumstance. The most common fossil reptile groups, i.e., pachypleurosaurs and ichthyosaurs, yielded the best growth series so far. Furthermore, less comprehensive growth series are available for placodont reptiles, nothosaurs, and the early archosauromorph genera *Tanystropheus* and *Macrocnemus*. Limb development is studied in the four genera of pachypleurosaurs (three species of *Neusticosaurus* and one species of *Serpianosaurus*) for the first time, and it is compared to other sauropterygian taxa, as well as with modern marine and non-marine reptiles, i.e., turtles and squamates. Long bone histology is used to access data on growth and paleoecology. It is inferred that it took ten to fifteen years for a specimen of *Mixosaurus* to reach an overall body length of approximately 100 cm. *Paraplacodus* long bone histology is similar to that of *Placodus*, i.e., pachyostotic in a broad sense, with the bones appearing more dense (osteosclerotic) than in the latter.

69th Annual Meeting of the Society of Vertebrate Paleontology (SVP) and 57th Symposium of Vertebrate Palaeontology and Comparative Anatomy (SVPCA), 23.-26.9.2009 in Bristol / United Kingdom. Journal of Vertebrate Paleontology 29 (3): Supplement, 177A.

Fossilised Ontogenies: Morphology and Ossification Sequence Studies of Limbs in Sauropterygian and Ichthyosaurian Clades from the UNESCO World Heritage Site of Monte San Giorgio, Switzerland, with a Comparison to Recent Reptiles

Jasmina Hugi, Torsten M. Scheyer, Christian Mitgutsch, Marcelo R. Sánchez-Villagra

The Unesco World Heritage site of Monte San Giorgio in Switzerland has yielded excellently preserved specimens of several basal sauropterygians and ichthyosaurs, in some cases even growth series from embryo to adult. These findings do not only provide information on adaptations of reptiles secondarily adapted to life in water, they also provide interspecific data of ossification sequences. Limbs are highly adaptive showing convergences for similar modes of life and also contain phylogenetic information. Limb ossification sequences were studied in four sauropterygians (pachypleurosaurs: *Serpianosaurus mirigiolensis*, *Neusticosaurus pusillus*, *N. peyeri*, *N. edwardsii*) and one ichthyosaur genus (*Mixosaurus* spp.). In addition, limb morphology was studied in placodonts, pachypleurosaurs, and nothosaurs, as well as in two ichthyosaur taxa. The aim of this study was to elucidate basal or derived adaptations to life modes in early marine reptiles such as a change in the predominance of the ossification sequence, a shortening of the stylo- and zeugopods, hardening of joints, and decrease/increase of the phalangeal formula. Results are compared to limb morphology and ossification sequences of modern marine reptiles, e.g. cryptodiran and pleurodiran turtles, and non-marine squamates (e.g., *Liopholis whitii*, Scincidae). Results of the ossification sequences of the genera *Neusticosaurus* and *Serpianosaurus* are: (1) acceleration of the hind limb compared to the forelimb in beginning ossification sequence. (2) acceleration of the forelimb compared to the hind limb in ending ossification sequence. (3)

ossification with a postaxial dominance in the sequential beginning formation of metapodials. (4) ossification with a preaxial dominance in the sequential ending formation of metapodials. (5) ossification with a postaxial dominance in the sequential beginning formation of phalanges. (6) ossification with a preaxial dominance in the sequential beginning formation of phalanges. (7) carpalia start ossification first endochrondrally before showing perichondral ossification. (8) tarsalia start ossification first perichondrally before showing endochondral ossification. The (1), (3) and (5) observations confirm previous stated characteristics of amniotes, whereas (4) and (6) is a characteristic of anamniotes. Swimming *Neusticosaurus* spp. and *Serpianosaurus* sp. use their hind limbs for steering while propulsion is provided by axial movement. Preaxial dominance of ending ossification of phalanges is regarded as derived adaptation to a life in water; preaxial digits (especially digit I), have first to be strengthened for resisting water flow. Ossification sequences in the phalanges of living reptiles are variable, as exemplified by comparisons among living turtle and squamate taxa.

69th Annual meeting of the Society of Vertebrate Paleontology (SVP) and 57th Symposium of Vertebrate Palaeontology and Comparative Anatomy (SVPCA), 23.-26.9.2009 in Bristol / United Kingdom. Journal of Vertebrate Paleontology 29(3): Supplement, 118A.

Ontogenetic and Histological Approaches to the Study of Limb Evolution in Pachypleurosaurs, with Comparison to Recent Forms

Jasmina Hugi, Torsten M. Scheyer, Marcelo R. Sánchez-Villagra

The UNESCO World Heritage site of Monte San Giorgio in Switzerland has yielded excellently preserved specimens of several basal sauropterygians. Due to great quantities of the fossil material, growth series can be found ranging in some cases even from embryo to adult individuals. Limb ossification sequences were studied in four pachypleurosaurs (*Serpianosaurus mirigiolensis*, *Neusticosaurus pusillus*, *N. peyeri*, *N. edwardsii*), with comparison to those of recent lizards. Reptilian limbs offer an excellent opportunity to explore the persistence of, as well as the mechanisms behind, morphological trends. Here, limb ossification sequence of the studied pachypleurosaurs deals with two aspects: (1) developmental sequence of phalanges, (2) secondary endosteal compactation of the bones. There are two different developmental stages of osteogenesis: (1) onset of ossification (i.e. primary endosteal and periosteal calcification of cartilage), (2) subsequent mineralization processes of the bones as revealed by compactation patterns (here referred to as “ending sequence” of ossification), also recognized for example in other marine eureptilian taxa like *Claudiosaurus germaini*. Results show that elements of the forelimb start ossification before corresponding elements of the hind limb. Conversely, the ending sequence shows the reverse order. Further results of the beginning sequence of pachypleurosaurs confirm the general ossification pattern of amniotes (i.e. ossification proceeds from proximal to distal across the limb, with a postaxial dominance in the zeugopodial and autopodial region) also

conserved in the ossification sequence of studied lizards without limb reduction. Interestingly, the results of the ending sequence show a different order of ossification: the postaxial ossification gradient shifts into a preaxial dominance in both the zeugopodial and autopodial regions, which is characteristic for anamniotes. Additionally, phalanges now show a distoproximal gradient. In pachypleurosaurs, ossification sequences of the limb bones are probably related to the aquatic life mode of these animals. Pachypleurosaurs use their webbed hind limbs for steering, while propulsion is provided by axial movement. Preaxial dominance of ending ossification sequence in the phalanges and often in the metapodials is regarded as a derived adaptation to a life in water; preaxial digits have first to be strengthened for resisting water flow.

Jahrestagung der Paläontologischen Gesellschaft, Bonn, 5.-7.Oktober 2009. Terra Nostra 54: 79.

On Becoming Aquatic: the Case of the Marine Iguana (*Amblyrhynchus cristatus*) and the Pachypleurosaurs from the Triassic of Monte San Giorgio, Switzerland

Jasmina Hugi, Torsten M. Scheyer, Marcelo R. Sánchez-Villagra

Aquatic tetrapods usually reflect specific histological imbalances between bone resorption and accretion. Positive imbalance leading to an increase in bone compactness is mainly observed in secondary aquatic reptiles living near-shore and feeding on plants or immobile prey. Those animals often show no or minor resorption in their bones reflecting the entire life history. To gain insight into the life history of secondary aquatic reptiles hypothesized to be ecologically similar, thin sections of long bones of extinct (Pachypleurosauridae: *Serpianosaurus mirigiolensis* and *Neusticosaurus* spp. from Monte San Giorgio, Switzerland) and extant marine reptiles and of closely related terrestrial taxa (Iguanidae) were studied. We show that bone compactness changes distinctly from terrestrial to secondary aquatic extant iguanids and the extinct pachypleurosaurs by continuous deposition of periosteal and endosteal bone and by no or only minor resorption.
The marine iguana (*Amblyrhynchus cristatus*) and the *N.* spp. show similar histological and skeletochronological patterns in their long bones, regarding for example the cortical growth and the age of reaching sexual maturity. The stratigraphically older *S. mirigiolensis* shows similarities with completely terrestrial iguanas.
Long bones of the marine iguanas exhibit dense, nearly avascular pachyostotic bones surrounding a medullary cavity. Their innermost periosteal layers (up to two) show fast growing bone tissue (woven-fibered bone grading into parallel-fibered bone) followed by the accretion of lamellar-zonal bone. The pachypleurosaurs from Monte San Giorgio, Switzerland, show the same bone tissue types as the marine iguanas. However, their bone compactness additionally increases by retaining a calcified cartilaginous core in the endosteal region. However, results also revealed that the *N.* spp. show less compact bones compared to their stratigraphically older relatives. The former exhibit higher vascularization in the periosteum and lower vascularization in the endosteal

region where the calcified cartilage is often entirely replaced by trabeculae.
This study focuses on two related reptilian lineages demonstrating similarities in the evolution of the life history in secondary aquatic members.

70th Annual Meeting of the Society of Vertebrate Paleontology (SVP), 10.-13.10.2010 in Pittsburgh. Journal of Vertebrate Paleontology 28(3): 108A.

Comparing the long bone microstructure of the marine iguana (*Amblyrhynchus cristatus*) with that of extinct marine reptiles (Pachypleurosauridae) from the Triassic of Monte San Giorgio, Switzerland/Italy
Jasmina Hugi

The long bones of vertebrates are informative structures to study life histories using histological data, because the microstructure is often altered as a result of changes in the endogenous biological rhythm or due to external factors. Marine iguanas (*Amblyrhynchus cristatus*) of the Galapagos Archipelago are highly dependant on one external factor, the availability of macrophytic algae, which are their only food supply. Does their bone histology indicate changes as a result of the amphibious lifestyle?
The aim of this study was primarily to assess the life history of the marine iguanas and compare this to the more terrestrial iguanid relatives, based on changes in the microstructure of the long bones. Results were then compared to the bone histology of four marine sauropterygian reptiles, *Serpianosaurus mirigiolensis*, *Neusticosaurus pusillus*, *N. peyeri* and *N. edwardsii* (Pachypleurosauridae), from the Middle Triassic of Monte San Giorgio in order to obtain further information about their life histories and secondary adaptations to an aquatic life.
Histological data of the marine iguanas indicate differences in microstructure and bone compactness values compared to terrestrial iguanid relatives, most likely as a result of their amphibious lifestyle. A characteristic spacing pattern of growth cycles distinguishes them from equivalent data of terrestrial lizards, indicating elongated phases of constantly low bone deposition rates. The marine iguana and its sister taxon, the Galapagos land iguana (*Conolophus subcristatus)*, share a specific alignment of the collageneous fibres, which results in a distinct light and extinction pattern visible in polarised light. The life history pattern of the marine iguana reconstructed with bone histology is strikingly congruent with observations provided by ecological studies. In comparison, the stratigraphically oldest and youngest of the four pachypleurosaurids (*Serpianosaurus mirigiolensis*, *N. edwardsii*) share similar histological features with the marine iguana based on the spacing pattern of the growth cycles, as well as the distinct light and extinction pattern. The skeletochronological data of the two other pachypleurosaurids (*Neusticosaurus pusillus*, *N. peyeri*) are comparable to the ones of terrestrial lizards. The bone microstructure might be linked to different habitat preferences within the pachypleurosaurids.

First International Symposium on Paleohistology, 18.-20.July 2011, Barcelona.

Appendix 4:

Curriculum Vitae

HUGI Jasmina

Geburtsdatum:	9.05.1983
Heimatort:	Winterthur ZH

Ausbildung:

1998-2002	Kantonsschule im Lee, Winterthur, Eidgenössische Matura Typus B
2003-2008	Studium von Biologie, Universität Zürich
2008	Master in Biologie: The axial and posterior appendicular morphology of the first theropod skeleton (Saurischia, Dinosauria) of Switzerland (Late Triassic; Frick, Canton Aargau)
2008-2011	Doktorandin am Paläontologischen Institut und Museum der Universität Zürich

Publikationen während des Promotionsstudiums:

Artikel

- Werneburg, I., Hugi, J., Müller, J., Sánchez-Villagra, M. R. 2009. Embryogenesis and Ossification of *Emydura subglobosa* (Testudines, Pleurodira, Chelidae) and Patterns of Turtle Development. *Developmental Dynamics* 238: 2770-2786.
- Hugi, J., Mitgutsch, C., Sánchez-Villagra, M. R. 2010. Chondrogenic and ossification patterns and sequences in White's skink *Liopholis whitii* (Scincidae, Reptilia). *Zoosystematics and Evolution* 86 (1): 21–32.
- Hugi, J., Hutchinson, M. N., Sánchez-Villagra, M. R. Heterochronic shifts in the ossification sequences of surface and subsurface dwelling skinks are correlated with the degree of limb reduction. Submitted, *Zoology.*
- Hugi, J., Scheyer, T. M., Sander, P. M., Klein, N., Sánchez-Villagra, M. R. 2011. Long bone microstructure gives new insights into the life of pachypleurosaurids from the Middle Triassic of Monte San Giorgio, Switzerland/Italy. In press, *C. R. Palevol* xxx (2011) xxx–xxx.

- Hugi, J., Scheyer, T. M. Ossification sequences and associated ontogenetic changes in the bone histology of pachypleurosaurids from Monte San Giorgio, Switzerland/Italy. In review, *Journal of Vertebrate Paleontology.*
- Hugi, J., Sánchez-Villagra, M. R. Life history and skeletal adaptations in the Galapagos Marine Iguana (*Amblyrhynchus cristatus*) as reconstructed with bone histological data - a comparative study of iguanines. In review, *Journal of Herpetology.*
- Hugi, J. The long bone histology of *Ceresiosaurus* (Sauropterygia, Reptilia) in comparison to other eosauropterygians from the Middle Triassic of Monte San Giorgio (Switzerland/ Italy). Submitted, *Swiss Journal of Paleontology.*

Abstracts für Vorträge an Fachtagungen

- Werneburg, I., Hugi, J., Mitgutsch, C., Müller, J., Sánchez-Villagra, M. R. Position of Turtles within Amniota: Approaches in Comparative Embryology. 1st European BioSyst Meeting and 11th Tagung der Deutschen Gesellschaft für Biologische Systematik (GfBS), 10.-14.8.2009 in Leiden / Netherlands, Conference Abstract Booklet, page 137.
- Hugi, J., Scheyer, T. M., Sánchez-Villagra, M. R. Fossilised ontogenies: morphology and ossification sequence studies of limbs in sauropterygian and ichthyosaurian clades from the UNESCO World Heritage site of Monte San Giorgio, Switzerland, with a comparison to recent reptiles. 69th Annual meeting of the Society of Vertebrate Paleontology (SVP) and 57th Symposium of Vertebrate Palaeontology and Comparative Anatomy (SVPCA), 23.-26.9.2009 in Bristol / United Kingdom. Journal of Vertebrate Paleontology, 29(3): Supplement, 118A.
- Scheyer, T., Hugi, J., Delfino, M., Sánchez-Villagra, M. R. Fossilized ontogenies: osteological and bone microstructural case studies of marine reptiles from the Unesco World Heritage Site of Monte San Giorgio, Ticino, Switzerland. 69th Annual Meeting of the Society of Vertebrate Paleontology (SVP) and 57th Symposium of Vertebrate Palaeontology and Comparative Anatomy (SVPCA), 23.-26.9.2009 in Bristol / United Kingdom. *Journal of Vertebrate Paleontology*: 29(3), Supplement, 177A.
- Werneburg, I., Hugi, J., Mitgutsch, C., Müller, J., Sánchez-Villagra, M. R. Embryological evidence for a basal position of turtles within Amniota. 69th Annual meeting of the Society of Vertebrate Paleontology (SVP) and 57th Symposium of Vertebrate Palaeontology and Comparative Anatomy (SVPCA), 23.-26.9.2009 in Bristol / United Kingdom. *Journal of Vertebrate Paleontology* 29(3), Supplement, 199A.
- Hugi, J., Scheyer, T. M., Sánchez-Villagra, M. R. Ontogenetic and histological approaches to the study of limb evolution in pachypleurosaurs, with comparison to recent forms. Jahrestagung der Paläontologischen Gesellschaft, Bonn, 5.-7.Oktober 2009. Terra Nostra 54: 79.
- Hugi, J., Scheyer, T. M., Sánchez-Villagra, M. R. On Becoming Aquatic: the Case of the Marine Iguana (*Amblyrhynchus cristatus*) and the Pachypleurosaurs from the Triassic

of Monte San Giorgio, Switzerland. 70th Annual Meeting of the Society of Vertebrate Paleontology (SVP), 10.-13.10.2010 in Pittsburgh. *Journal of Vertebrate Paleontology* 28(3): 108A.

- Hugi, J. Comparing the long bone microstructure of the marine iguana (*Amblyrhynchus cristatus*) with that of extinct marine reptiles (Pachypleurosauridae) from the Triassic of Monte San Giorgio, Switzerland/Italy. First International Symposium on Paleohistology, Barcelona 2011.